ISSUE RESOLUTION STATUS REPORT

KEY TECHNICAL ISSUE: UNSATURATED AND SATURATED FLOW UNDER ISOTHERMAL CONDITIONS

Division of Waste Management
Office of Nuclear Material
Safety & Safeguards
U.S. Nuclear Regulatory Commission

Revision 1
September 1998

Volume II
(Attachments)

9908270110 981007
PDR WASTE
WM-11 PDR

ATTACHMENT A

DRAFT FIGURES ILLUSTRATING ELEMENTS OF THE NRC STAFF'S TOTAL SYSTEM PERFORMANCE ASSESSMENT

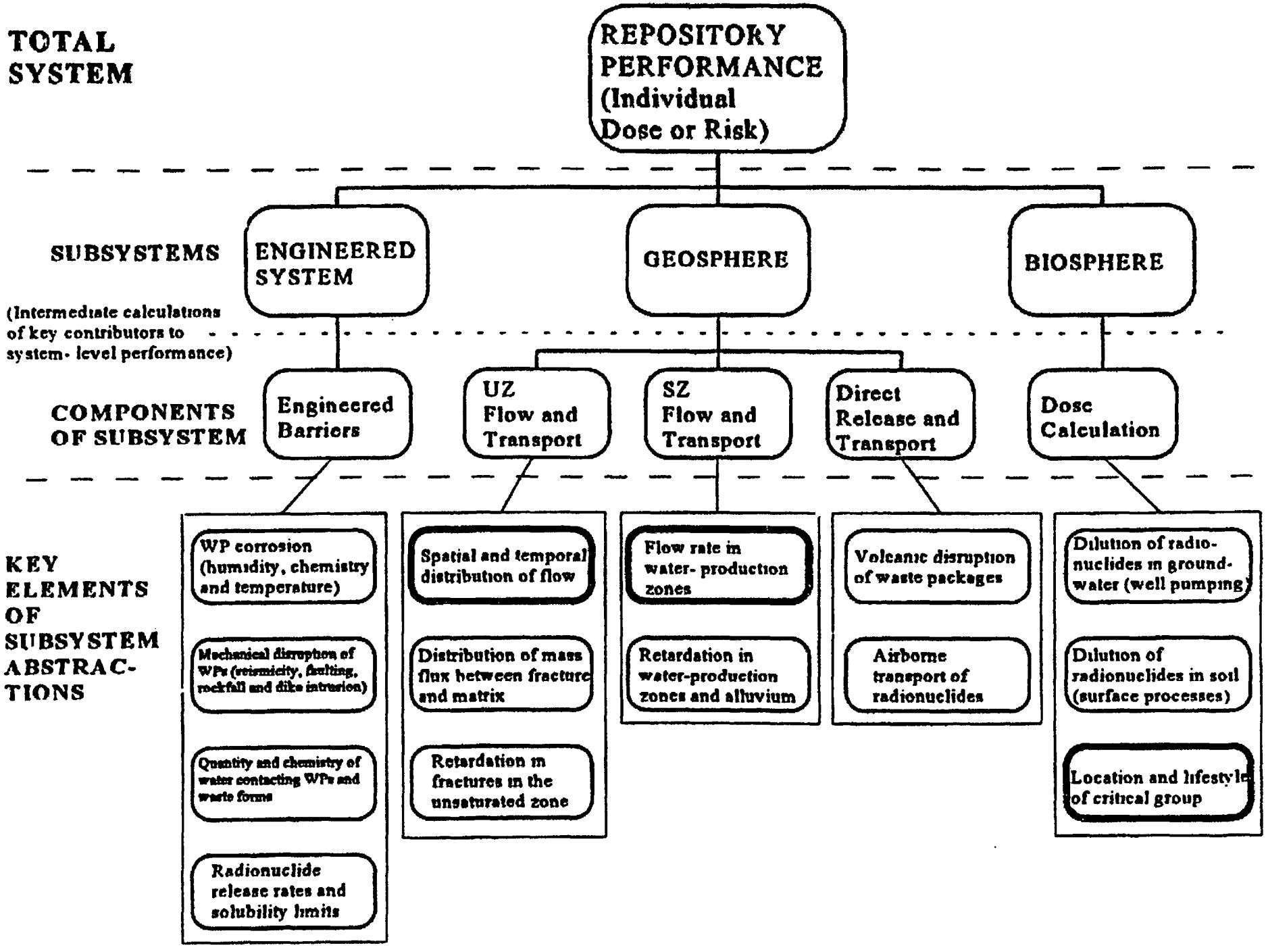
TOTAL SYSTEM
REPOSITORY PERFORMANCE (Individual Dose or Risk)
SUBSYSTEMS
(Intermediate calculations of key contributors to system- level performance)
ENGINEERED SYSTEM
GEOSPHERE
BIOSPHERE
COMPONENTS OF SUBSYSTEM
Engineered Barriers
UZ Flow and Transport
SZ Flow and Transport
Direct Release and Transport
Dose Calculation
KEY ELEMENTS OF SUBSYSTEM ABSTRAC-TIONS
WP corrosion (humidity, chemistry and temperature)
Mechanical disruption of WPs (seismicity, faulting, rockfall and dike intrusion)
Quantity and chemistry of water contacting WPs and waste forms
Radionuclide release rates and solubility limits
Spatial and temporal distribution of flow
Distribution of mass flux between fracture and matrix
Retardation in fractures in the unsaturated zone
Flow rate in water- production zones
Retardation in water-production zones and alluvium
Volcanic disruption of waste packages
Airborne transport of radionuclides
Dilution of radio-nuclides in ground-water (well pumping)
Dilution of radionuclides in soil (surface processes)
Location and lifestyle of critical group

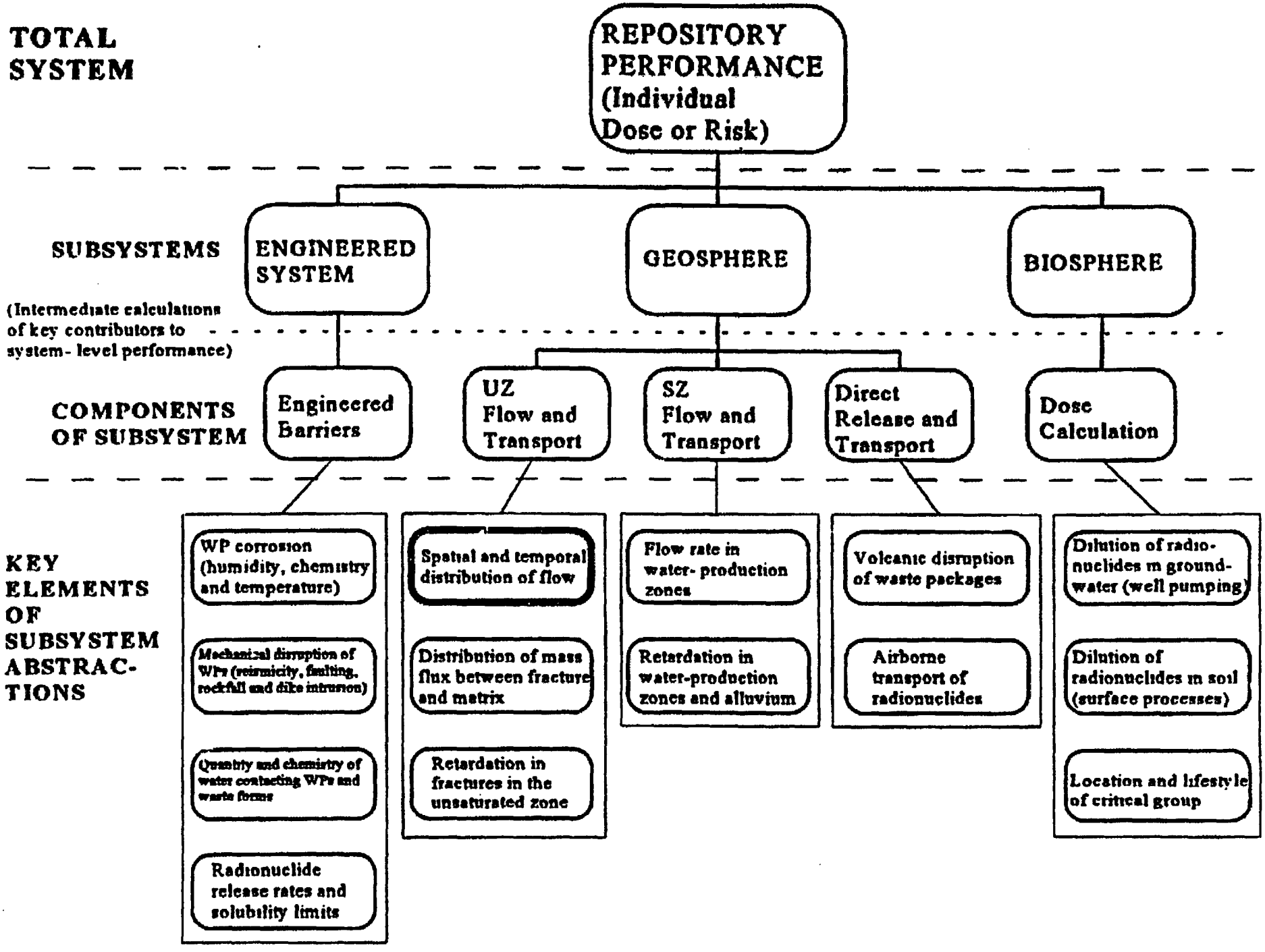
TOTAL SYSTEM
REPOSITORY PERFORMANCE (Individual Dose or Risk)
SUBSYSTEMS
(Intermediate calculations of key contributors to system- level performance)
ENGINEERED SYSTEM
GEOSPHERE
BIOSPHERE
COMPONENTS OF SUBSYSTEM
Engineered Barriers
UZ Flow and Transport
SZ Flow and Transport
Direct Release and Transport
Dose Calculation
KEY ELEMENTS OF SUBSYSTEM ABSTRAC-TIONS
WP corrosion (humidity, chemistry and temperature)
Mechanical disruption of WPs (seismicity, faulting, rockfall and dike intrusion)
Quantity and chemistry of water contacting WPs and waste forms
Radionuclide release rates and solubility limits
Spatial and temporal distribution of flow
Distribution of mass flux between fracture and matrix
Retardation in fractures in the unsaturated zone
Flow rate in water- production zones
Retardation in water-production zones and alluvium
Volcanic disruption of waste packages
Airborne transport of radionuclides
Dilution of radio-nuclides in ground-water (well pumping)
Dilution of radionuclides in soil (surface processes)
Location and lifestyle of critical group

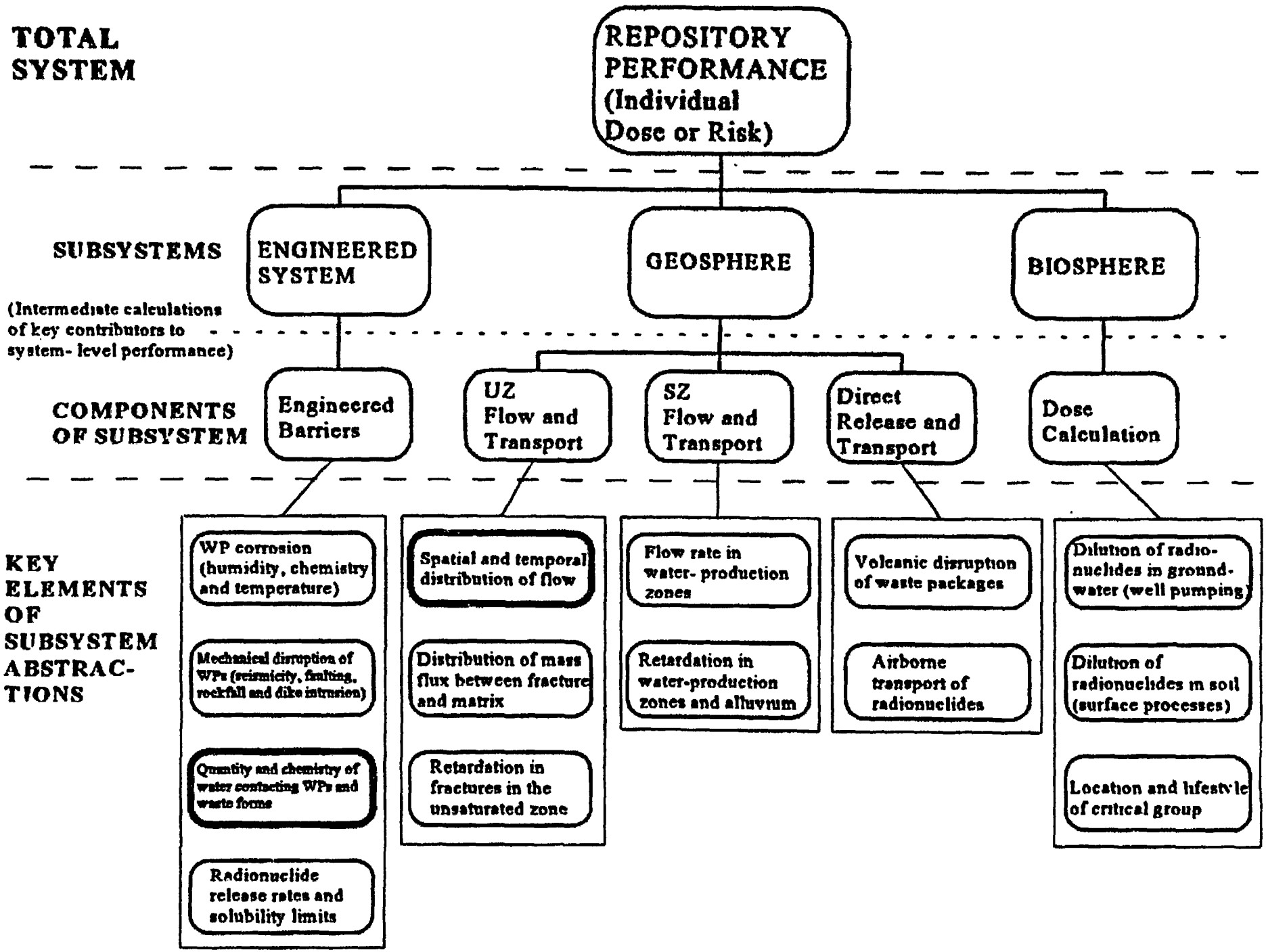
TOTAL SYSTEM
REPOSITORY PERFORMANCE (Individual Dose or Risk)
SUBSYSTEMS
(Intermediate calculations of key contributors to system- level performance)
ENGINEERED SYSTEM
GEOSPHERE
BIOSPHERE
COMPONENTS OF SUBSYSTEM
Engineered Barriers
UZ Flow and Transport
SZ Flow and Transport
Direct Release and Transport
Dose Calculation
KEY ELEMENTS OF SUBSYSTEM ABSTRAC-TIONS
WP corrosion (humidity, chemistry and temperature)
Mechanical disruption of WPs (seismicity, faulting, rockfall and dike intrusion)
Quantity and chemistry of water contacting WPs and waste forms
Radionuclide release rates and solubility limits
Spatial and temporal distribution of flow
Distribution of mass flux between fracture and matrix
Retardation in fractures in the unsaturated zone
Flow rate in water- production zones
Retardation in water-production zones and alluvium
Volcanic disruption of waste packages
Airborne transport of radionuclides
Dilution of radio-nuclides in ground-water (well pumping)
Dilution of radionuclides in soil (surface processes)
Location and lifestyle of critical group

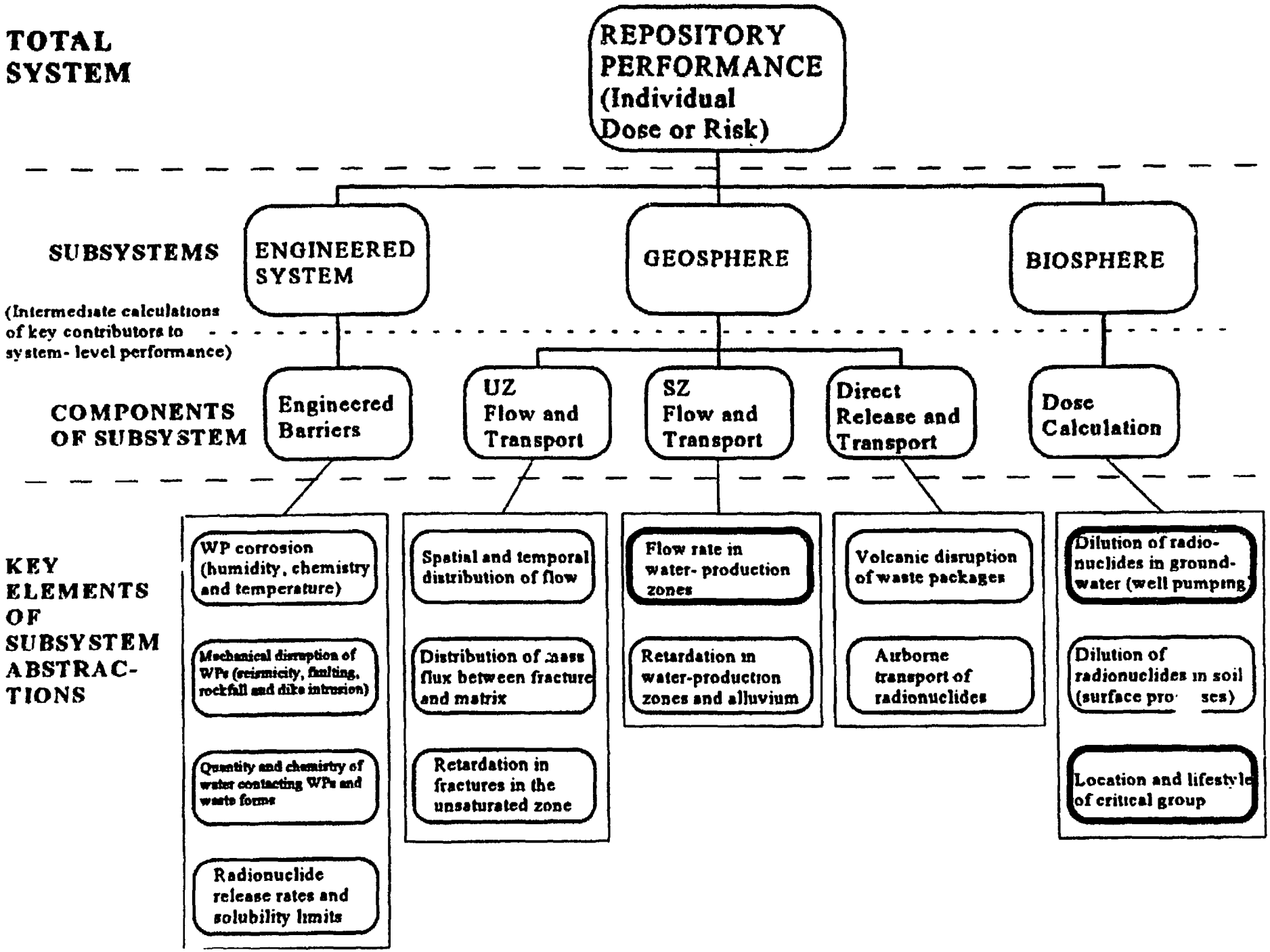
TOTAL SYSTEM
REPOSITORY PERFORMANCE (Individual Dose or Risk)
SUBSYSTEMS
(Intermediate calculations of key contributors to system- level performance)
ENGINEERED SYSTEM
GEOSPHERE
BIOSPHERE
COMPONENTS OF SUBSYSTEM
Engineered Barriers
UZ Flow and Transport
SZ Flow and Transport
Direct Release and Transport
Dose Calculation
KEY ELEMENTS OF SUBSYSTEM ABSTRAC-TIONS
WP corrosion (humidity, chemistry and temperature)
Mechanical disruption of WPs (seismicity, faulting, rockfall and dike intrusion)
Quantity and chemistry of water contacting WPs and waste forms
Radionuclide release rates and solubility limits
Spatial and temporal distribution of flow
Distribution of mass flux between fracture and matrix
Retardation in fractures in the unsaturated zone
Flow rate in water- production zones
Retardation in water-production zones and alluvium
Volcanic disruption of waste packages
Airborne transport of radionuclides
Dilution of radio-nuclides in ground-water (well pumping)
Dilution of radionuclides in soil (surface pro sses)
Location and lifestyle of critical group

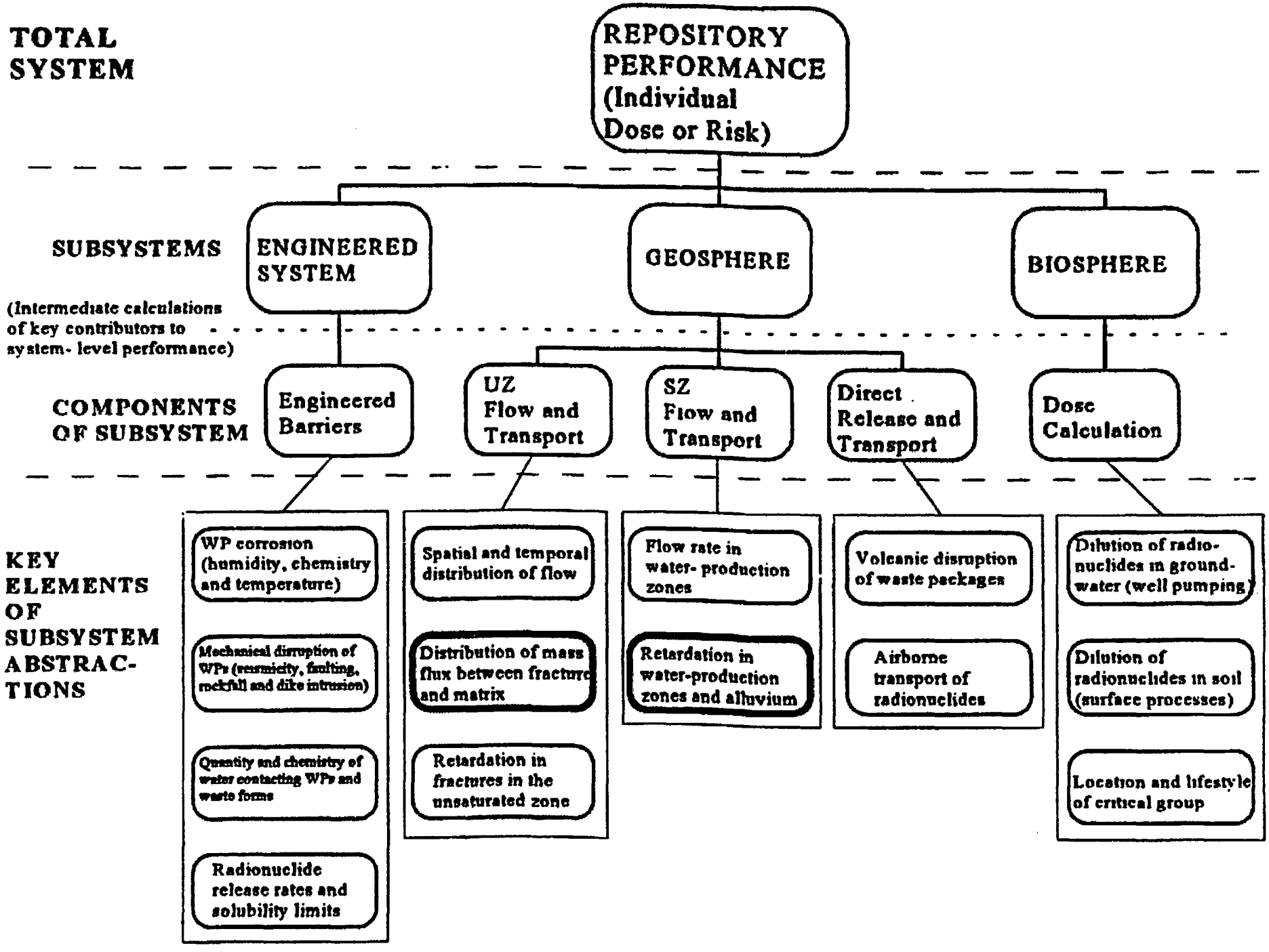
TOTAL SYSTEM
REPOSITORY PERFORMANCE (Individual Dose or Risk)
SUBSYSTEMS
(Intermediate calculations of key contributors to system- level performance)
ENGINEERED SYSTEM
GEOSPHERE
BIOSPHERE
COMPONENTS OF SUBSYSTEM
Engineered Barriers
UZ Flow and Transport
SZ Flow and Transport
Direct Release and Transport
Dose Calculation
KEY ELEMENTS OF SUBSYSTEM ABSTRAC-TIONS
WP corrosion (humidity, chemistry and temperature)
Mechanical disruption of WPs (seismicity, faulting, rockfall and dike intrusion)
Quantity and chemistry of water contacting WPs and waste forms
Radionuclide release rates and solubility limits
Spatial and temporal distribution of flow
Distribution of mass flux between fracture and matrix
Retardation in fractures in the unsaturated zone
Flow rate in water- production zones
Retardation in water-production zones and alluvium
Volcanic disruption of waste packages
Airborne transport of radionuclides
Dilution of radio-nuclides in ground-water (well pumping)
Dilution of radionuclides in soil (surface processes)
Location and lifestyle of critical group

ENCLOSURE

ACKNOWLEDGMENTS

This report has been prepared jointly by staff from the U.S. Nuclear Regulatory Commission and the Center for Nuclear Waste Regulatory Analyses (CNWRA). Primary authors of the report are, in alphabetical order, Amit Armstrong, Jeff Ciocco, Neil Coleman, Randall Fedors, Latif Hamdan, Stuart Stothoff, David Turner, James Winterle, and Gordon Wittmeyer. The authors offer special thanks to David Brooks, Budhi Sagar, and English Pearcy for their excellent reviews.

Valuable technical assistance was provided by William Murphy, David Ferrill, John Stamatakos, and English Pearcy. Special thanks to Ronald Martin for providing assistance with figures. This report would not have been possible without the assistance of Carrie Crawford, Corky Gray, Annette Mandujano, and Arturo Ramos.

QUALITY OF DATA, ANALYSES, AND CODE DEVELOPMENT

DATA: NRC and CNWRA-generated original data contained in this report meet quality assurance requirements described in the CNWRA Quality Assurance (QA) Manual. Sources for other data should be consulted for determining the level of quality for those data.

ANALYSES AND CODES: The TPA Version 3.1.1 code has been developed following the procedures described in CNWRA Technical Operating Procedure, TOP-018, which implements the QA guidance contained in the CNWRA QA Manual. The code was used to perform the sensitivity studies described in Section 3.

INTERNET WEBSITES

The reader can find informative discussions about the Yucca Mountain Project by visiting internet web sites and associated links. A partial list is provided below. The U.S. Nuclear Regulatory Commission (NRC) web site provides general information about agency programs and nuclear wastes. The U.S. Nuclear Waste Technical Review Board (NWTRB) website in particular provides many additional important links.

U.S. Nuclear Regulatory Commission	http://www.nrc.gov http://www.nrc.gov/ACRSACNW/
U.S. Department of Energy (DOE)	http://www.ymp.gov [and] http://www.rw.doe.gov
U.S. Nuclear Waste Technical Review Board	http://nwtrb.gov
Nevada Nuclear Waste Project Office	http://www.state.nv.us/nucwaste/
Nye County, Nevada	http://site206087.primehost.com/index.htm
Los Alamos National Laboratory	http://ees13.lanl.gov/!ees-13y.htm
Lawrence Livermore National Laboratory	http://energy.llnl.gov/Yucca.html
Earnest Orlando Lawrence Berkeley National Laboratory	http://www-esd.lbl.gov/NW/yuccamtn.html
Sandia National Laboratories	http://ntp.nwer.sandia.gov/nwmp/ymp.htm
U.S. Environmental Protection Agency	http://epa.gov/rpdweb00/yucca.index.html

Americium and plutonium were significant contributors to maximum TEDE for a receptor group 5 km away from the repository. This indicates that sorption does not become effective in the model for these radionuclides. Although these radionuclides have a great tendency to sorb to most types of earth minerals, they are experiencing little retardation. This low retardation resulted from modeling assumptions where flow is predominantly through fractures for the 5 km receptor group, allowing little contact with sorbing minerals. Normally, americium and plutonium would not be expected to migrate significant distances unless associated with substantial colloidal transport.

The following aspects were identified as requiring additional characterization and examination: (1) well pumping rates (5 km and 20 km receptor groups); (2) mixing zone thickness (5 km and 20 km); (3) maximum hydraulic head in the SZ; and (4) width of the streamtubes at 20 km. Also, the treatment of matrix diffusion and/or the parameters related to sorption of radionuclides such as americium and plutonium need confirmation. Sorption is addressed in detail in the IRSR on Radionuclide Transport (NRC, 1998d).

4.0 REVIEW METHODS AND ACCEPTANCE CRITERIA

The staff's technical review of DOE's treatment of subissues under unsaturated and saturated flow under isothermal conditions will be based on the completeness and applicability of data and analyses. The staff will determine whether DOE has reasonably complied with the acceptance criteria listed in this section for each subissue.

4.1 CLIMATIC CHANGE

See Section 4.2.

4.2 HYDROLOGIC EFFECTS OF CLIMATE CHANGE

Review methods, acceptance criteria, and technical bases for the subissues (climate change and hydrologic effects of climate change) were provided in a previous version of this IRSR which is attached as Attachment E (NRC, 1997a). The acceptance criteria, with slight modification, are repeated below for the convenience of the reader.

4.2.1 ACCEPTANCE CRITERIA

(1) Climate projections based primarily on paleoclimate data are acceptable for use in performance assessments of the YM site. During its review, the staff should determine whether DOE has made a reasonably complete search of paleoclimate data that are available for the YM site and region, and has satisfactorily documented the results. Staff should determine that, at a minimum, DOE has considered information contained in Forester, et al. (1996); Winograd, et al. (1992); Szabo, et al. (1994); and other reports that may become available.

(2) DOE's projections of long-term climate change are acceptable if these projected changes are consistent with evidence from the paleoclimate data. Specifically, staff

should determine whether DOE has evaluated long-term climate change based on known patterns of climatic cycles during the Quaternary, especially the last 500 ky The current analysis indicates that these cycles included roughly 100-ky cycles of glacial/interglacial climates, with interglacials lasting about 20 ky Current information also suggests that past climate conditions were cooler and wetter than today, about 60 to 80 percent of the time.

(3) The staff will not require climate modeling to estimate the range of future climates. If DOE uses numerical climate models, staff will determine whether such models were calibrated with paleoclimate data before they were used for projection of future climate, and that their use suitably simulates the historical record.

(4) Values for climatic parameters (time(s) of onset of climate change; mean annual precipitation (MAP); mean annual temperature (MAT); etc.) to be used in DOE's safety case should be adequately justified. Determine whether appropriate scientific data were used reasonably interpreted, and appropriately synthesized into parameters such as MAP, MAT, and long-term climate variability. The current knowledge about these parameters, coupled with past climate change, will require that, as a bounding condition, a return to full pluvial climate (higher precipitation and lower temperatures) be considered for at least a part of the 10-ky period (current information does not support persistence of present-day climate for a duration of 10 ky or more). The current interpretations of paleoclimate data indicate an increase in MAP by a factor of 2 to 3 and a lowering of MAT of 5-10 °C (9-18 °F) during the pluvial climate episodes.

(5) If DOE uses expert elicitation to arrive at values of climate parameters, staff will determine whether the guidance in the Branch Technical Position on Expert Elicitation (NRC, 1996a) was followed by DOE.

(6) Bounding values of climate-induced effects (for example water-table rise) based primarily on paleoclimate data will be acceptable. Staff should determine whether DOE has made a reasonably complete search of paleoclimate data pertinent to water-table rise and other effects (for example, changes in precipitation and geochemistry) of climate change that are available for the YM site and region, and has satisfactorily documented the results. In evaluating DOE's analyses, staff should determine whether, at a minimum, DOE has fully considered information contained in Paces, et al. (1996a), Szabo, et al. (1994), Forester, et al. (1996), and other reports that may become available.

(7) It will be acceptable for DOE to use regional and sub-regional models for the saturated zone to predict climate-induced consequences if these models are calibrated with the paleohydrology data. Staff should determine whether DOE's models of the consequences of climate change are consistent with evidence from the extensive paleoclimate data base. Specifically, climate-induced water-table rise is expected to occur in response to elevated precipitation during future pluvial climate episodes, and the staff should determine whether DOE's estimates of climate-induced, water-table rise are consistent with the paleoclimate data. The current estimate of water-table rise during the late Pleistocene is 120 m (394 ft). Staff should determine whether DOE's

assumptions about climate-induced, water-table rise over 10 ky, if different from 120 m (394 ft), are adequately justified.

(8) Based on judgment and analysis, staff will determine whether DOE has adequately incorporated future climate changes and associated effects in its performance assessments. Current information does not support an assumption that present-day climate will persist unchanged for 10 ky or more. The staff should keep in mind that the consequences of climate change may be coupled to other events and processes and therefore the projections of water-table rise that are used in total system performance may be different from those based solely on climate change.

(9) The collection, documentation, and development of data, models, and computer codes have been performed under acceptable QA procedures. If they were not subject to an acceptable QA procedure, they have been appropriately qualified.

4.2.2 Technical Basis for Review Methods and Acceptance Criteria

See NRC (1997a) for a description of the technical basis for review methods and acceptance criteria for the subissues of climate change and hydrologic effects of climate change. An important new paper on Devils Hole was published in 1997, and the main conclusions are presented below. These do not lead the NRC staff at this time to change the previously developed acceptance criteria. Winograd, et al. (1997) examined the Devils Hole paleoclimatic record in light of the widely held view that interglaciations lasted 11 ky to 13 ky and constituted only about 10% of middle-to-late Pleistocene climatic cycles. They concluded that the previous interglacial (Sangamon, or substage 5e) lasted significantly longer, about 22 ky, consistent with the Vostok ice core record which suggests a duration of about 19 ky for this event in Antarctica. The three preceding interglacials in the Devils Hole record (analogs of marine isotopic substages 7e, 9c, and 11c) lasted 20 ky to 26 ky. The warmest intervals of each interglacial in the Devils Hole record indicate apparent climatic stability for periods lasting 10 ky to 15 ky. Winograd, et al. (1997, p. 153) also note that "Phase offsets of thousands of years are likely between different climate proxy records (especially temperature and ice volume) of the same interglaciation." They also speculated about the possible duration of our current interglacial climate, assuming only natural variation. With no anthropogenic warming, Holocene-like temperatures could remain with us for up to another 5 ky, or alternatively, the next millennium could experience steadily lowering temperatures.

NRC (1997a) discussed the fact that, during the Wisconsin, the water table at YM may have risen 10 times higher than at Devils Hole, given the proximity of YM to areas of higher elevation where recharge would have been greater, and also due to higher transmissivities in the Paleozoic carbonate aquifer at Devils Hole. It should also be mentioned that the Wisconsin-age rise of the potentiometric surface at Devils Hole may have been controlled, to some extent, by local topography. The present water table is only 17 m below the land surface (Szabo, et al., 1994). Areas close to Devils Hole occur at lower elevations where surface discharges of groundwater could occur during times of elevated water tables. This could perhaps limit the Wisconsin-age rise of the water table to less than 10 m at Devils Hole, as inferred from calcites in the subterranean Browns Room.

The NRC staff has previously recommended (NRC, 1997a, p. 8) a pragmatic approach to address climate change. Under this approach, the effects of global, enhanced, greenhouse warming would be presumed to last no more than several thousand years, and that, about 3 ky into the future, the climate at YM will resume or continue the global cooling predicted by the Milankovitch orbital theory of climate. Pluvial conditions should be expected to dominate at least several thousand years of the next 10 ky. Current information suggests that past climate conditions were cooler and wetter than today, about 60 to 80 percent of the time.

4.3 PRESENT-DAY SHALLOW INFILTRATION

Review methods, acceptance criteria, and technical bases for the subissue of present-day shallow infiltration were provided in a previous version of this IRSR which is provided as Attachment F (NRC, 1997b). The acceptance criteria, with slight modification, are repeated below for the convenience of the reader.

4.3.1 Acceptance Criteria

(1) Staff shall determine whether DOE has estimated shallow infiltration for use in the PA of YM using mathematical models that incorporate site-specific climatic, surface, and subsurface information. Staff will also determine whether DOE provided sufficient evidence that the mathematical models were reasonably verified with site data. These data would include measured infiltration data and indirect evidence such as geochemical and geothermal data. DOE may choose to use a vertical one-dimensional (1D) model to simulate infiltration. However, in that case, DOE should reasonably show that the fundamental effects of heterogeneities, time-varying boundary conditions, evapotranspiration, depth of soil cover, and surface-water runoff have been considered in ways that do not underestimate infiltration.

(2) Staff shall determine whether DOE has: (1) appropriately analyzed infiltration at appropriate time and space scales; and (2) has tested the abstracted model against more detailed models to assure that it produces reasonable results for shallow infiltration under conditions of interest. Recent studies by NRC (Stothoff, et al., 1996) and the DOE (Flint, et al., 1994; Flint and Flint, 1995; Flint, et al., 1996a) suggest that shallow infiltration is relatively high in areas where rocks are covered with shallow soils or channels and relatively low in areas where soil cover is deep. In addition, infiltration takes place episodically in time with areas having a shallow soil cover contributing more frequently.

(3) Staff shall determine whether DOE has characterized shallow infiltration in the form of either probability distributions or deterministic upper-bound values for PA, and whether DOE has provided sufficient data and analyses to justify the chosen probability distribution or bounding value. DOE's expert elicitation on unsaturated zone flow (Geomatrix, 1997) resulted in various estimates of a related parameter, the groundwater percolation flux at the depth of the proposed repository (see Attachment F of this report, Table C-2). The estimated aggregate mean flux was approximately 10 mm/yr. The panelists estimated the 95th-percentile percolation flux over a range from 10 to 50 mm/yr, with an aggregate estimate of 30 mm/yr. An independent staff assessment of an

upper bound for yearly shallow infiltration under present climatic conditions is about 25 mm, which is somewhat less than the aggregate 95th percentile flux estimated by the expert panel.

(4) DOE's estimates of the probability distribution or upper bound for present-day shallow infiltration need not be refined further if DOE demonstrates through TSPA and associated sensitivity analyses that such refinements will not significantly alter the estimate of total-system performance.

(5) If used, expert elicitations should have been conducted and documented using the guidance in the Branch Technical Position on Expert Elicitation (NRC, 1996), or other acceptable approaches.

(6) Staff will determine whether the collection, documentation, and development of data, models, and computer codes have been performed under acceptable QA procedures. If they were not subject to an acceptable QA procedure, they have been appropriately qualified.

4.3.2 Technical Basis for Review Methods and Acceptance Criteria

See NRC (1997b) for a description of the technical basis for review methods and acceptance criteria for the subissue on present-day shallow infiltration.

4.4 DEEP PERCOLATION (PRESENT AND FUTURE)

The staff's technical review of DOE's treatment of deep percolation will be based on an evaluation of the completeness and applicability of the data and evaluations presented by DOE. It is expected that DOE will summarize or document the results of all significant-related studies that have been conducted in the YM vicinity. The staff will determine whether DOE has reasonably complied with the acceptance criteria listed below.

4.4.1 Acceptance Criteria

(1) It will be acceptable for DOE to estimate present-day deep percolation by using (1) a reasonable upper bound based on available data; or (2) through a demonstration in TSPA and associated sensitivity analyses that further refinement of the estimate will not significantly alter the estimate of total-system performance. In the latter case, the staff will conduct an independent analysis to judge the appropriateness of the estimate. In the VA analysis, it will be acceptable to use the aggregate distribution for areally averaged percolation flux estimated through the expert elicitation (i.e., Geomatrix, 1997). DOE's current infiltration map (e.g., Flint, et al.,1996a) may be used to account for spatial variations in percolation.

(2) DOE's estimate of future percolation will be acceptable if it provides a reasonable basis for assumed long-term average net infiltration and percolation flux. It will be acceptable to apply spatial- and temporal-average values of deep percolation through the use of an abstracted deep percolation model in PA. In arriving at spatial- and temporal-average values: variability is appropriately considered; model parameters are averaged over

appropriate time and space scales; and the abstracted model is tested against more detailed models and field observations to assure that it produces reasonably conservative dose estimates. The current understanding is that a vertical one dimensional (1D) model, capable of considering heterogeneities and time-varying boundary conditions at the ground surface, may be sufficient for such calculations above the repository, while a vertically oriented, two dimensional (2D) model or three dimensional (3D) model may be necessary below the repository.

(3) It will be acceptable for DOE to conservatively assume that the fraction of deep percolation that intercepts disposal drifts also drips onto waste packages. Technical bases should be provided for deep percolation that is considered to bypass emplacement drifts. These technical bases should use field observations, experimental data from the ESF facility, calculations based on mass balance, tracer studies, and data from natural analog sites. Likely changes in percolation rates and patterns due to climate change should also be considered. Also, the abstracted model used in PA should be tested against more detailed models and field observations to assure that it produces reasonably conservative dose estimates. It is known that the amount of deep percolation into the waste emplacement drifts is sensitive to fast flow in fracture zones. Such flow paths need to be considered in DOE's calculations.

(4) It will be acceptable for DOE to conservatively assume that all deep percolation below the repository level bypasses the bulk of the units of the CHn formation, either by lateral movement above the units or through vertical flow through fractures and faults. Technical bases should be developed for any deep percolation considered to flow vertically through the matrix of the nonwelded zone. Such technical bases should consider spatial and temporal variability and the scales at which model parameters have been averaged. Also, the abstracted model has been tested against more detailed models and field observations to assure that it produces reasonably conservative dose estimates.

(5) If used, DOE's expert elicitations should have been conducted and documented using the guidance in the Branch Technical Position on Expert Elicitation (NRC, 1996), or other acceptable approaches.

(6) Staff will determine whether the collection, documentation, and development of data, models, and computer codes have been performed under acceptable QA procedures. If they were not subject to an acceptable QA procedure, they have been appropriately qualified.

4.4.2 Technical Basis for Review Methods and Acceptance Criteria

- **Definitions**

To ensure clarity, the staff have developed definitions for various terms related to deep percolation. The terms infiltration, shallow infiltration, net infiltration, percolation, seepage, and recharge refer to flow across a boundary or datum. The NRC staff associates the term infiltration with near-surface processes and the term percolation with processes deeper in the

unsaturated zone. Emphasis is placed on the types of processes as well as on the vertical delineation in the following definitions:

Shallow Infiltration Flux - The liquid-water flux that has moved beyond the zone of evapotranspiration and remains in the rock is called shallow infiltration. In other words, this is the fraction of precipitation that has penetrated the ground surface and moved just below the zone of evaporation and the zone of plant roots. Relative to the entire UZ column, shallow connotes both a spatial delineation and a distinction of the type of processes affecting flow. Shallow infiltration incorporates the surface and near-surface processes of precipitation, runoff, heat flux, and evapotranspiration. These processes impact groundwater flow in the colluvial and alluvial sediments as well as the top few meters of bedrock. Although there may be evaporation from the fracture system down to the PTn and further, especially as suggested by the high air permeability in the TCw, the amount is not considered significant with respect to the MAI. Net infiltration is used interchangeably with shallow infiltration.

Deep Percolation Flux - The liquid-water flux below the zone of shallow infiltration that moves downward through the UZ is called deep percolation flux. Excluding lateral flow, the upper bound for the magnitude of average vertical deep percolation flux is the average shallow infiltration flux. The zone of deep percolation covers the 500 to 700 meters of the unsaturated domain below the shallow infiltration zone down to the water table. Percolation is governed by flow processes in the fractured bedrock comprising the portion of the UZ below the impact of evapotranspiration, hence the deep portion of the unsaturated column. The study of deep percolation addresses flow processes above, near, and below the repository horizon, including lateral flow, perched water formation, and matrix/fracture interaction.

Seepage Flux - The fraction of the deep percolation at the repository horizon that enters the drifts is the seepage flux. The physics of flow at the interface of the bedrock and the drift, such as capillary diversion of matrix flow around the drift and the spatial relationship between fractures and drift, determine the fraction of percolation flux above the drifts that becomes seepage flux into the drift.

Recharge - The downward liquid-water flux across the boundary delineated by the water table.

Under the assumptions of steady state and downward flow with no lateral component, all of these flux values are equal in magnitude. At YM, the assumptions are not likely valid at the drift boundary and below the repository.

Evaluation of the following topics provided key support for review methods and acceptance criteria for deep percolation.

General discussion about deep percolation
Measurements and modeling related to deep percolation at YM (Bodvarsson, et al., 1997a)
Conceptualization of site-scale flow from the near surface to the water table (Geomatrix, 1997)
Conceptualization of small-scale flow in fractures and fracture/matrix interactions
Estimates of deep percolation from geochemical, thermal, and water distribution data (Bodvarsson, et al., 1997a)

Estimates of deep percolation based on numerical simulations (Bodvarsson, et al., 1997a)
Past evidence and impact of future climate changes on deep percolation (NRC, 1997b)
Pneumatic responses at YM (Ahlers, et al., 1996; 1997)
Evidence for fast pathways (Fabryka-Martin, et al., 1997)
Calculated distribution of percolation at the repository horizon (Flint, et al., 1996a; NRC, 1997b)
Summary of deep percolation topics that warrant further analysis

4.4.2.1 General Discussion About Deep Percolation

It can be simply (and conservatively) assumed, for the purposes of PA, that all net shallow infiltration (i.e., water entering the subsurface below the root zone) within and updip of the repository footprint enters the waste packages (WP) and contacts waste. However, this assumption is not realistic. Geometric arguments alone suggest that only a small fraction of this total flux should be intercepted by the emplacement drifts because the area occupied by drifts is a small fraction of the area of the repository footprint. There are several additional ways that the fraction of shallow infiltration contacting waste may be reduced or that some portion may bypass the WPs, including

- Evaporation from below the root zone
- Lateral diversion due to capillary or permeability contrast, such as might occur at the Paintbrush Tuff nonwelded (PTn) unit
- Local lateral diversion due to capillary or permeability contrast, such as might occur at the rock/drift interface
- Lateral diversion within the drift (e g., by drip shields or other engineered systems)

On the other hand, some heterogeneities such as fracture and fault zone may focus the infiltration into flow paths that may carry a larger fraction of flux than would normally be expected from geometric arguments alone.

If flow is predominately within the matrix, the drifts would tend to be protected through capillary-barrier effects, and migration through the UZ would tend to be quite slow (e.g., assuming 1 mm/yr fluxes and 10 percent average moisture content, water travel times for 100 m would be 10^4 yr and sorption processes might retard many radionuclides further). The relatively low permeabilities of the matrix at the repository horizon would tend to require large saturations everywhere in space and many drifts might be affected by matrix fluxes. On the other hand, if flow is predominantly through the fractures, the drifts would be less well-protected through capillary-barrier effects and travel times to the water table would be drastically reduced. Also, as permeabilities of the fractures are rather large relative to the current estimates of percolation flux, it is possible that relatively few fractures might carry the bulk of the water and only a few drifts would be contacted by a flowing fracture. Accordingly, it is important to characterize percolation flux in terms of the capacity for driving fracture flow at and below the repository horizon.

Net vertical infiltration from the ground surface is the predominant source of moisture for deep percolation, with the water table potentially contributing a small amount of water through capillary rise and vapor redistribution due to the geothermal gradient. Deep percolation patterns can be strongly dependent on the nature of infiltration due to the intermittent pattern of precipitation in arid and semiarid climates. For example, consider a homogeneous fractured welded tuff with a matrix saturated hydraulic conductivity (K_{sat}) of 10 mm/yr and a fracture K_{sat} of 10^4 mm/yr. If a source of water is applied at a steady rate of 5 mm/yr, then the fractures will not be active due to capillary effects. On the other hand, if the same total volume of water is due to an extreme precipitation event and is applied over a short period, for example 1 month out of every 10 yr, the average flow during that month is equivalent to 600 mm/yr and, at best, the matrix can carry 1.7 percent of the total flux, leaving the remainder to the fractures. Higher flux rates may occur, as a significant rainfall might be 1 cm over a period of a day (equivalent to 3,650 mm/yr). Even larger proportions of total flux may be carried in the fractures if the same total inflow is focused into small areas, such as stream channels. If the pulses are not attenuated with depth, one would expect flows at the repository horizon to be episodic and dominated by fracture flow. On the other hand, if the pulses are strongly attenuated with depth, such that average infiltration rates are sufficiently low, flows would tend to be matrix-dominated at the repository horizon. Accordingly, the episodicity of infiltration, the localization of influx, and the ability of the vertical profile to attenuate the wetting pulses are issues that should be appropriately evaluated in order to characterize the behavior of deep percolation. The use of steady-state percolation fluxes may significantly misrepresent the partitioning of deep percolation into matrix and fracture fluxes.

The ability of any method to estimate deep percolation under climatic variation is another issue to be considered. This issue is only briefly discussed in this IRSR. However, the performance of the potential repository should be assessed over periods of time long enough that climatic variation will be a factor. Percolation flux changes in response to climatic variations may be translated from changes to shallow infiltration and may primarily be reflected both in magnitude and distribution of flux. Therefore, methods for estimating deep percolation that are suitable for such long time periods are more useful for PA than methods that can only be applied for current climatic conditions.

4.4.2.2 Measurements and Modeling Related to Deep Percolation at Yucca Mountain

A wide variety of methods are used to model the movement of water in fractured porous media. Good overviews of some of the more common methods to study rock fractures and fluid flow are presented in Evans and Nicholson (1987), Bear, et al. (1993), and National Research Council (1996). Prior to the intensive work at YM, unsaturated flow in fractured porous media received little attention. Saturated fractured porous media received more attention due to topics of water supply, petroleum, and potential nuclear repository sites in other countries (Canada, Sweden, France). The development of methods to study unsaturated flow in fractured rock domains was primarily driven by YM as evidenced by the appropriate sections of Evans and Nicholson (1987), Bear, et al. (1993), and National Research Council (1996) on unsaturated flow. The methods have evolved as new information was gained. As such, the following sections contain descriptions of the current status of methodologies applied to YM, which taken as a whole, present a convergence of estimates for percolation for present day

conditions. However, specific aspects of flow at YM remain unclear thus necessitating a close review of the methods used; appropriate comments are discussed in each section.

The primary source of integrated information for UZ flow at YM is the work on the site-scale model by Lawrence Berkeley National Laboratory (LBNL). The LBNL UZ model of YM (Wittwer, et al., 1995; Bodvarsson and Bandurraga, 1996; Bodvarsson, et al., 1997a) is an ongoing synthesis of data focused on the development of numerical models that capture the important features of flow both at the site scale and at the smaller drift scale. Concurrent studies of site scale processes at Sandia National Laboratories (SNL) (Arnold, et al., 1995; Altman, et al., 1996) and at Los Alamos National Laboratory (LANL) (Robinson, et al., 1997) focus on groundwater velocities and transport of radionuclides through the UZ. Concurrent drift-scale experiments (niche and alcove) and modeling is being done by Lawrence Livermore National Laboratories (Nitao, 1997) and LBNL (Wang, et al., 1998; Birkholzer, et al., 1997a).

- **Unsaturated Zone Hydrostratigraphy**

The LBNL site-scale UZ hydrogeologic model of YM (Bodvarsson, et al., 1997a) has been the primary mechanism of data synthesis for numerical simulations. Recently the Geologic Framework Model (GFM) ISM2.0, created by the Management and Operations (M&O) contractors at YM, became the standardized model.

Following Montazer and Wilson (1984), the primary hydrostratigraphic units consist of alternating zones of moderately to densely welded, highly fractured tuffs and non- to partially-welded, highly porous tuffs. From highest to lowest, these units are:

- The Tiva Canyon Welded (TCw) unit, consisting of the moderately to densely welded portions of the Paintbrush Group.
- The PTn unit, consisting of the partially welded to nonwelded portions of the Tiva Canyon Tuff underlying the TCw, alternating layers of bedded tuffs of the Yucca Mountain Member and Pah Canyon Member and the partially welded to nonwelded portions of the Topopah Springs Tuff.
- The Topopah Springs Welded (TSw) unit, consisting of the moderately to densely welded portions of the Topopah Spring Tuff.
- The CHn unit consisting of the formations underlying the basal vitrophyre of the TSw and including the nonwelded to partially welded portions of the lower part of the Topopah Spring Tuff, the Calico Hills formation, the Prow Pass Tuff of the Crater Flat Group, and the nonwelded to partially welded portion of the Bullfrog Tuff of the Crater Flat Group.
- The Crater Flat Undifferentiated (CFu) units consisting of the lower Bullfrog and Tram Tuffs of the Crater Flat Group (only found in the UZ below Yucca Crest south of the repository).

Table 1, taken from Hinds, et al. (1997), illustrates the relationship between the hydrostratigraphic units and the geologic units as delineated by Buesch, et al. (1996). The geologic units are illustrated in cross-sections (Figure 2) from Hinds, et al. (1997). Detailed geologic descriptions of the PTn subunits are in Moyer et al. (1996) with the description of the fracture characteristics in Sweetkind, et al. (1995, 1997). Descriptions of the CHn and Prow Pass Tuff are found in Moyer and Geslin (1995) and Loeven (1993). Measurements of core samples including porosity, saturation, bulk density, and permeability for the major hydrostratigraphic units are reported in Flint (1997). A synthesis of the stratigraphic and fracture data, as combined with a geologic site-scale model into a hydrostratigraphic model, is described in Bandurraga and Bodvarsson (1997) and Sonnenthal, et al. (1997a).

In general terms, the nonwelded bedded tuffs have high porosities and low fracture frequencies, whereas the welded tuffs typically have low matrix porosities and high fracture frequencies (Hinds, et al., 1997). In terms of fracture data, there is a high density of fractures near vitric (both crystal-rich and crystal-poor) and nonlithophysal units, relatively high fracture density within nonlithophysal as compared to lithophysal units, relatively lower fracture density within the nonwelded PTn, and very low fracture density within the CHn. Features that increase matrix porosity and hydraulic conductivity are a lower degree of welding and the presence of lithophysae in the welded units.

The TCw hydrostratigraphic unit is subdivided into 3 model layers (Table 1) for the LBNL site-scale model. As an indication of the importance of fracture flow in the TCw, the delineations preserve units of generally similar fracture characteristics (Sweetkind, et al., 1997). As the uppermost unit, the TCw varies in thickness based on erosional features. The PTn

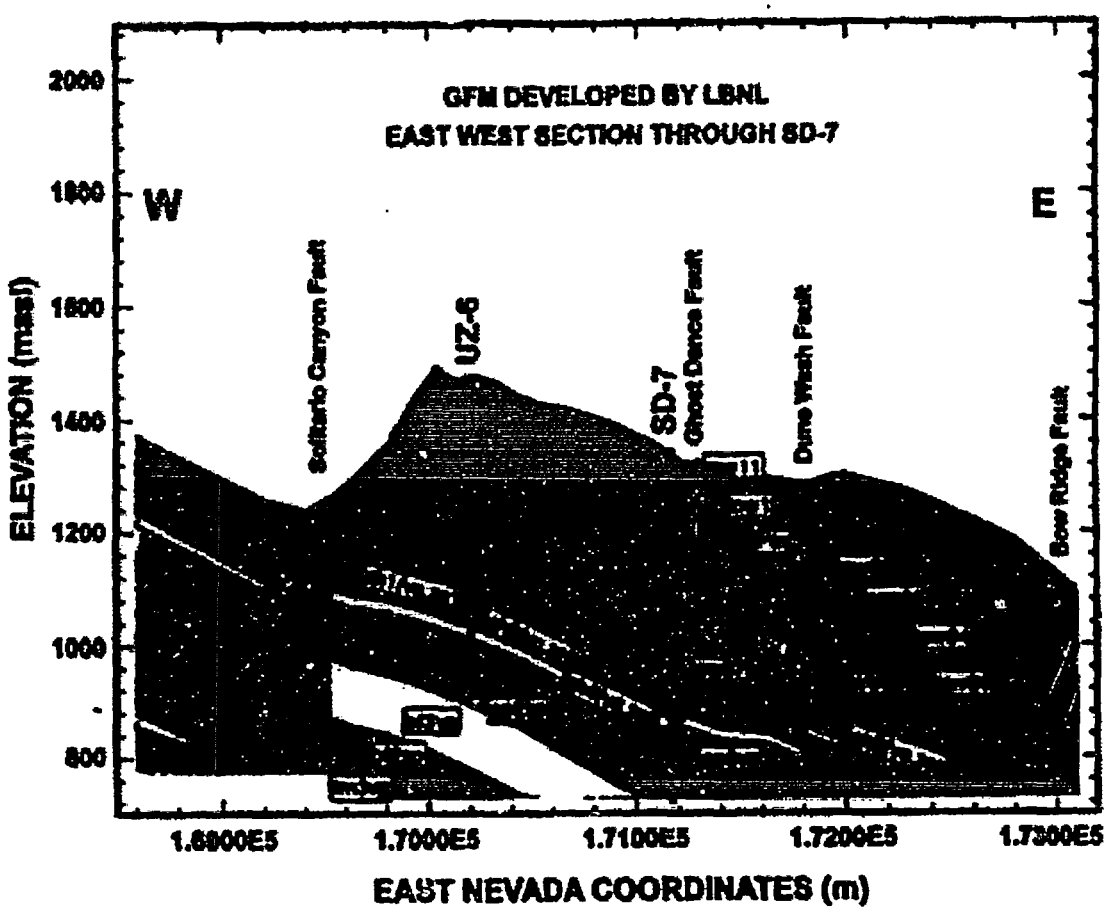

Figure 2. East-west geologic cross-section across the repository from Hinds, et al. (1997).

Table 1. Relationship between model hydrogeological units and geological formation (Lawrence Berkeley National Laboratory geological model from Hinds, et al., 1997)

Geological Unit	Welding Intensity/Formation Name (Buesch, et al., 1996)	Model Layer Name	Hydrogeological Unit
Paintbrush Group			
Tiva Canyon Tuff	M,D[1] (Tpcxxxx)	tcw11 tcw12	Tiva Canyon
	D-Basal vitrophyre (Tpcpv3) M (Tpcpv2)	tcw13	
	N,P (Tpcpv1)	ptn21	Paintbrush
Bedded Tuff	N (Tpbt4)		
Yucca Mountain Tuff	N,P,M (tpy)	ptn22	
Bedded Tuff	N (Tpbt3)	ptn23	
Pah Canyon Tuff	N,P,M (Tpp)	ptn24	
Bedded Tuff	N (Tpbt2)	ptn25	
Topopah Spring Tuff	N,P (Tptrv3)		
	M (Tptrv2) D-Upper vitrophyre (Tptrv1)	tsw31	Topopah Spring
	M,D (Tptrn)	tsw32	
	M,D,L[2] (Tptrl) M,D,L (Tptpul)	tsw33	
	D (Tptpmn)	tsw34	
	M,D,L (Tptpll)	tsw35	
	D (Tptpln)	tsw36	
	D-Basal vitrophyre (Tptpv3)	tsw37	
	N,P,M; may be altered (Tptpv1, Tptpv2)	ch1(vc or zc)	Calico Hills
Bedded Tuff	N; may be altered (Tpbt1)		
Calico Hills Formation	N; unaltered (Tac-vitric)	ch2(vc or zc)	
	N; altered (tac-zeolitic)	ch3(vc or zc)	

Geological Unit	Welding Intensity/Formation Name (Buesch, et al., 1996)	Model Layer Name	Hydrogeological Unit
Bedded Tuff	N; may be altered (Thtbt)	ch4(vc or zc)	
Crater Flat Group			
Prow Pass Tuff	N; may be altered (Tcp) Unit 4[3]		
	P,M Unit 3	pp3vp	
	N,P; generally altered Units 2,1	pp2zp	
Bedded Tuff	N; generally altered (Tcpbt)		
Upper Bullfrog Tuff	N;P; generally altered (Tcb)		
Middle Bullfrog Tuff	P,M	bf3vp	
Lower Bullfrog Tuff	N,P; generally altered		Crater Flat Undifferentiated
Bedded Tuff	N; generally altered (Tcbbt)	bf2zp	
Upper Tram Tuff	N,P; generally altered (Tct)		
Older tuffs and lavas	Generally altered (Tct)	tr3zp	
		tr2zp	

[1]Welding Intensity N=Non P=Partially; M=Moderately; D=Densely
[2]L=Lithophysal Zone
[3]Units per Moyer and Geslin (1995)

hydrostratigraphic unit is subdivided into 5 model layers that generally correspond to both the lithostratigraphic units of Buesch, et al. (1996) and the delineations based on pneumatic testing (Sweetkind, et al., 1997). The overall thickness of the PTn varies from about 20 m in the south to 170 m in the north in the area of the LBNL site-scale model (Wittwer, et al., 1995). The 7 model layers of the TSw hydrostratigraphic unit correspond to lithostratigraphic units of Buesch, et al. (1996). The delineations correspond to variations in porosity, saturation, and capillary pressure measurements. The overall thickness of the TSw is greatest in the center of the LBNL site-scale model area and decreases to the north, varying from 340 m to 50 m thick (Wittwer, et al., 1995). The Calico Hills hydrostratigraphic unit is divided into 7 model layers of which the top 4 model layers may transition from vitric to zeolitic. The Calico Hills hydrostratigraphic unit includes a portion of the basal TSw vitrophyre, the Calico Hills Formation, Prow Pass, and upper portion of the Bullfrog Tuffs. The thickness of the Calico Hills

Formation ranges from about 30 m in the southwest to 300 m in the north, whereas the Prow Pass Tuff varies from about 200 m in the east to 80 m in the west (Moyer and Geslin, 1995).

The LBNL and the ISM2.0 models correlate well except for several instances of grouping of layers in the latter model, and for the delineation of units below the TSw (Hinds, et al., 1997). The Calico Hills hydrostratigraphic unit is a zone of the geologic section that is particularly important to repository performance. The LBNL model uses altered zones as a basis for sublayering and delineates a transition within each sublayer based on a threshold zeolite weight percent. The LBNL model follows the Moyer and Geslin (1995) interpretation that describes a gap in the alteration in the southwest portion of the repository that extends through all sublayers of the CHn. However, Chipera, et al. (1997) state that there is no gap in the alteration. LANL site-scale modeling (Robinson, et al., 1997) uses the ISM2.0 geologic framework model and adds a mineralogic model that modifies CHn sublayer properties in order to incorporate hydrologic properties of zeolites in the CHn unit. In contrast, the LBNL modeling (Hinds, et al., 1997) assigns appropriate hydrologic property values to zeolitic and to vitric model sublayers of the CHn. This topic is discussed in more detail in a later section.

Structural features of importance to flow in the UZ are faults, fractures, joints, and bedding planes. These discontinuities form interconnected networks at varying scales. The central part of YM is a relatively undeformed block of Miocene tuff bounded on the west by the Solitario Canyon Fault (SCF) and by the Bow Ridge fault (BRF) located about 3.5 km to the east (see Figure 2). These block-bounding faults have predominantly dip-slip separations with cumulative displacements between 100 and 1000 m (Day, et al., 1997; Scott, 1990). Both dip moderately to steeply to the west (Day, et al., 1997). Within the YM block are north-south striking normal and northwest-southeast striking dextral strike-slip faults. These secondary faults are often discontinuous or *en echelon* and have displacements between 1 and 50 m. The Ghostdance Fault (GDF) is one of the largest intrablock faults, having up to 25 m of dip-slip offset separation. It is discontinuous at the surface. The Sundance (SDF) and Drill Hole Wash (DHW) faults are two of the better known strike-slip faults. Because of localized fracturing and the possible connectivity through numerous thermal mechanical units associated with the structures, these faults can be important to groundwater flow in the UZ. On a smaller scale, the fracture and joint systems and bedding planes are also important to groundwater flow in the UZ. Fracture systems may cross or interfinger across lithologic and thermal-mechanical boundaries. Cooling joint systems are generally confined within thermal-mechanical units (e.g., Sweetkind, et al., 1997). Each thermal-mechanical unit has a characteristic set of fracture and joint attributes, including orientation, distribution, intensity, and length (e.g., Sweetkind and William-Stroud, 1996). Lateral flow along sub-horizontal cooling joints, fractures, and bedding planes can be locally important to flow in the UZ. Layering in the fault blocks dip 5 to 15 degrees to the east (Day, et al., 1997). Details of the important structural features and lithologic and thermal mechanical layering of YM are summarized in the Structural Deformation and Seismicity (SDS) IRSR (NRC, 1998a).

4.4.2.3 Conceptualization of Site Scale Flow from the Near Surface to the Water Table

The NRC conceptual model of flow from the near surface to the water table is broadly similar to the conceptual model proposed by Montazer and Wilson (1984). The Montazer and Wilson (1984) conceptual model has been generally supported by subsequent field studies and

modeling. The work presented by Bodvarsson and Bandurraga (1996) and Bodvarsson, et al. (1997a), using available field observations to calibrate 1D, 2D, and 3D models, provides updated support for the Montazer and Wilson (1984) conceptual model. The conceptual models and measurements were reviewed by an expert-elicitation panel (Geomatrix,1997), reinforcing the general agreement on conceptual models and elucidating disagreements. The following discussion presents the NRC conceptual model.

Water that flows through the zone of potential evapotranspiration, thus becoming net shallow infiltration, is believed to proceed via rapid flow through the highly fractured and relatively impermeable TCw matrix to the less fractured but highly porous and permeable PTn unit. The notion that fast flow occurs through the TCw is supported by the extensive presence of bomb-pulse ^{36}Cl throughout the TCw and into the top of the PTn. Pneumatic pulses are minimally attenuated within the TCw, suggesting that fast pathways are available for moisture flow as well. Rapid changes in gas pressure and temperature in boreholes, attributed to a pulse of water from a previous season (Bodvarsson and Bandurraga, 1997), are additional evidence suggesting that water moves quickly through the TCw. Velocities in the TCw may be as high as tens of meters per year based on the ^{36}Cl, temperature and gas pressure data. Once water moves below the rooting zone, some removal of vapor is believed to occur due to air flow within the TCw bedrock. Estimates for vapor removal, in terms of water flux, range from 0.1 mm/yr for a local value (Rousseau, et al., 1996) to 0.02 mm/yr (E. Weeks, presentation at the Unsaturated Zone Expert Elicitation Workshop, February 4, 1997).

As the water enters the PTn unit, the rate (and perhaps direction) of flow changes. Capillarity and the large storage capacity of the PTn may strongly dampen infiltration pulses, as is shown by numerous modeling studies. Depending on the fluxes from infiltration and the hydraulic properties of the PTn, water may pass through the PTn to the TSw unit through several pathways:

- Predominantly vertical movement through the matrix of the PTn, thereby strongly damping out infiltration pulses.

- Predominantly vertical movement through the PTn, with some local lateral flow focusing water into slump faults, thereby damping out infiltration pulses to a lesser extent.

- Predominantly vertical movement through local fast pathways formed by small-scale heterogeneities in the PTn matrix, thereby bypassing the bulk of the matrix and not strongly damping out infiltration pulses. In modeling exercises, this component of movement is termed fracture flow, but field observations do not support significant fracture flow *per se*.

- Lateral movement downdip at a permeability barrier at the base of the PTn, thereby damping pulses but perhaps significantly redistributing water to the east. The redistributed water may be focused into larger faults or may move into the fracture system to the west of the Ghost Dance Fault. Infiltration pulses are expected to be strongly dampened.

- Lateral movement downdip at the capillary barrier at the base of the TCw, again with a potential for focusing flows into larger faults or the fracture system. TCw matrix waters are likely to move downdip at a steady state, but only a small component of flux is likely to be involved. TCw fracture waters are likely to move downdip in (possibly large) transient pulses if the stratabound TCw fractures are not well connected to the PTn matrix.

There is substantial evidence suggesting that fast flow paths exist through the PTn (e.g., geochemical and bomb-pulse data below the PTn). These fast flow paths may carry a substantial portion of the entire infiltration flux. The actual pathways by which flow bypasses the PTn have not been determined. Most current DOE modeling efforts predict that bypass flows are predominantly vertical, as does expert elicitation (Geomatrix, 1997).

As with the TCw unit, flow in the TSw is believed to be predominantly in the fracture and fault systems. Strong damping of wetting pulses in the PTn would cause all flows below the PTn to be approximately steady state. The TSw matrix is likely to be approximately at a steady state regardless of the PTn, due to its low matrix permeability. If bypass fluxes are minimally damped, TSw fracture flows may be transient. The TSw matrix water contents are near saturation values, with little capacity for capillary action, and thus minimal fracture/matrix interaction is expected. The disparity between geochemical signatures of pore waters and perched waters further suggests that the matrix has little connection with fast paths. The fine pores of the TSw matrix are likely to provide a strong capillary barrier to entry into mined cavities, even if backfill were to be emplaced, so that water in the matrix is likely to be diverted around the cavities. On the other hand, TSw fracture flows have less of a capillary barrier to overcome in order to enter mined cavities, particularly if backfill were emplaced, so that the dominant mode of water entering drifts is likely to be through TSw fracture flow.

Portions of the vitric non-welded tuff in the Calico Hills formation have been altered into zeolitic horizons. These zeolitic horizons may represent the single most effective barrier for radionuclides between the repository horizon and the water table. Combined with the hydraulic barrier represented by low fracture densities and low matrix permeability, the large adsorptive capacity of these zeolitic horizons provides a significant geochemical barrier to radionuclide transport (RT), realized only if flows do not bypass the bulk of the zeolitic horizons through vitric horizons or fast pathways. Perched-water bodies are present in portions of the repository footprint where significant zeolitization is present, suggesting that vertical percolation is slow in these areas. The absence of perched water bodies where the vitric units have not been zeolitized suggests that any percolation fluxes entering these zones can be accommodated through vertical percolation. Further, lateral flow from the perched water bodies may divert substantial quantities of water away from the zeolitic units into vertical flow through the vitric units. There may also be substantial lateral flow into faults such as the GDF, or downdip to the east of the GDF. If lateral flow is significant along the top of zeolitic units, the volume of the perched water bodies may be controlled by geometric factors (e.g., particular perching height may be required to encounter a lateral fast pathway) rather than by the hydrostatic pressures required to force waters through low-permeability zeolitic zones. If any of these potential lateral-flow pathways carry significant quantities of water, rapid transport to the water table may be considerably facilitated.

The factors affecting deep percolation most, from the standpoint of repository performance, are related to initiation and sustenance of fast-pathway flow. Transport of radionuclides from non-backfilled drifts is likely to be minimal if there is not significant fracture flow in the TSw. Transport from the repository to the water table is likely to be very slow for pathways significantly occurring within the matrix. Accordingly, later sections address issues regarding fast pathways and fracture/matrix interactions in some detail.

4.4.2.4 Conceptualization of Small-Scale Flow in Fractures and Fracture/Matrix Interactions

Flow through an unsaturated, fractured rock involves two systems - matrix and fracture - that exhibit greatly different hydraulic behavior. Assuming isothermal conditions, liquid flow is governed by capillary, gravity, and viscous forces. As these effects are relatively well understood in the porous media representation of the matrix, most of the uncertainty in combined systems is associated with describing flow in the fractures. In contrast to porous media flow and transport theories, there are no widely acceptable theories for the study of fracture flow under unsaturated conditions (Bagtzoglou, et al., 1994). The flow process that dominates repository performance, flow in the fracture system, is also the process with the most uncertainty. Four issues pertinent to fracture flow in the UZ will be discussed in this section: flow in small-aperture fractures, flow in large-aperture fractures, matrix/fracture interaction, and the distinction between discrete fracture and dispersed fracture flow.

The classical view of flow in unsaturated, fractured rocks is that flow will not occur in fractures unless the matrix is saturated. Unsaturated fractures were viewed as barriers to flow because of capillary forces that preferentially draw water into finer matrix pores. Given low estimates of average annual infiltration rates for YM, minimal flow in fractures would be expected due to the capillary forces. Another model of flow in fractured rocks is based on transient wetting pulses in the fractures, occurring due to precipitation events that promote fracture saturation at the ground surface. The wetting front in the fractures is not likely to coincide with the front in the matrix unless the matrix and fractures are strongly coupled. A pulse initiated near the ground surface penetrates to depth based on the connectivity of the fracture system and the properties and conditions of the pathway. These two views of flow in fractured rocks can be considered as modes corresponding to different stresses at the ground surface (National Research Council, 1996).

Fractures are void spaces. An understanding of the control that void space geometry plays on hydraulic flow properties is important in ascertaining the appropriateness of models developed to match conditions or predict future behavior. Fractures are often visualized as parallel plates separated by a gap, the fracture aperture. A more accurate and meaningful conceptualization accounts for areas where surfaces are in contact and areas with no contact, which can also be viewed as large-scale differences in roughness between the two sides of the fracture (National Research Council, 1996). The points of roughness between the two sides of the fracture will lead to partial saturation of the fracture as the matrix saturation is increased. Following the model of Peters and Klavetter (1988), flux in the fracture begins to exceed the flux in the matrix as the matrix becomes saturated. Any amount of percolation above the transmission capacity of the matrix will be in fractures. Often used for quick estimates, transmission capacity of the matrix is generally taken as a direct function of the effective conductivity at the steady state

matrix saturation; the limiting case, assuming no ponding above the matrix, is a unit gradient under saturated conditions.

The voids of a fracture form a planar interconnected network, thus the analogy with porous media. However, the fracture voids are limited to a 2D (albeit not necessarily smooth) plane, thus increasing the possibility of phase interference over that of 3D porous media. Phase interference, or capillary exclusion, occurs when one phase in the plane of the fracture creates barriers to flow of the other phase. Fine fractures imbibe water, which then has the potential to block further water movement because of capillary effects in small apertures. In large-aperture fractures, film flow may occur that is impacted not by capillary forces across the width of the fracture but rather by the roughness of the fracture wall on which flow is occurring (Brown, 1987). For unsaturated flow in fractures, therefore, the geometry of the flowing pulse may differ from the aperture geometry (Glass, et al., 1996).

Transient, nonequilibrium flow in response to surface infiltration processes is another mechanism that initiates and sustains fracture flow. Flint, et al. (1996a) suggested that significant infiltration events occur at YM, on the average, once every 5 yr, noting that there were major runoff events in 1969, 1983-84, 1991, and 1995. Based on watershed modeling in Solitario Canyon using historical precipitation data, Woolhiser, et al. (1997) suggest that large runoff events, and hence large possible infiltration events, occur once or twice every 10 yr. A large pulse of water entering the fracture system near the ground surface may percolate at a high rate in large open fractures as sheet or rivulet flow. Fracture flow in this situation will be driven by a combination of viscous and gravity forces, and the 2D pore structure of the fracture.

Factors which affect the depth to which transient pulses of water may travel are the matrix saturation adjacent to the fracture, the water sorptivity of the matrix, the presence of fracture coatings, and the fracture aperture. Near-saturation matrix water contents, low matrix sorptivity, and low-permeability fracture coatings will all promote penetration of transient pulses to greater depths. Measurements by Thoma, et al. (1992) and simulations by Soll and Birdsell (1998) illustrate the strong impact that fracture coatings have on imbibition into the matrix. Small-aperture fractures would have the tendency to produce more tortuous paths and a higher possibility of phase interference due to capillary forces; if positive pressure heads drive the pulse, however, the impact of capillarity is lessened. If the flow of water is along rivulets in the rough-surfaced fractures rather than as sheet flow along smooth fractures (Kapoor, 1994), pulse penetration to greater depths is supported by reduction of the surface area available for imbibition. Measurements and observations by Tokunaga and Wan (1997) demonstrate that water preferentially flows in fractures with rougher walls. Flow in rough-walled fractures has been numerically simulated by Preuss and Tsang (1990), Tsang (1984), Tsang, et al. (1988), Brown (1987), and Silliman (1989). Coatings on the footwall and not the hanging wall of some fractures or faults at YM indicate that sheet or rivulet flow occurs in at least some fractures or faults at YM.

Paces, et al. (1998a) describe the distribution and isotopic composition of hydrogenic minerals in fractures and cavities in the ESF. The presence or absence of coatings in fractures may not be a good indicator of which fractures would likely carry flow. The chemistry of the fluids migrating down the fracture system would be expected to control whether precipitation or flushing (dissolution) is occurring. The fluids could either be undersaturated or oversaturated with respect to the minerals in the coatings. For example, percolating water that is

undersaturated with respect to calcite would not lead to precipitation of calcite along the water pathways, and hence, the fractures with no coatings would be expected to carry the percolating water. If the percolating water is oversaturated with respect to calcite, then calcite would be precipitated along the flow path, and hence, the fractures with coatings would be expected to carry the percolating water. Another possibility is that the percolating water is initi undersaturated with respect to calcite, but evaporation along the pathway causes the water to become oversaturated. Coatings on open fractures in the ESF imply that the percolating sheet flow was either oversaturated initially or became oversaturated due to evaporation. For the latter case, the strong air connectivity of some large fault features to the atmosphere at the surface may allow for evaporation to be significant even at large depths. If a significant amount of the percolation occurs in large aperture fractures, where coatings occur on the footwall, the implication for fracture/matrix interaction is that the portion of the fracture surface across which flow to the matrix may occur could be reduced. Dependent on the hydraulic properties of the coatings, they may restrict or enhance fracture/matrix interaction. Since the water chemistry of percolating water is poorly constrained at YM, it is prudent to consider that all possibilities of water chemistry occur, and therefore, all fracture pathways should be considered.

Approaches used to model fracture flow and matrix/fracture interaction draw on classic porous flow concepts. Parameters used for the modeling are briefly described below along with brief mention of some of the limitations due to molding classic porous media concepts to fracture flow. Under the assumption that the fractures can be modeled as a classic porous media continuum, hydraulic properties valid for a representative elementary volume of fractures are needed. Air-permeability tests are used to infer indirect information on, and constrain the range of values for, the unsaturated constitutive relationships for water retention and relative permeability. However, inverse modeling is relied upon for their determination for each sublayer in the LBNL model (Bandurraga and Bodvarsson, 1997). Conceptually, the step from air permeability to constitutive relations is through variability of fracture spacing and fracture apertures. The constitutive relationships used for porous media are applied to estimate the fracture-continuum properties. No measurements of unsaturated-fracture constitutive relationships have been made at YM, although they may be highly variable given the range of fracture geometries and the nature of unsaturated flow in rough-walled fractures. Glass, et al. (1996) demonstrated that air entrapment in fractures can lead to prominent hysteresis in the constitutive relations. Reitsma and Kueper (1994) illustrate a technique to measure water retention curves on a single fracture; however, they noted that the Brooks-Corey relation was more applicable than the van Genuchten relation (which is usually used at YM) due to the physics of water entry into fractures. Given the small amount of hydrologic data on fractures at YM, the unsaturated parameters are primarily determined by inverse modeling (Bandurraga and Bodvarsson, 1997).

Two parameters have been introduced into unsaturated zone modeling at YM to link flow in the tuff matrix to flow in the fracture system. The first factor, matrix/fracture conductance, is essentially the fracture surface area multiplied by an imbibition rate into the matrix. Model calibrations suggested that the potential conductance was too large to match the data (Bandurraga and Bodvarsson, 1997). Accordingly, the fracture surface area fraction became a calibration parameter, justified by qualified observations of channeling or rivulet flow in fractures. A second factor, satiation, was included in models using similar arguments of difficulty in matching model results to field observations. Capillary theory dictates that flow from the matrix into a fracture will not occur until the matrix is fully saturated (Bear, et al., 1993). The

term satiation was introduced to account for flow initiating in the fractures at pressure heads slightly less than atmospheric. In measurements of flow along fractures in the nonwelded Bishop tuff, Tokunaga and Wan (1997) found that film flow in the fracture had velocities of 2 to 40 m/d at -250 Pa, although the volumetric rate may not be significant. Tokunaga and Wan (1997) note that similar behavior may occur at much greater suctions in welded tuffs. Three reasons can be used to justify using a satiation value less than full saturation. The first argument is based on small-scale heterogeneities leading to local areas of saturated matrix adjacent to fractures even though the larger-scale average of matrix saturation is less than one. A second argument is nonequilibrium of the matrix in the vicinity of the fracture. Matrix saturations may reach full saturation adjacent to the fracture, but the rest of the matrix, some distance from the fracture, remains relatively drier. The third argument addresses the conceptualization of fractures as smooth parallel plates. Small-scale surface roughness on the fractures, or heterogeneities of the fracture surface leading to "point connections" (Glass, et al., 1996), may lead to wetted regions and contact points where water may enter the fracture.

The NRC staff considers that spatial and temporal variations in flux through the YM unsaturated flow system are dominated by the fracture flow system, particularly in welded and altered layers. Defining the flow system requires either detailed data on the fractures, especially those that dominate the flow system, or detailed information on the hydrologic response. At YM most of the available fracture data for the UZ has been obtained from the ESF. The east-west drift (enhanced characterization of the repository block, or ECRB) will likewise add to the fracture data base. However, it is difficult to directly evaluate modes and rates of water flow through fractures and faults in unsaturated rocks. In addition, little is known about the mechanisms and parameters that control flow: (i) between matrix and fracture; (ii) in open and coated fractures; (iii) in capillary films, sheets, or rivulets in open fractures; and (iv) along fracture planes and intersections. When insufficient data are present, the necessary fracture flow parameters can be estimated by inverse modeling given the constraints of other information at YM such as thermal and geochemical data and the presence and extent of perched water bodies. Groundwater tracers such as ^{36}Cl and ^{3}H are especially useful for detecting zones of enhanced downward flow in the UZ. Given the uncertainty, field observations and measurements should be a critical part of validating both site-scale and drift-scale models.

4.4.2.5 Estimates of Deep Percolation Based on Geochemical, Thermal, and Water Distribution Data

There is a wide variety of information and approaches for estimating deep percolation at YM. Geochemical, thermal, and water saturation conditions can potentially be used to indirectly estimate residence times, percolation rates, or volumetric flux rates. Table 2 contains a partial list of shallow infiltration and percolation flux estimated using different methods. Here, percolation flux is taken to be equal to the shallow infiltration rate under the assumptions of steady state, vertical flow. Most estimates prior to 1990 were less than 5 mm. Over time the estimates have increased, with an apparent convergence on the range 1 to 10 mm/yr for an areally averaged mean annual rate of percolation. Locally, infiltration and deep percolation can exceed this average range or can approach zero.

Table 2. Estimates of shallow infiltration and deep percolation rates under current climatic conditions using different methods (in approximate chronologic order).

Estimate (mm/yr)	Location	Methodology	Source
1.5	YM	elevation & precipitation	Rush (1970)
2	Yucca Flat	parameter values	Winograd (1981)
1 to 10	YM	drill hole geothermal	Sass and Lachenbrush (1982)
4	YM	elevation & precipitation	Rice (1984)
0.5	YM	matrix Ksat data	Sinnock, et al. (1984)
0.5 to 2	YM	elevation & precipitation	Czarnecki (1985)
0.1 to 0.5	UZ-1	core & *in situ* data	Montazer, et al. (1988)
2 to 5	YM	drill hole geothermal	Sass, et al. (1988)
0 to .001	H-1	core data	Gauthier (1993)
4 to 35.1	UZ-4,5,7	Tritium and ^{14}C	Kwicklis, et al. (1993)
0.6 to 1.9	YM	1D modeling	Long and Childs (1993)
0 to 5.4	YM	Cl mass balance	Fabryka-Martin, et al. (1994)
6 to 16	YM channel	bomb-pulse ^{36}Cl	Fabryka-Martin, et al. (1994)
0 to 13.2	YM	outcrop Ksat data	Flint and Flint (1994)
0.001 to 0.5	YM	3D UZ site-scale	Wittwer, et al. (1995)
0.1 to 10	YM	inverse modeling	Bodvarsson and Bandurraga (1996)
1.7	YM	1D modeling	EPRI (1996)
6.5	YM	100-yr 1D modeling	Flint, et al. (1996)
0.1 to 18	north YM	heat flux	Rousseau, et al. (1996)
0.001 to 0.29	north YM	perched water balance	Rousseau, et al. (1996)
1.8 & 3.4	ESF	fracture coatings	Marshall, et al. (1998)
1 to 15	YM	3D UZ site-scale	Wu, et al. (1998)
3.9 to 21.1	YM	expert elicitation	Geomatrix (1997)

Some of the methods provide only indications of pathways whereas other methods provide flux estimates that may be reflective of bulk response of the system. Percolation rate is taken to be a Darcy flux, the average flow perpendicular to a cross-sectional area. Pore-water velocity, particle velocity, and seepage velocity all refer to the velocity of a solute or water particle from one point to another point. The Darcy flux is related to the particle velocity by an effective porosity, or water content if unsaturated, through which the flow occurs. The effective porosity, or water content, may be difficult to determine, especially for the individual portions of dispersec fracture and fast-pathway fracture flow. The presence of environmental tracers at different depths at YM provides indications of pore-water velocity along a pathway with no indication of the amount of flow between two locations unless a mass balance can be developed, or it can be shown that the environmental tracer moved in all the fractures pathways, not just a portion.

The following subsections focus on various approaches for estimating rates of deep percolation Key citations are noted.

In Situ Observations and Measurements (Wang, et al., 1997)

Net Shallow Infiltration Related to Deep Percolation (Flint and Flint, 1994; Flint, et al., 1996a).

Temperature Gradients and Heat Fluxes (Sass, et al., 1988; Wittwer, et al., 1995)

Isotopes (Fabryka-Martin, et al., 1997; Yang, et al., 1996b)

Chloride Mass Balance (Fabryka-Martin, et al., 1997)

Saturation and Water Potential (Flint, 1997)

Fracture Coatings (Paces, et al., 1996b; Marshall, et al., 1998)

Perched Water (Wu, et al., 1996)

- ***In Situ* Observations and Measurements**

Damp fractures or joints that quickly evaporate due to the required ventilation have been observed at the ESF. Seeps in niches and alcoves of the ESF also evaporated rapidly when exposed to the ventilation. Closing off niche 3566 (near the SDF) after finding a seep allowed re-equilibration of the relative humidity in the niche but no visual rewetting of the seep, reported Wang, et al. (1997). Damp features have also been noted in niche 3650 and the ESF directly. At the Expert Elicitation for Unsaturated Flow (Geomatrix, 1997), reference was made to an estimate of deep percolation based on vapor flow and the shutdown of the ventilation system o weekends. It was established that the average moisture flux from the rocks into the ESF was 50 mm/yr (Geomatrix, 1997). The ambient percolation flux within the rock does not exceed the transfer rate with the ESF in place, hence the 50 mm/yr would be an upper limit.

Given its close proximity and similar lithology, Rainier Mesa is considered a possible analog sit for YM. Percolation estimates from seepage into the tunnels at Rainier Mesa are approximatel 24 mm/yr under current mean annual precipitation of 320 mm (Russell, et al., 1987; Wang, et al., 1993), or about 8 percent of the precipitation.

- **Net Shallow Infiltration Related to Deep Percolation**

Infiltration is the source of virtually all deep groundwater flux in the UZ. This section summarizes, for completeness, the detailed discussion of infiltration modeling approaches of both NRC and DOE at YM that was provided by NRC (1997b). Models of infiltration processes provide information on the spatial and temporal variation of net infiltration, which can then be used as boundary conditions in models of deep subsurface processes. Infiltration models and deep subsurface models consider time scales so disparate that it would be computationally infeasible to consider infiltration processes and deep subsurface processes simultaneously. There are sufficient uncertainties arising from the use of infiltration models, including lack of understanding of flow processes, lack of knowledge of parameters, and lack of resolution, that infiltration models cannot be relied on to provide accurate estimates of infiltration magnitudes without significant corroborating evidence. Infiltration models can provide estimates of the spatial distribution of relative magnitudes and frequencies of wetting pulses. Most importantly, infiltration models may provide the primary source of information regarding infiltration and deep percolation under future climates.

The infiltration maps provided by Flint, et al. (1996a) (based on detailed 1D numerical modeling) have superseded the maps by Flint and Flint (1994) (based on matrix properties of bedrock outcrops) for use in boundary conditions in DOE site-scale and cross-sectional studies (Bodvarsson and Bandurraga, 1996; Bodvarsson, et al., 1997a; Robinson, et al., 1997). The Flint, et al. (1996a) map is derived from sequences of 50 to 100 yr of weather, applied with a daily time step, using a 30-m by 30-m grid of independent 1D infiltration simulations. The 1D bucket model for each grid element considers evapotranspiration but not lateral redistribution.

The Flint, et al. (1996a) map is generally supported by neutron-probe observations during the period of October 1984, through April 1995, which Hudson and Flint (1996) used to create an infiltration map based on regressions taking into account precipitation, elevation, geomorphic class, and soil thickness. These maps suggest that infiltration occurs primarily on ridgetops and sideslopes, where surficial materials are shallow, and little infiltration occurs where alluvium is deeper than 1 to 2 m. The base infiltration map used by Bodvarsson, et al. (1997b) provides 6.7 mm/yr infiltration over the repository footprint and 4.9 mm/yr over the site-scale model.

The NRC model (Bagtzoglou, et al., 1997; NRC, 1997b), based on abstractions of detailed nonisothermal 1D simulations, predicts roughly three times as much infiltration as does the Flint, et al. (1996a) model, but is broadly in agreement with USGS predictions of the spatial distribution of mean annual infiltration (MAI). The NRC model neglects transpiration but has much finer spatial and temporal resolution than the USGS model. The agreement between the USGS and NRC models is not unexpected, as both are based on 1D approaches and both neglect lateral redistribution.

- **Temperature Gradients and Heat Fluxes**

This section outlines the use of borehole temperature measurements at YM to estimate percolation. Solution of the conduction equation using borehole temperature measurements to infer temperature gradients, heat conductivity of each unit, estimates of heat flux, and the assumption that the heat flow in YM is controlled by conduction, leads to a temperature profile

which differs from the actual profile. The difference is interpreted to be due to either downward flux of cool water or upward flux of vapor.

Temperature data from boreholes, reported by Sass, et al. (1988) for a regional study, and by Rousseau, et al. (1996) in an area near the North Ramp of the ESF, were compared by those authors to predictions from models using the conductive heat equation. Although most of the heat flux could be explained by the conductive model, vertical heat-flux deficits were present that could be explained either by percolating water or by evaporation of water. Sass, et al. (1988) estimated that either 2 to 5 mm/yr percolation through the PTn and into the TSw or 0.1 mm/yr vaporization with 15 m/yr upward air discharge would account for the apparent deficits. The spatial distribution of infiltration rates estimated by Sass, et al. (1988), using the approach outlined above, is generally consistent with infiltration maps produced by Flint, et al. (1996a). Although vaporization and advective transport of vapor may be locally important in the highly fractured, densely welded tuffs such as the TCw, site-scale numerical modeling suggests that these effects are secondary to the effects of percolation (Rousseau, et al., 1996), particularly below the pneumatic barrier represented by the PTn. Temperature data from boreholes UZ#4 and UZ#5, in Pagany Wash, suggest that percolation may be on the order of 10 to 20 mm/yr (Rousseau, et al., 1996). In both studies, an average heat flux for the area was assumed in order to estimate percolation. Sass, et al. (1988) noted that the actual heat fluxes used in the analysis.are difficult to measure.

Bodvarsson, et al. (1997c) re-analyzed the borehole data without assuming an average heat flow for the area. Percolation fluxes were estimated by matching the borehole temperature data with predictions from analytical solutions for the layered system, using both constant heat flux and constant temperature lower boundary conditions. Estimates ranged from 0 to 63 mm/yr. Low heat-flux boreholes appeared to be affected by vapor transport in the TCw, and high heat-flux boreholes appeared to be affected by proximity to fault zones. In both cases, the assumptions for the analytical solution are violated. For the remaining 18 boreholes, percolation estimates ranged from 0 to 15 mm/yr.

The thermal properties of the welded and nonwelded tuffs used in the studies are summarized by Wittwer, et al. (1995), Rautman, et al. (1995), and Rautman and McKenna (1997). Heat flux modeling by Rousseau et al. (1996) and by Bodvarsson, et al. (1997c) found that the regression equation of Rautman, et al. (1995) for thermal conductivity of the welded and nonwelded lithologies as a function of porosity, temperature, and saturation worked well in their modeling of the temperature profiles.

The different thermal properties and heat flow in the TCw, TSw, and CHn are reflected in the temperature profiles and subsequent percolation estimates. Estimates of percolation flux through the CHn are less than those estimated for the TSw (Bodvarsson, et al., 1997c). The temperature gradient through the CHn is much larger than that of the TSw, which, in part, may be explained by the lower effective thermal conductivity of the CHn. Another possible explanation is lateral flow above the zeolitic horizons of the CHn. The thermal conductivity of the CHn varies depending on the vitric or zeolitic content of the layer as well as the degree of welding and the water content Temperature gradients and heat flux estimates in the TCw may be problematic due to the effects of vapor flow on the temperatures.

An indication of the temporal aspect of a percolating pulse was noted by Sass, et al. (1988). In 1983, about 15 months after the previous reading, temperature perturbations were observed in UE-25a#7 following a major storm. Borehole UE-25a#7 lies on or near the Drillhole Wash fault zone. The temperature response was recorded to a depth of 150 m, which Sass, et al. (1988) assessed as possibly attributable to perturbation along the borehole-annulus. If temperature fluxes along the annulus of UE-25a#7 were significant, the temperature anomalies are meaningless. Since the temperature anomaly persisted for at least 1 yr and was different from previous conditions, the anomaly may represent an infiltration event moving through the fault. If so, the moisture penetrated 47 m of alluvium, 4 m of TCw, 42 m of PTn, and 58 m of TSw in about 15 months.

- **Isotopes**

Environmental isotopes ^{36}Cl, ^{14}C, and $^{87}Sr/^{86}Sr$ have been used to estimate percolation rates and residence times as well as to confirm the presence of fast pathways at YM. As discussed by Tyler and Walker (1994), the use of bomb-pulse tracers, however, can overestimate recharge by an order of magnitude or greater when the impact of transpiration on the flow velocities is neglected.

Elevated levels of ^{36}Cl in the ESF and in boreholes at YM are traceable to global fallout in the nuclear tests from 1952 to 1958 (Levy, et al., 1997). A report by Fabryka-Martin, et al. (1997) contains the currently available set of ^{36}Cl measurements from boreholes and the ESF. Of 247 samples from the ESF, 13 percent had an unambiguous bomb pulse signal. In a straightforward approach, the presence of unambiguous bomb pulse ^{36}Cl in the ESF suggests pore-water velocities on the order of 7.5 m/yr assuming a depth of 300 m and onset of testing as 40 yr ago. However, these pore-water velocities may only represent a fraction of pathways, those that are faster preferential pathways, and may not be directly used to estimate percolation rates even for the fast pathways, since the effective porosity (or water content) for fast pathways is also unknown.

Another environmental tracer, ^{14}C, has been used not only for calculation of residence times of water but has also been used to infer velocities. Interpretation of the ^{14}C data is complex because of its transport mechanism, movement both in the aqueous and vapor phases, and carbon exchange with older calcite or younger gas. Yang, et al. (1996b) report a wide range of isotopic dates from ^{14}C data in the CHn that may support multiple origins for the perched water. The ambiguity of ^{14}C dating carries over to estimates of percolation rates. From data at a depth of 100 m in borehole UZ-25, Murphy (1995) estimated pore-water velocities of 20 to 100 mm/yr. Flow and transport models with varying degrees of geochemical complexity incorporated have been used to model borehole ^{14}C data. Using tritium and ^{14}C data, estimates are 35.1 and 20 mm/yr for UZ-4 and 4 mm/yr for UZ-5 (Kwicklis, et al., 1993). Moridis, et al. (1997) used optimization of two 1D models for wells UZ-1 and UZ-14 to determine a percolation rate of 4.2 mm/yr.

Strontium isotope ratios in pore waters are a function of dissolution and exchange with the rock as well as total strontium concentration and water percolation rates. Strontium geochemistry and isotopic ratios have been measured at only a few boreholes. Based on the analysis at one

borehole (SD-7), using the dissolution rate from fractured basalts, an estimate of percolation based on $^{87}Sr/^{86}Sr$ ratios ranges from 0.5 to 5 mm/yr (Sonnenthal, et al., 1997b).

- **Chloride Mass Balance**

The percolation flux at depth can be estimated by a meteoric chloride mass balance method by using the average precipitation rate, Cl concentration corresponding to the typical near-surface infiltrating water, and Cl^- concentration in a well-mixed reservoir at depth (Fabryka-Martin, et al., 1997). This method assumes that precipitation, net infiltration, and chloride deposition rates have been constant for sufficient time to reach steady state and further assumes that matrix and fracture waters have fully mixed. The chloride mass balance approach also assumes piston-like flow, a uniformly downward movement of water that displaces the initial water in the profile (Scanlon, et al., 1997). This assumption may not be valid at YM because of the potential for preferential fast flow paths in the unsaturated zone.

Estimates of percolation tabulated by Fabryka-Martin, et al. (1997, Table 5-2) were calculated using the geometric mean of Cl^- values for hydrostratigraphic units in six wells, 170 mm/yr for precipitation, and a Cl^- concentration of 0.62 mg/L for near-surface infiltrating water. Percolation estimates calculated using the Cl mass balance method described above for the PTn range from 1.1 to 3.4 mm/yr with an average of 2.0 mm/yr. Similarly calculated percolation estimates for the CHn range from 2.2 to 5.3 mm/yr with an average of 3.9 mm/yr, while estimates for the perched water range from 11 to 23 mm/yr with an average of 16 mm/yr. Assuming unit gradients and values of saturated hydraulic conductivity of 0.9 and 1.9 mm/yr for the TCw and TSw units, respectively, it is noted that percolation in the units above the PTn and CHn exceed their transmission capacity, the difference being indicative of the portion of total flow due to flow in fractures. Higher fractions due to fracture flow would result if effective conductivity was used instead of saturated hydraulic conductivity. Another important observation is that the perched water has lower concentrations of Cl^-, and, hence, larger percolation estimates, than the PTn. The implication is that the water reaching the perched zone either bypassed the PTn or percolated quickly through the PTn through fast paths, possibly as nonuniform fronts.

Yang, et al. (1996b) report Cl concentrations in perched water of 4.1 to 15.5 mg/L, with 15 of the 17 reported values no greater than 8.3 mg/L and a Cl concentration of 7 mg/L at NRG-7a (the nearest borehole to UZ-4 and UZ-5 with a reported perched-water sample). Using the same precipitation rate (170 mm/yr) and Cl concentration for near-surface infiltrating water (0.62 mg/L) as Fabryka-Martin, et al. (1997) and assuming that the perched water is well mixed with the matrix waters, calculated net infiltrations are 25.7, 12.7, and 6.8 mm/yr for concentrations of 4.1, 8.3, and 15.5 mg/L, respectively. A percolation value of about 26 mm/yr would represent an upper bound based upon the perched-water chloride data; if the matrix waters do not mix completely with the perched water, percolation values may be lower. The estimated percolation values are more consistent with the shallow infiltration estimates than the estimates from the pore-water of the PTn (NRC, 1997b), suggesting that a considerable portion of the percolating water may bypass the PTn matrix.

- **Saturation and Water Potential**

Observations of both saturation/water content and water potential can yield independent estimates of water fluxes, in addition to providing calibration data for numerical simulators. When the hydraulic characteristics of a matrix sample are known, saturation, water content, and water potential each can be used to estimate the unsaturated hydraulic conductivity. Knowing the unsaturated hydraulic conductivity at a particular water content and assuming gravity drainage, the percolation rate is directly calculated using Darcy's law. If capillary effects are negligible, so that the assumption of gravity drainage is appropriate, the vertical flux is numerically equal to the unsaturated hydraulic conductivity.

The question of whether or not gravity drainage is an appropriate assumption was addressed by Rousseau, et al. (1996) who presented *in situ* water potential measurements from five boreholes (UZ-1, UZ#4, UZ#5, NRG-6, and NRG-7a). None of the profiles had unequivocally returned to initial conditions in the time frame examined (several months to years), but, generally, it appears that, upon equilibration, all five boreholes will exhibit minimal vertical variation in water potential (implying gravity drainage) and no profile will be drier than five bars of suction. In boreholes UZ#4 and UZ#5, available core sample potentials are scattered within one or two bars of the *in situ* values; overall, the core values tend to be wetter than the *in situ* values.

The expert elicitation process (Geomatrix, 1997) revealed limitations on the use of water content and potentials for estimating percolation rates. There are two primary sources of saturation and water potential data: (1) measurements from core samples obtained during drilling; and (2) *in situ* measurements. A great number of core-sample measurements were obtained during drilling the more recent boreholes (Flint, 1997). Although care was taken during sampling to preserve *in situ* conditions in the core, some drying apparently occurred during sampling and the resulting data should be considered suspect (L. Flint, 1997, presentation to Site-Scale Unsaturated-Zone Flow Model Expert Elicitation Panel). Drying becomes more of an issue as the degree of welding increases, as the same amount of evaporation distorts the data more by removing a larger fraction of the available moisture. Independent estimates of fluxes obtained from these potentials are dependent on the independent estimates of hydraulic properties, particularly saturated hydraulic conductivity and van Genuchten α. A factor of two change in van Genuchten α (which is small compared to the uncertainty associated with the parameter) may change estimates of relative permeability by an order of magnitude. Accordingly, estimates of flux obtained from *in situ* saturations or water potentials are not considered reliable.

- **Fracture Coatings**

The percolation flux can be estimated from fracture coatings of calcite and silica (e.g., opal). It has been proposed that all of the fracture coating in the UZ was precipitated from downward percolating waters (Johnson and DePaolo, 1994). The finely layered coatings suggest periodic deposition with no textural indication of chemically undersaturated water from large pulses to dissolve the coating (Paces, et al., 1996b). In the ESF, Paces, et al. (1996b) noted that fracture coatings occurred exclusively on the footwall, that the thickest deposits were in the low-angle fractures, and that coatings occurred where apertures generally exceeded several millimeters.

Paces, et al. (1996b) and Marshall, et al. (1998) provide preliminary estimates of the percolation fluxes required to deposit calcite and opal in the form of fracture fillings and lithophysae coatings at YM. Assuming that the fracture characteristics and filling patterns observed in the ESF are representative of the entire UZ, all cations are deposited within the UZ, and infiltrating water has the composition observed under current conditions, the average percolation flux rate required to match the observed patterns is calculated to be 2.1 mm/yr for calcite and 0.3 mm/yr for opal (Paces, et al., 1996b). Marshall, et al. (1998) updated these to 3.4 and 1.8 mm/yr, respectively. As noted by Paces, et al. (1996b), these are minimum estimates, as almost certainly not all calcium and silica in the percolating water is deposited as coatings.

Dating of fracture coatings using ^{14}C measurements range from 16 to 44 kya, whereas, the ages calculated using $^{230}Th/U$ measurements range from 28 to over 500 kya (Simmons, 1996; Paces, et al., 1996b). However, sampling difficulties due to the fine layering make interpretations of the fracture coating ages using isotopic measurements difficult. The older ages for the coatings may be consistent with calcite deposition models that suggest that deposition will only occur where flux is slow. Fast moving pulses of water in the fractures might be expected to dissolve the existing calcite. The use of isotopes to date layers of fracture coatings does not appear to have produced reliable information. This may be a result of apparent ages of fracture coatings being representative of mixtures of older and younger minerals, or representative of precipitation, dissolution, and re-precipitation along flow paths.

- **Perched Water**

A summary of perched water data from YM is provided by Wu, et al. (1996). The presence of perched water in and immediately above the CHn unit can be used as a lower constraint for estimation of percolation flux. Estimates of residence times, volume estimates, material properties, and head gradients can be used in this regard. Volume of perched water is also an important constraint on calibrating the site-scale model, as noted by Wu, et al. (1997); adjustment of rock properties in the layers in and adjacent to the perched zones was required to match the volumes of water in the perched zone.

A flux estimate required to form and sustain perched water above the CHn in the vicinity of UZ-14 was made by Rousseau, et al. (1996). Seepage rates both laterally along and through the perched zone and seepage rates through adjacent vitric zones were weighted by their areal distribution to estimate the percolation through the TSw in the combined areas of the vitric and the perched zones. In addition to the residence time data, estimates of head gradient, permeability, perched water volume, and area were required. Flux through the vitrophyre below the perched zone was estimated to range from 0.0014 to 0.29 mm/yr, a range corresponding to effective porosity values between 0.001 to 0.10 (Rousseau, et al., 1996). However, since the origin of the perched water is not clear and the presence of two distinct waters in the CHn is indicated by geochemical data (Yang, et al., 1996a), estimates of percolation flux may not be reliable.

- **Summary of Deep Percolation Estimates**

There is a wide range of flux estimates, based on various methods and assumed climatic conditions. Concurrence of values from widely different approaches leads to confidence in the

estimates, leaving the extreme values as an indication of less reliability. The UZ Expert Elicitation Panel provided estimates of deep percolation, considering all presented approaches, with estimated mean values ranging from 4 to 21 mm/yr (Geomatrix, 1997).

The use of tracers to robustly estimate percolation rates in the YM area is limited. Difficulties with estimating the impacts of lateral flow and multiple pathways would appear to limit their use over most of the repository footprint. Nevertheless, unambiguous bomb pulse signatures observed at depth in the ESF are interpreted as occurring where high infiltration occurs over a zone having a fault that provides a fast pathway through the PTn unit (Levy, et al., 1997). The bomb pulse data were instrumental in demonstrating that fast pathways exist and, by implication, that, at least locally, there are areas where infiltration might be much higher than previously thought.

Despite the limitations on tracer methods, the chloride mass balance technique does provide a means of estimating an upper bound for net infiltration. The upper bound value obtained by chloride mass balance on perched water, 26 mm/yr, is remarkably consistent with the upper-bound value obtained by geothermal heat-flux calculations.

Collectively, the geochemical, thermal, and water distribution data suggest that flow in the UZ is better represented by conceptual models that consider fast pathways and limited matrix/fracture interactions than by models which consider predominantly matrix flow. The NRC staff review should ensure that fast pathways and limited matrix/fracture interaction are reasonably represented by DOE numerical models.

4.4.2.6 Estimates of Deep Percolation Based on Numerical Simulations

Numerical modeling of flow processes at YM is unavoidable due to the large spatial and temporal scale of the repository performance relative to the scope of conceivable investigation. Numerical modeling enables observations at limited observational points and times to be extended in time and space. In modeling flow through the UZ at YM, it is important to capture both fracture flow and matrix flow processes. However, fracture flow may be more important from the perspective of PA, as releases and transport are apparently more strongly affected at YM by fracture flow than matrix flow.

A wide variety of methods and formulations have been applied to site- and drift-scale modeling at YM. Current estimates of the spatial distribution of percolation using the site-scale model of LBNL (Bodvarsson, et al., 1997a) are developed using separate, but interacting, continua for matrix and fracture systems. For drift-scale modeling, no definitive choice has been made (TRW Environmental Safety Systems, Inc., 1997a), although Birkholzer (1998) recently presented a fracture continuum model. Inherent in both scales of modeling are the estimates of physical and hydraulic parameters. As such, the first portions of this section discuss issues related to parameter estimation for matrix and fracture systems. The last portion of this section discusses alternative methods and formulations for modeling flow at YM.

- **Matrix Properties and Parameter Estimates**

A large database of bedrock physical and hydraulic properties for units at YM has been collected, correlated to lithologic structure, and analyzed for spatial trends, using samples collected from outcrops and from boreholes (Peters, et al., 1984, Klavetter and Peters, 1986; Flint and Flint, 1990, 19[illegible] Rautman and Flint, 1992; Istok, et al., 1994; Cromer and Rautman, 1995; McKenna and Rautman, 1996; Rautman, et al., 1995; Schenker, et al., 1995; Flint, et al., 1996b; Moyer, et al., 1996; Rousseau, et al., 1996; Flint, 1997; Rautman and McKenna, 1997). Easily measured physical properties (i.e., porosity and bulk density) have been collected for most of these samples, but hydraulic properties have only been sparsely collected. Rautman and McKenna (1997) summarize the available data, much of which is described by Flint (1997) in greater detail, and extrapolate the data to model grids. Bodvarsson and Bandurraga (1996) and Bodvarsson, et al. (1997a) use much of this information to constrain values of grid-block-scale hydraulic parameters derived through inverse modeling.

Porosity is generally used as a surrogate variable for K_{sat} (Flint, 1997; Rautman and McKenna, 1997), because: (1) porosity has been measured on virtually all core samples; (2) values of other hydraulic properties have not been determined for most core samples; and (3) porosity appears to be fairly well correlated to hydraulic properties. Interestingly, a staff comparison of *in situ* water saturation and core-sample K_{sat} suggests that saturation may be a better predictor of K_{sat} than porosity. This correlation may warrant further study. In addition to K_{sat}, the van Genuchten parameters for the UZ constitutive relations are required for UZ flow modeling. Matrix retention parameters require the most effort to obtain and, therefore, have only been determined for a small number of core samples; many of the measurements exhibit a great deal of scatter both within units and for similar rock types. Accordingly, estimates of matrix retention parameters have a great deal of uncertainty.

Measurements from core samples are at a much smaller scale than typical model grid blocks (i.e., several cubic centimeters as opposed to grid blocks 1 to 100 m on a side, which is at least 8 orders of magnitude difference). One way to reconcile the disparity in scales is through inverse modeling to obtain effective properties [e.g., the LBNL 3D site-scale model approach (Bodvarsson and Bandurraga, 1996; Bodvarsson, et al., 1997a)]. Since inverse modeling approaches are inherently mathematically ill-posed and nonunique, it is most effective when only a few parameters need to be determined; thus, heterogeneity is not easily accommodated. For this reason, the LBNL inverse-modeling approach assumes that all parameters are homogeneous within each layer. It appears that each physical layer is modeled with at most two computational layers, which may tend to mask processes occurring on a sub-layer scale such as lateral diversion in the PTn unit (Wilson, 1996). Further, the LBNL inverse-modeling does not use an approach that estimates all properties simultaneously, and inconsistently estimates some properties using the assumption of 1D vertical flow despite the lateral flow exhibited in subsequent 2D and 3D simulations using the parameters. The NRC staff considers that the LBNL 3D site-scale model may be too coarse to provide more than a general indication of subsurface processes at YM but notes that significant model refinement may be computationally infeasible. Despite these reservations, NRC staff endorse the LBNL philosophy of using all available sources of information to calibrate the site-scale model, and agree that, for many purposes, homogeneous effective properties for each layer obtained through inverse modeling may be adequate.

Another way to reconcile the disparity in scales is through upscaling. Schenker, et al. (1995), attempting to estimate layer-wide hydraulic properties from core-sample data, recognized that bulk variability is usually less than the core-sample variability and, therefore, reduced the coefficient of variation for hydraulic properties according to the vertical correlation length and layer thickness.

The sophisticated approach adopted by Rautman and McKenna (1997), building upon a series of previous SNL efforts, generates heterogeneous parameter fields based on cross-correlation of hydraulic conductivity, bulk density, and thermal conductivity. A significant advantage of this approach, relative to the inverse-modeling approach, is that heterogeneity readily can be accommodated into modeling efforts. Porosity, K_{sat}, and thermal conductivity (in the TSw unit) are considered by Rautman and McKenna (1997), although the methodology could be extended to include retention parameters. The Rautman and McKenna (1997) methodology minimizes statistical artifacts potentially introduced by faults by using the depositional environment (before faulting occurred) to perform statistical analyses, although this procedure may add statistical anomalies when considering alteration (which occurred after faulting).

Despite the attractive characteristics of the Rautman and McKenna (1997) procedure, it appears that the procedure projects core-scale properties to the grid-block scale (100 m × 100 m × 2 m) rather than projecting averaged or upscaled properties. Rautman and McKenna (1997) note that the procedure does not address the issue of upscaling. However, the procedure could be adapted to generate a fine-scale set of hydraulic properties on a subgrid within each grid block; the fine-scale properties could then be formally upscaled to arrive at effective properties. Formal upscaling that accounts for flow characteristics may generate effective properties that are different from averaged properties, as noted by Rautman and McKenna (1997), who further note that advective processes (e.g., percolation) are more likely to be affected by upscaling issues than diffusive processes (e.g., heat conduction).

If one upscales using the many-tubes approximation, which assumes that the porous medium is composed of many tubes (at the scale of core samples) in parallel, all with vertical gravity flow and all at the same suction (essentially assuming that local lateral flow is not restricted), staff analysis determined that a small percentage of the tubes (local fast pathways) carry the bulk of the flow when the cores are as heterogeneous as those reported by Flint (1997) for the PTn subunits. The assumption of locally unrestricted lateral flow may be appropriate for bedding planes in bedded units such as the PTn. If, in fact, local fast pathways carry the bulk of the percolating water, most observations from the PTn used for calibration would be representative of the bypassed portion of the matrix. Further, flow along these fast pathways may penetrate the PTn rapidly enough to account for bomb-pulse observations, even accounting for potentially tortuous lateral paths. Unfortunately, hydraulic parameters that are upscaled, accounting for the local flow paths during ambient conditions, may not be appropriate during the repository thermal pulse, during which all of the matrix would presumably participate in flow redistribution.

Modeling efforts rely heavily on these laboratory-determined rock properties, upscaling, or inverse modeling. As a check on consistency, Winterle and Stothoff (1997) modeled imbibition, using METRA (Seth and Lichtner, 1996) to verify that the hydraulic parameters used by Bodvarsson, et al. (1997a) would reproduce sorptivity measurements by Flint (1997). If reported rock properties are accurate, and the underlying physics of the UZ flow models are

correct, then models should be able to predict rock matrix sorptivity that is very close to the observed sorptivity. However, comparison of model-predicted sorptivity and observed sorptivity yielded an interesting result: numerically determined sorptivity was consistently greater than the observed sorptivity. Furthermore, the ratio of modeled to observed sorptivity varied in proportion to K_{sat}. This relationship was interpreted by Winterle and Stothoff (1997) to be suggestive of hysteretic behavior in rock moisture retention characteristics. That is, at a given saturation, capillary suction is less in a rock that is undergoing a wetting cycle that it would be in the same rock undergoing a drying cycle. Moisture retention characteristics reported by Flint, et al. (1996b) were measured in the laboratory by incrementally oven drying rock samples and measuring capillary suction; however, imbibition is a wetting process. Thus, laboratory-reported values of van Genuchten's α parameter may be too low for use in models where the flow of infiltration pulses in fractures is of interest. Implications are that infiltration at YM may travel farther in fractures than would be predicted by models using moisture-retention characteristics based on drying curves. Interestingly, calibration of the YM site-scale UZ flow model (Bandurraga and Bodvarsson, 1997) required an increase in the α values relative to mean values reported by Flint (1997).

The NRC staff considers that approaches used by DOE to estimate parameters for flow and transport simulations generally use sound methods, particularly in the most recent work. The NRC staff notes, however, that subgrid heterogeneity is not explicitly and transparently addressed in the approaches and caution that failure to consider subgrid heterogeneity may lead to qualitatively incorrect results. Small-scale modeling of heterogeneous zones is one approach that may be used to support use of uniform properties in hydrostratigraphic units of the site-scale UZ flow model.

- **Hydraulic Properties of the Fracture System**

A general understanding of fracture geometry, surface characteristics (e.g. roughness), size distributions, and spatial variation is important for modeling UZ flow in the fracture bedrock of YM. These characteristics will affect hydraulic conductivity, hydraulic connectivity, matrix imbibition, chemical diffusion, and flow channeling in the fracture system. This section includes a discussion of fracture characteristics in relation to hydraulic properties. An analysis of the fracture system characterization at YM is included in the SDS IRSR (NRC, 1998a).

Fracture characteristics are used both to estimate hydrologic properties of the fracture system and to constrain conceptual models of UZ flow at YM. Fracture geometries, orientations, and distributions, combined with permeability measured by air injection testing and modeling of pneumatic response to atmospheric pressure changes, have been the source of data used to estimate physical and hydrologic properties for the fracture system for numerical modeling of the UZ at YM. There are no direct measurements of hydrologic properties of fractures or fracture systems in the UZ, only indirect calculation of hydrologic properties based on gas permeability data and constraints by thermal and geochemical evidence. Air injection and gas permeability data are used to estimate apertures and aperture distributions that are then used to estimate hydraulic properties of the fracture systems. Since air-injection testing is a critical component of estimating hydraulic properties of fracture system, and there was some controversy about methods and interpretation of previous air-injection testing at the site, a peer review was performed by an independent, three-member panel. Recommendations of the peer

review are summarized in attachments to a U.S. Geological Survey letter (USGS, 1995). The estimates of hydraulic fracture property values are used to constrain the range of possible values in the LBNL site-scale UZ inverse modeling; as such, the fracture parameters of saturated hydraulic conductivity and van Genuchten alpha are calibrated values.

Hydrogeologic parameters for fractures are difficult to characterize through direct measurement at YM because fractures vary widely in length, connectivity, orientation, aperture, and coating type and amount. These parameters depend on the scale of observation. For example, scale dependency in conductivity of a fractured rock is attributed to three properties: (1) the variation of length or consistency of the fractures; (2) the distribution of the fractures as related to the connectivity of the fracture system; and (3) the variation in conductivity or transport capacity. Sonnenthal, et al. (1997a) provide the best available summary and analysis of data on hydrologic properties of fractures and faults in the UZ, based on data from the detailed line surveying (DLS), borehole measurements, and the air injection tests (for permeability) (Ahlers, et al., 1996; Anna, 1996; Sweetkind and Williams-Stroud, 1996; LeCain, 1997; LeCain and Patterson, 1997; Sweetkind, et al., 1997). The summary provides estimates about fracture frequencies, orientations, and connectivities in the Topopah Spring Tuff, fracture frequencies from borehole measurements, permeabilities from air-injection tests, fracture apertures, van Genuchten parameters, fracture porosity, and heterogeneity of fracture distributions. The summary also includes pneumatic responses of faults and provided estimates of fault hydrologic properties, such as pneumatic permeability and porosity of the fracture continuum. The data are organized into a consistent set to be used with the UZ hydrostratigraphic model Table 7.7 of Sonnenthal, et al. (1997a)), including mean values for fracture spacing, frequency, trace length, intensity, and the proportion longer than 1 m for 16 zones in the upper 12 sublayers of the UZ model. These are 12 hydrostratigraphic sublayers from the ground surface to the repository horizon.

A brief discussion of fracture properties as related to hydrologic properties by hydrostratigraphic unit is included below. A detailed discussion of the fracture properties can be found in the SDS IRSR (NRC, 1998a). The nonwelded PTn sublayers generally have larger fracture spacing (i.e., lower density), lower frequency, and larger trace lengths than the overlying and underlying welded tuffs of TCw and TSw, although on a sublayer basis, there is considerable overlap between the units. There are as yet few data for the CHn nonwelded unit. However, the Busted Butte test facility should provide the needed information.

In the TCw, fracture spacing is significantly smaller than the fracture length thus implying the likelihood of connectivity of fractures. Geometric connectivity is an important criterion for fracture flow capability. Air injection tests performed on the drift-scale in the ESF demonstrated the connectivity and showed that the fracture network generally behaves as a continuum, with the mean fracture permeability generally increasing as the scale of the system increases (Sonnenthal, et al., 1997a). Pneumatic responses supported by gas chemistry data led Thorstenson, et al. (1998) to conclude that vertical permeability to air of the PTn was 1 to 3 orders of magnitude less than in the TCw or TSw. Thorstenson, et al. (1998) correctly noted that the gravity force acting on water percolating through the PTn is orders of magnitude greater than the buoyant forces acting on air, hence, the "gas permeability contrast does not preclude a high rate of water percolation through the PTn."

Because the repository will be in the TSw, a more detailed reporting of fractures in the TSw was organized by Sonnenthal, et al. (1997a). In looking at all of the fractures in the TSw (down to a length of 0.3 m) and over a 100-m scale, the middle nonlithophysal unit has higher fracture densities than the other layers. The vertical air permeabilities of the other TSw units measured from boreholes in the ESF are about 2 to 3.5 times the horizontal air permeabilities, while the ratio for the nonlithophysal layer is only about 1.3 (uniform over a distance of over 1,200 m in the ESF). However, the water permeability could be underestimated if it is based directly on air permeability, especially for horizontal water permeability where blockage by water could impact air permeability testing. Also for the TSw, the number of fractures was found to be inversely proportional to fracture size, and over half of the fractures are found in the 0.3- to 1.0-m range. This would indicate that the earlier cutoff length of 1.0 m used for the average values in the different zones of the UZ model probably skewed the data input to the model (Sonnenthal, et al., 1997a).

Two important features of the model layer properties in Sonnenthal, et al. (1997a) are worth underscoring here. One, for most of the sixteen zones (in the upper 12 hydrostratigraphic sublayers), the standard deviations for fracture spacing and fracture intensity are greater than the mean values. Therefore, use of mean values in flow models will underestimate the lateral and vertical variability of permeability in the UZ. Two, more than a third of all the fractures are eliminated from the analysis due to use of a 1 m fracture-length cutoff (fractures shorter than 1 m were not measured and counted). Elimination of short fractures from nonwelded, lithophysal, or densely fractured units could lead to an underestimation of hydrologic properties, such as porosity, permeability, and fracture connectivity. Elimination of fractures less than 1 m also may modify fracture intensity interpretations near faults such as for the GDF in the ESF where the 1 m cutoff for trace length leads to extremely different fracture intensity estimates over a wide zone (Sweetkind, et al., 1997).

Major faults in the vicinity of the repository include the north-south trending GDF, SCF, Bow Ridge, and Dune Wash Faults, which are normal faults, and the northwest trending Sundance, Drill Hole, and Tea Cup Faults, which are strike-slip faults. Hydraulic properties of fault zones are impacted by the degree of associated fracturing, the geometric character of the fracturing, and the nature of the fault gouge, all of which can vary vertically and laterally. The limited pneumatic monitoring and air-injection testing on fault zones at YM is summarized in Sonnenthal, et al. (1997a). The geologic characterization of faults at YM is analyzed in detail in the SDS IRSR (NRC, 1998a).

Sonnenthal, et al. (1997a) made several recommendations for additional data collection that are worth restating here. First, that fracture mapping data should be obtained from the east-west drift to compare and combine with data from the ESF. The proposed emplacement zones all lie west of the ESF loop. Second, additional borehole testing data are needed for units below the proposed repository horizon to better constrain the fracture distribution and permeability structure of zeolitic units. And finally, if faults are expected to play a large role in formulating UZ waste isolation strategy, then additional investigations are needed to better define fault widths, frequencies, interconnectedness, and gouge properties.

It should be noted that the current NRC/CNWRA modeling approach emphasizes relatively rapid fracture flow in the UZ. Our approach places little emphasis on retardation of radionuclides in the UZ, with repository performance being much more affected by properties of

the SZ. Under this approach, bounding values are probably acceptable for hydraulic properties of fractures, reducing the need for extensive characterization of UZ fracture networks. One exception to this would be the need for ESF data on fractures within the TSw. A reasonable understanding of general fracture patterns in the ESF is needed to refine conceptualizations of conditions under which water may enter emplacement drifts and drip onto waste packages. Data from the ESF and the east-west drift should provide an acceptable reference base.

- **Model Formulations**

There are two main approaches to modeling flow in unsaturated fractured tuffs: continuum methods and discrete-fracture methods (Evans and Nicholson, 1987). Continuum methods treat the matrix and fracture systems with various levels of interaction [e.g., methods using an equivalent continuum model (ECM), a dual-porosity model, a dual-permeability model (DKM), and a multiple interacting continua (MINC) model]. Discrete-fracture models may either account for or ignore interactions with the matrix. The models are discussed by Altman, et al. (1996). The continuum models are evaluated to investigate prediction differences by Doughty and Bodvarsson (1996, 1997). The observations of fast-path bomb-pulse ^{36}Cl detected in the ESF, coupled with newer estimates of MAI that exceed matrix permeabilities, have required a shift from matrix-dominated flow models (such as the ECM approach) toward fracture-dominated methods (such as the DKM approach), to enable some portion of percolation fluxes to occur in fast pathways.

Model dimensionality is another factor that may have a large impact on transport times. One dimension simulations cannot find fast pathways through lateral flow, thereby, magnifying the impact of low-permeability zones, while 2D and 3D simulations provide increasingly greater latitude for lateral flow.

The ECM formulation, developed by Klavetter and Peters (1986), merges matrix and fracture continua into a single equivalent continuum by assuming that the pressure in the matrix and fracture continua are in hydraulic equilibrium at each spatial location, resulting in considerable computational efficiency. In general, the fracture system only carries flow when the matrix system is essentially saturated. Early versions of the 3D UZ site-scale model developed by LBNL used the ECM formulation (Bodvarsson and Bandurraga, 1996), but subsequent analyses have largely abandoned the approach in favor of the DKM approach (Bodvarsson, et al., 1997a). The GWTT-94 analyses performed by SNL used the ECM approach, but the GWTT-95 analyses used the DKM approach. A modified ECM approach was used in TSPA-95 (Andrews, et al., 1994), with a heuristic disequilibrium assumed between matrix and fractures, but DOE intends to use a DKM approach for TSPA-VA (S. Sevougian, presentation at DOE/NRC Technical Exchange on Total System Performance Assessment, March 17, 1998). The NRC staff supports the use of the DKM approach relative to the ECM approach for site-scale flow modeling as long as DOE demonstrates that the results bound the effect of episodic pulses.

Doughty and Bodvarsson (1997) conclude that the ECM is most appropriate for steady state conditions and gas-flow problems at YM, as the assumption of matrix/fracture pressure equilibrium is best met under these conditions. Doughty and Bodvarsson (1997) and Tsang (1997) find that the DKM predictions significantly differ from the ECM predictions under transient conditions, with transport times significantly slower in the ECM. The DKM provides

prediction more consistent with simulations of a ponded-infiltration experiment examining flow processes in TSw bedrock at Fran Ridge (Eaton, et al., 1996) than the ECM predictions. Doughty and Bodvarsson (1997) further conclude that the additional complexity of the MINC approach is most necessary near faults.

Discrete-fracture approaches have not been used frequently at YM but have not been ignored completely. The WEEPS model (Gauthier, et al., 1992; Sandia National Laboratories, 1994), used to assess fluxes onto a WP for TSPA, assumes that all percolation is within fractures and is gravity-driven. The model uses geometric arguments to map the intersection between flowing fractures and WPs in order to arrive at total flux onto WPs. The model apportions the available flux into flowing fractures, with a primary uncertainty being the aperture distribution of the flowing fractures.

Individual fracture segments within a fracture network are explicitly represented in a discrete-fracture formulation, with each segment having individual hydraulic and pneumatic properties. The explicit-fracture method is attractive at scales where continuum behavior is not observed (i.e., at scales small relative to fracture density) but becomes intractable once many fractures are considered. Discrete-fracture methods are not practical for use at a YM-site scale as there are an estimated 10^9 significant fractures at YM (Doughty and Bodvarsson, 1997). Anna (1996) attempted to model a portion of the North Ramp using a discrete-fracture formulation with limited success. The generated network of fractures was based on ESF observations and had generally low connectivity, but pneumatic testing suggested that fracture connectivity should have been much larger. The discrepancy between simulated and inferred connectivities may be due to those fractures not considered in the discrete-fracture model (i.e., fractures less than 1 m in trace) or to the partial pneumatic connection through the matrix not included in the formulation.

The most appropriate application at YM for discrete-fracture methods may be drift-scale modeling, as there are few enough fractures that discrete-fracture discretization requirements may be tractable, and continuum approaches may be invalid. Nevertheless, DOE drift-scale studies for isothermal flow have invariably used continuum approaches: (1) matrix continuum, with fractures included as heterogeneous pathways (Wang, presentation to Site-Scale Unsaturated Zone Expert Elicitation Panel, 1997); (2) fracture continuum, with no consideration of matrix interaction (Birkholzer, et al., 1997a); (3) equivalent continuum (Nitao, 1997); and (4) DKM (Tsang, 1997). The DOE conceptual model for seepage into drifts is not well enough defined, nor is the uncertainty reasonably enough constrained to determine, a single appropriate model at this time (TRW Environmental Safety Systems, Inc., 1997a). However, seepage and moisture studies are ongoing at YM to better evaluate the drift seepage processes, percolation fluxes, and the capillary barrier system. These investigations are titled "Percolation in the Unsaturated Zone - Exploratory Studies Facility." The objective is to conduct *in-situ* ambient cross-hole pneumatic and liquid-release niche seepage studies and alcove surface infiltration studies.

Wang, et al. (1998) presented the Phase 1 preliminary test results and numerical model analysis of seepage into drifts. This included test results of the first seepage tests at Niche 3650 and sensitivity analysis of drift seepage with two and three-dimensional numerical models. The numerical models were then tested to predict the wetting-front arrival time of the planned

infiltration test for Alcove 1. This report is the third technical report for the drift seepage testing and moisture analysis.

According to the Master Scientific Notebook YMP-LBNL-JSW-6.0, ongoing field studies include: (1) the Phase 2 drift scale seepage test; (2) field tests of flow propagation through the heterogeneous and fractured Paintbrush nonwelded tuff (PTn); (3) investigation of fracture flow and storage effects in the PTn; (4) horizontal diversion of flow along interfaces between different subunits, (5) fracture flow, fracture-matrix interaction, and matrix imbibition tests of the middle nonlithophysal unit of Topopah Springs welded unit; and (6) Alcoves 1 and 7 testing. The results of these field investigations will feed the site-scale and drift-scale models calibrated against on-going field test results in support of the TSPA for YM.

4.4.2.7 Past Evidence and Impact of Future Climate Changes on Deep Percolation

The primary sources of information for future predictions of climatic change are the paleo records. Local data include the isotopic record from Devils Hole, pack rat middens, paleospring deposits, and water table fluctuations recorded by isotopic data, while the global data include information such as the integrated marine record (see Attachment E, NRC, 1997a; Forester, et al., 1996).

The single most important data set for predicting deep percolation under pluvial conditions is net shallow infiltration. According to Forester, et al. (1996), shallow infiltration may increase by a factor of 2 to 3 as a consequence of 5 to 10 °C drops in temperature, so that significant changes in vegetation may occur (NRC, 1997b). The factor for the increase in infiltration due to climatic change (pluvial) may be larger due to the nonlinear response of infiltration to increased precipitation and cooler temperatures. The staff is currently evaluating climate analog sites to incorporate in infiltration estimates the effects of soil characteristics, vegetation, and surface water runoff phenomena.

For deep percolation, the effect of climatic changes would be expected to impact the magnitude and pattern of percolation rates, including seepage into the drifts and flow below the repository. Increased percolation through the TSw is expected to be through the fracture system as the low matrix permeabilities will not take a significantly larger magnitude of the flow. The seepage-to-percolation ratio for seepage into drifts increases (Birkholzer, et al., 1997a) due to the fractures taking up a higher fraction of the flow as percolation increases. The spatial pattern of percolation might be expected to change as different portions of the fracture system begin to carry more flow as percolation increases. Below the repository, both the perched water and water table levels might be expected to change.

Site-scale modeling of potential future climatic impacts by Ritcey, et al. (1997b) using the ECM formulation suggests increased fluxes over the northwestern portion of the repository, though there is little significant change in pattern for other areas at the repository horizon or below the repository. Ritcey, et al. (1997b) noted that modest increases, less than 10 m, in the elevation of perched water tables resulted from doubling the shallow infiltration rates.

The question of how much to increase percolation rate to account for possible climatic changes requires a linkage of paleoclimatic conditions to the shallow infiltration. Linkage of the top

boundary condition of shallow infiltration to both general and local paleoclimate information led Gauthier (1998) to use precipitation multipliers of 1 for the current dry conditions, 2 for the long-term average conditions, and 3 for the super pluvial conditions. Over the past four hundred thousand years, the long-term average conditions occurred about 80 percent of the time (Forester, et al., 1996). A constraint on the conditions is the paleo position of the maximum 100-m rise of the water table as indicated by the strontium data from calcite fracture filling and paleosprings deposits in Crater Flats (Forester, et al., 1996).

4.4.2.8 Pneumatic Responses at YM

A major topic of study at YM has been the movement of unsaturated zone gases, mainly water vapor, in response to barometric pressure changes. There have also been concerns about the possible interference of exploratory shafts and tunnels on testing in the UZ. The NRC staff developed an open item on pneumatic issues during our review of the Site Characterization Plan (see SCA, 1989, p. 4-92). Our comment (no. 123) stated that:

> The effects of ventilation of the exploratory shafts and the underground testing rooms may have been underestimated in the evaluation of the potential interference with testing and the potential for irreversible changes to baseline site conditions; also, there is not an adequate analysis of the effects of ventilation in the ESF on the ability of the site to isolate waste.

DOE (1990) responded that the exploratory shaft would be lined with poured concrete that would isolate the rock from the ventilation air. The staff did not close the open item at that time because it was not clear whether the shaft would be lined, and secondary effects of ventilation on baseline conditions were not addressed. Since that time, DOE has chosen to construct the underground exploratory facility and the east-west drift using a tunnel boring machine (TBM) rather than build vertical access shafts.

Another open item had been raised by the staff regarding possible interference by the ESF on gas chemistry sampling. This item was closed in a 1994 letter from NRC to DOE (NRC, 1994). The staff's remaining concern was with pneumatic pathways.

Early in 1993, the State of Nevada wrote to NRC questioning whether DOE could adequately characterize pneumatic pathways before the UZ was disturbed by construction of the ESF. The State felt that the potential loss of data could prevent the NRC from making a licensing finding on the issue of the fastest pathway for radionuclide release. The State's letter was forwarded to DOE by NRC staff along with a reminder that the staff also had related concerns. The topic was discussed at a meeting of the NWTRB on October 19, 1993. Then, during January 26-27, 1994 a forum was convened by the YM Affected Units of Local Government (AULG). Proceedings of this roundtable have been published (AULG, 1994).

The concern that characterization of pneumatic pathways could be precluded by penetrating the PTn with a TBM was a valid one. It was thought that if the PTn was an effective pneumatic barrier, distinction between the pneumatic system above, in, and below the PTn could be determined by responses to changes in barometric pressure. If, however, the PTn were breached by the large diameter ESF, the distinction might have been masked. Knowledge of

the effectiveness of a pneumatic barrier above a hot nuclear waste repository could be important to performance assessment.

DOE, in its Accelerated Surface-Based Testing Program, committed to collect data on ambient pneumatic conditions and perturbations caused by ESF excavation. DOE installed pressure monitoring systems in boreholes NRG-6 and NRG-7a in October and November, 1994. These holes were located along the north ramp portion of the planned ESF Data were collected from these holes for over two years, ending in December 1996 The staff had no objections to DOE's decision to discontinue monitoring in these holes because, by that time, the TBM was almost two miles away constructing the south ramp of the ESF. The TBM was no longer within the repository horizon and, therefore, NRG-6 and NRG-7a were no longer yielding new information.

Pneumatic information was also obtained from boreholes UZ-4, UZ-5, UZ-7a, NRG-4, NRG-5, SD-7, SD-9, SD-12, and ONC-1. NRG-4 and ONC-1 were instrumented by the Nye County cooperative study program. Locations of pneumatic testing and monitoring boreholes had been sited based on the ESF layout, allowing large-scale seasonal barometric responses to be monitored along with responses to ESF construction. To give a time perspective to progress of the TBM, the front of the TBM passed closest to NRG-4 on June 16, 1995 and penetrated through the PTn into the Topopah Spring unit on June 20, 1995. The TBM passed closest to UZ-4 and UZ-5 on September 2, 1995, and closest to SD-9 on November 16, 1995. It passed SD-12 on April 4, 1996, and SD-7 on June 5, 1996 (Ahlers, et al., 1996).

Summaries of the pneumatic response data are provided by Ahlers, et al. (1996; 1997). They reported that the ESF can affect pneumatic pressures from a large distance where faults are involved. They recommended that any new pneumatic monitoring boreholes be located far enough from the ESF that the data would not be affected by the tunnel. If additional drifts are planned (such as the east-west drift), boreholes along the drift alignments should be considered. Faults were identified as fast pneumatic pathways in the PTn and the TSw. Ahlers, et al. (1997, p. 10-28) concluded that:

> Overall, simulation of pneumatic conditions at Yucca Mountain using the three-dimensional site-scale UZ model has been successful. Though some minor modifications to the model are warranted by the simulation results, the technique for pneumatic calibration produces reasonable pneumatic parameter sets. These parameter sets should be acceptable for simulation of future scenarios and predictions at Yucca Mountain.

As noted in Section 5, and based on the above discussion, the staff now considers SCP open item Comment 123 to be resolved. Sufficient data on baseline conditions have been obtained and data were collected during the construction of the ESF. Pneumatic monitoring and testing is continuing at various locations in the ESF. As of June 1998, recording of pneumatic data continues at boreholes UZ-4, UZ-5, UZ-7a, SD-12, NRG-7a, and SD-7. Nye County, Nevada, continues to record pneumatic data in NRG-4 and ONC-1.

4.4.2.9 Evidence for Fast Pathways

Early conceptualizations of flow processes at YM discounted the possibility of significant fast-pathway flows below the TCw unit, based on low infiltration rates and the large capacity of the PTn to dampen wetting pulses. The associated concept, that the TCw matrix conducted all percolation fluxes at a steady state with little or no fracture flow, was strongly challenged by observations of bomb-pulse ^{36}Cl and other radionuclides far below the PTn. It is difficult to provide strong limits on fluxes using bomb-pulse evidence, as mixing of waters distorts interpretations, so that bomb-pulse observations are only evidence of fast pathways and not necessarily focused-flow pathways. However, additional evidence that significant flux occurs in fast pathways at YM has been mounting steadily, forcing revision of conceptual models for both infiltration and subsurface flow processes.

Isotopes arising from nuclear testing worldwide in the 1950s provide the strongest evidence that fast-flow pathways exist in the subsurface of YM. Although ^{36}Cl is the bomb-pulse isotope providing the most unambiguous indication of fast water flow paths, since ^{36}Cl moves only with liquid-phase water, ^{3}H and ^{14}C (despite moving both in the air and the liquid phases) also provide supporting evidence for fast flow (Yang, et al., 1996a; Fabryka-Martin, et al., 1997). Elevated isotope levels are found in the fracture systems in the ESF and in perched water bodies. Elevated isotope levels are also found in the boreholes in the TCw (fracture-dominated flow) and at the top of the PTn. The absence of elevated ^{36}Cl in the lower portions of the PTn in most boreholes, but its presence in TSw fractures and in perched water above the CHn, is indicative of fast pathways bypassing the PTn.

Geochemical data from UZ matrix waters, perched waters, and the saturated zone suggest that fast pathways, having little interaction with the matrix, exist through the UZ. Ca^{2+}, Mg^{2+}, and Cl are up to 10 times more concentrated in the matrix pore water than either the perched water or the saturated zone water (Yang, et al., 1996b). The Cl^- concentrations are indicative of percolating water bypassing pore water in units above the perched water. Chloride concentrations in some portions of the CHn range from 4 to 8 mg/L (Yang et al., 1996b), which is closer to the near-surface estimate of 0.6 mg/L than to the matrix concentrations of 60 to 228 mg/L in the PTn (Fabryka-Martin, et al., 1997). Indicative of little mixing in the UZ, dissolved SiO_2 levels are consistently 50 percent higher in the matrix pore water than in perched or SZ waters.

Hydrogen and oxygen isotope ratios in perched waters are similar to the current winter-precipitation meteoric ratios, indicating that there is little evaporative loss before recharge (Wu, et al., 1996). Lateral flow from Solitario Canyon or vertical fast-pathway percolation may explain the isotope-ratio data. The similarity to current meteoric water and dissimilarity to waters north of the repository is evidence that perched water is not formed from fluids migrating from the north. Preliminary ^{14}C dates show a trend of younger water to the south (Wu, et al., 1996), providing further evidence that perched water near the repository may not be related to the high gradient zone to the north.

Carbon-14 isotopic dating provides apparent ages of 5,000 to 10,000 yr for perched waters, while apparent ages of the PTn pore waters are about 1,000 yr (Rousseau, et al., 1996; Patterson, et al., 1996). However, ^{14}C measurements in deeper portions of the CHn have indicated ages similar to or younger than 1,000 yr (Rousseau, et al., 1996). The ^{14}C data for the CHn water not only suggests fast preferential flow but also a more complex mechanism for

formation of the perched zones. Lateral flow from Solitario Canyon or vertical fast-pathway percolation may explain a portion of the water in perched zones of the CHn.

In a study of transport and water-rock interaction by Johnson and DePaolo (1994), strontium isotope data in water, whole rock, and calcite fracture fillings in the TSw were found to be consistent with fast pathway movement of water.

Studies at Rainier Mesa support the possibility of fast-pathway flow through fractured nonwelded tuffs. A sequence of lithologies similar to YM is present at Rainier Mesa, including alternating welded and nonwelded tuffs capped by a moderate-to-densely-welded tuff. However, the sequence at Rainier Mesa is primarily nonwelded with a thick sequence of zeolite-altered tuffs (Wang, et al., 1993). Percolation estimates from seepage into the tunnels, based on discharge at the portal and vapor flow, are approximately 24 mm/yr with a mean annual precipitation of 320 mm (Russell, et al., 1987; Wang, et al., 1993), or about 8 percent of the precipitation. Suggestive of fracture or fault flow, there is a distinct difference between the geochemistry of the matrix pore water and the water in the seeps (Murphy and Pabalan, 1994). The saturated zone water geochemistry is similar to that of the seeps. Residence times estimated from tritium data suggest travel times less than 6 yr from ground surface to the observation tunnels at a depth of 350 m (Wang, et al., 1993). Bomb-pulse ^{36}Cl observations in the seeps provide additional evidence for fast-path movement of water. Using the precipitation record, seep discharge rates, gross water chemistry, stable isotope composition, and two tracer tests, Russell, et al. (1987) concluded that: (1) the seep water was meteoric in origin with winter as the principal period of recharge based on hydrogen and oxygen isotope ratios; (2) the period of hydrologic response was at least 4 months; and (3) the travel time from surface to tunnel was at least 1 yr and less than 6 yr (Wang, et al., 1993). The period of hydrologic response is the time it takes for a given recharge event to cause a corresponding increase in discharge at the seeps in the tunnels. In spite of the large matrix permeabilities of the nonwelded tuffs, fault systems intercepted by the tunnels within the zeolitic horizons provide the bulk of the discharge. An estimate of 10 percent of the total percolation is from 2 seeps in the U12n tunnel while 50 to 60 percent of the 112 mapped faults in the U12e tunnel supplied most of the total discharge from the tunnel system (aqueous discharge through the portal and vapor discharge through the air ventilation system). The analogy to YM is weakened by the observation that nuclear testing probably altered the flow system, but the extent of alteration is unknown.

Observations at the Apache Leap Test Site (ALTS) featuring a sequence of fractured tuffs also suggest fast pathway flow along fractures, although the fracture system at ALTS has far wider apertures than exist at YM; mean aperture is 760 μm at ALTS (Bassett, et al., 1994) and the range of mean apertures is 131 to 497 μm for all units at YM (Sonnenthal, et al., 1997a). At ALTS, intermittent recharge from a stream penetrates to a tunnel 150 m below the ground within days to weeks (National Research Council, 1996). Infiltration tests by Rasmussen and Evans (1993) demonstrated the possibility of high water intake rates on exposed fractured rock surfaces at the Apache Leap site.

The portion of flow that occurs through fast pathways is an important consideration for repository performance. Seepage into the repository is dependent on the partitioning of percolation flux into matrix, dispersed fractures, and fast-pathway fractures or faults. Transmission capacity for matrix flow in the welded units is about 1 mm/yr assuming, that

percolation is gravity-dominated, based on effective conductivities and typical water saturations provided by Flint (1997). Any additional percolation flux is carried in discrete pathways, typically in small-aperture (capillary-dominated) fractures appropriate for continuum approaches or large-aperture (gravity-dominated) fractures or faults that may not be appropriate for continuum approaches. Partitioning between the two fast-pathway alternatives, in part, is related to the physics of flow through small-aperture fractures versus large-aperture fractures, but it is also controlled by focusing mechanisms at the ground surface and at depth. Despite the evidence presented in this section demonstrating that fast pathways occur at YM, it is difficult, however, to estimate the portion of the repository that might be contacted by fast pathways.

The discussion of mass balance of ^{36}Cl in Section 4.4.3.1 looked at the fraction of the perched water having the bomb pulse signature, with roughly 1 to 50 percent ascribable to water infiltrating in the past 50 yr. Murphy (1998) estimated that the bomb-pulse ^{36}Cl signature was primarily evident in three ESF zones, comprising 23 percent of the tunnel, which implies that roughly a quarter of the repository may experience fracture flow if the ESF is representative of the remainder of the repository footprint. Note that Murphy (1998) used a lower threshold to identify bomb pulse ^{36}Cl than was used by Fabryka-Martin, et al. (1997) in order to account for bomb-pulse dilution through mixing.

4.4.2.10 Calculated Distribution of Percolation at the Repository Horizon

A map of estimated spatial distribution of shallow infiltration, on a mean annual basis, was presented in NRC (1997b). The distribution was in qualitative agreement with the map of Flint, et al. (1996a). Using the presumption that flow above the repository is predominantly vertical, the magnitude and distribution of percolation flux at the repository horizon is equal to that of the shallow infiltration. The assumption of vertical flow means that no lateral flow at the PTn is recognized. Current efforts by the NRC staff are focused on further refining percolation estimates by adding the impact of plants and lateral flow at the bedrock interface with the alluvium, colluvium, or atmosphere.

4.4.3 Summary of Deep Percolation Topics That Warrant Further Analysis

Significant variability of flow and transport pathways and travel times is expected to occur at YM due to the natural heterogeneity, stratification, alteration, fracturing, and other characteristics of the site. The extent to which such heterogeneities of the flow system should be incorporated into the DOE site-scale UZ flow model depends on their importance for estimating seepage into the repository and flow below the repository. Conceptualizations of flow in the UZ at YM have ranged from single-continuum models, to equivalent continuum models, to dual- and multiple-continuum models, to discrete-fracture models, as the importance of particular components of the flow system was examined. Given the matrix permeability values (Flint, 1997) and assuming a unit hydraulic gradient, groundwater flowing only in the matrix would move sufficiently slowly that it would take many tens of thousands of years for shallow infiltration to go through the repository horizon and arrive at the SZ. In contrast, both geochemical evidence and transient-flow modeling have suggested that a significant amount of groundwater flux occurs in the fracture system, and that these fluxes can travel at much faster rates than in the matrix. Fluxes in the fracture systems may move sufficiently fast that some component of shallow infiltration reaches the water table in tens to hundreds of years. Differing conceptualizations of the link between the matrix and fracture systems and flow processes in

the fractures cause important differences between alternative conceptual models. The differences in the conceptualizations can have a strong impact on PA modeling and, as such, are the focus of the discussion in this section.

The development of both the repository-scale and drift-scale conceptual models at YM may be partitioned into:

- Percolation processes above the repository, which affect the spatial and temporal distribution of water moving through the repository horizon
- Percolation processes at the drift scale, which affect the release of radionuclides from the repository
- Percolation processes below the repository, which affect the transport of radionuclides from the repository to the SZ

An assessment of current understanding of these three parts of the conceptual model is summarized below for flow above, at, and below the repository.

4.4.3.1 Percolation Processes Above the Repository

Percolation processes above the repository have a direct impact on flow processes at the drifts, by affecting the amount of water that arrives at the repository horizon and the partitioning of that water between matrix and fractures. As discussed in the IRSR related to shallow infiltration (NRC, 1997*b*), water infiltrates into the subsurface in pulses following precipitation events. Some portion of this infiltrating water (net infiltration) eventually escapes downward from the root zone to become deep percolation. Both within wash channels above the repository and where bedrock cover is shallow (i.e., less than 0.5 m), the magnitude of the infiltration pulse can be much larger than the permeability of underlying moderately to densely welded tuff. As there is typically a plentitude of fractures within the Tiva Canyon bedrock, it is anticipated that infiltration pulses below the root zone primarily enter the bedrock fracture system and move under the dominant influence of gravity. There may be some fracture/matrix transfer within the TCw unit, but the percolating water should generally move vertically downward until a zone is reached with increased matrix permeability or reduced fracture permeability. If the fracture system exhibits numerous subhorizontal cooling joints, significant lateral flow may occur within the fractures leading to either a spreading or a coalescing of flow.

Available evidence supports the interpretation of rapid penetration of infiltration pulses into the TCw unit where bedrock alluvial or colluvial cover is shallow (i.e., less than 2 m, which corresponds to all of the repository footprint except for some wash bottoms). Neutron-probe data have been obtained for a network of 99 boreholes, with records extending nearly 10 yr for some boreholes (Flint and Flint, 1995). As discussed by Flint and Flint (1995), the average wetting-pulse penetration depth in the years 1990 through 1993 that was detected by the neutron-probe apparatus was at least 5 m for 12 of the 14 ridgetop and sideslope boreholes considered, with average wetting pulses penetration greater than 10 m in 8 of the boreholes. The neutron-probe methodology is relatively insensitive to fracture flow, so that deeper wetting pulses may have occurred without having been detected.

Further corroboration of rapid penetration of infiltration pulses is indicated by bomb-pulse ^{36}Cl found within borehole ream-bit cuttings. As discussed by Fabryka-Martin, et al. (1997), bomb-pulse ^{36}Cl has been transmitted well into the fractured bedrock (e.g., 20 to 80 m) at all but one of the shallow boreholes examined that has alluvial cover less than 2 m (most have less than 1 m of cover). Bomb-pulse ^{36}Cl was found within the PTn unit in several of the boreholes, penetrating to the TSw unit in one borehole. Bomb-pulse ^{36}Cl evidence (Fabryka-Martin, et al., 1996b) suggests that lateral flow may occur in the TCw and PTn units, based on the existence of multiple peaks in several of the boreholes.

Aside from the lower portion of the west flank of YM, which exhibits outcrops of the TSw unit, the bedded tuffs within the PTn unit form the first barrier to fracture-dominated flow within the repository footprint. These bedded tuffs have relatively large primary permeability and relatively few fractures, and the fracture system tends to be strata-bound (i.e., fractures within the PTn unit are poorly connected to those within the overlying TCw unit and the underlying TSw unit). Montazer and Wilson (1984) hypothesized that the PTn has the potential to significantly attenuate infiltration pulses due to these factors. Simulations (Buscheck, et al., 1991; Nitao, et al., 1992) suggest that an infiltration pulse penetrating to the PTn unit, either in the matrix or in fractures, should end up entirely within the PTn matrix by the time the pulse reaches the bottom of the PTn unless the fracture and the flow rates are quite large, due to strong capillary uptake from the fractures to the matrix. Furthermore, the large storage capacity of the PTn is thought to provide a strong buffer, almost completely damping out the pulse by the time it reaches the bottom of the PTn. If the PTn does damp out infiltration pulses both spatially and temporally, fluxes in the underlying TSw unit may be nearly steady state and total fracture flux would be significantly smaller than in the TCw unit, although the flow in the fractures may still be widespread. However, if the PTn causes lateral diversion and, thereby, focuses flow, fracture flow may be spatially infrequent, but those areas with fracture flow may have large fluxes. As the PTn unit thins from north (roughly 80 m) to south (roughly 20 m) within the repository block (Moyer, et al., 1996), the effects of the PTn unit should diminish from north to south.

The perched water at the base of the TSw unit does not carry a strong geochemical signature of having passed through the PTn matrix, suggesting that the bulk of the perched water may have bypassed the PTn matrix (Bodvarsson and Bandurraga, 1997; Striffler, et al., 1996; Yang, et al., 1996a,b). In particular, the chloride concentration is far larger in the PTn unit than in the perched water. The perched water may be largely the result of lateral flow from Solitario Canyon directly entering the TSw, thereby bypassing the PTn, or from lateral flow from the area of the large hydraulic gradient to the north of the repository footprint. If the perched water primarily results from net infiltration occurring above the repository, the discrepancy between the signatures of the PTn matrix and the perched water suggests that a large component of deep percolation does not pass through the PTn matrix. Flow starting above the PTn unit may bypass the PTn matrix in several ways:

- Connected fracture pathways with fracture coatings that reduce matrix/fracture interaction
- Fine-scale matrix pathways formed by heterogeneity and/or fingering
- Systematic down-dip movement within the fractures above the PTn until a fast pathway, such as a fault, is encountered that focuses flow

The different mechanisms for water moving through the PTn have different influences on flux distributions at the repository horizon within the underlying TSw unit. The TSw unit is similar to the TCw unit: densely welded, with low permeability and extensive fracturing. Matrix fluxes within the PTn unit would tend to preferentially move into the more fine-pored TSw matrix through capillarity, to the extent possible, with the excess perhaps moving downdip until sufficient pressure builds up to overcome the matrix/fracture capillary barrier. Flux pulses bypassing the PTn matrix via fractures may tend to remain within fractures in the TSw if the fracture sets are connected. As bypass fluxes become large, it becomes increasingly unlikely that the TSw matrix can conduct all percolation flux and more likely that fracture flow is initiated where the bypass fluxes contact the TSw unit.

The chloride mass balance technique, as applied by Fabryka-Martin, et al. (1996b), assumes that average chloride concentration multiplied by total flux is conserved, and flows are approximately steady state. To roughly estimate the relative components of PTn matrix flux and bypass flux, assume that:

- $C_m Q_m + C_b Q_b = C_p (Q_m + Q_b)$, where C represents concentration, Q represents flux, and the m, b, and p subscripts represent matrix, bypass, and perched components, respectively.

- Bypass fluxes arrive at the perched water body with the chloride concentration of rainfall (0.62 mg/L) that was used by Fabryka-Martin, et al. (1996b)

- PTn fluxes arrive with an average chloride concentration of 62 mg/L [a number near the middle of the range of observed PTn values reported by Fabryka-Martin, et al. (1996b)]

- Chloride concentration in perched waters is 6.2 mg/L [a typical value from Yang, et al. (1996a)]

Using these chloride concentrations in a simple mass-balance calculation, which requires that chloride from both matrix and bypass fluxes fully mix in the perched waters, suggests that bypass fluxes are roughly ten times as great as PTn matrix fluxes. As the chloride concentration in the bypass fluxes increases (indicating evaporation within the subsurface), the ratio of bypass flux to matrix flux also increases.

Using a similar mass balance technique for ^{36}Cl, the ^{36}Cl signatures from both perched water and pore waters can be used to roughly estimate flux rates for the bomb-pulse portion of the perched waters. Based on Table 4-16 by Fabryka-Martin, et al. (1997), the ratio of ^{36}Cl to chloride in perched waters obtained from boreholes NRG-7a, SD-7, SD-9, UZ-1, and UZ-14 ranges from 449×10^{15} to 999×10^{15} with a mean of 590×10^{15}. Comparable ratios from 5 samples from the TSw unit [SD-12 and ONC boreholes in Table 4-11 of Fabryka-Martin, et al. (1997)] are 235×10^{15}, while the deepest non-bombpulse sample obtained from the PTn unit in boreholes N37, N53, N54, UZ-14, and UZ-16 average 345×10^{15} [Table 4-10 of Fabryka-Martin, et al. (1997)]. Seven borehole observations within the PTn unit were greater than $10{,}000 \times 10^{15}$, with a peak value of $32{,}400 \times 10^{15}$. Within the ESF, 21 of the 141 samples obtained from formations in or below the upper lithophysal zone of the TSw unit

(station 18+00 to 69+00) were above 1,250 × 10^{15}, with a maximum of 4,100 × 10^{15}. Several calculations can be made:

- Assuming that the perched-water ratio is 590 × 10^{15}, pore waters have the TSw ratio (235 × 10^{15}), and fast-path ratio is 4,100 × 10^{15}, about 10 percent of perched water has a bomb-pulse signature.

- Assuming that pore waters have the PTn ratio (345 × 10^{15}), and the fast-path ratio is the largest observed at YM (32,400 × 10^{15}), about 0.8 percent of perched water has a bomb-pulse signature.

- Assuming that pore waters have the TSw ratio (235 × 10^{15}), and the mean fast-path ratio is 1,250 × 10^{15}, more than 50 percent of perched water has a bomb-pulse signature.

- Assuming that fast-path fluxes are 10 times greater than matrix fluxes, and pore waters have the PTn or the TSw ratio, the fast-path ratio is 626 × 10^{15} and 615 × 10^{15}, respectively.

From these considerations, it is likely that at least one percent, and perhaps more than half, of the perched water infiltrated in the past 50 yr. However, flux information derived from the chloride calculations yields an estimated ratio so low that it is unlikely that all of the bypass fluxes are younger than 50 yr unless a significant portion of the perched waters come from post-bomb-pulse waters. The magnitude and spatial distribution of fracture fluxes within the TSw are likely to have a profound impact on repository performance. As discussed in Section 4.4.2.4, capillary effects tend to preclude entry of liquid into open cavities in unsaturated porous media, particularly when the medium is as fine-grained as is the TSw matrix, so that flows in the matrix will tend to divert around the drifts rather than entering the drifts. Capillary-exclusion effects are less important for fractures, especially larger fractures, so that flows in fractures are less likely to divert around drifts. The larger the flow in a fracture, the less important capillary forces are relative to gravity and the less likely that diversion will occur around a drift intercepted by the fracture. If the fracture supports film flow, only viscous and gravity forces significantly affect the flow (Kapoor, 1994) so that capillary forces are unlikely to prevent entry into the drift.

As with the TCw unit, matrix/fracture interactions are likely to be relatively limited within the densely welded TSw unit, and flows are likely to be predominantly vertical. Hence, the distribution of fracture flows initiated in the TSw at the bottom of the PTn is likely to be propagated vertically downward to the repository horizon with some spreading or coalescing of flow paths possibly occurring.

- **Modification of Percolation Due to the Paintbrush Nonwelded Unit**

The possibility that the PTn unit may cause lateral diversion due to capillary effects (at the TCw/PTn interface) or permeability effects (at the PTn/TSw interface) has long been recognized (Montazer and Wilson, 1984). The effectiveness of the PTn unit in attenuating pulses or causing lateral diversion has been examined by numerous researchers (Prindle and Hopkins, 1989; Ross, 1990; Buscheck, et al., 1991; Nitao, et al., 1992; Brown, et al., 1993, Altman, et al.,

1996; Bodvarsson and Bandurraga, 1996; Fabryka-Martin, et al., 1996a, b, 1997; Moyer, et al., 1996; Robinson, et al., 1996, 1997; Rousseau, et al., 1996; Wilson, 1996; Wolfsberg, et al., 1996; Fairley and Wu, 1997; Wu, et al., 1997; Ofoegbu, et al., 1997). In general, the PTn matrix is considered to have the potential to strongly attenuate pulses, due to large storage capacity, high matrix permeability, and capillary effects that strongly imbibe fracture waters into the matrix. The strong attenuation potential within the PTn, which would tend to reduce fluxes below the PTn to nearly steady, is often used to justify the modeling assumption that fluxes are at a steady state throughout YM. Depending on model assumptions and model parameters, however, disparate results for lateral diversion are obtained. For example, Prindle and Hopkins (1989) and Ross (1990) suggest lateral diversion increases as net infiltration increases while modeling studies reported by Bodvarsson and Bandurraga (1996) suggest that the capillary barrier effect decreases with increasing net infiltration.

Several factors appear to play a major role in determining the role of the PTn unit in attenuating and diverting infiltration pulses:

- Fracture/fault interaction with the PTn matrix
- Infiltration model
- Hydraulic properties
- Stratigraphy

Early models generally assumed that infiltration was quite small (less than 1 mm/yr) and at steady state; the PTn unit did not have significant fractures or fractures were included using the ECM conceptual model; hydraulic properties were based on early measurements reported by Peters, et al. (1984) and Klavetter and Peters (1986); hydraulic properties within layers were homogeneous; and microstratigraphy was usually not considered (e.g., several bedded-tuff layers were consolidated into the PTn unit). With such small and steady infiltration rates, the (assumed-homogeneous) matrix is sufficiently permeable to carry all percolation fluxes and fracture flow is inhibited due to capillary effects. These early models tend to indicate that significant lateral flow may occur. Significant lateral flow may be generated in the PTn in the absence of vertical discontinuities even when detailed microstratigraphy and updated hydraulic properties are considered (Moyer, et al., 1996).

Sampling from within the ESF and in deep boreholes has revealed bomb-pulse ^{36}Cl and ^{3}H in numerous locations (Fabryka-Martin, et al., 1996a, 1997; Yang, et al., 1996b), which requires that for at least some flow paths travel times are less than 50 yr to the repository horizon and the base of the TSw unit. In addition, calcite and opal fillings (their origins may be associated with fracture-flow paths) have been observed in numerous fractures within the ESF, and the portions of the PTn penetrated by the ESF exhibit numerous small-offset (slump) faults. Spurred by these observations, conceptual models have been modified to emphasize the role of fractures and faults and to consider the role of transient infiltration pulses. Recent models tend to exhibit predominantly vertical flow, less lateral diversion, and a small component of the flow bypassing the PTn matrix in fast pathways. However, significant systematic lateral flow (e.g., 500 m) is still produced with some calibration parameter sets (Bodvarsson, et al., 1997a).

Sweetkind, et al. (1995) conclude that observations of fractures in the PTn unit at 22 outcrop locations do not support interpretations of significant fracture flow within the PTn unit, due to the generally stratabound nature of the observed fractures and lack of alteration products within the fractures (although calcite fillings were observed in some of the fractures). If correct, this conclusion implies that fast pathways within the PTn, if they exist, are fault-derived or due to heterogeneity-derived channels in the matrix.

Field evidence for lateral flow within the PTn unit is derived primarily from geochemical data, such as inversions in concentration as depth increases. Kwicklis (1996) suggests that at least limited lateral redistribution may be indicated by inversions of aqueous ^{14}C data with depth in borehole UZ-14, although these inversions may also be due to fracture flow. Fabryka-Martin, et al. (1997) suggest that a model postulated by Paces, et al. (1997), in which percolating waters with two distinct strontium isotopes (resulting from areas with ridge crests and sideslopes without thick calcretes, and areas with thick calcite- and Sr-rich soils) requires mixing through lateral flow in the PTn unit to explain observed profiles within borehole SD-7.

The UZ expert elicitation panel had based its conclusions on available evidence for infiltration and deep percolation as of the end of 1996. The panel noted that lateral diversion might be expected at the TCw/PTn and PTn/TSw interfaces, and perhaps within the PTn itself, if textural differences alone were considered (Geomatrix, 1997). However, the panel generally agreed that the series of small slump faults observed in the ESF within the PTn would serve to capture flow moving laterally, diverting the flow vertically down the faults. Thus, the expert panel concluded that lateral diversion might occur over a few meters to tens of meters, but lateral diversion would not be expected to occur over a much larger scale. Most of the experts, accordingly, expected that the spatial distribution of percolation flux at the repository level is similar to the spatial distribution of net infiltration, although perhaps smoothed. One expert believed that there may be focusing processes as well as smoothing process, perhaps funneling flow into locally high-flux zones.

Two mechanisms that promote bypassing of the PTn matrix apparently have not been quantified to date: (1) potential lateral fluxes, in response to large infiltration pulses, in a TCw fracture system that is strata-bound (i.e., that terminates above the PTn); and (2) vertical fluxes in localized pathways within the PTn matrix. In the first case, large pulses of water may proceed rapidly down to the base of the fracture system. If the fractures are strata-bound or are filled with alteration products that drastically reduce fracture permeabilities, the infiltration pulse may tend to rapidly redistribute downdip until a fast pathway is encountered. If faults are not ubiquitous or if the moist conditions at the bottom of the TCw have caused widespread alteration, lateral redistribution within the TCw fracture system may be significant. In the second case, heterogeneity within the PTn matrix may cause local fast pathways within the matrix, which may not be captured by current estimates of grid-block-scale parameters. Potential causes and effects of misrepresenting heterogeneity are discussed in Section 4.4.2 3.

The NRC staff concludes that systematic lateral flow within the PTn may not occur in the vicinity of the ESF observations and would be similarly unlikely if the PTn is generally faulted over the repository block. The PTn unit is observed only in a relatively small portion of the ESF east of the GDF, and it is possible that the observed faulting is not typical of the relatively less distorted areas west of the GDF. If small-scale PTn faulting is much less frequent over the repository block, lateral flow diverting into faults may serve to localize flow rather than to prevent localized

flow. In the absence of evidence to the contrary, however, the NRC staff endorses use, in PA, of the assumption that general lateral diversion does not occur above the repository, as this conservatively passes all net infiltration generated within the repository footprint to the repository horizon.

- **Focusing of Flow Due to Faults**

There is solid evidence that faults have large permeabilities, based on observations of barometric attenuation and phase lag during the excavation of the ESF (Ahlers, et al., 1996; Nilson, et al., 1991; Patterson, et al., 1996). The character of barometric response was altered kilometers from the ESF (e.g., in borehole ONC-1), apparently due to the interaction of faults with the ESF. Faults therefore represent potential fast pathways providing water to the deep subsurface. If water is diverted laterally into the fault, these potential fast pathways may carry substantial quantities of flow. However, if no waste is emplaced close to the faults, then this water is not intercepted by those waste packages. Fault-permeability estimates presented by Sonnenthal, et al. (1997a) (their figure 7.7) range from 3×10^{-13} to 6×10^{-10} m^2. Sonnenthal, et al. (1997a) further categorize faults into normal faults (large- and small-displacement) and strike-slip faults, all with different deformation features (fracturing gouge) resulting from different formation processes.

Observations of bomb-pulse ^{36}Cl in the ESF have prompted LANL and USGS researchers to hypothesize that three conditions are required for observations of flowing water to occur within the ESF (Fabryka-Martin, et al., 1997):

- A continuous fracture path must extend from the surface to the sampled depth (implying that a fault must cut through the PTn)
- Values of MAI at the surface must be at least 1 mm/yr (in order to initiate and sustain fracture flow)
- The residence time of water in alluvium must be less than 50 yr (alluvial thickness must be less than 3 m)

As noted by Fabryka-Martin, et al. (1997), predictions based on these conditions appear to be reasonably consistent with observations in the northern half of the ESF but are inconsistent with the paucity of bomb-pulse ^{36}Cl observations in moist fractures in the southern half of the ESF. Fabryka-Martin et al. (1997) suggest that, if the conceptual model for observations of bomb-pulse ^{36}Cl in the ESF is correct, requiring that the PTn be cut by a fault, then there may be significant connection between the fault and fractures in the welded unit. This suggestion is based on observations of bomb-pulse ^{36}Cl spread laterally downdip from the Sundance Fault (SDF) in a swath 300 m wide within the ESF (Levy, et al., 1997), which appears to travel laterally as much as 200 m within subhorizontal cooling joints in the middle nonlithophysal zone. An important implication of these observations is that significant downdip redistribution may occur within the fractures of at least some densely welded units, although fracture permeabilities are inferred to be as much as ten times greater in the vertical than the horizontal direction (Sonnenthal, et al., 1997a). Nicholl and Glass (1995) offer further evidence that considerable spreading can occur within the TSw fracture system, demonstrated with a ponded infiltration experiment at Fran Ridge where the TSw unit crops out. Thus, even if systematic

lateral redistribution in and above the PTn unit does focus flow into faults, these locally concentrated fluxes may be significantly smoothed through lateral spreading before reaching the repository horizon

Water will not enter a fault in the UZ unless the matrix is sufficiently saturated to overcome the capillary barrier represented by the fault. Other barriers, such as low permeability fracture coatings, may also be present. In order to focus flow within a fault possessing a significant capillary or other barrier, it is necessary for water to collect updip of the fault. This collected water will tend to make the updip side of the fault, where water is entering the fault, wetter than areas further updip from the fault, and thereby may cause enhanced vertical flows below the wetter region. As the main drift of the ESF parallels the GDF on the updip side, inferences drawn from observations within the ESF may be unrepresentatively wetter than the repository block as a whole if vertical fluxes are enhanced through significant collected water above the ESF. Note that waters within the GDF are likely to exit through gravity, so that the matrix in the immediate vicinity of the west-dipping fault is likely to increase in wetness as the fault is traversed from west to east at the ESF elevation.

The impact of a fault is likely to be most significant when the fault is perpendicular to the stratigraphic dip. From geometric arguments (all else being equal), north-trending faults at YM (e.g., the GDF) may tend to have a greater impact on UZ flow than north-west-trending faults (e.g., the SDF) as flows can divert around north-west-trending faults, to some extent. On the other hand, different fault-forming mechanisms may yield significantly different hydraulic properties, which may override the geometric arguments.

The focusing or spreading of flow, and the flow pathways in general, under current conditions does not necessarily reflect that under future conditions. A change in the amount and distribution of infiltration may lead to a change in the predominant flow pathways, or at least change the proportions of flow in various pathways. Also, active tectonic stresses on the YM block may alter the flow pathways by modifying the hydrologic properties along the fault or by creating new pathways. It is likely that reductions in fault and fracture apertures in one area may be accompanied by the dilation of other discontinuities. The NRC staff review of DOE methods may need to consider the potential impact of structural changes to the fault system. One approach would be to analyze the sensitivity of repository performance to altered patterns of percolation.

- **Influx on the West Flank**

Solitario Canyon may provide sources of infiltrating water with potential for impacting repository performance. These sources include infiltration from numerous small channels incised into the bedrock of the west flank of YM, distributed infiltration from the shallow colluvial cover and bedrock exposures on the west flank of YM, and percolation along the SCF. The potential for these sources to impact repository performance has not been quantitatively evaluated to date.

Portions of the west flank of YM lie above the repository footprint but below the PTn outcrop, so that infiltration in these areas may reach the western edge of the repository with none of the PTn buffering discussed in Section 4.4.2.3. Although the west flank of YM is steep, fractured bedrock has minimal surface cover in many locations, which may enable significant infiltration. Any waters infiltrating below the PTn outcrop may flow directly to the repository or may continue

to the TSw/CHn interface and flow laterally to form part of the perched water bodies observed at this interface. The possibility of direct recharge within the TSw outcrop was noted by the State of Nevada (Lehman, 1992; L. Lehman, letter to E. Smistad and A. Van Luik, November 14, 1994).

The main Solitario Canyon channel is west of the SCF and does not lie above the footprint. Based on geometric arguments and the predominance of vertical flow, it does not appear likely that flow from the main channel during large runoff events will move laterally towards the repository. However, the SCF offsets sufficiently near the repository block to juxtapose the PTn unit, to the west of the fault, with the TSw unit, to the east of the fault. Under these conditions, it is plausible to expect that any lateral diversion occurring in Solitario Canyon will intercept the SCF (Lehman, 1992). Since there is no evidence for or against flow moving across the fault zone in the UZ, and there is little evidence for lateral flow in the PTn above the repository footprint, it is considered unlikely that groundwater flow from beneath the channel during runoff events will laterally move towards the repository along stratigraphic boundaries.

However, any laterally diverted percolation fluxes from Solitario Canyon may pass across the steeply west-dipping SCF and proceed vertically to the CHn unit. The diverted waters from Solitario Canyon may then form a significant portion of the perched water bodies observed at the TSw/CHn interface. This scenario has implications for the formation of the perched water beneath the repository as well as implications for dilution of radionuclides below the repository.

The potential for influx from Solitario Canyon was considered briefly and dismissed by two expert panels (Unsaturated Zone Hydrology Peer Review Team, 1991; Geomatrix, 1997) without quantitative justification. Nevertheless, there is potential for significant inflow arising from along the west flank of YM in Solitario Canyon to pass through the repository footprint. The SCF impacts repository design in terms of standoff distance from fault zones and flow in along the fault may contribute to the perched water bodies.

4.4.3.2 Percolation Processes at the Drift Scale

An understanding of the nature of water flow into drifts is important for two reasons: first, water in the vicinity of WP may elevate relative humidity, thereby, accelerating corrosion and WP failure; second, almost all radionuclides are expected to have a dominant release pathway of water traveling through drifts, contacting waste, and transporting dissolved or colloidal waste through the geologic setting.

- **Nature of Flow Into Drifts (Drift Seepage)**

The conceptual model developed for unsaturated flow through repository drifts depends, to a large extent, on whether drifts will be backfilled after waste emplacement and, if so, on the type of backfill material used. If backfill is to be used, it is necessary to take into consideration the moisture retention and permeability properties of the backfill before an effective assessment of the effects on flow can be considered. For example, a coarse, well-sorted backfill would allow water to pass easily through the drift; it would have a very low residual water content; and it would not produce enough capillary suction to imbibe water from drift walls. Conversely, a fine or poorly-sorted backfill would have a lower permeability, a higher residual water content than the well-sorted backfill, and could imbibe water out of drift walls toward the WP, depending on

the saturation of the ESF wallrock. Although the higher capillary suction of a fine, poorly-sorted backfill can result in more uniform contact of water with the WP surface, the same capillary suction could prevent water from entering the WP. Shotcrete coatings on walls of tunnels or emplacement drifts, if applied, would have an effect on dripping patterns. This would have to be independently evaluated by the staff. The USGS (1998) has submitted to DOE a level 4 milestone report, SPH261M4, regarding the hydraulic properties of backfill materials. The staff have not yet evaluated this report.

In the absence of backfill, water dripping from the drift crown is the only mechanism for water to directly contact the WP. In this case, there are several factors that should be considered in estimating the amount of water that could potentially drip onto a WP. For example, the angle that a fracture intersects a drift will affect the potential for fracture flow to divert laterally around the drift. The dip angle will also affect the amount of water required to overcome any capillary barrier to dripping. The hydraulic properties of a fracture affect the fluxes within the fracture and the degree to which a capillary barrier between fractures and the open drift will act to divert flow around the drift. Several other factors, such as fracture frequency, fracture intersections, fracture coatings, and degree of heterogeneity, should also be considered. Long-term dripping from fractures is also likely to result in stalactite formation—especially in the high-evaporation environment that could result from WP heating. Formation of stalactites tends to focus fracture dripping on constant locations.

The case of partial filling of the drifts with backfill will exhibit features of both the full backfill and no backfill scenarios. Diversion of matrix flow and dripping from fractures may occur at the crown of the drift The dripping water plus water imbibed from sidewalls of the drift will be somewhat distributed around the WP, although vertical flow through the backfill from a dripping crown would concentrate some of the moisture.

A conservative approach to incorporating drift seepage into PA models is to assume that 100 percent of the percolation flux that intersects a drift will enter the drift opening and contact a WP. Only a fraction of percolating waters is likely to enter drifts based on geometric arguments, i.e., the relatively small percentage of repository area that will contain waste packages. Also, because of the capillary barrier imposed by the drift opening, some percolation flux is expected to be diverted around the drift. Presumably, there is a percolation threshold, below which no seepage into the drift will occur. The DOE PA model currently takes credit for diversion of flow around drifts; their characterization of drift seepage is based on both modeling and field studies. A more conservative approach than 100 percent of the percolation flux intersecting the drift may be envisioned if focusing or funneling of flow incorporates flow from a larger area than the repository into the repository. Given the intensity of fracturing in the TSw, NRC staff believe that, on the average, the amount of flow funneled to the repository will be the same as the amount funneled away from the repository. New information on the fracture system in the TSw may change the NRC staff views on seepage into drifts.

Wang, et al. (1997) reported preliminary results of field seepage tests conducted in two niches in the ESF. Of the five tests conducted, one did not result in flow into the niche; another induced flow to reach the ceiling and migrate along the mined surface as film flow, but water did not drip into the niche; and dripping from fractures into the niches was observed in the remaining three tests. Of the three tests where dripping was observed, the mass of water collected in the fluid collection system ranged from 9.5 to 27 percent of injected mass. The

NRC believes that the niche and alcove tests are extremely useful for corroborating drift-scale numerical model and that measurements and experiments in the east-west drift will similarly provide useful information.

Birkholzer, et al. (1997a,b) used a 3D fracture continuum model to simulate seepage into drifts under both isotropic conditions and anisotropic permeability conditions. Heterogeneity was applied to the permeability field with no consideration of possible correlation between permeability and fracture α values. The modeled steady-state percolation fluxes ranged from 5 mm/yr to 1,000 mm/yr. Seepage into drifts was found to start when steady-state percolation fluxes were on the order of tens of millimeters per year, with heterogeneity in the fracture continuum being a key factor controlling the rate of seepage. The same fracture continuum model was used to simulate the niche studies, with generally good agreement between the model and observations, reportedly occurring with no calibration or fitting (Birkholzer, 1998).

A similar modeling effort was conducted using 2D and 3D dual-permeability models with a fracture-matrix interface factor to allow for a reduced wetted contact area between fractures and matrix. Results of this effort, reported by Tsang (1997), indicate that the inclusion of fracture-matrix interaction is only important when percolation flux occurs as transient pulses.

A continuum model requires definition of a representative elementary volume (REV). This requires that any heterogeneities should be incorporated at a scale either much smaller than the grid scale (i.e., subgrid heterogeneity) or much larger than the grid scale (i.e., parameter variability within the model). Accordingly, the assumption of a fracture continuum requires that the fractures either be numerous relative to the grid scale (subgrid) or be explicitly accounted for (parameter variability within the model). Sonnenthal, et al. (1997a) report that measured fracture frequencies in the TSw unit (counting only fractures at least 1 m in length) range from 0.48 to 4.45 m^{-1}. If the continuum approximation requires numerous fractures, a continuum approximation for fractures of this size and larger may require tens of meters to achieve a representative elementary volume, which is larger than the drift diameter. Using an *ad hoc* criterion of 5 fractures per grid block length to enable the fracture-continuum assumption, drift-scale simulations with 0 5-m grid blocks (fairly coarse) would require fracture frequencies of roughly 10 m^{-1}, implying that the assumption of a fracture continuum may be violated at the drift scale and models assuming a fracture continuum may misrepresent important fracture/drift interactions.

The assumption of uniform, steady-state infiltration in the fracture continuum model does not take into account potential episodic fracture flow. Modeling results that indicate that the PTn unit has a large capacity to attenuate large infiltration pulses, together with the presence of the PTn over almost all of the repository footprint, support the assumption of steady-state conditions at the repository horizon. However, given the existence of perched water at the base of the TSw that shows geochemical evidence of having partially bypassed the PTn (e.g., Striffler, et al., 1996; Yang, et al., 1996a,b), the potential for episodic infiltration pulses should not be discounted entirely

In a fracture continuum model, diversion of percolation flux around the drift is possible at all spatial locations, due to the continuum assumption, and diversion is controlled by random heterogeneities. In reality, the diversion path of fracture flow around a drift is controlled by geometric factors, particularly, fracture orientation: fractures that intersect the drift at highly

oblique angles require a longer flow path for diversion and, thus, are more likely to result in dripping. NRC staff believe that correlation structures used in the DOE fracture continuum model do not appear to capture this effect of increased diversion path length caused by oblique fractures. Moreover, continuum models do not account for fracture intersections, which may form highly permeable linear pathways that can focus flow toward drifts. Furthermore, it is assumed in the fracture continuum model that all water in fractures is influenced by capillarity; the possibility of sheet-type flow in large-aperture fractures is not considered. Because sheet flow along surfaces of large-aperture fractures is not held by capillary forces, it is more likely to result in dripping where such flows intersect drifts. The predominance of sheet-type flow in fractures at the ESF horizon may be supported by the predominance of fracture coatings (Paces, et al., 1998b) occurring on only one side of the fractures.

Fracture permeability distributions used in the DOE fracture continuum model are based on drift-scale air permeability measurements, analysis of cores, and ESF fracture mapping. Estimations of fracture α values are based on calibration of the Site-Scale UZ Model (Bodvarsson and Bandurraga, 1997a). In general, narrow-aperture fractures are expected to have lower permeability and more capillary suction (lower α values), with the opposite being true for wide-aperture fractures. Inclusion of such a correlation in seepage models would cause low-permeability fractures to have higher saturations than high-permeability fractures, which may affect both seepage into, and diversion around, drifts. Correlation between fracture permeability and fracture α value is not considered in the DOE model, although it is recognized that both fracture frequency and fracture aperture affect fracture permeability, while only fracture aperture affects fracture α. Dual-permeability drift scale-model results, reported by Tsang (1997), predict a reduction in drift seepage, when fracture α values are correlated to fracture permeability. Based on this result, a lack of correlation between these parameters in a seepage model can be considered a conservative assumption.

An additional caution regards the use of air-permeability testing to infer fracture hydraulic permeability. There is a possibility that water-bearing fractures could exhibit low air permeability because of water filling the fracture voids. This would be especially true for narrow-aperture horizontal fractures with high capillary suction, which can wick away significant quantities of water. In areas where the horizontal fractures have smaller apertures than the vertical apertures, capillary suction may generate a moisture-dependent anisotropy for water that is primarily horizontal rather than vertical at low saturations.

- **Distribution of Drifts with Potential for Seepage**

The quantity and distribution of water that seeps into drifts depends on the amount and spatial variability of deep percolation that reaches the repository horizon, and on the variability in hydraulic properties of fractures that intersect drifts. Two quantities are used to parameterize seepage into drifts for the DOE model: the seepage fraction and the seep flow rate. The seepage fraction is defined as the fraction of WP contacted by seeps while the seep flow rate is the flow rate onto those packages that are contacted by seeps. Ranges for these parameters are estimated stochastically, using the 3D heterogenous fracture continuum model described in the previous section; they are based on weighted distributions of fracture permeabilities and α values, and a broad range of percolation fluxes are used in this estimation method. It is assumed that there is no correlation between these model input parameters. Based on the distribution of fracture properties, a distribution of seepage threshold fluxes is calculated, and

the seepage fraction is the fraction of drifts that receive percolation flux above their respective seepage thresholds while the seep flow rate is the portion of percolation flux in excess of the seepage threshold. In the DOE PA model, seepage is calculated for six repository regions under present climate conditions, long-term average climate, and a super-pluvial climate. It is presently assumed by DOE that all seepage that enters the upper half of a drift will contact a WP.

The NRC approach to incorporating seeping drifts into a PA model is currently based on the approach used in TSPA-95 (TRW Environmental Safety Systems, Inc., 1995), assuming that the matrix will carry all fluxes up to the matrix K_{sat} with any excess flows occurring in the fractures. Matrix fluxes are assumed to divert around the drift, while fracture flows enter the drift, with both the matrix K_{sat} and the percolation fluxes assumed to be independent and lognormally distributed.

An option under consideration by DOE for emplacement of canisters is to create a stand-off distance from fault systems that have been recently active on a geologic time scale. An active fault is one that has indications of movement over the last 2 million yrs (Elater and Nolting, 1996). Stand-off of 60 m is limited to the active faults, such as the SCF, the Drill Hole Fault, and the Abandoned Wash Fault. However, for the GDF, the distance that canisters should be shifted away from the fault is 120 m due to the large air permeability values and large fracture zone width (Elater and Nolting, 1996). The NRC staff review of methods used for determination of stand-off distance should consider variability along fault systems, both the dip of the fault and the strike of the fault relative to the drift, and the geochemical evidence suggestive of spreading laterally away from faults. In the ESF, ^{36}Cl appears to have spread laterally away from the main fault trace of the SDF over 200 m along the cooling joint system (Levy, et al., 1997).

4.4.3.3 · Percolation Processes Below the Repository

The nature of percolation below the repository horizon affects the formation of perched water, the spatial distribution of flux to the water table, groundwater velocities, and radionuclide advection, dispersion, sorption, and decay. If percolation is dominated by matrix flow through the CHn rather than fast pathways, slow travel times, increased adsorption (with resulting augmentation of retardation and decay), and mixing with the relatively large volume of water in the matrix pores are expected to occur. The potential for adsorption is particularly great in zeolitic horizons.

Flow paths from the repository horizon to the base of the TSw unit are expected to be predominantly vertical within the TSw fracture system. At the base of the TSw unit and below, flow paths are more uncertain. In nonwelded vitric units, flows are expected to be predominantly vertical within the matrix, but fracture flow may occur as well. In areas with significant zeolitization, there may be complex combinations of matrix and fracture flows, with strong possibilities of lateral flow. The nature of flow through the CHn is the primary source of uncertainty in flow paths and travel times from the repository to the water table.

- **Flow Through Non-Welded Vitric and Zeolitic Horizons**

Percolation in the TSw unit is expected to occur primarily in the fracture system. The highly fractured TSw basal vitrophyre overlies the porous nonwelded CHn, leading to the possibility of

lateral flow and perched water in areas where the vertical transmission rate of the CHn is exceeded. The presence of perched water above altered units in the CHn signifies slow vertical percolation within the altered units, providing the potential for lateral flow to bypass the altered zones and enter faults or unaltered zones. The absence of perched water above the vitric portions of the CHn suggests that percolation is rapid enough to conduct fluxes under current climatic conditions.

The vitric zones are sufficiently permeable that percolation may be primarily within the matrix. Zeolitic alteration of glassy tuffaceous material has been shown to drastically reduce permeability without significantly affecting porosity (Loeven, 1993). Measured permeabilities in the vitrified and de-vitrified horizons are generally 1 to 2 orders of magnitude higher than in the altered zones. Hydraulic conductivity measurements of 5 vitric samples from the CHn range from about 1×10^{-5} to 5×10^{-6} m/s, whereas, zeolite-altered core measurements ranged from about 3×10^{-7} to less than 1×10^{-12} m/s [the lower limit of the measurement technique (Flint, 1997)]. The saturations in vitric units are generally lower than those in altered units, indicating greater drainage properties for the vitric versus the altered (zeolitic).

Flow in the vitric portions of the CHn may also be through fractures. The characteristics of fractures and fast pathways in the vitric portion of the CHn are not well known. However, there are indications that water moved quickly into the vitric zones. Major element chemistry and ^{14}C data suggest that matrix water below the perched water is distinct from the perched water (Fabryka-Martin, et al., 1997; Rousseau, et al., 1996). The underlying matrix water appears to be younger, and to have bypassed the perched water in the CHn layers. This could be explained either by fracture flow through the vitric or matrix flow through a small thickness of the vitric layers followed by lateral flow beneath the perched zone. Where the vitric overlies the zeolitic alteration, the transitional contact in the north is less than 20 m below the basal TSw vitrophyre in the north and 460 m below in the southwest (Rousseau, et al., 1996).

The impact of large structural features on travel times could be significant. According to Ritcey, et al. (1997a), the fastest travel times are expected for paths in the center of the repository block where a greater amount of fracture flow would occur or where flow might be along stratigraphic contacts to structural features such as the GDF and Dune Wash Fault. The hydraulic properties of the faults dictate whether perching or drainage down the fault to the saturated zone will occur. Wu, et al. (1996) hypothesized that travel paths south of Dune Wash divert to the east, and, if the GDF is neither a barrier nor a conduit, continue eastward in the fractured TSw to meet the water table near the Bow Ridge Fault. However, the perched water noted in boreholes SD-7, SD-12, SD-9, NRG-7, UZ-1, UZ-14, G-2, and WT-6 is an indication that the GDF is likely (at least locally) to be a barrier with relatively low permeability, and possibly altered near the perched water. There are insufficient data on the lateral characteristics of the GDF to determine the continuity of perched zones at YM.

The CHn mineralogy is highly variable, with both lateral and vertical gradational variations, due to nonuniform alteration of parent tuffs. The general distribution of zeolitic alteration in the repository block is described by Moyer and Geslin (1995) and Carey, et al. (1997). Based on the interpretations of Moyer and Geslin (1995) and Hinds, et al. (1997), there is a gap in the zeolite alteration in the southwestern portion of the repository area (Figure 3). The LBNL model (Hinds, et al. 1997) is based on four layers in the geologic stratigraphy from the basal TSw,

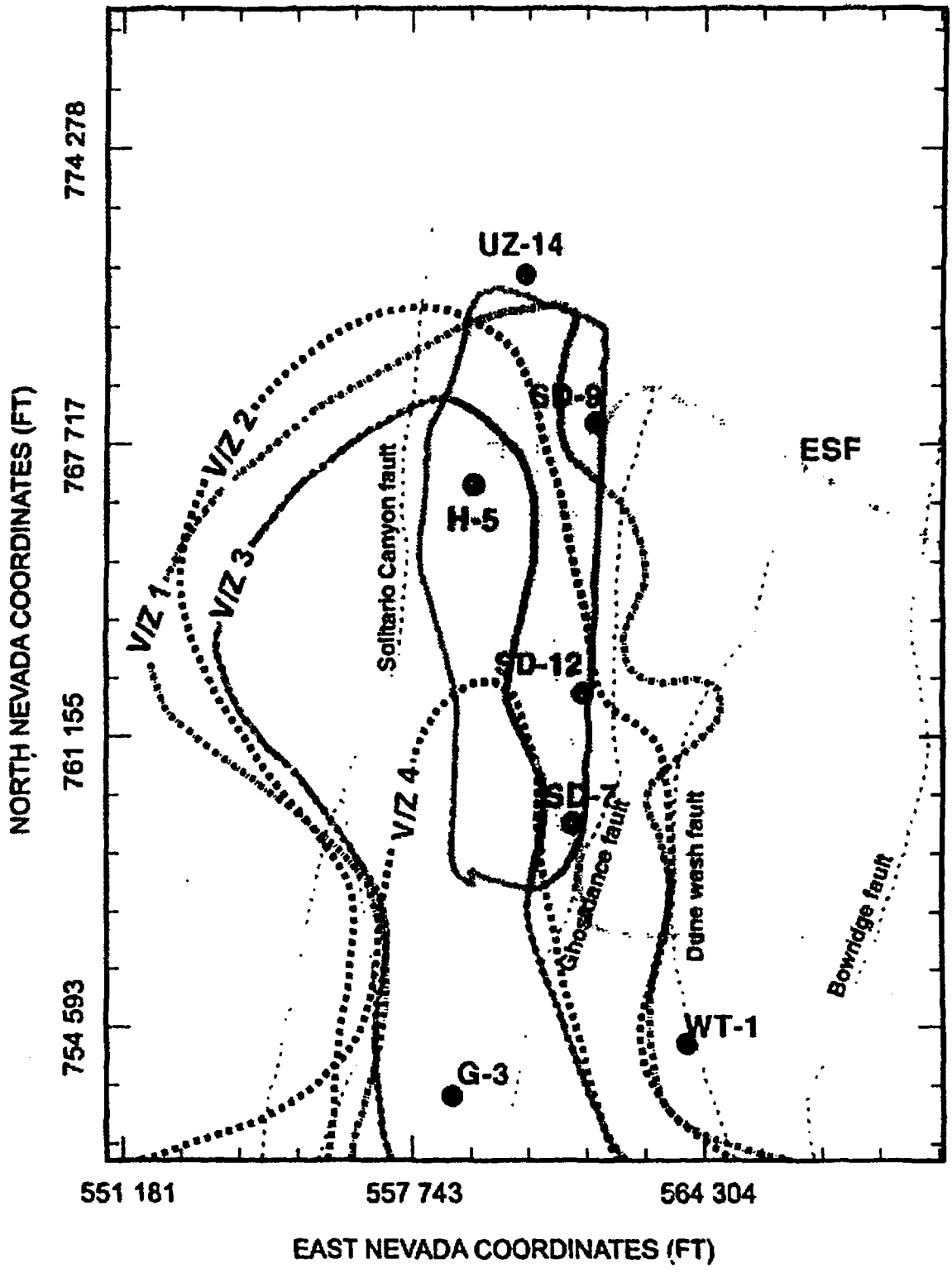

Figure 3. Transitions from zeolitic to vitric zones in the basal vitrophyre of the Topopah Springs Tuff, the Calico Hills Unit, and upper Prow Pass Tuff used by Lawrence Berkeley National Laboratory in the site-scale unsaturated zone model. The model accounts for fo layers, all of which include a transition (V/Z) from vitric to zeolitic. This figure is a modifie version of Figure 4-8 (page 4-12) of Bodvarsson, et al. (1997a).

through the CHn, to the upper Prow Pass unit Each sublayer is divided into a homogeneous layer of vitric or zeolitic portions as delineated by a threshold of ten weight percent zeolite alteration. In the LBNL model, appropriate hydrologic properties for each zone are assigned, but are kept uniform throughout each zone. However, given the limited data available to support this generalized description of the zeolite distribution, new information may significantly change the interpretation

In contrast to the LBNL interpretation, the LANL site-scale flow and transport modeling (Robinson, et al., 1997) used the ISM2.0 geologic framework and adds a mineralogic module that modifies the CHn sublayer properties based on the amount of zeolite alteration; hence, heterogeneous properties are incorporated into the numerical model for flow and transport. The mineralogic model is based on the work of Chipera, et al. (1997) and Carey, et al. (1997), where the x-ray data from boreholes were interpolated onto the geologic section using a program called STRATAMODEL. In their conceptual model, Robinson, et al. (1997) assumed that flow would more readily occur in the vitric and the slightly altered zones. Zones of heavy zeolite alteration would have low permeability, thus, promoting lateral flow around, rather than vertical flow through, the zeolites. However, a small amount of zeolites may not impact the permeability of the vitric zone. Hence, the predominance of sorption of radionuclides would be postulated to occur in the slightly altered zones rather than the heavily altered zones. The wide range, from 10 to 10,000 yr, in the particle tracking results of Robinson, et al. (1997) captures the uncertainty in flow paths through the CHn unit, with short times reflective of fast pathways through faults and long times reflective of flow through zeolitic matrix. Thus, understanding the detailed distribution of the mineralogy in the Calico Hills Unit is of utmost importance for flow and transport below the repository.

A total of 1503 records from 20 boreholes in the YM block extend into or cross the CHn; 18 of the boreholes fall in the area outlined in Figure 3. Typically, there are 10 to 35 analyses in the zone from the basal TSw unit to the upper Prow Pass units. The area below the western portion of the repository is poorly constrained (Carey, et al., 1997) due to data available in only three boreholes of which only one is considered reliable (G-3, one mile south of repository). Chipera, et al. (1997) report thinly intercalated layering of the vitric and zeolitic zones that would have been easily missed by the previous sampling intervals of 15 to 40 m. They also contend that there are no data to support the "misconception" of holes in the zeolite layers, indicating instead, that there are intercalated vitric and zeolitic layers at each borehole.

Figures 4 and 5 represent the interpolated data from the LANL STRATAMODEL program conformally mapped onto the GFM3.0 geologic section (Geologic Framework Model; documentation not yet released). The geologic portion of ISM2.0 and the GFM3.0 models do not differ in the region around the zeolites. In the figures, the zeolite weight percent is conformally mapped to the Tac and the Tacbt (basal part of Thtbt) units using 0.1 as a vertical factor to support the lateral continuity of the altered zones. Figure 3 represents the distribution in the vicinity of the contact between the Tac and the Tacbt. Figure 5 represents the distribution on a plane that is a slice at the elevation of 826 m msl. Figures 4 and 5 would be expected to illustrate the V/Z 4 transition in Figure 3. These figures are presented not as a more accurate representation of the zeolite distribution but rather indicative of the lack of data to constrain the distribution of zeolites in the CHn and the representative hydrologic properties for those zones. The purported hole in the zeolite alteration in the southwestern portion of the

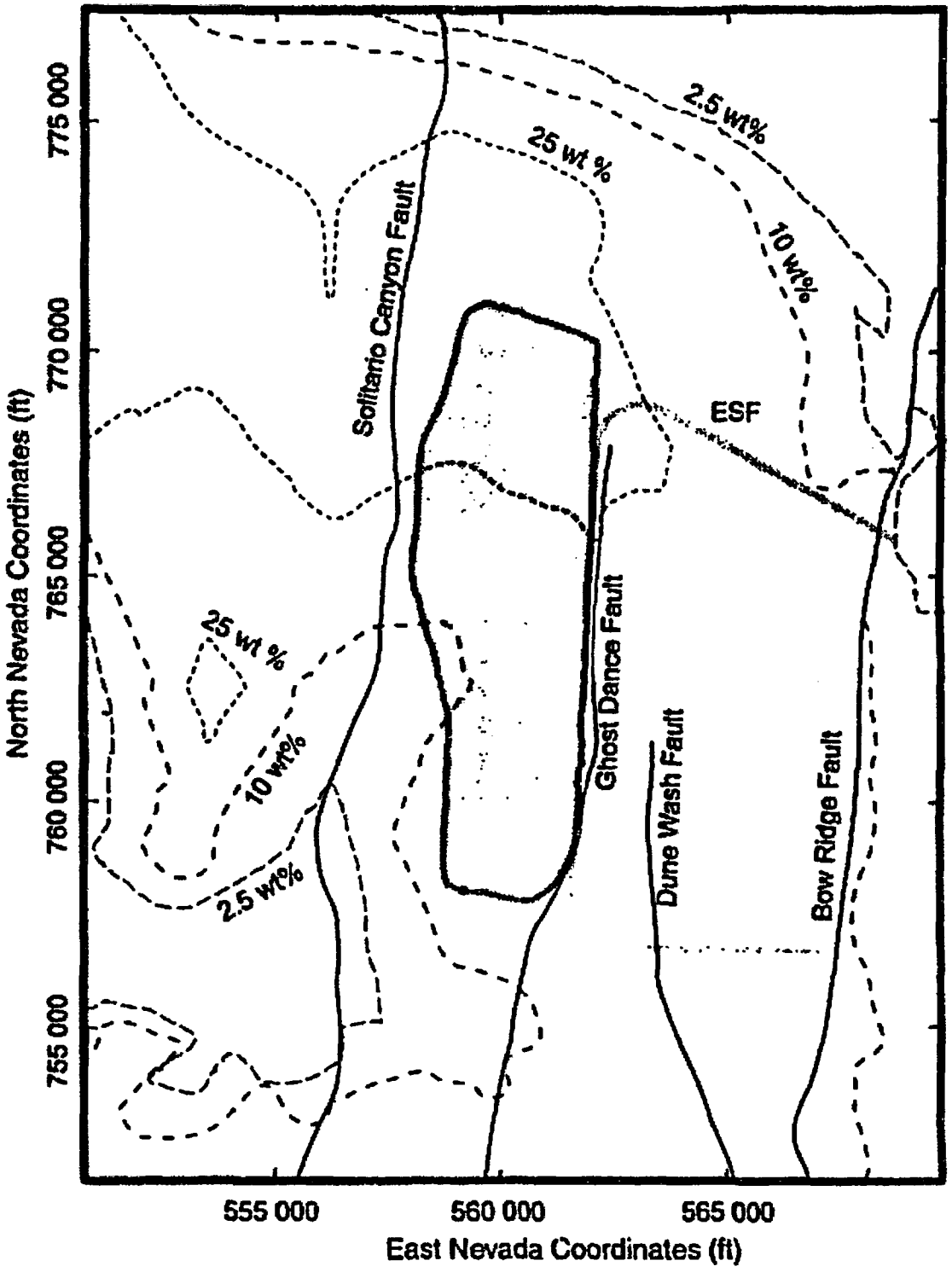

Figure 4. Zeolite weight percent contours over the same area as Figure 3 using interpolated data referenced in Carey, et al. (1997) in the lower portion of the Calico Hills Formation.

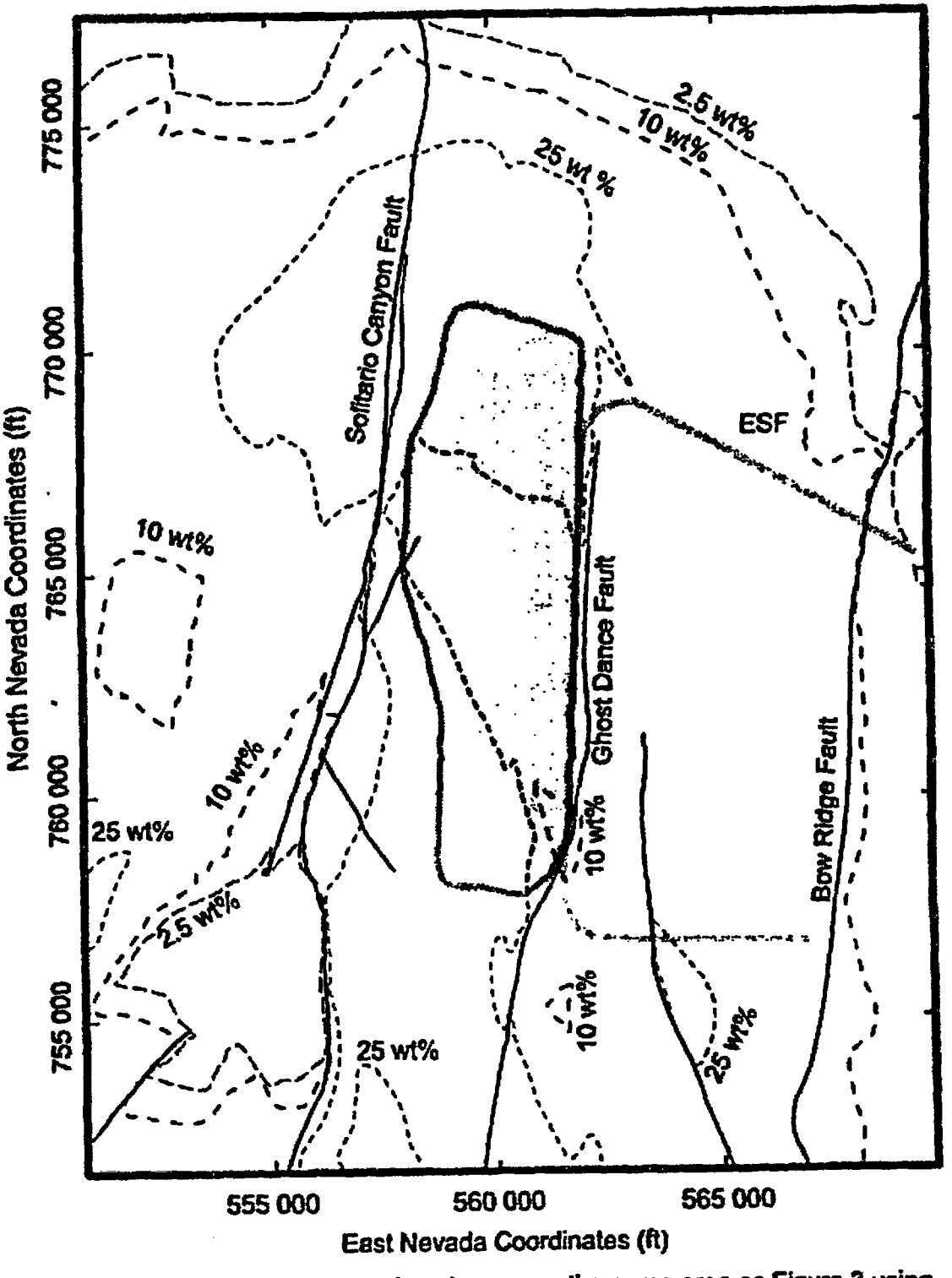

Figure 5. Zeolite weight percent contours over the same area as Figure 3 using the interpolated data referenced in Carey, et al. (1997) at the 2709 foot elevation (above mean sea level).

ATTACHMENT B

INITIAL ASSESSMENT OF DILUTION EFFECTS INDUCED BY WATER WELL PUMPING IN THE AMARGOSA FARMS AREA

INITIAL ASSESSMENT OF DILUTION EFFECTS INDUCED BY WATER WELL PUMPING IN THE AMARGOSA FARMS AREA

Prepared for

Nuclear Regulatory Commission
Contract NRC-02-97-009

Prepared by

R.W. Fedors
G.W. Wittmeyer

Center for Nuclear Waste Regulatory Analyses
San Antonio, Texas

Revised
January 1998

ABSTRACT

A preliminary study was undertaken to gain insights into the factors controlling borehole dilution effects in the Amargosa Farms area from a potential release at the proposed Yucca Mountain repository. Dilution in individual boreholes depends on the fractions of water drawn from contaminated and uncontaminated production zones, which in turn depend on the depth of the well, screened intervals, aquifer hydraulic parameters, pumping rates, and distribution of radionuclides across a plume. Dilution arising from infiltration or groundwater mixing underneath the repository was not included in this analysis.

The fundamental question addressed by this study includes how variations in well construction practices, hydraulic parameters of the basin-fill aquifer, and pumping rates affect capture of radionuclide plumes of specified shapes. Detailed statistical analysis of magnitude and spatial distributions of water usage and well bore construction practices was conducted for the Amargosa Farms area. A sensitivity analysis for borehole dilution was performed to assess the effects of reasonable variations in aquifer hydraulic parameters, well depths, screening practices, and variations in pumping rates of irrigation and domestic supply wells for various radionuclide plume configurations. A distinction is made between dilution factors based on volumetric fluxes of the capture and plume areas and those based on dispersion during transport. In general, the volumetric flux-based dilution due to wellbore mixing reduced radionuclide concentrations by less then an order of magnitude. The range of dilution was primarily affected by pumping rates and plume thickness. The choice of modeling the plume with significant vertical dispersion (thick plume) versus little or no vertical dispersion (thin plume) had a significant impact on the borehole dilution factors. The dispersion (transport)-based dilution factors ranged from one to two orders of magnitude with the conservative lower bound delineated by the ratio of the source concentration and the centerline concentration of a plume.

CONTENTS

Section Page

1 INTRODUCTION 1-1
1.1 GEOSPHERE RELEASE PATHWAYS CONSIDERED IN TSPA 1-4
1.2 LITERATURE REVIEW 1-4
1.3 METHODS USED TO CONDUCT STUDY 1-5
1.4 LIMITATIONS OF STUDY 1-6

2 HYDROGEOLOGY OF THE AMARGOSA DESERT 2-1
2.1 STRUCTURE AND DEPOSITIONAL HISTORY 2-1
2.2 BASIN-SCALE GROUNDWATER FLOW 2-2

3 WELL CONSTRUCTION AND WATER USE IN THE AMARGOSA FARMS AREA . . . 3-1
3.1 NUMBER AND DISTRIBUTION OF WELLS 3-1
3.2 STATISTICAL ANALYSIS OF WELL CONSTRUCTION PRACTICES 3-2
3.3 ESTIMATION OF WATER USE 3-2

4 THREE-DIMENSIONAL CAPTURE ZONE ANALYSIS AND PLUME DELINEATION . 4-1
4.1 DETERMINATION OF FLOW FIELD AND CAPTURE ZONE 4-3
4.1.1 Description of the Analytic Element Method 4-3
4.1.2 Ranges for Parameter Values 4-3
4.1.3 Sensitivity Analysis for Capture Zone 4-4
4.2 RADIONUCLIDE PLUME SHAPE AND LOCATION 4-8
4.2.1 Transport Parameters 4-10
4.2.2 Plume Dimensions for 3D Dispersion from Constant Concentration Source 4-11
4.2.3 Plume Dimensions Neglecting Vertical Dispersion for Constant Concentration Source 4-12
4.3 BOREHOLE DILUTION FACTORS BASED ON VOLUMETRIC FLUX 4-13
4.3.1 Domestic Wells 4-14
4.3.2 Irrigation Wells and Plumes with No Vertical Dispersion 4-19
4.3.3 Irrigation Wells and Plume with Vertical Dispersion 4-19
4.4 BOREHOLE DILUTION FACTORS BASED ON DISPERSIVE TRANSPORT 4-24
4.4.1 Domestic Wells 4-24
4.4.2 Irrigation Wells 4-24

5 CONCLUSIONS 5-1

6 REFERENCES 6-1

APPENDIX A — DETAILED WATER USE TABLES FOR 1983, 1985–1996
APPENDIX B — CAPTURE ZONE DELINEATION TABLE
APPENDIX C — TABLE OF BOREHOLE DILUTION FACTORS

FIGURES

Figure		Page
1-1	Lower Amargosa Desert region south of proposed Yucca Mountain repository site (R) including Amargosa Valley and Amargosa Farms	1-2
3-1	The distribution of domestic and quasi-municipal wells based on range and township from well driller's logs	3-4
3-2	Distribution of annual water use (acre-ft) by type and by range and yownship for commercial, irrigation, quasi-municipal wells for the year 1996	3-7
3-3	Distribution of water use by type for the year 1996	3-8
4-1	Comparison of plume cross-section (P), irrigation well capture area (I), and domestic well capture area (D)	4-2
4-2	This plot illustrates the effect of well penetration depth (60, 190, 500, and 1,000 m) on a small irrigation capture zone width and thickness	4-5
4-3	Effect of combinations of transmissivity (200, 300, 400 m^2/d) and hydraulic head gradient (0.001, 0.002, 0.003, 0.005) on a large irrigation well's capture zone width and thickness	4-6
4-4	Effect of combinations of transmissivity (50, 100, 200, 300, 400 m^2/d) and hydraulic head gradient (0.001, 0.0025, 0.005, 0.01) on a domestic well's capture zone width and thickness	4-7
4-5	This plot illustrates the effect of pump rate (range 1 to 2000 m^3/d) on the capture zone width and thickness	4-9
4-6	Effect of pump rate (range 1 to 75 m^3/d) on the flux-based borehole dilution factor for plumes of thickness 10 m and 25 m (no vertical dispersion)	4-15
4-7	Effect of screen position for domestic-sized wells on the flux-based borehole dilution factor for plumes of thickness 10 m and 25 m (no vertical dispersion)	4-16
4-8	Effect of transmissivity (10, 50, 100, 400 m^2/d) on the flux-based borehole dilution factor for plumes of thickness 10 m and 25 m (no vertical dispersion)	4-17
4-9	Effect of the regional gradient (0.001, 0.0025, 0.005, 0.01) on the flux-based borehole dilution factor for a domestic-sized well and plumes of thickness 10 m and 25 m (no vertical dispersion)	4-18
4-10	Effect of pump rate on flux-based borehole dilution factors for irrigation wells and a 25 m thick plume with no vertical dispersion	4-20
4-11	Effect of pump rate on dilution factors for irrigation sized wells and a plume with 3D dispersion	4-21
4-12	Effect of transmissivity (50 to 400 m^2/d) on dilution factors for irrigation sized wells and a plume with 3D dispersion	4-22
4-13	Effect of regional hydraulic gradient (0.001 to 0.0005) on dilution factors for irrigation-sized wells and a plume with 3D dispersion	4-23
4-14	Effect of pumping rate (1-75 m^3/d) for domestic wells on transport dispersion-based borehole dilution factor for two different plume configurations: a thin plume with no vertical dispersion and a 3D dispersion plume both with dispersivity ratios as noted in the plot	4-25

FIGURES (Cont'd)

Figure		Page
4-15	Effect of transmissivity (10–400 m^2/d) for domestic wells (Q = 3 m^3/d) on transport dispersion-based borehole dilution factor for two different plume configurations: a thin plume with no vertical dispersion and a 3D dispersion plume, both with dispersivity ratios as noted in the plot	4-26
4-16	Effect of pumping rate (300–2,000 m^3/d) for irrigation wells on transport dispersion-based borehole dilution factor for four different plume configurations: two thin plumes with no vertical dispersion and two 3D dispersion plumes, all with dispersivity ratios as noted in the plot	4-27
4-17	Effect of transmissivity (50–400 m^2/d) for large irrigation wells (Q = 2116 m^3/d) on transport dispersion-based borehole dilution factor for two different plume configurations: two 3D dispersion plumes with dispersivity ratios as noted in the plot	4-28

TABLES

Table Page

3-1 Distribution of wells by water use across Townships T15,16,17S using well driller's logs . 3-3
3-2 Statistics for well construction practices and water level positions for wells recorded in GWSI database in Amargosa Valley and Amargosa Farms area 3-3
3-3 Annual estimates of water use by type; International Minerals Venture Floridan (IMV), American Borate (AB), quasi-municipal (QM), commercial (COM) 3-5
3-4 Summary statistics of individual irrigation users on an annual basis 3-6

4-1 Plume configuration and point dilution factor at 15 km from the source area for a range of dispersivity values. C_c is the centerline concentration. The source area is 25 m thick by 500 m wide. 4-13
4-2 Plume configuration and point dilution factor at 25 km from source area for a range of dispersivity values 4-13
4-3 Plume configuration in terms of width at 15 and 25 km and point dilution factor for a source area width of 500 m and no vertical dispersion 4-14

ACKNOWLEDGMENTS

This report was prepared to document work performed by the Center for Nuclear Waste Regulatory Analyses (CNWRA) for the Nuclear Regulatory Commission (NRC) under Contract No. NRC-02-97-009. The activities reported here were performed on behalf of the NRC Office of Nuclear Material Safety and Safeguards (NMSS), Division of Waste Management (DWM). The authors thank Chad Glenn (NRC) for his assistance in obtaining data from the Nevada Division of Waster Resources, Ron Martin for his assistance with geographic information (GIS) data; J. Winterle, A. Armstrong, and R. Baca for their technical reviews; and B. Sagar for his programmatic review. The authors would also like to thank C. Gray for his editorial review and C. Garcia for secretarial support. The report is an independent product of the CNWRA and does not necessarily reflect the views or regulatory position of the NRC.

QUALITY OF DATA, ANALYSES, AND CODE DEVELOPMENT

DATA: CNWRA-generated original data contained in this report meet quality assurance requirements described in the CNWRA Quality Assurance Manual. Sources for other data should be consulted for determining the level of quality for those data.

ANALYSES AND CODES: The GFLOW Version 1.1, PATCHI Version 1.1, and STRIPI Version 1.1 computer codes were used for analyses contained in this report. These computer codes are controlled under the CNWRA Software Configuration Procedures.

1 INTRODUCTION

Yucca Mountain (YM), Nevada, was originally proposed as a deep geologic repository for high-level radioactive waste due in part to its favorable hydrogeologic regime. Moisture fluxes within the 700 m thick unsaturated zone at YM were presumed to be small (< 0.1 mm/yr) due to the region's arid climate and the low permeability of the tuff units comprising the mountain (U.S. Department of Energy, 1988). Low moisture fluxes should reduce the rate of waste canister corrosion, subsequent dissolution of the exposed waste form, and transport of radionuclides to the accessible environments. However, recent studies (Stothoff, 1997; Flint and Flint, 1994) suggest that mean annual infiltration at YM may be as high as 15 mm and provide convincing evidence that there are fast pathways, albeit probably spatially focused, from the surface of YM to at least the depth of the repository (Fabryka-Martin et al., 1996). Radionuclides not sorbed by the zeolitized bedded tuffs that underlie the repository (e.g., technetium, iodine, neptunium), or diffused from fluid-conducting fractures into the rock matrix within welded tuff units, will enter the water table, which, based on current engineering designs, lies 250 to 300 m below the repository. Current hydrogeologic studies (Czarnecki and Waddell, 1984; TRW Environmental Safety Systems, Inc., 1995) indicate that radionuclides that enter the saturated zone beneath YM would generally flow to the south-southeast into western Jackass Flat within the welded tuff aquifer and then south-southwest into the Amargosa Desert where the water table lies within an alluvial aquifer. In order to demonstrate compliance with a risk- or dose-based standard, mixing that occurs due to saturated zone transport and active pumping of wells may play a major role in reducing radionuclide concentrations.

Saturated zone dilution of radionuclide concentrations depends on the bulk flow rate of water beneath YM at locations where radionuclides enter the water table, the degree of mixing caused by large-scale variations in the groundwater velocity field in the welded tuff and alluvial aquifers, and mixing in boreholes where water may be pumped for domestic or agricultural use. Clearly, the amount of dilution depends on the duration and degree of mixing along the radionuclide transport path, while the estimated risk or dose depends on the ultimate use of water pumped from the aquifer. Estimating dose or risk requires definition of a potentially exposed population and the potential biosphere pathway by which an individual would be exposed to released radionuclides (TRW Environmental Safety Systems, Inc., 1995). In the TSPA-95 (TRW Environmental Safety Systems, Inc., 1995), it was assumed that the peak dose to the maximally exposed individual is received by a person drinking 2 L of water per day pumped from the welded tuff aquifer at a location just outside the boundary of the controlled area (5 km outside the repository footprint). However, National Academy of Sciences recommendations may require determining the peak dose to the average member of a critical group, based on current water and land use practices in the YM area. Therefore, it is prudent to consider populations currently residing downgradient from YM, such as the Amargosa Farms area (figure 1-1), that produce at least a portion of the food they consume using local groundwater to irrigate their crops. However, one should consider variations in individual expected dose within the critical group due to differences in well locations, well construction, and pumping rates.

As noted in Kessler and McGuire (1996), dispersive transport processes are relatively ineffective at reducing contaminant concentrations in a steady-state groundwater flow regime. If there are large temporal variations in the magnitude and direction of the groundwater velocity field, then mixing and attendant dilution during transport may be significant. Current conceptual models of the YM saturated groundwater system would suggest that the flow regime is relatively unperturbed by fluctuations in the magnitude and location of recharge and discharge. However, increased pumping for irrigated agriculture in the Amargosa Farms area over the past 30 yr may have had some effect on the groundwater flow

Scale 1:250000

Figure 1-1. Lower Amargosa Desert region south of proposed Yucca Mountain repository site (R) including Amargosa Valley and Amargosa Farms

regime. Nonetheless, in the present study it is assumed that pumping has no effect on the groundwater flow regime between YM and receptor locations. If the primary effect of pumping on the flow regime is enhanced mixing or more rapid transport, the assumption of steady state flow conditions, if not realistic, is at least conservative from the standpoint of radionuclide dose.

Dilution factors can be defined in a number of ways. Each of the three definitions mentioned in this report are based on a particular approach to addressing dilution. The first approach addresses dilution that results from dispersion of a solute during transport; the dilution factor is calculated as the ratio of concentration at the source area to that at the receptor point. The second approach addresses dilution due to mixing and is calculated as the mass release rate divided by the largest flux of water into which the solute may be mixed and used by a critical group. The third approach addresses dilution due to the intersection of the capture zone of a pumping well with the plume configuration at the withdrawal location. In this case, the dilution factor is calculated as the ratio of the plume area intercepted by the capture area and the entire capture area. The third approach is used in this report to describe borehole dilution from the geometric standpoint and it may be linearly combined with the first approach for a total borehole dilution factor. Usage of the first two approaches is described further below.

Baca et al. (1997) and Kessler and McGuire (1996) used the first approach to calculate point dilution factors (P-DF) where point refers to concentration at a single point. Under assumptions of steady state flow, estimated dilution factors due to dispersive mixing along the saturated zone transport pathway from the proposed YM repository to locations 20 to 30 km to the south have ranged from 5 to 50 (Baca et al., 1997) and from 4 to 44 (Kessler and McGuire, 1996). In both analyses, the reported dilution factors were determined by solving the advection-dispersion equation. Baca et al. (1997) contoured the P-DF while Kessler and McGuire (1996) tabulated P-DFs based on centerline concentration. In TSPA-93 (Wilson et al., 1994), TSPA-95 (TRW Environmental Safety Systems, Inc., 1995), and Iterative Performance Assessment Phase 2 (Nuclear Regulatory Commission, 1995) it was assumed that additional dilution occurs at the receptor location due to mixing of clean and contaminated water in the borehole and, in the case of TSPA-95, due to mixing of waters from groundwater basins influent to the central region of the Amargosa Desert.

In the ongoing NRC Iterative Performance Assessment (IPA) Phase 3, the borehole dilution factor corresponds to a single well that is pumped at a rate sufficient to supply all water needs for the critical group in question. For example, if there are assumed to be 12 quarter-section, center pivot irrigation plots under cultivation with alfalfa at Amargosa Farms, the equivalent annual well discharge[1] is 9,300,000 m^3. If the critical group consists of a residential community of 500 persons located 5 km south of YM, the equivalent annual well discharge[2] would be 103,700 m^3. Borehole dilution factors can be computed directly for the critical groups if the volume of contaminated water captured by the well is known. For example, if, the volume of contaminated water captured by the well at Amargosa Farms is 930,000 m^3, the dilution factor is 10. However, in order to determine a dose, one must compute the radionuclide concentration in the borehole and, hence must also know the concentration of radionuclides in the contaminated water captured by the well. Inherent in this approach, the assumption is that the entire radionuclide plume is captured and that there is no well-to-well variation in the concentration. This report

[1] 12 plots × 126 acres/plot × 5 ft of water/year = (8.107 × 10^{-4} m^3/acre-ft).

[2] 150 gal/person-day × 500 persons × 365.25 days/yr × 3.785 × 10^{-3} m^3/gal.

addresses the validity of this assumption considering the concept of borehole dilution as well as the distribution of pumping well locations and pump magnitudes.

1.1 GEOSPHERE RELEASE PATHWAYS CONSIDERED IN TSPA

Farming in the Amargosa Farms region is partially related to the accessibility to well water. The combination of non-arable land and large depths to the water table restrict farming-based population growth to the area immediately south of the town of Amargosa Valley. The water table gradually approaches the land surface toward the southern reaches of the Amargosa Farms area. Exposure scenarios are assumed to occur through a combination of drinking water and ingestion of locally raised produce and livestock. The lengths of the groundwater flow paths from YM to domestic and commercial wells and irrigation wells are approximately 25 and 30 km, respectively.

1.2 LITERATURE REVIEW

In groundwater hydrology, the term borehole dilution is used to describe several phenomena including: (i) contaminant sampling biases resulting from improper monitor well construction, (ii) the effectiveness of pump and treat remediation systems, and (iii) capture zone analysis. Borehole dilution is used to explain one to two order-of-magnitude differences in values between concentrations measured in sampling wells and concentrations measured in the aquifer; however, the concentration in the borehole may be greater than the *in situ* or resident concentration. Borehole dilution is also the name of a procedure used to estimate permeabilities or seepage velocity in a single well bore through analysis of the dilution rate after release of a solute in the wellbore. Borehole dilution in the present work refers to dilution of the resident contaminant concentrations in a wellbore due to pumping a well that captures both contaminated and uncontaminated portions of the aquifer.

Six factors that may significantly affect the borehole concentration are: (i) well pump rate and well distribution in the well field, (ii) regional hydraulic gradient, (iii) transmissivity, (iv) hydrostratigraphy and anisotropy, (v) well penetration depth and length of screen, and (vi) vertical and horizontal contaminant plume distribution. Analytical solutions for flow can incorporate the effects of well pump rates, well design, and regional gradients under certain restrictions for a sensitivity analysis. Complex numerical models are generally required to analyze the effects of heterogeneity in the hydraulic properties and simulate complex plume configurations, especially if three-dimensional (3D) effects are considered to be important. An increase in the spacing of the wells may increase the capture zone horizontally but may decrease the capture zone vertically and may introduce gaps in the capture zone between wells where contaminants may escape. An increase in the regional hydraulic gradient will act to decrease the capture area. An increase in the anisotropy will increase the capture zone horizontally but decrease it vertically.

Analytic solutions (Schafer, 1996; Faybishenko, et al., 1995; Grubb, 1993) and analytic element methods (Strack, 1989; Haitjema, 1995) have been published for estimating capture zones for partially penetrating wells in steady state 3D flow fields. Sensitivity analyses of effects that include vertical movement of water or solute in a heterogeneous domain require the use of numerical models. A good illustration of the factors that affect capture zone size and shape is found in Bair and Lahm (1996). Bair and Lahm (1996) used a finite difference method to determine the steady state flow field and particle tracking to delineate the size and shape of the capture zone. They determined the magnitude of changes to the capture zone area due to perturbations in the regional gradient, well penetration, pump rates, well

configuration, and degree of hydraulic conductivity anisotropy in the context of an idealized pump and treat design.

Three published articles on numerical simulation of 3D flow in and around a wellbore contain pertinent information for refined modeling in the vicinity of a single well. Chiang et al. (1995) simulated 3D flow and advective solute transport in the vicinity of a partially penetrating well in order to understand the order of magnitude difference in contaminant concentrations between well samples and point aquifer samples. The concentration profile in the aquifer was known. The well bore was modeled as separate elements with a permeability in the range of that predicted for laminar flow in a tube. They noted that their transient simulation results asymptotically approached the simple, mass balance-based result which assumes a flat water table.

Akindunni et al. (1995) simulated 3D flow near a well for various screen and plume positions. They approximated the well using a Neumann boundary condition at the edge of the domain at which the discharge was equally apportioned to the nodes along the screened length of the well. They compared vertically averaged values of concentration for both the wellbore and the aquifer. In the transient simulations, concentrations differed significantly in the well and aquifer. Concentrations in the wellbore were higher or lower than the vertically averaged aquifer value depending on the relative position of the plume depth and screened interval. However, over long times, the concentration in the wellbore asymptotically approached the vertically averaged aquifer value. In addition to screen position and plume position, they also investigated the dependence on screen length and anisotropy. Again, initial concentrations differed significantly but long time concentrations appeared to approach the vertically averaged aquifer value. As expected, simulations with large anisotropy ratios for hydraulic conductivity exhibited less vertical mixing than the isotropic case.

Reilly et al. (1989) also modeled the wellbore as a column of hydraulically connected cells; however, their focus was on wellbore flow in a monitoring well with implications for sampling bias and cross-contamination. In a monitoring well, cross-contamination will act to dilute the plume. Of note was their conclusion that greater than half the aquifer-to-wellbore flow occurred in the top ten percent of the screened length while greater than half the wellbore-to-aquifer flow occurred in the bottom ten percent of the screened length. Hence, solute plumes approaching the top of the screened portion will enter the wellbore while plumes approaching the bottom will tend to flow around the well. This finding may be pertinent for the Amargosa Farms area when irrigation wells are shut down, but is probably irrelevant during periods of pumping.

1.3 METHODS USED TO CONDUCT STUDY

Wellbore design and pumping practices in the Amargosa Farms region may have a significant effect both on the capture of a potential plume and, from another perspective, on the radionuclide concentration of the water pumped from the wells. Existing databases were analyzed in order to characterize the location, design, and production of wells. An important feature of the wells in the Amargosa Farms region is that they partially penetrate the alluvial aquifer thickness. The first wells encountered in a path of a simulated plume released from the proposed repository site are low pumping rate domestic, commercial, and quasi-municipal wells at a distance of approximately 25 km. Large pumping rate irrigation wells capable of lowering the water table over square kilometers of area are located at a distance of approximately 30 km.

The analytic element method is used to model 3D flow in the vicinity of a partially penetrating well. Particle tracking is used to delineate a capture area for different well designs, pumping rates, and regional flow characteristics. The capture area is determined at an upgradient point from the well location where the flow is essentially one-dimensional (1D); for example, no longer 3D. Also, the cross-sectional area of a plume entering the Amargosa Farms region is approximated by using two-dimensional (2D) and 3D solutions to the advection-dispersion equation. Geometric arguments are utilized to estimate dilution factors due to the portion of the plume captured. For dilution factors based on dispersive transport, numerical integration is used to estimate a representive concentration for the portion of the plume captured.

1.4 LIMITATIONS OF STUDY

The geometric borehole dilution factors reported here account only for borehole dilution due to pumping in the Amargosa Farms area. Dilution due to mixing with clean water, either underneath the repository or at the northern portion of Fortymile Wash, or from any interbasin transfers is not included. The dilution factors calculated using the different approach may not be linearly combined nor directly compared except under certain restrictions. A comparison of the Total-system Performance Assessment (TPA) streamtubes of Baca et al. (1997) with the geometries of the capture zone and plume configuration are not possible since they are derived from different phenomena.

Three significant assumptions are used in this study, in part due to the scarce amount of data for the groundwater in the alluvial sediments of Amargosa Farms region. Material properties are considered to be homogeneous and isotropic, the flow field is assumed to be uniform, and steady state pumping rate and contaminant transport are assumed to represent the effects of borehole dilution. The latter assumption specifically addresses that the irrigation pumping patterns can be approximated by an annual pump volume. The dilution factors calculated for steady state flow and transport provide an upper bound for those that would result from a transient analysis.

This study addresses borehole dilution induced by a single well, pumping at a rate comparable to an actual well in the Amargosa Farms area. This differs from the IPA Phase 3 approach where the entire volume of water needed by the critical group is used in determining radionuclide concentrations for dose calculations, hence all the wells are assumed equally mixed.

2 HYDROGEOLOGY OF THE AMARGOSA DESERT

The Amargosa Desert is a northwest-trending, triangular-shaped alluvial basin bounded on the north by Bare Mountain, YM, and the Specter Range, on the east by the Resting Spring Range, and on the west by the Funeral Range and Black Mountains. Elevations on the valley floor range from 975 m mean sea level (msl) at the Amargosa River narrows near Beatty and 720 m (msl) at the proximal edge of the fan formed by Fortymile Wash as it discharges from Jackass Flat to less than 610 m (msl) at Franklin Lake playa south of the Amargosa Farms region.

2.1 STRUCTURE AND DEPOSITIONAL HISTORY

The Amargosa Desert is an alluvial valley that resulted from large-scale block faulting in the Basin and Range Province (Plume, 1996; Bedinger et al., 1989). Sediments deposited in depressions created by Tertiary to Quaternary block faulting can be classified as alluvial fan, lake bed, and fluvial deposits. In general, the coarsest materials (gravels and boulders) were deposited near the mountains, and the finer materials (silts and clays) were deposited in the central part of the basin. The distribution of sediment is generally associated with distance from the mountains. Alluvial fans with steep gradients and coarse sediments flatten and coalesce basinward, interfingering with the lake bed deposits. Within the alluvial fans there is a complex interfingering and interbedding of fine and coarse sediments due to shifting of fluvial processes across the top of the fan. The finer grained, distal portions of the fans merge laterally and interlayer with the lake deposits. The lake bed deposits can include beach sand and gravel lenses, silts and clay layers, and evaporites from playa-type environments. The fluvial deposits of recent times consist of sand and gravel lenses along present or ancestral streams. These exhibit a greater degree of sorting than the alluvial fan deposits.

Repeated upheaval events led to a complex interbedding and interlayering of the proximal and distal facies of the alluvial basin sediments. The repeated upheavals, together with the lateral and down gradient transitions within the alluvial fan and grading into the lake bed or playa deposits, has strong implications for flow and transport on a basin-wide scale.

The Amargosa Farms region is in the distal portion in terms of sediment facies of an alluvial basin where lowland fans and lake beds would comprise much, but not all, of the stratigraphic section. Geologic lithologies and maps are described in Burchfiel (1966), Denny and Drewes (1965), Fischer (1992), Naff (1973), Swadley (1983), Swadley and Carr (1980), and Walker and Eakin (1963). Recent maps of the central Amargosa Desert area have followed the lithologic characterization of Hoover et al. (1981). Local features pertinent to the hydrogeology include the presence of tuffaceous beds (ash fall), limestone horizons, perched water systems (especially where the Funeral Mountain fanglomerates overlie lake sediments), common occurrence of caliche, and cementation of sand and gravel units. The high east-west hydraulic gradient, in the otherwise north-south regional gradient, between Amargosa Farms and Ash Meadows is thought to be due to low permeability lake bed sediments faulted into juxtaposition with the conductive Paleozoic carbonates of Ash Meadows.

The thickness of the alluvial sediments in the Amargosa Farms region in not well known. Bedinger et al. (1989) report the basin-fill as greater than 1,300 m, possibly as thick as 2,000 m for basins in the Death Valley Region. Oatfield and Czarnecki (1991) used geophysical data to estimate the thickness of the alluvial valley fill sediments in the range 800 to 1,100 m for the Amargosa Farms area.

Laczniak et al. (1996) infer depths up to 1,140 m on their east-west cross-section across the Amargosa Farms area.

2.2 BASIN-SCALE GROUNDWATER FLOW

Hydrographically, Amargosa Desert is part of the Death Valley groundwater flow system, which is a series of topographically closed intermontane basins connected at depth by the Paleozoic carbonate aquifer. The Death Valley groundwater system is further subdivided into three basins: (i) the Alkali Flat-Furnace Creek Ranch sub-basin; (ii) the Ash Meadows sub-basin; and (iii) the Oasis Valley sub-basin. The Amargosa Farms region is in the southern portion of the Alkali Flat-Furnace Creek sub-basin and adjacent to the Ash Meadows sub-basin (D'Agnese et al., 1996; U.S. Department of Energy, 1988). The Ash Meadows sub-basin, which drains the eastern and northeastern basins of the Death Valley regional flow system, is not believed to be influent to Alkali Flat-Furnace Creek Ranch sub-basin in the vicinity of the primary agricultural pumping area.

The diverse mix of geochemical signatures in the Amargosa Desert area suggests that the groundwater comes from a combination interbasin flow, upwelling from the deep Paleozoic carbonate aquifer, and intrabasin flow from the northwest and from the north (Winograd and Thordarson, 1975). Due to high evapotranspiration rates for the Amargosa Desert, most of the recharge occurs through the ephemeral stream channels (Osterkamp et al., 1994; Savard, 1995). Since the stream channels in the Amargosa Farms portion of the Amargosa Desert rarely have flow, the recharge estimates of Osterkamp et al. (1994) are about 0.5 percent of precipitation. Precipitation is generally between 100 and 200 mm for the Amargosa River basin (Osterkamp et al., 1994).

The groundwater contribution from the proposed YM repository area is a small portion of the southward flow along Fortymile Wash. The contribution from the Ash Meadows springs area to the Amargosa Farms area may be minimal. The Ash Meadows springs line and high gradient toward the Amargosa Farms area is a reflection of the hydraulic conductivity contrast across a gravity fault which abuts the carbonates of Ash Meadows on the east side with the confining playa deposits on the west side (Naff, 1973).

3 WELL CONSTRUCTION AND WATER USE IN THE AMARGOSA FARMS AREA

Characterization of well construction practices and water use specific to the Amargosa Farms area is presented in this section. Some aspects have been presented elsewhere (e.g., U.S. Department of Energy, 1988) but either the level of detail was not sufficient or data were included for other areas of the Amargosa Desert region.

Four sources of information were used to characterize well construction and water use in the Amargosa Farms area. The well permit database, well driller's logs, and annual water use estimates were obtained from the Nevada Division of Water Resources (Nevada Division of Water Resources, 1997a,b,c; Bauer and Cartier, 1995). A fourth source was the Ground-Water Site Inventory (GWSI) portion of the National Water Information System developed and maintained by the U.S. Geological Survey (USGS) (U.S. Geological Survey, 1989). The well permit tables, well driller's logs, and annual water use tables are recorded by location using the standard range, township, section, quarter section, and possibly quarter-quarter section coordinate system. The tables are organized by hydrographic basin with the Amargosa Desert being defined as basin 230. The Amargosa Farms area of the Amargosa Desert includes townships (T) 15, 16, and 17 south (S) and ranges (R) 48 and 49 east (E), as well as the western half of R50E.

The GWSI database uses both the township-range coordinate system as well as the longitude-latitude coordinate system. The wells in Amargosa Farms and Amargosa Valley are taken as those bounded by −116° 21' 34" to -116° 37' 15" west longitude and 36° 40' 10" to 36° 20' 53" north latitude. For graphical purposes, township-range coordinates and latitude and longitude coordinates are converted to UTM section 11 coordinates using the NAD27 datum. The former conversion is made directly to UTM by assuming a well is in the middle of the smallest reported area (e.g., quarter section). The latter conversion is made using a USGS-supplied conversion program.

3.1 NUMBER AND DISTRIBUTION OF WELLS

A division of wells into two categories based on water use is made here for the purpose of presentation of separate results for different receptor pathways. Domestic and quasi-municipal wells can be characterized as having low but continuous pump rates throughout the year. Irrigation wells and commercial and industrial wells constitute the large pump rate category. Although irrigation wells operate intermittently through the growing season, they are approximated in this study as a continuously pumping well at the annual rate estimated from the annual volume pumped.

There are no municipal wells in the Amargosa Farms area. Instead, quasi-municipal wells and domestic wells support direct human use. In addition, a portion of the irrigation wells (well driller's logs) and industrial wells (Buqo, 1996) may also supply water for direct human use. Five percent of the total irrigation wells recorded in the well driller's log also listed domestic use. Dependent on the State Engineer's concurrence, the water use category associated with a permit may be changed at a later date.

There are 508 wells recorded in the State of Nevada's well driller's logs which date back to at least 1921. Many of these wells are no longer in operation. The GWSI database contains 224 well records for approximately the same area of central Amargosa Desert. The well permit database contained 185 certificated or permitted water rights entries. The estimated water use tables from the Nevada State

Engineer tracked as many as 72 entries in one year (1996) and a combined 126 different entries over the span 1983-1996. Individual domestic wells are not recorded in the state water use tables, nor were quasi-municipal wells prior to 1996 for Hydrographic Basin 230.

The distribution of wells spatially and across water use categories is illustrated in table 3-1 by Township and figure 3-1 by Range and Township. The U.S. Department of Energy (DOE) (1988) identifies nine quasi-municipal wells, five commercial wells, and three industrial wells that were active. Changes in water use category may occur on permitted or certificated water rights. A majority (70 percent) of all wells were drilled in T16S. Figure 3-1 shows that the domestic wells are concentrated in T16S and R48-49E. Locations of sections where 14 or more (up to 40) domestic wells have been drilled according to the well drillers logs are also marked in figure 3-1.

3.2 STATISTICAL ANALYSIS OF WELL CONSTRUCTION PRACTICES

The GWSI database (U.S. Geological Survey, 1989) also contains information on well construction. Of the 227 wells from the Amargosa Farms region listed in the database, 188 records included water table depth, 113 included screen positions, and 15 records included specific discharge data. Although 18 wells had multiple screened portions, a majority of the screened portions are closely spaced. This is reflected in the fact that there is only a 1-m difference between the average of the sum of the screened portions and the average of the length of the combined screened portion. Table 3-2 is a statistical summary of relevant well characteristics. Of note are the averages of 11 and 62 m depths from the water table to the top and bottom of the screened portions, respectively.

3.3 ESTIMATION OF WATER USE

For the Amargosa Desert, designated as Hydrographic Basin 230, the state has estimated the perennial yield to be 24,000 acre-ft-yr (Buqo, 1996). Committed water use, which includes both certificated and permitted water use, is over 41,000 acre ft-yr. This situation makes it unlikely that new permits will be granted by the State Engineer. In the past few years, proceedings for water users to demonstrate beneficial use have led to thousands of acre-feet of forfeiture for well permits. These proceedings may have had an impact on the number of water users reported in the basin during the mid-1990's (Buqo, 1996).

On a volume basis, the water pumped in the Amargosa Farms region is predominantly used for irrigation and mining. The bulk of the mining related water use is in the playa area, which lies south of the farming area. The St. Joe Bullfrog Gold Mine is also a large-volume water user as reported in the tables for the Amargosa Desert but it is not located in the Amargosa Farms region. Historically, groundwater pumping for irrigation increased significantly in the late 1950's (D'Agnese, 1994; and Buqo, 1996). Irrigation use was 3,000 acre-ft by 1962, 9,300 acre-ft by 1967, and 7,300 acre-ft in 1973. Kilroy (1991) reports rapid declines in the water table during the 1970's and less severe declines in the 1980's. The declines are 20 to 30 ft in three different areas of Amargosa Farms with the largest being a northeast-trending trough near the Nevada-California border in T16S, R48E.

Since 1983, the Nevada State Engineer has tabulated water use for individual users and summarized annual use by category, although data for 1984 were not recorded. Table 3-3 is the annual summary of water use with both the Amargosa Desert total and the Amargosa Farms portion total. The

Table 3-1. Distribution of wells by water use across Townships T15,16,17S using well driller's logs. There are 34 log entries classified as other. See figure 3-1 for layout of Townships and Ranges.

Township	Domestic	Irrigation	Industrial/ Commercial	Quasi-Municipal
T15S	12	5	2	1
T16S	207	120	1	3
T17S	55	65	1	1

Table 3-2. Statistics for well construction practices and water level positions for wells recorded in GWSI database in Amargosa Valley and Amargosa Farms area.

Well Characteristic	Average	Standard Deviation	Number	Minimum	Maximum
Distance from Water Level to Top of Screen (m)	11	13.0	113	0	66.0
Distance from Water Level to Bottom of Screen (m)	62	36.7	113	1.7	219
Distance from Water Level to Screen Centerline (m)	35	23.1	113	1.2	124
Total Screen Length (m)	52	33.2	113	0.9	191
Distance from Top to Bottom of Screens (m)	53	33.1	113	0.9	191
Depth of Well (m)	83	42.6	172	0.9	229
Wellbore Diameter (m)	0.31	0.08	112	0.032	0.41
Specific Discharge (m^2/hr)	32.3	33.4	15	2.34	104

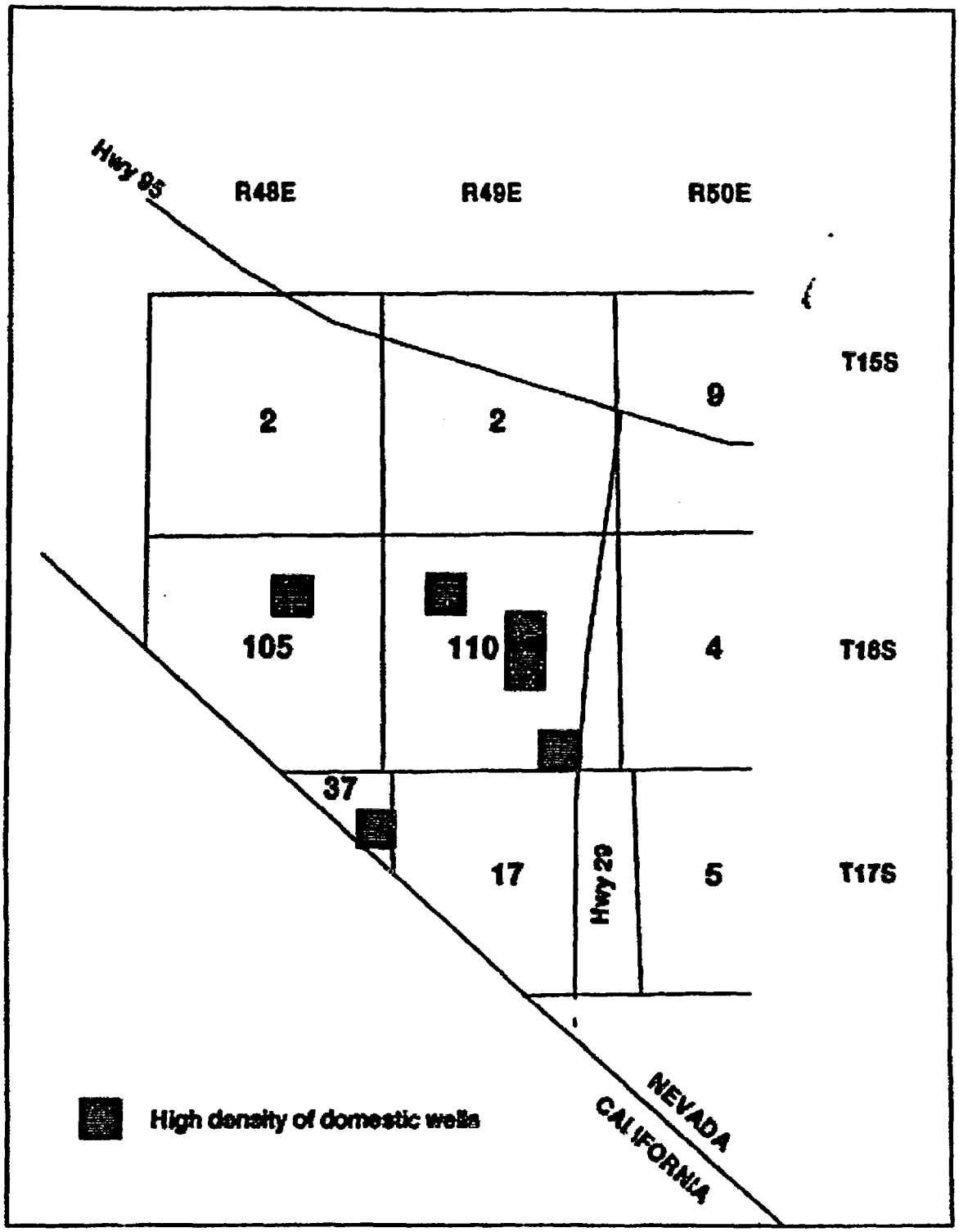

Figure 3-1. The distribution of domestic and quasi-municipal wells based on range and township from well driller's logs. The number of wells in each range and township includes those listed for dual usage, domestic, and irrigation. Locations of sections (1 square mile) with 14 or more domestic wells are highlighted.

Table 3-3. Annual estimates of water use by type; International Minerals Venture Floridan (IMV), American Borate (AB), quasi-municipal (QM), commercial (COM),

Year	Basin-230 Total Acre-ft	Irrigation Acre-ft	IVM/AB Acre-ft	QM/COM Acre-ft	Domestic Acre-ft	Amargosa Farms Total Acre-ft
1996	13,613	11,033	1,019	204	50	12,306
1995	15,035	12,354	780	10	100	13,244
1994	12,595	9,977	717	10	100	10,804
1993	11,300	8,659	1,007	10	100	9,776
1992	8,164	5,711	654	10	100	6,475
1991	6,122	4,942	450	10	100	5,502
1990	7,807	4,953	887	10	125	5,975
1989	3,921	1,566	1,413	10	125	3,114
1988	4,109	2,978	996	10	125	4,109
1987	6,137	5,700	302	10	125	6,137
1986	7,238	6,553	550	10	125	7,238
1985	9,672	8,472	950	20	230	9,672
1983	9,500	9,105	125	20	230	9,500

annual totals increased significantly from 1993 to 1996 due to large increases in irrigation use with the largest volume being 13,244 acre-ft in 1995.

Individual domestic water use is not recorded in the State Engineer's tables, and individual records for quasi-municipal water users did not start until 1996. Annual estimates were lumped together for the domestic and quasi-municipal/commercial use for each year, although there is some recategorization occurring in 1996. A 1 acre-ft annual usage is assumed for every household, although this may be an over-estimate (Buqo, 1996). However, the DOE (U.S. Department of Energy, 1988) states that the annual household usage estimate is 1,800 gpd. One acre-ft is about 895 gpd or about 3.4 m^3/d.

Individual records for each irrigation user are tabulated (appendix A) for the years 1983, 1985–1996 and pertinent summaries are included in table 3-4. For individual users, the maximum annual pump volume for any particular user in 3,960 m^3 (1,170 acre-ft). The average for all years for an individual irrigation user is 828 m^3 and the range in any particular year is 348 to 1,300 m^3. The number of irrigation users for any year ranged from 15 in 1991 to a high of 55 in 1996. Most of the groundwater

Table 3-4. Summary statistics of individual irrigation users on an annual basis.

Year	Average (m^3/d)	Number of Users	Minimum (m^3/d)	Maximum (m^3/d)
1996	772	5[illegible]	3.4	2,707
1995	886	51	6.8	2,928
1994	771	44	3.4	3,960
1993	711	41	3.4	3,960
1992	645	30	3.4	3,368
1991	1116	15	67.7	3,960
1990	645	26	16.9	2,675
1989	348	16	16.9	1,354
1988	503	20	8.5	2,370
1987	900	20	8.5	2,912
1986	1300	17	8.5	2,928
1985	1134	25	76.9	2,928
1983	1083	26	16.9	2,116
Overall	828	–	–	–

pumping occurs in T16S, R48-49E, and T17S, R49E. Figure 3-2 shows the distribution of groundwater pumping for the year 1996 by township and range based on the individual records (no domestic wells are recorded). Figure 3-3 shows the distribution for 1996 relative to the streamtube model boundaries used in Baca et al. (1997). In combination, figures 3-2 and 3-3 illustrate two important points based on 1996 data. One, domestic or quasi-municipal wells are likely to be the first wells encountered by a plume migrating from the proposed YM repository. Two, large pumping rate wells capable of capturing a plume are not encountered until about 30 km from the proposed YM repository.

In summary, the typical pump rates range from 300 to 2,000 m^3/d for irrigation wells and 3 to 6.8 m^3/d for domestic wells. Although the Hydrographic Basin of Amargosa Desert is over-appropriated, actual usage has remained less than 65 percent of the estimated perennial yield. Groundwater pumpage in the Amargosa Farms portion of the Amargosa Desert has led to a decline in the water table locally up to 10 m.

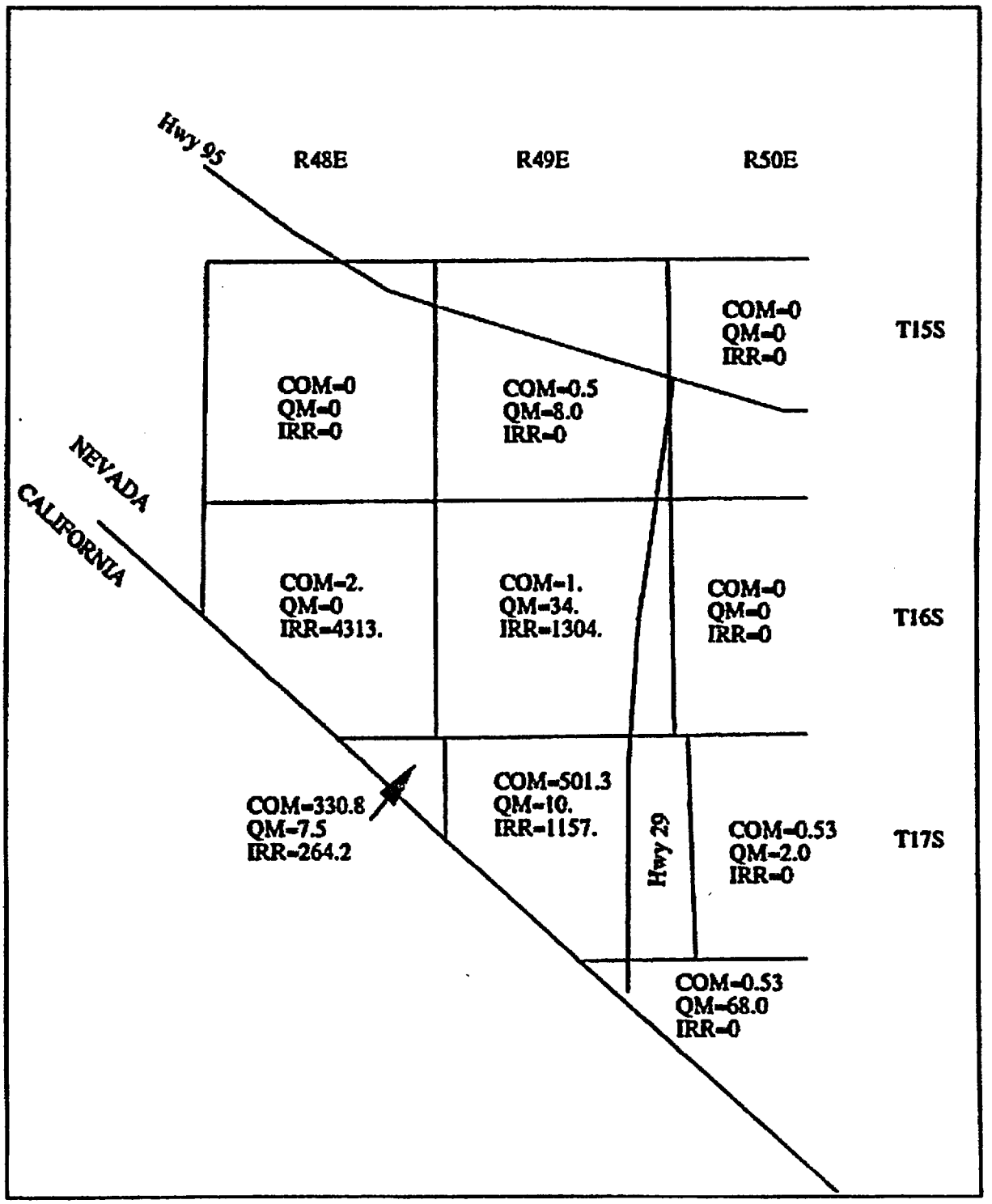

Figure 3-2. Distribution of annual water use (acre-ft) by type and by range and yownship for commercial, irrigation, quasi-municipal wells for the year 1996.

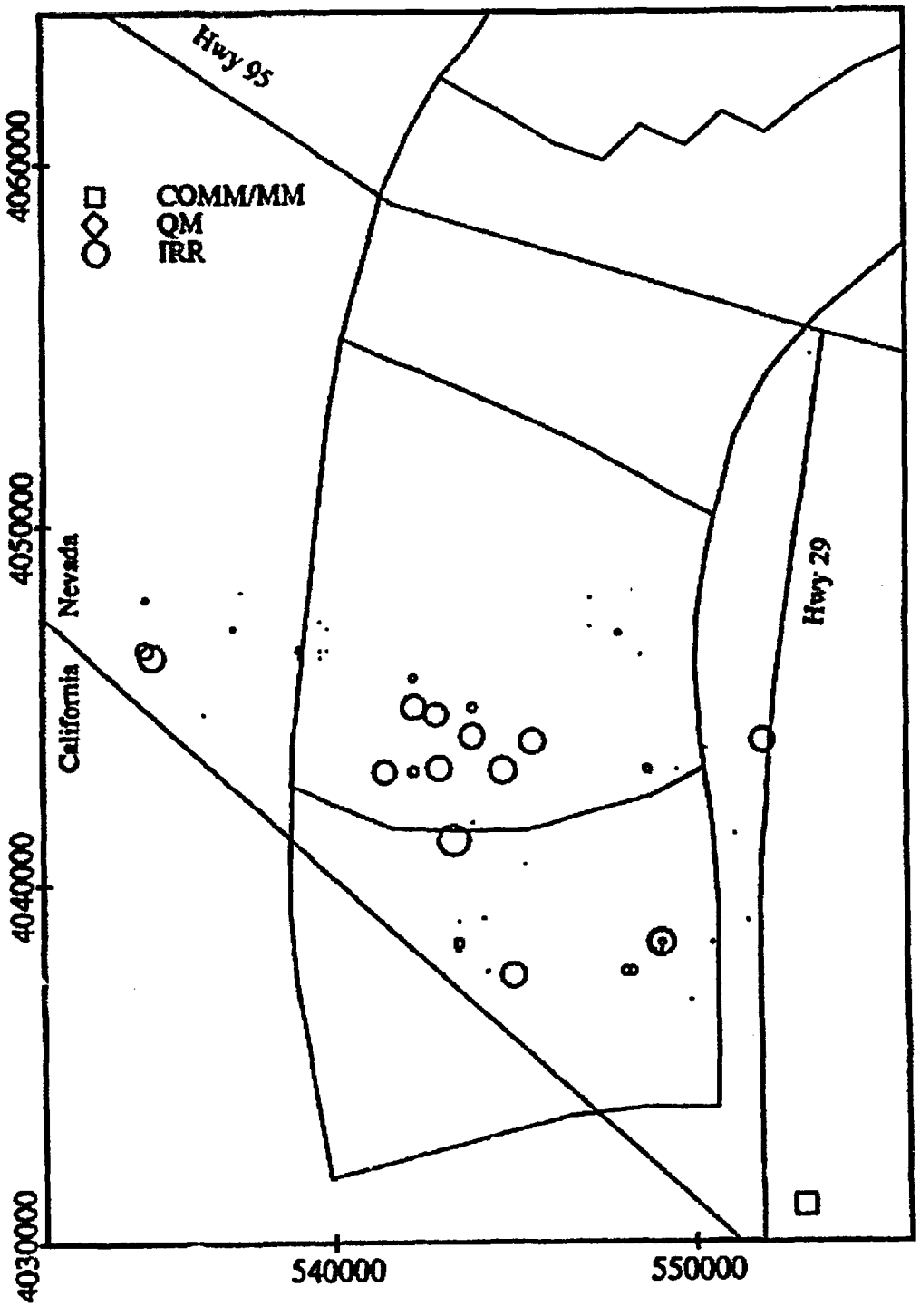

Figure 3-3. Distribution of water use by type for the year 1996. The symbol size for each category is scaled to the magnitude of groundwater pump volume. Data are from Nevada Division of Water Resources (1976b) and are converted to Universal Transverse Mercator Section II coordinates so as to correspond with the streamtube model of Baca et al. (1997).

4 THREE-DIMENSIONAL CAPTURE ZONE ANALYSIS AND PLUME DELINEATION

The approach used here to estimate borehole dilution factors in the Amargosa Farms region is to separate them into two components; one, the factor due to volumetric-flux; and two, the factor due to dispersion during transport. The factor due to volumetric flux is a comparison of the cross-sectional areas of a capture zone of a pumping well to the intercepted portion of a contaminant plume. In all cases, the areas discussed here refer to the cross-sectional area normal to the principal direction of regional flow. The second component of borehole dilution is the effect due to dispersion during transport. It is calculated as the ratio of the source concentration to the areal average concentration of the portion of the plume which is captured by a pumping well.

Other types of dilution factors include that used by Baca et al. (1997) and Kessler and McGuire (1996) based on normalized concentration variations during passive transport, and that used in IPA Phase 3 based on a mass release rate into a total volumetric flux potentially used by a critical group. The dilution factor due to dispersive transport used in this report accounts for the distribution of concentration across a plume whereas that used by Kessler and McGuire (1996) only accounts for concentration reduction along the centerline of the plume. Direct usage or comparison of the borehole dilution factor and the IPA Phase 3 dilution factor is restricted by the reference to different volumetric fluxes.

Different configurations for the intersection of the plume and the capture area are possible. For domestic wells, the capture area is generally much smaller than the cross-sectional area of a plume that has undergone transverse spreading due to macro-dispersion during transport along a 20- to 30-km pathway (figure 4-1). Hence, there would be little borehole dilution even if the well was aligned along the center of the plume, and any borehole dilution that did occur would be due to vertical gradients in the plume concentration. For a 2D plume of prescribed thickness, the location of the plume relative to the capture area affects the dilution factor. For irrigation wells, or any high discharge wells, the capture area is generally thicker than the plume. The capture area may be wider or narrower than the contaminant plume depending on the problem. In all cases, the well is assumed to be in the transverse center of the plume which is the conservative assumption.

The effects of the regional gradient, transmissivity, pumping rate, and screen position and length on the area of the capture zone can be described in qualitative terms. An increase in transmissivity or the regional gradient will decrease the width of the capture area. An increase in the pumping rate will increase the capture area. An increase in the depth of a partially penetrating well will increase the vertical capture area but decrease the horizontal capture area. The position and distribution of the plume in relation to the capture zone will control the dilution of the solute in the well bore.

At present, there are few data for the hydraulic properties, well construction, and pumpage in the Amargosa Desert or Amargosa Farms. Moreover, the size, location, and shape of a plume are uncertain and usually must be obtained from large-scale transport modeling. Because of the relative paucity of site-specific data, the focus of this study is relating dilution trends to generic well design and plume configuration.

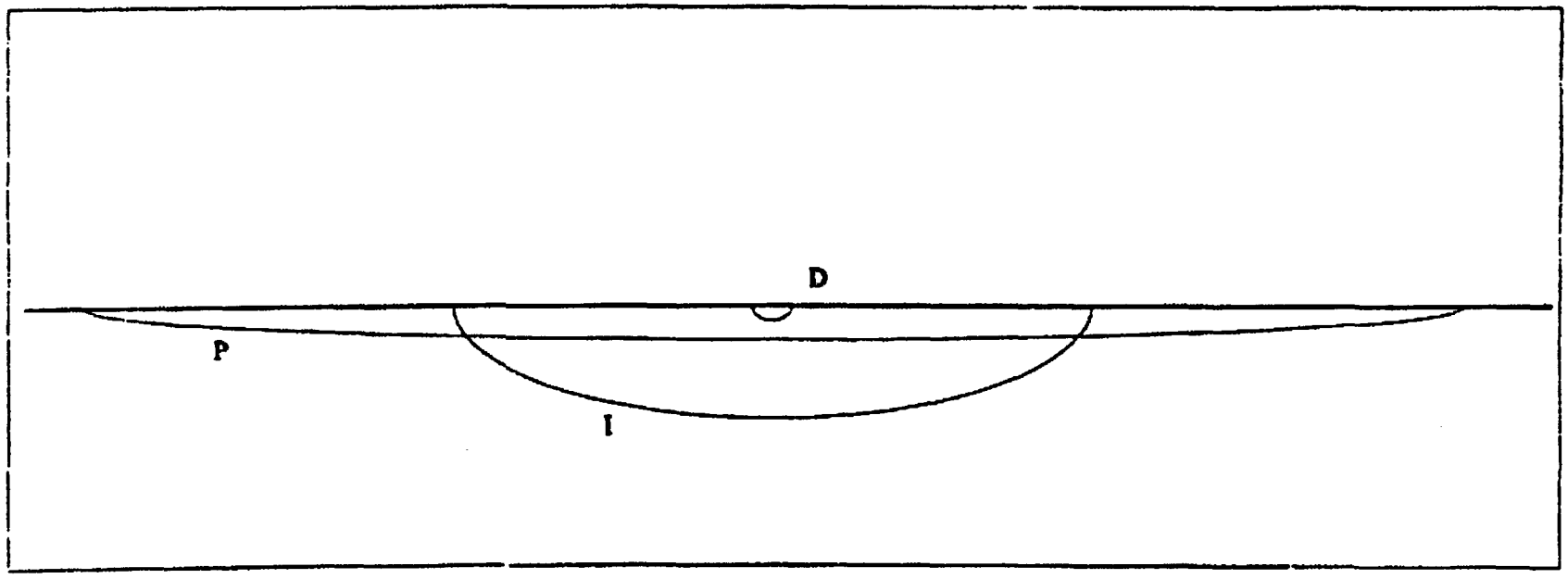

Figure 4-1. Comparison of plume cross-section (P), irrigation well capture area (I), and domestic well capture area (D).

4.1 DETERMINATION OF FLOW FIELD AND CAPTURE ZONE

The groundwater flow simulation program GFLOW Version 1.1 (Haitjema, 1995), that is based on the analytic element method, was used to estimate the size and shape of capture zones for individual wells. GFLOW is designed to simulate partially penetrating wells in a uniform regional gradient. There are other types of elements in GFLOW for modeling groundwater flow fields that were not used. The 3D effects of the partially penetrating well are superimposed on the 2D regional flow field. At some distance from the well, the vertical components due to pumping become negligible. Forward or backward particle tracking is used in GFLOW to determine a capture area at some distant, upgradient point where vertical flux components become insignificant. This capture area is a vertical plane normal to the direction of regional flow.

4.1.1 Description of the Analytic Element Method

The Analytic Element Method (AEM) provides a composite analytic solution which satisfies the differential equation in an unbounded domain. Delineation of streamlines is more precise than with standard numerical methods since both the head and the velocities are known at every point, rather than solely at computational nodes. Combined 2D and 3D modeling is accomplished by superposition of 3D effects on the general 2D solution. For example, near a partially penetrating well, a 3D solution is used. However, at a location sufficiently far from the well, the vertical flow components are negligible and a 2D approximation to the well may be superimposed on the solution. AEM is not well suited for complex flow problems in which material property heterogeneity is large.

The equations for flow in AEM are written in terms of discharge potentials instead of hydraulic head. The discharge potential is defined differently for confined, unconfined, 1D flow, 2D flow, or for any analytic element. An advantage of the AEM is that the solution to the equation for flow written in terms of the discharge potential is not dependent on whether the problem domain being solved is confined or unconfined. Once the strength of the potential is known for each analytic element, the head or groundwater discharge may be determined at any point in the flow domain. The solution for the partially penetrating well is based on work by both Muskat and Polubarinova-Kochina (Haitjema, 1995) for the representation of the strength distribution along a line sink (point sinks along a line) while constraining the discharge to a fixed value.

4.1.2 Ranges for Parameter Values

Four parameters are varied to test their effects on the capture area including: (i) pump rate, (ii) well screen position and length, (iii) regional gradient, and (iv) hydraulic conductivity or transmissivity. The pump rates range from those typical of domestic wells to those typical of irrigation wells. A reasonable range to use for the pump rates for domestic or quasi-municipal wells is 1 to 75 m^3/d. The DOE estimate (U.S. Department of Energy, 1988) for a single household is 1,800 gpd (6.8 m^3/d) while the State of Nevada uses 1 acre-ft per household (3.4 m^3/d) noting that this value is probably too high (Buqo, 1996). The high end of the domestic range corresponds to a quasi-municipal well or to multiple domestic wells modeled as a single well. For example, the first wells in a potential plume's path are multiple domestic, quasi-municipal, and small commercial wells near the junction of highways 95 and 29 at Amargosa Valley. For irrigation wells, pumping may be as high as 4,000 m^3/d; however, a more typical large irrigation pump rate is 2,116 m^3/d (625 acre-ft/yr). The average pump rate from 1983–1996 was about 800 m^3/d while the lowest was 300 m^3/d for any particular year.

The average screened length of the wells in the Amargosa Farms region (top to bottom) is 53 m while the maximum screen length is 190 m (table 3-2). The typical screen position starts 11 m below the static water level at the time of construction. Hence, the typical well modeled here will be screened from the water table to 60 m below the water table. Sensitivity analysis for the screen position, for domestic wells only, will account for the adjustment steps of about one standard deviation of the screen position.

The range of regional hydraulic gradients considered is 0.01 to 0.001. Bedinger et al. (1989) list a value of 0.003 for generic basin-fill environments in the Death Valley Region. Estimates for the Amargosa Farms area made from water table maps by Kilroy (1991), the DOE (U.S. Department of Energy, 1988), and Nichols and Akers (1985) fall within the 0.001 to 0.01 range. Most estimates are in the 0.001 to 0.005 range; the 0.01 values are from the east-west gradients immediately south and east of Amargosa Valley and may reflect the abrupt decrease in transmissivity across the northern end of the so-called Gravity fault, which has been inferred along the Ash Meadows spring line.

The range of transmissivities reported for basin-fill alluvium in the Death Valley Region is 10 to 400 m^2/d (Plume, 1996; U.S. Department of Energy, 1988; and Winograd and Thordarson, 1975). Since Amargosa Farms is in the area of sediments facies of lower fans and lowland sediments, rather than the coarser sediments of the upper and middle fan deposits, the saturated hydraulic conductivities should encompass a wide range and be highly heterogeneous relative to other basin-fill. Plume (1996) estimates a range of 0.006 to 43 m/d for saturated hydraulic conductivity while the DOE (U.S. Department of Energy, 1988) reports a range of 0.21 to 2.9 m/d. The transmissivity is a product of the saturated hydraulic conductivity and the saturated thickness of the aquifer. The aquifer thickness is assumed to be 1,000 m for all modeling scenarios.

4.1.3 Sensitivity Analysis for Capture Zone

The effects of reasonable variations in transmissivity, regional gradient, and pumping rate for all well types are presented in this section. In addition, the effects of screen position and length for domestic wells are presented. Due to their large discharge rates and small degree of well penetration relative to the aquifer thickness, the effects of screen position and length are negligible for irrigation wells. The capture area is determined at an upgradient point from the well location where the flow is essentially 1D, for example, no longer 3D. At this upgradient point, the width and thickness are at a maximum for the capture area. A table of the widths and depths of the capture area results is included in appendix B.

The effect of a partially penetrating well compared with that of a fully penetrating well is shown in figure 4-2 for a small irrigation well pumping at 300 m^3/d. The maximum screen length of 190 m is marked as maximum on the figure. The capture width of the fully penetrating well is about 44 percent of that for the typical partially penetrating well.

Figure 4-3 represents the capture zone width and thickness for combinations of regional gradients and transmissivities for a large pumping rate well of 2,116 m^3/d (625 acre-ft/yr). The combination of a regional gradient of 0.001 and transmissivity of 200 m^2/d (the lowest represented here) leads to a capture width of about 5,600 m, which captures nearly the entire width of a streamtube (Baca et al., 1997) that brackets the repository. Conversely, a larger gradient (0.005) and higher transmissivity (400 m^2/d) lead to a much smaller capture area, 1,800 m wide by 720 m deep. A similar trend also occurs for low-discharge, domestic wells (figure 4-4). Maximum capture areas are created either by the smallest regional gradient (0.001) or the lowest transmissivity (10 m^2/d) for capture thicknesses up to

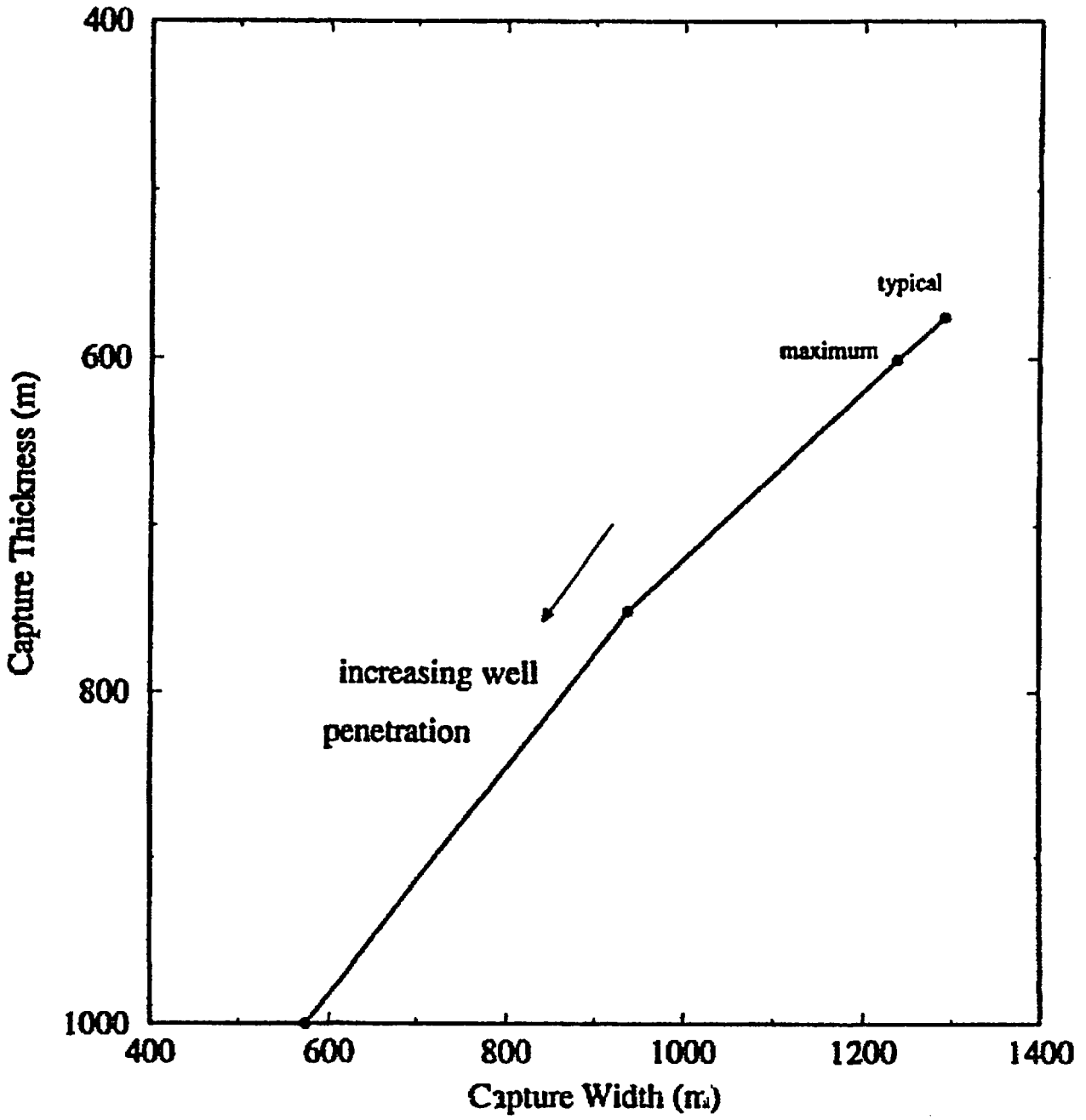

Figure 4-2. This plot illustrates the effect of well penetration depth (60, 190, 500, and 1,000 m) on a small irrigation capture zone width and thickness. A pump rate of 300 m^3/d and regional gradient of 0.005 are used. The "maximum" denotes the maximum well penetration depth and "typical" denotes the typical well penetration depth for the Amargosa Farms region.

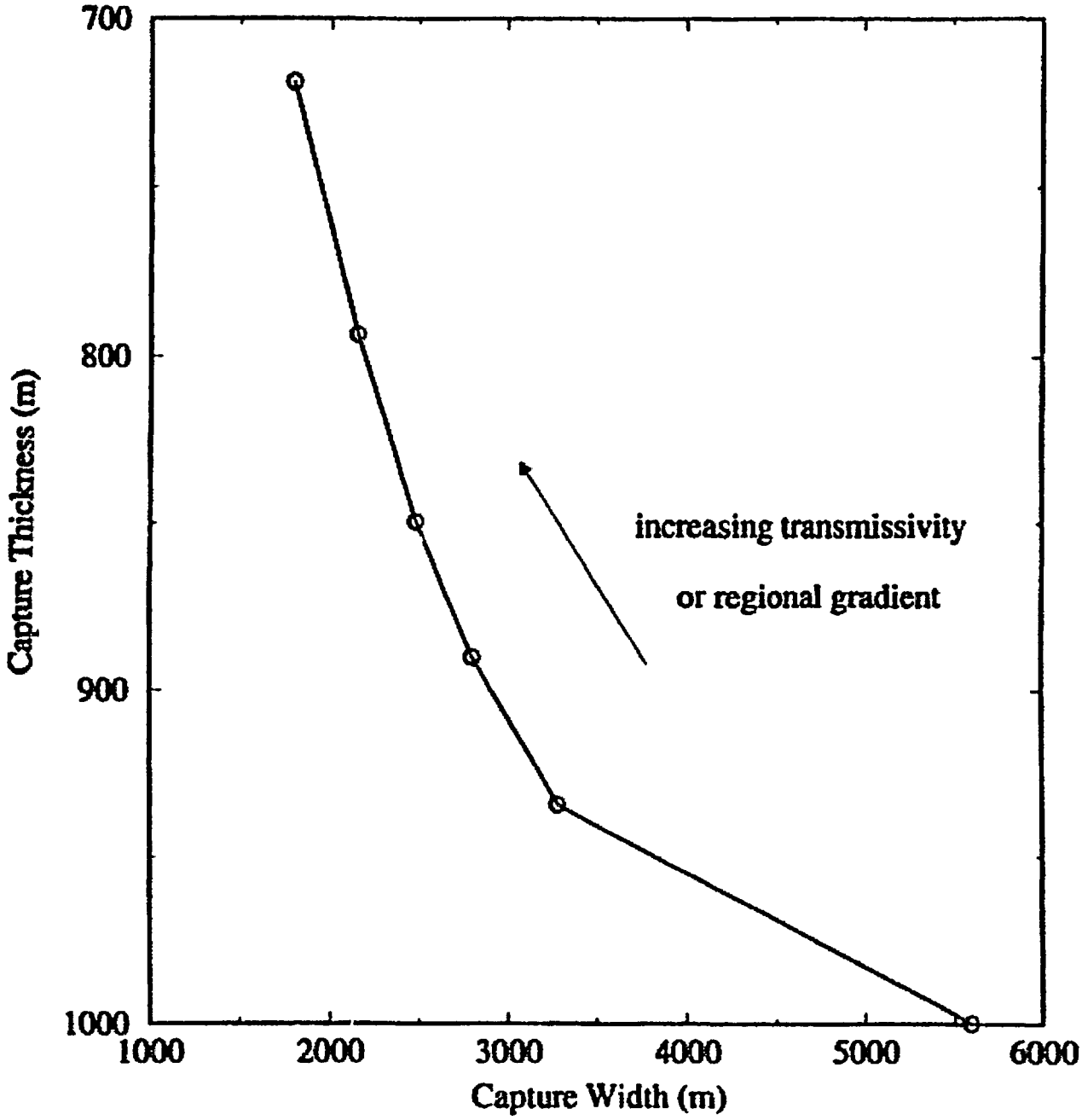

Figure 4-3. Effect of combinations of transmissivity (200, 300, 400 m^2/d) and hydraulic head gradient (0.001, 0.002, 0.003, 0.005) on a large irrigation well's capture zone width and thickness. A pump rate of 300 m^3/d is used.

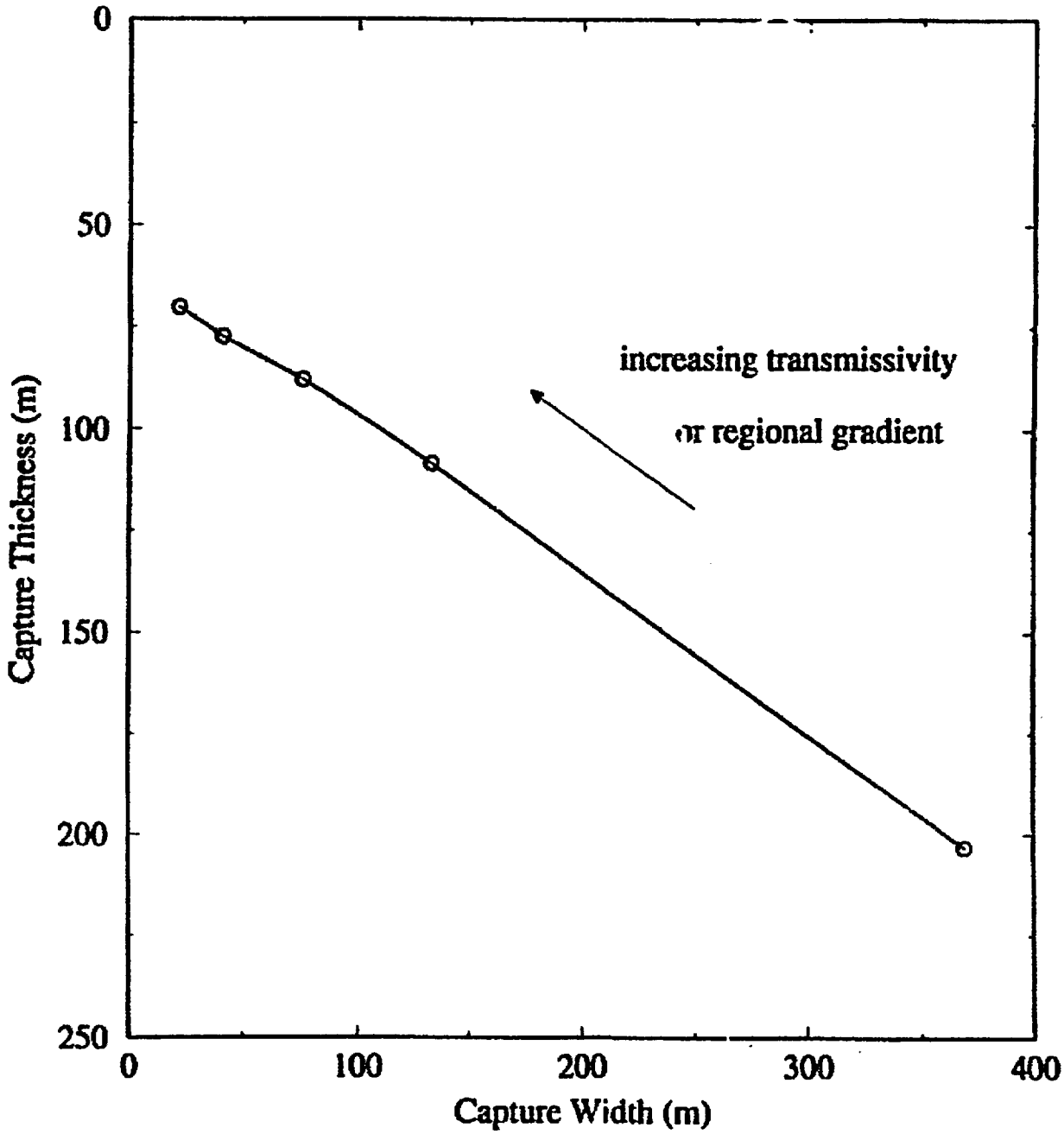

Figure 4-[illegible] Effect of combinations of transmissivity (50, 100, 200, 300, 400 m^2/d) and hydraulic head gradient (0.001, 0.0025, 0.005, 0.01) on a domestic well's capture zone width and thickness. A pump rate of 3 m^3/d and the screened portion is 60 m long starting from the water table.

200 m. Since the Darcy velocity is a function of the hydraulic conductivity and hydraulic gradient, figures 4-3 and 4-4 also illustrate the effect of Darcy velocity on capture width and thickness.

The effect of pump rate on the capture area is presented in figure 4-5. A gradient of 0.005 and transmissivity of 100 m^2/d are used for all pump rates. Of significance for borehole dilution is that all wells in the low pump rate range (< 75 m^3/d) will have capture areas that would be much less than the plume area based on 3D advection-dispersion equation modeling.

4.2 RADIONUCLIDE PLUME SHAPE AND LOCATION

The potential release and subsequent movement of radionuclides from the YM repository is likely to follow a path generally southeast to Fortymile Wash and then continue south to southwest toward the Amargosa Valley and Amargosa Farms areas. A more precise delineation of the flow path under current conditions is a point of debate due to a lack of data and the absence of any detailed hydrogeologic study in the Fortymile Wash and lower Amargosa Desert areas. The shape of the plume at a 30-km distance from the proposed repository, in particular the amount of vertical dispersion which leads to an increase in the plume thickness, is yet another unknown. Vertical dispersion may be limited by the possible presence of confining horizons (Naff, 1973) in the lake bed facies of the basin-fill sediments.

Given the uncertainty of the plume configuration, two scenarios were analyzed. The first scenario was a plume modeled for 3D dispersion. The second scenario is a plume for which no vertical dispersion is incorporated. Both scenarios are simulated to a steady state solution to assess the maximum dimensions of a plume reaching a well.

Dispersion, adsorption, and radioactive decay of the radionuclides will occur along this transport path. Adsorption and decay depend on the particular radionuclide. However, most of the radionuclides of concern in the far field (e.g., ^{237}Np, ^{129}I, ^{99}Tc) have half-lives greater than 10,000 yr Adsorption also depends on the surface mineralogy of the porous media as well as the chemistry of the groundwater. There are no site specific data for adsorption in terms of distribution coefficients for the valley fill sediments. Considering these points, the conservative approach of neglecting both decay and adsorption is adopted.

In order to evaluate dilution due to both vertical and horizontal capture of clean water by a pumping well, an estimate of the shape of a potential plume is needed. Specifically, the configuration of the cross-sectional area perpendicular to the direction of flow is needed. Analytic solutions to the advection-dispersion equation were previously used to describe the plume shape at downgradient points from YM in TSPA-95 (TRW Environmental Safety Systems, Inc., 1995 and Kessler and McGuire, 1996). The advection-dispersion equation for 3D dispersion and 1D flow is

$$\frac{\partial C}{\partial t} = D_x \frac{\partial^2 C}{\partial x^2} + D_y \frac{\partial^2 C}{\partial y^2} + D_z \frac{\partial^2 C}{\partial z^2} - V \frac{\partial C}{\partial x} \qquad (4\text{-}1)$$

where C is the concentration, D_x, D_y and D_z are the dispersion coefficients in the coordinate directions, V is the seepage velocity in the principal direction of flow, and t is time.

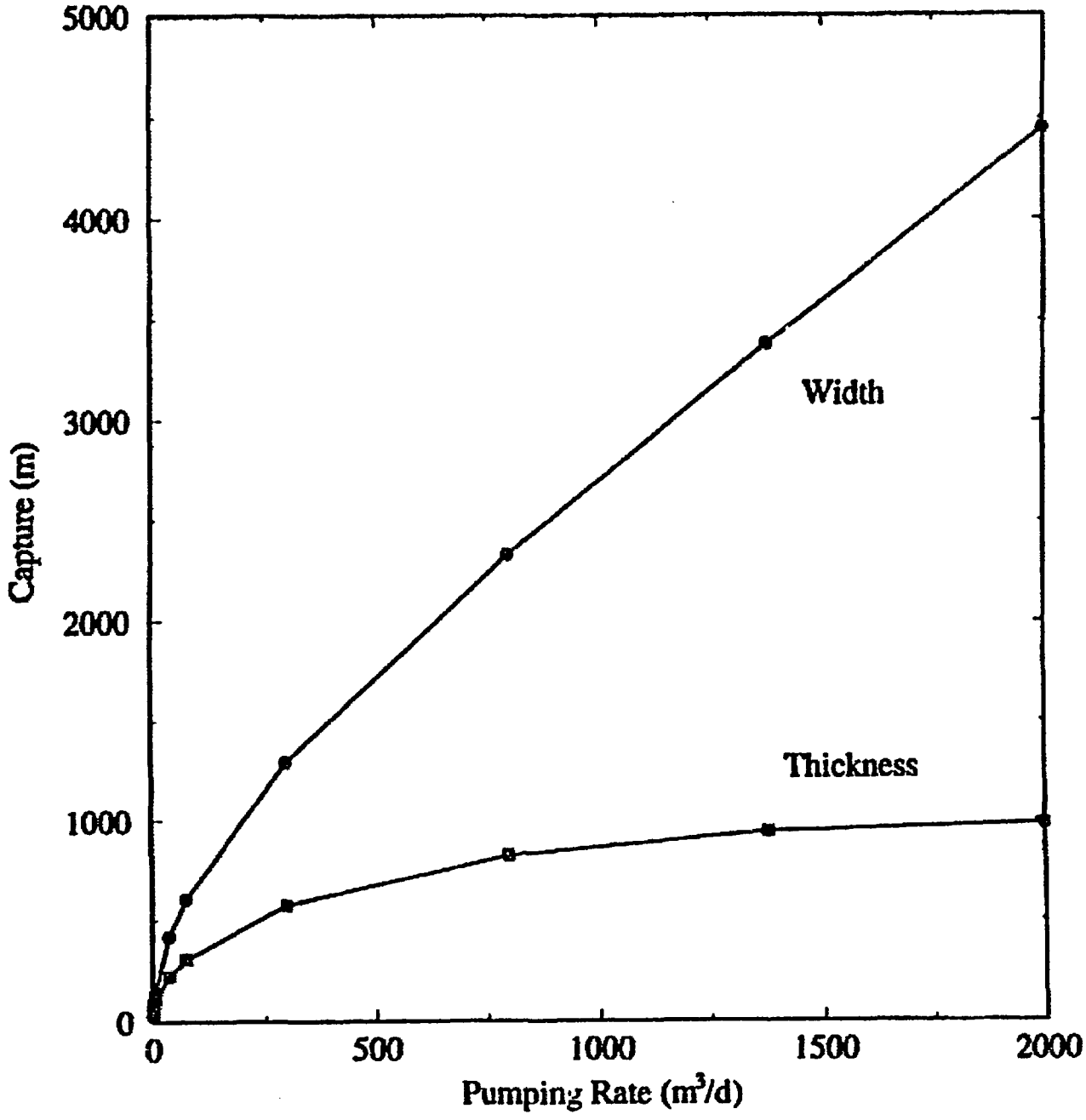

Figure 4-5. This plot illustrates the effect of pump rate (range 1 to 2000 m^3/d) on the capture zone width and thickness. A transmissivity of 100 m^2/d and regional gradient of 0.005 are used.

4.2.1 Transport Parameters

The initial source size, seepage velocity, and the dispersivities all control the plume configuration after 30 km of advective-dispersive transport. Kessler and McGuire (1996) noted the inverse relationship between source size and mean concentration reductions. They also found that a doubling of the source thickness led to an increase of 17 percent in the plume width at 25 km. Similarly, a 60-percent increase in the source width led to an increase of 6 percent in the plume width at 25 km. In this study, the source size will be held constant at 500 by 25 m for the 3D dispersion plumes and 500 m wide for the 2D dispersion plumes.

Since transport simulations were run to steady state in order to determine maximum plume dimensions, a reasonable value of the seepage velocity along the flow path from the repository, or from the accessible environment, to Amargosa Farms is needed. Seepage velocity is related to the Darcy flux by porosity. The Darcy flux for the transport analysis need not be the same as that for the capture zone analysis since the former represents the porous media and hydraulic head gradients from the repository to Amargosa Farms while the latter represents the Amargosa Farms area. Seepage velocity for transport was chosen to represent the mean pathway velocity from the tuff through the alluvium. Baca et al. (1997) report calculated ranges of Darcy flux of 0.01 to 3.7 m/yr for the saturated tuff aquifer and 0.4 to 0.7 m/yr for the alluvium. Assuming a porosity of 0.3 for the alluvium, the seepage velocity would be in the range of 1.3 to 2.3 m/yr. Kessler and McGuire (1996) used a seepage velocity of 1.76×10^{-6} m/s (55 m/yr) although it is not clear whether site-specific information (gradient, hydraulic conductivity, porosity) was used to obtain this estimate. The value of 2.4 m/yr used here for seepage velocity is closer to that approximated from the Darcy flux values reported by Baca et al. (1997).

The value of the concentration at the source is chosen to approximate a mass release rate of 10 Ci/yr, which is taken as an upper bound for mass release rates as delineated by the ^{99}Tc example in Mohanty et al. (1997). Assuming that dispersion off the constant concentration boundary is negligible, the concentration corresponding to 10 Ci/yr is 4.38E−6 Ci/l for a source size of 500 by 25 m and a Darcy velocity corresponding to a seepage velocity of 2.4 m/yr with a porosity of 0.3. The assumption of negligible dispersion off the source boundary as compared to advective flux off the boundary is reasonable at long times. However, since the plume configurations scale directly for steady state problems, the value of the concentration at the boundary conditions does not affect dilution factor estimates; as long as normalized values of concentration are reported and not absolute concentrations.

Simulation of 3D dispersion requires values for the longitudinal, horizontal transverse, and vertical transverse dispersivities. Generally, dispersivities are considered to be scale dependent (Gelhar et al., 1992). TSPA-95 (TRW Environmental Safety Systems, Inc., 1995) assumed relatively large transverse dispersivities which resulted in exceptionally large plumes (especially in the vertical direction) and large dilution factors (10^3 to 10^5). Kessler and McGuire (1996) recognized that there is a limit to the heterogeneity scale that a plume would encounter, although they nonetheless used a vertical transverse dispersivity equal to the horizontal dispersivity. This seems unlikely in light of the lithologic layering in the alluvial basin sediments. Contaminant plumes generally exhibit limited vertical spreading (Gelhar et al., 1992) Thus, small vertical transverse dispersivities values are likely. In a literature review of measured dispersivity values and ratios, Gelhar et al (1992) note that horizontal to vertical transverse dispersivity ratios are often 1-2 orders of magnitude different. Furthermore, the measured vertical dispersivity values were all reported in Gelhar et al. (1992) to be less than 1 m; generally, in the range 0.06 to 0.3 m for scales ranging from 20 m to 10 km. In addition, the vertical transverse dispersivity

values exhibited no scale dependency. The longitudinal and horizontal transverse dispersivity are scale-dependent with their ratio equal to one order of magnitude. For the constant concentration source, the longitudinal dispersivity and the velocity do not affect the mean plume concentration in steady state transport. Plume size is controlled by the transverse dispersivities.

In this study, the location of the radionuclide source area is the same as that assumed by Kessler and McGuire (1996). A patch source area aligned perpendicular to the flow direction is located at the edge of the accessible environment or fence as described in Kessler and McGuire (1996), as opposed to locating the source area at the repository. The conceptual model consists of a release from the repository reaching the accessible environment from where it is modeled as a patch source to obtain a plume configuration 15 to 25 km further along Fortymile Wash to the Amargosa Farms area. Noting the variations in the flow path lengths, the accessible environment is approximately 5-7 km from the repository, the quasi-municipal and domestic wells first encountered at Amargosa Valley are about 15 km from the accessible environment, and the majority of irrigation wells first encountered are at about 25 km from the accessible environment.

4.2.2 Plume Dimensions for 3D Dispersion from Constant Concentration Source

The analytic solution to Eq. (4-1) for the constant concentration patch source as described in Wexler (1992) is

$$C(x,y,z,t)=\frac{C_0\, x \exp\left[\frac{Vx}{2D_x}\right]}{8\sqrt{\pi D_x}} \int_0^t \tau^{-\frac{3}{2}} \exp\left[-\left(\frac{V^2}{4D_x}+\lambda\right)\tau - \frac{x^2}{4D_x\tau}\right] \left[\operatorname{erfc}\left(\frac{(Y_1-y)}{2\sqrt{D_y\tau}}\right) - \operatorname{erfc}\left(\frac{(Y_2-y)}{2\sqrt{D_y\tau}}\right)\right] \left[\operatorname{erfc}\left(\frac{(Z_1-z)}{2\sqrt{D_z\tau}}\right) - \operatorname{erfc}\left(\frac{(Z_2-z)}{2\sqrt{D_z\tau}}\right)\right] d\tau \tag{4-2}$$

where C_0 is the concentration at the source, τ is a dummy variable of integration for time, λ is the decay coefficient, exp is the natural exponential, and erfc is the complementary error function. The dispersion coefficients in the x-, y-, and z-directions are defined as the products of the seepage velocity and the dispersivities in the x-, y-, and z-directions, respectively. This equation is the solution to the 3D solute transport equation for a vertical patch source aligned normal to the principal direction of flow where the patch dimensions are devined by $Y_2 - Y_1$ and $Z_2 - Z_1$. The solution to the advection-dispersion equation is valid for a 1D uniform flow field and 3D dispersion for a constant concentration source in an aquifer of infinite depth and lateral extent. Adsorption and radioactive decay of the solute are incorporated into the solution but were not used in this study. In the PATCH I Version 1.1 program, Wexler (1992) uses a Gauss-Legendre numerical integration technique to evaluate Eq. (4-2); however, possible round-off errors were reported for solutions at small distances and long times using this technique. For a similar problem, Domenico and Robbins (1985) simplify the integral problem by

summing over a specified number of continuous point sources in a patch. However, they too noted numerical errors at small distances and long times.

Tables 4-1 and 4-2 contrast plume width and thickness for various sets of dispersivity values at 15 and 25 km, respectively, from the source area located at the accessible environment. The longitudinal dispersivity value is reported in the tables but its magnitude is not a controlling factor for the results. The plume width and thickness are delineated at a threshold concentration of approximately $10^{-4} \times C_0$. The P-DF is also included in tables 4-1 and 4-2. These values will be used as a reference point for the dispersion-based dilution factors estimated in the following section. Where the centerline concentration can be used as a conservative estimate of the plume concentration, borehole dilution factors due to dispersion will be calculated by accounting for the distribution of concentration across a plume.

A reduction of the transverse dispersivities by 80 percent leads to a 46-percent reduction in plume width and thickness at 25 km. The ratio of the horizontal and vertical transverse dispersivities is kept at an order of magnitude. The percentages are approximately the same for the 15-km results. Similarly, a 50-percent reduction in the transverse dispersivities leads to a 24-percent reduction in plume width and thickness at 25 km.

4.2.3 Plume Dimensions Neglecting Vertical Dispersion for Constant Concentration Source

From the literature (Bedient et al., 1994), it is evident that existing plumes (caused either by accidental contamination or by deliberate injection of tracers for experimental purposes), typically show that plumes are often confined to a thin layer near the water table. Exceptions would occur in areas of high infiltration. The extreme case is to assume no vertical dispersion so the plume remains the same thickness as the source area but is dispersed laterally. This conceptual model for plume movement can be modeled using the following solution for 2D dispersion for a line source of specified width and constant concentration (Wexler, 1992):

$$C(x,y,t)=\frac{C_0 x}{4\sqrt{\pi D_x}}\exp\left(\frac{Vx}{2D_x}\right)\int_0^t \tau^{-\frac{3}{2}}\exp\left[-\left(\frac{V^2}{4D_x}+\lambda\right)\tau-\frac{x^2}{4D_x\tau}\right] \left[\operatorname{erfc}\left(\frac{(Y_1-y)}{\left(2\sqrt{D_y\tau}\right)}\right)-\operatorname{erfc}\left(\frac{(Y_2-y)}{\left(2\sqrt{D_y\tau}\right)}\right)\right] d\tau \quad . \tag{4-3}$$

The solution to Eq. (4-3) is implemented in the STRIPI Version 1.1 program of Wexler (1992). The solution for the line source can be extended to any source thickness.

In light of the arguments presented in the previous section, a reasonable selection of sets of dispersivities is 20:2, 50:5, and 100:10 for the longitudinal and transverse directions (table 4-3). These are depth-averaged dispersivity values which are not strictly comparable to the set of dispersivity values for 3D dispersion. When no vertical dispersion is included, the plume widths increase by between 16 and 29 percent for corresponding transverse dispersities.

Table 4-1. Plume configuration and point dilution factor at 15 km from the source area for a range of dispersivity values. C_c is the centerline concentration. The source area is 25 m thick by 500 m wide.

a_x:a_y:a_z (m)	Thickness (m)	Width (m)	P-DF = C_e/C_c
20:2:0.2	330	2,200	6
50:5:0.5	480	3,100	13
100:20:2	830	5,200	48
100:10:1	640	4,000	25
100:10:0.1	250	4,300	9

Table 4-2. Plume configuration and point dilution factor at 25 km from source area for a range of dispersivity values.

a_x:a_y:a_z (m)	Thickness (m)	Width (m)	P-DF = C_e/C_c
20:2:0.2	410	2,600	9
50:5:0.5	580	3,700	21
100:20:2	970	5,800	80
100:10:1	780	4,800	41
100:10:0.1	290	5,200	14

4.3 BOREHOLE DILUTION FACTORS BASED ON VOLUMETRIC FLUX

Volumetric flux-based borehole dilution factors (F-BDF) are determined by comparison of the plume and capture zone configurations (figure 4-1). The ratio of the cross-sectional area of the capture zone to the cross-sectional area of the portion of the plume which intersects the capture area in the plane perpendicular to the principal direction of flow is the dilution factor due to borehole mixing based on

Table 4-3. Plume configuration in terms of width at 15 and 25 km and point dilution factor for a source area width of 500 m and no vertical dispersion.

a_x:a_y (m)	Width (m) at 15 km	P-DF = C_o/C_c at 25 km	Width (m) at 15 km	P-DF = C_o/C_c at 25 km
20:2	2,330	1.5	2,860	1.8
50:5	3,410	2.1	4,230	2.6
100:10	4,640	2.8	5,800	3.6

volumetric flux comparisons. In other words, the F-BDF is the ratio of the capture and the intersection area. No credit is taken for the distribution of the concentration across the plume in the calculation of the F-BDF. All plumes in this section are modeled from a constant concentration source.

Generally, the plumes are wider than the capture zone but not as thick. Four plume scenarios are chosen to represent a range of conditions. The first and second scenarios are 10 m and 25 m thick plumes for which no vertical dispersion has occurred. The width of the plume depends on the horizontal transverse dispersivity that is used. For domestic wells, it does not matter what dispersivity is chosen since all plumes are wider than all domestic well capture zones. The third and fourth scenarios incorporate vertical dispersion with dispersivity ratios of 20:2:0.2 and 100:10:0.1. The F-BDF for the third and fourth scenarios are presented for the large pumpage irrigation wells.

4.3.1 Domestic Wells

The plume configuration that results from 3D dispersion from a constant concentration source will generally be larger than the capture area of a single domestic well, a closely spaced collection of domestic wells, or a quasi-municipal well for wells typical of the Amargosa Farms area. Hence, with the assumption of a uniform plume concentration, there will be no borehole dilution. Only for the smallest vertical transverse dispersivity values (less than 0.2) and for the largest pump volumes from a closely spaced collection of domestic and quasi-municipal wells will there be vertical gradients that are strong enough to capture clean water and provide borehole dilution.

The effects due to pumping rate, screen position, transmissivity, and regional gradient on the F-BDF are shown in figures 4-6 to figure 4-9. The plumes of thickness 10 and 25 m with no vertical dispersion are used for the calculation. As expected, the factors for the 10-m thick plume are greater than those for the 25-m plume. Again, the F-BDF do not include effects due to concentration differences in the plume.

For a typical domestic well that pumps 1,800 gpt, the F-BDF decreases from 10 to 4 when the plume thickness increases from 10 to 25 m at the 25-km distance (figure 4-6). The difference in the factors increases as the pumping rate increases. The F-BDF for the 10-m plume range between 7 and 26 for pumping rates in the range of domestic and quasi-municipal wells. Similarly, the F-BDF for the 25-m plume range between 3 and 10.

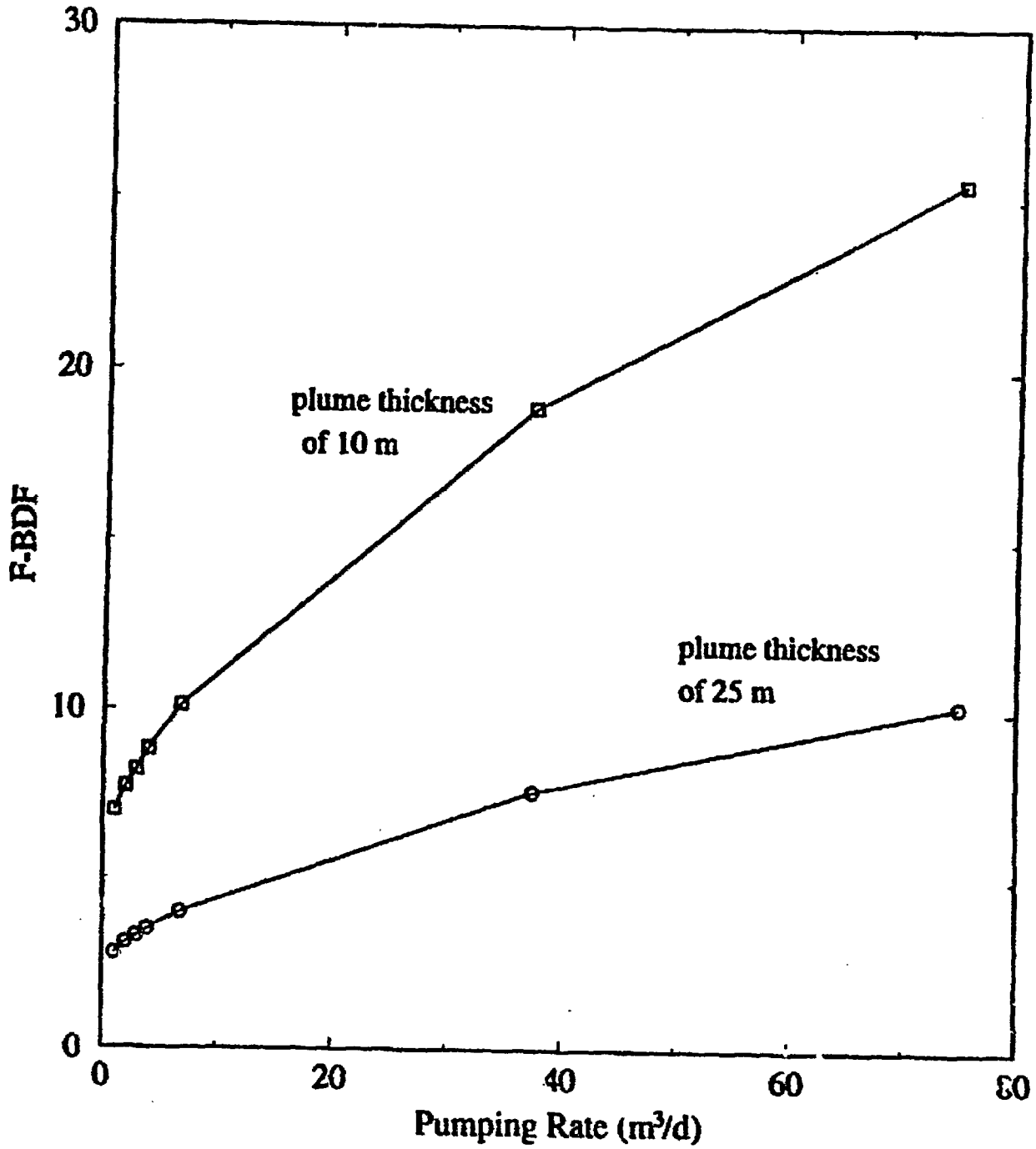

Figure 4-6. Effect of pump rate (range 1 to 75 m^3/d) on the flux-based borehole dilution factor for plumes of thickness 10 m and 25 m (no vertical dispersion). The regional gradient is 0.005 and the transmissivity is 100 m^2/d for all cases.

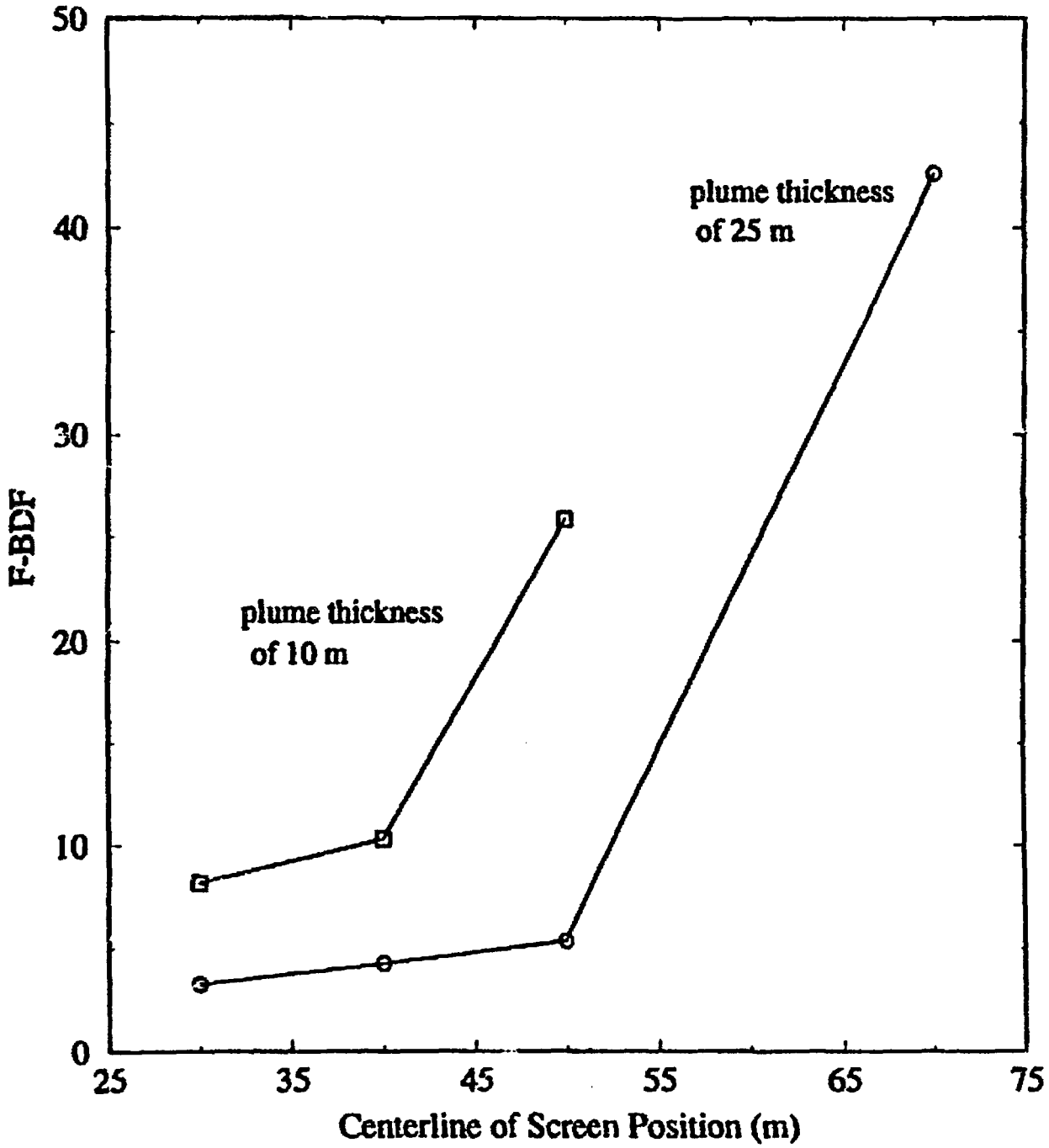

Figure 4-7. Effect of screen position for domestic-sized wells on the flux-based borehole dilution factor for plumes of thickness 10 m and 25 m (no vertical dispersion). All screen lengths are 60 m, the regional gradient is 0.005, and the transmissivity is 100 m^2/d for all cases.

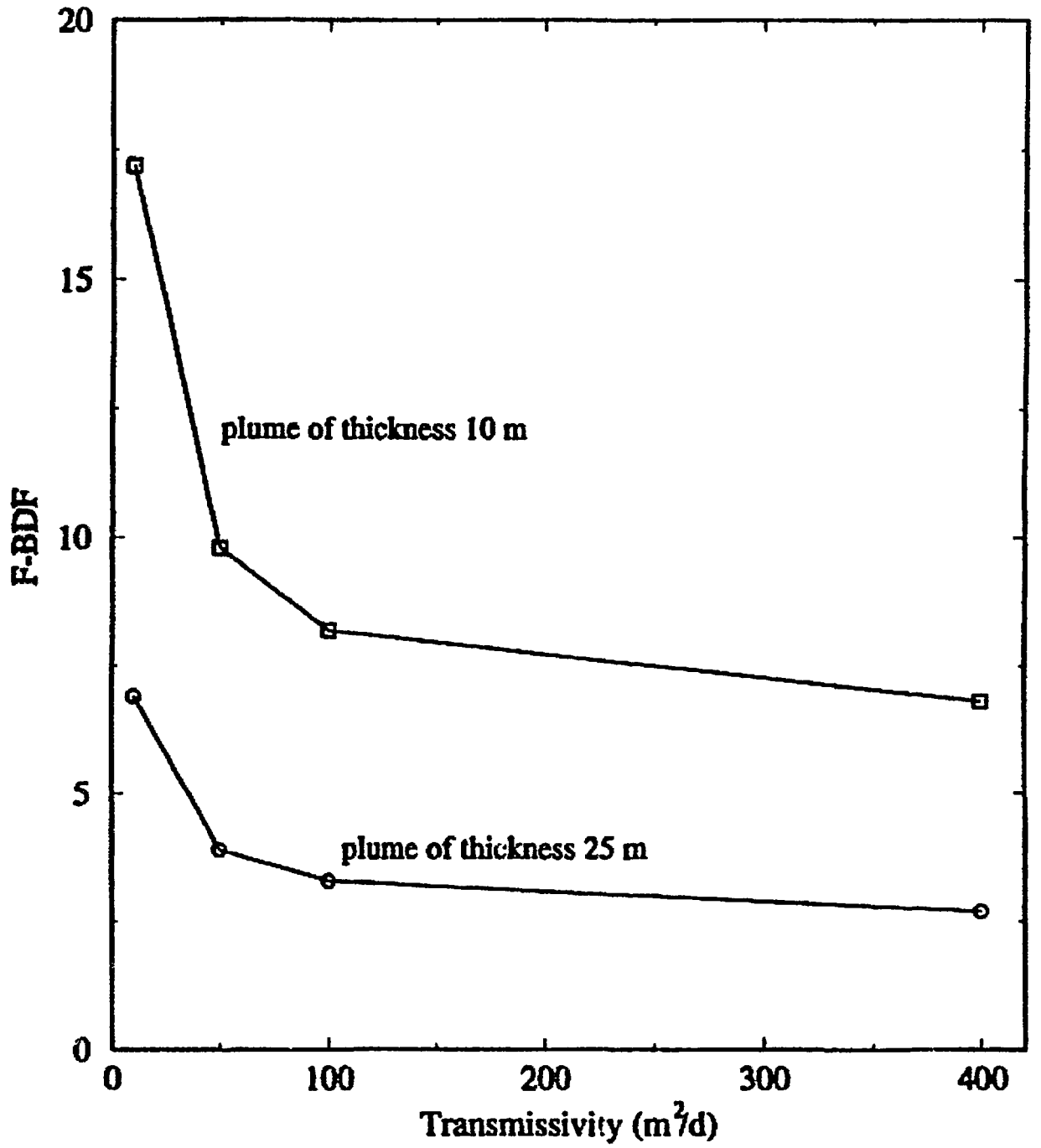

Figure 4-8. Effect of transmissivity (10, 50, 100, 400 m^2/d) on the flux-based borehole dilution factor for plumes of thickness 10 m and 25 m (no vertical dispersion). The regional gradient is 0.005 and the pump rate is 3 m^3/d for all cases.

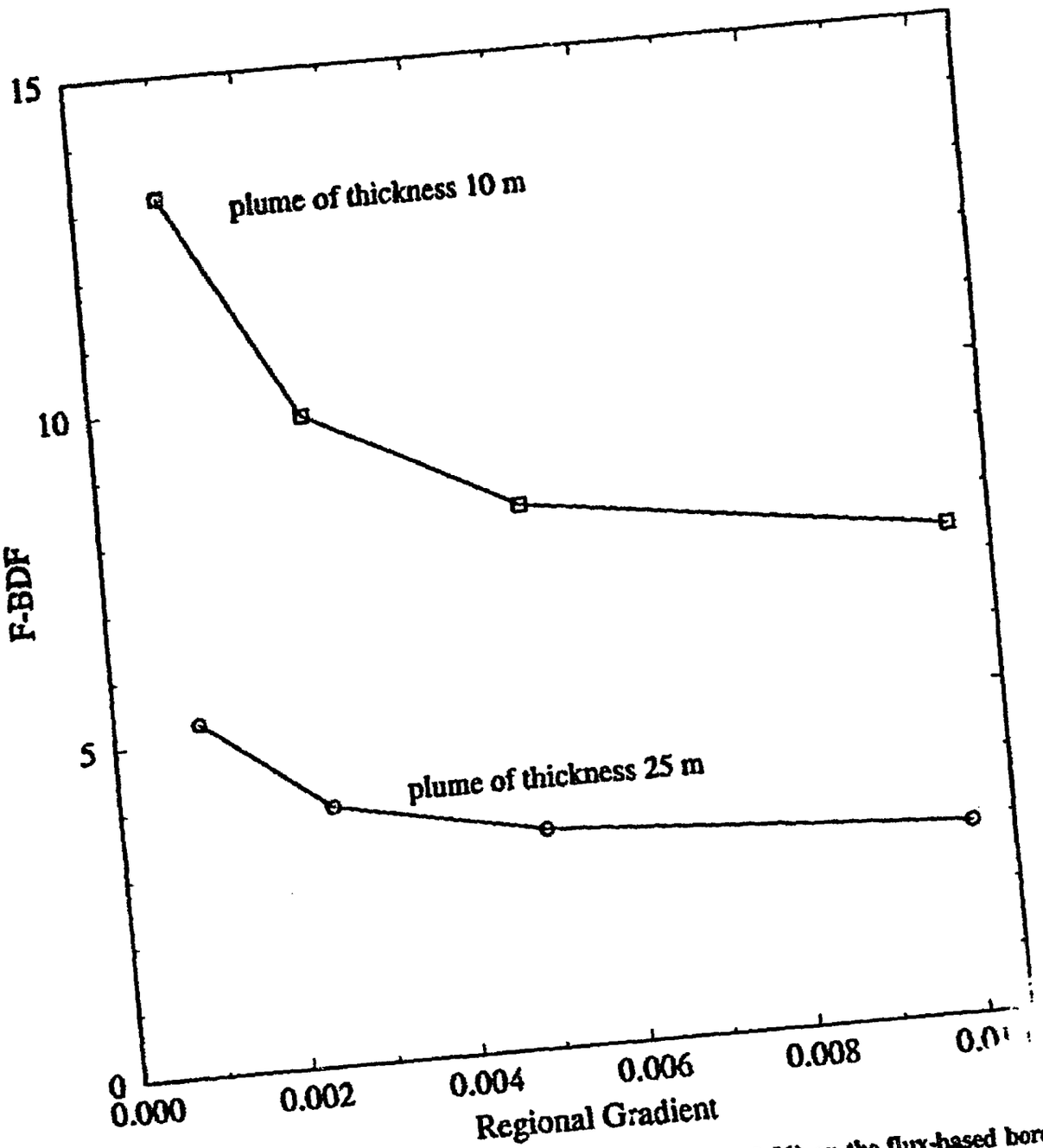

Figure 4-9. Effect of the regional gradient (0.001, 0.0025, 0.005, 0.01) on the flux-based borehole dilution factor for a domestic-sized well and plumes of thickness 10 m and 25 m (no vertical dispersion). The transmissivity is 100 m^3/d and the pump rate is 3 m^3/d for all cases.

The position of the screened portion of the well does not have a significant effect for domestic wells for the 25-m plume until screened portions are lower than three standard deviations from the average screen position (figure 4-7). The limited effect of screen position is due to a combination of the center of mass of the plume being near the water table as well as the small impact on the capture area due to different screen position and lengths. Within about two standard deviations from the average position of the screen, the F-BDF do not vary by more than a factor of 2. In all scenarios, the plume is assumed to be at the water table. The borehole dilution factors are in the 3 to 5 range and 8 to 10 range for the 25 and 10-m plumes, respectively, unless screen positions lower than three standard deviations from the average are considered.

The effect of transmissivity and regional gradient on F-BDF for the 10 and 25-m-thick plumes with no vertical dispersion are not significant until the smallest values of transmissivity and gradient are used (figures 4-8 and 4-9). For transmissivities greater than 50 m^2/d, the F-BDF is in the range of 7 to 10 for the 10-m-thick plume and 3 to 7 for the 25-m-thick plume. A regional gradient of 0.001 leads to a F-BDF of 13 for the plume thickness of 10 m while the larger gradients range from 7 to 10. The F-BDF for the 25-m-thick plume are between 3 and 5.

4.3.2 Irrigation Wells and Plumes with No Vertical Dispersion

The F-BDF were calculated for irrigation wells using the scenario of a 25-m-thick plume with no vertical dispersion. In this scenario, the large vertical gradients and deep capture for the wells lead to large amounts of clean water mixing in the borehole with the contaminated water from the plume. Depending on the capture zone width and the plume width, some horizontal mixing of clean and contaminated water may occur. The width of the plume depends on the transverse dispersivity. Figure 4-10 shows the F-BDF for a well pumping rate of 300 to 2,000 m^3/d for plumes using three different dispersivity values. Since the plume width decreases as the dispersivity decreases, the F-BDF increases as the dispersivity decreases. This effect is not present at the low pumping rates for the particular flow field parameters chosen for this comparison. The F-BDF range from 19 to 49 for all dispersivities sets. It must be re-emphasized that the F-BDF only reflects the effects of contaminant concentration reduction in the borehole and not the effects of dispersion on the resident or aquifer contaminant concentrations. This explains the otherwise counter-intuitive observation that, for high capacity wells, the F-BDF increases as the transverse dispersivity decreases.

4.3.3 Irrigation Wells and Plume with Vertical Dispersion

The F-BDF are calculated for irrigation wells using the scenario of a plume where 3D dispersion from a constant concentration source occurs. The effect of dispersion on the concentration during transport on the borehole dilution factor is not considered here; only the shape of the plume is considered in the dilution factors. Generally, the capture zones are thicker and narrower than the thin but wide plumes. Depending on the dispersivity values used for the plume and the pumping rate and hydraulic properties used for the capture zone, the capture zones may be wider than the plume. Only for low pumping rates are the plumes thicker than the capture zone; this occurrence leads to no volumetric-based borehole dilution.

Plume shapes using dispersivities of 100:10:0.1 m and 20:2:0.2 m are compared to capture areas in order to calculate F-BDF The plume for the 100:10:0.1 scenario is wider but thinner than the plume for the 20:2:0.2 scenario. Figures 4-11 to 4-13 show the effects of pumping rate, transmissivity, and regional gradient on the F-BDF which generally range from 1 to 5 regardless of dispersivity values used. For the pumping rate (figure 4-11) and the regional gradient (figure 4-13) curves, the two

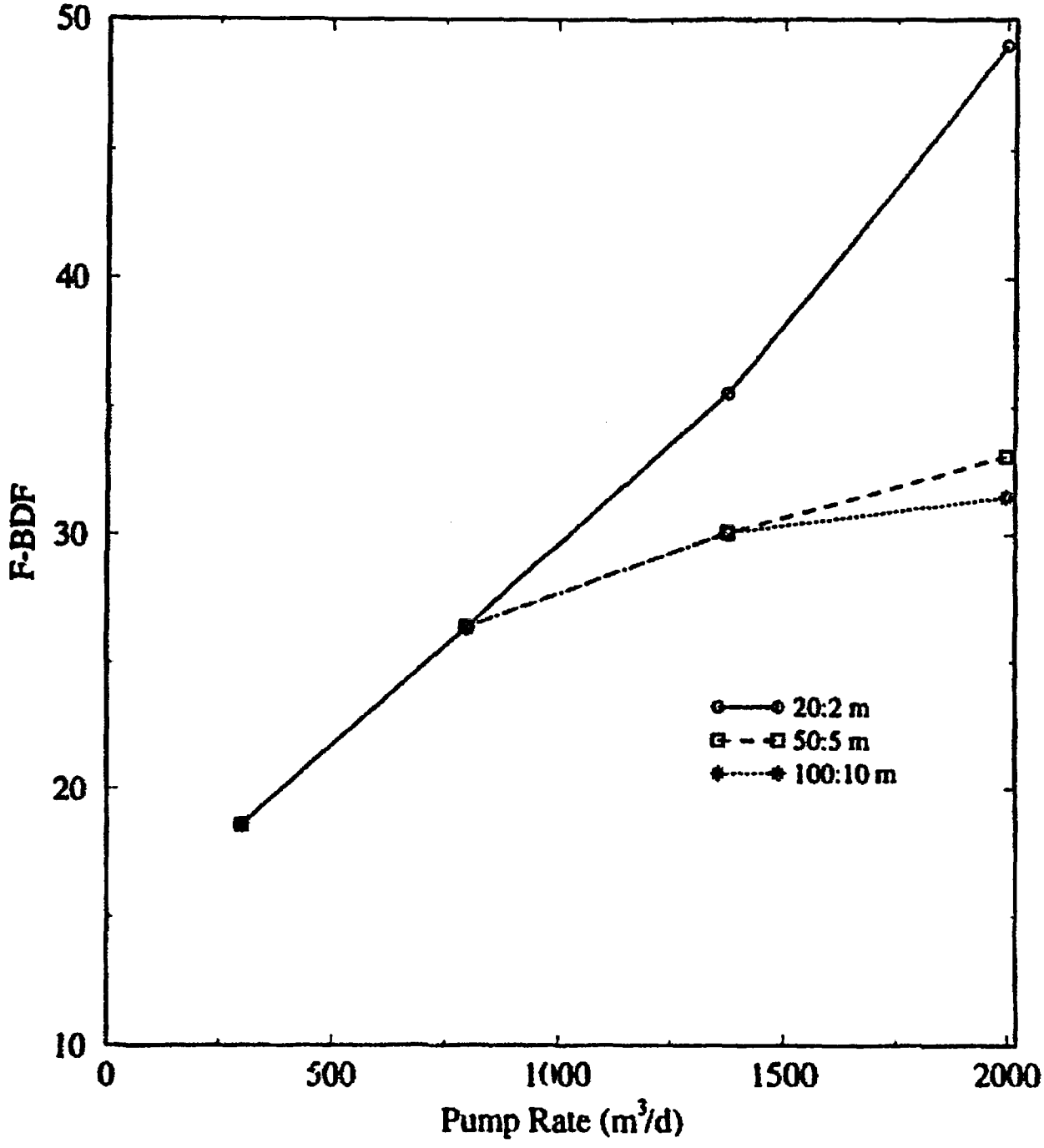

Figure 4-10. Effect of pump rate on flux-based borehole dilution factors for irrigation wells and a 25 m thick plume with no vertical dispersion. Three curves are plotted for different sets of dispersivity values.

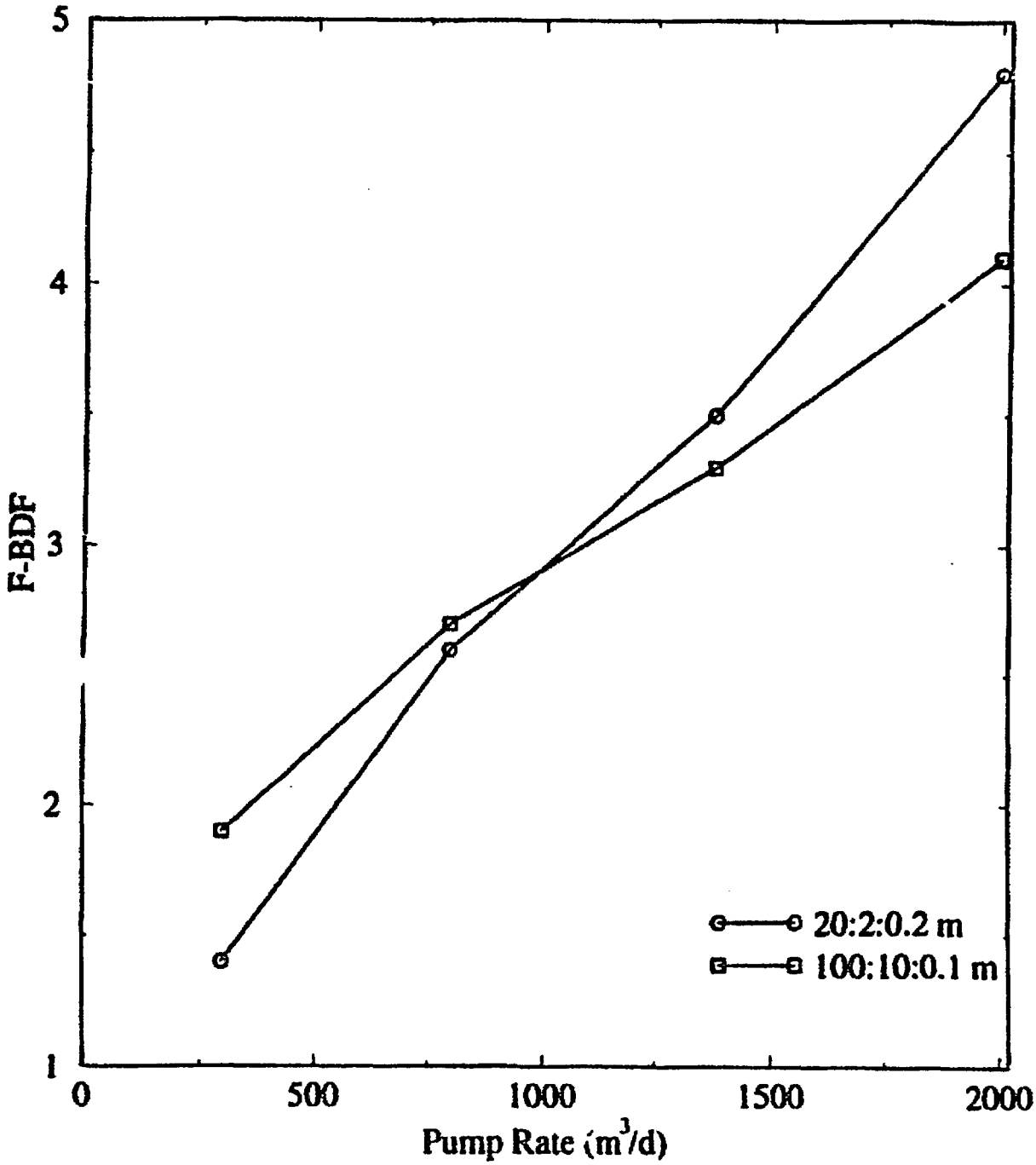

Figure 4-11. Effect of pump rate on dilution factors for irrigation sized wells and a plume with 3D dispersion. Curves are plotted for two sets of dispersivity values.

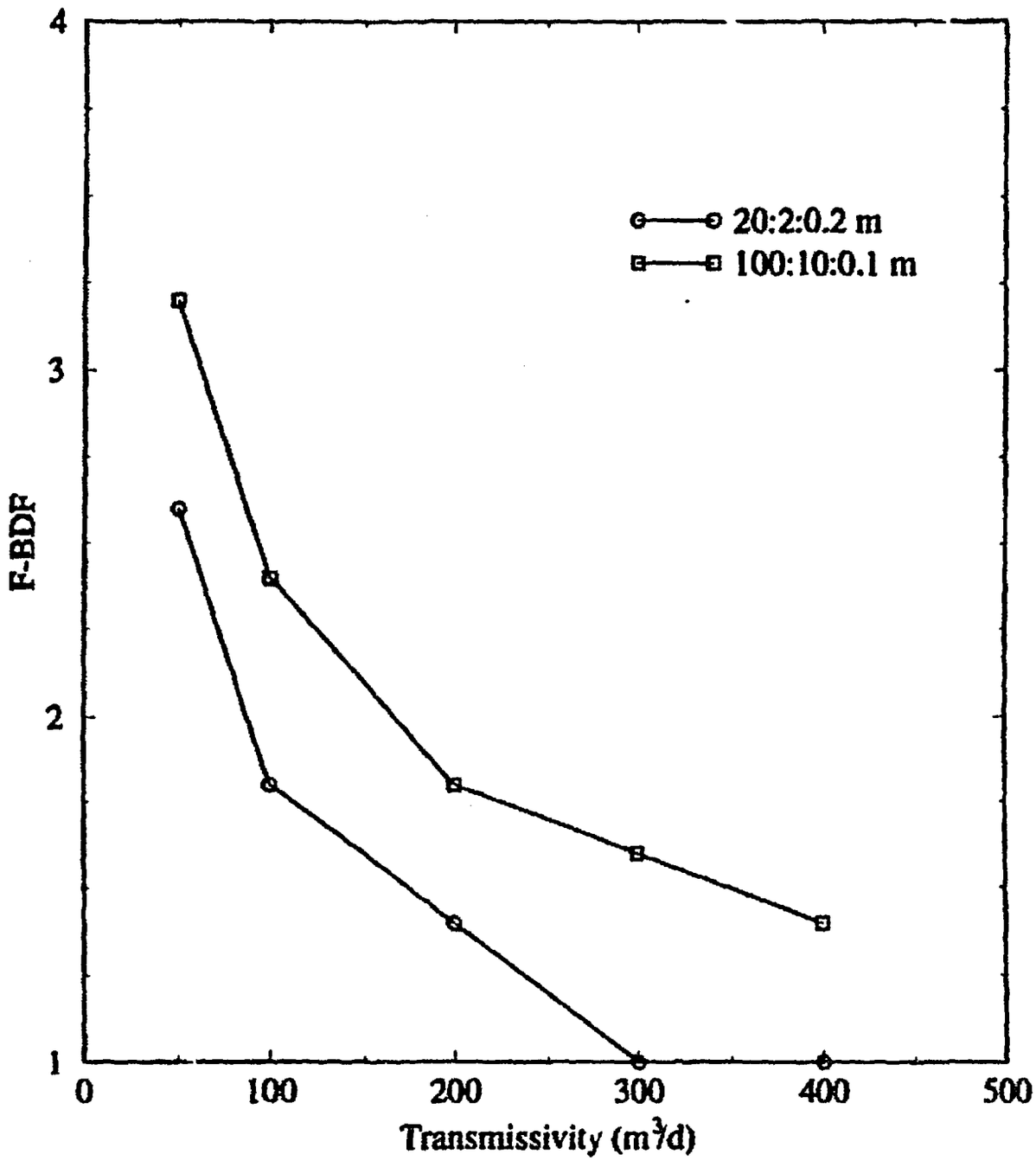

Figure 4-12. Effect of transmissivity (50 to 400 m²/d) on dilution factors for irrigation sized wells and a plume with 3D dispersion. Curves are plotted for two sets of dispersivity values.

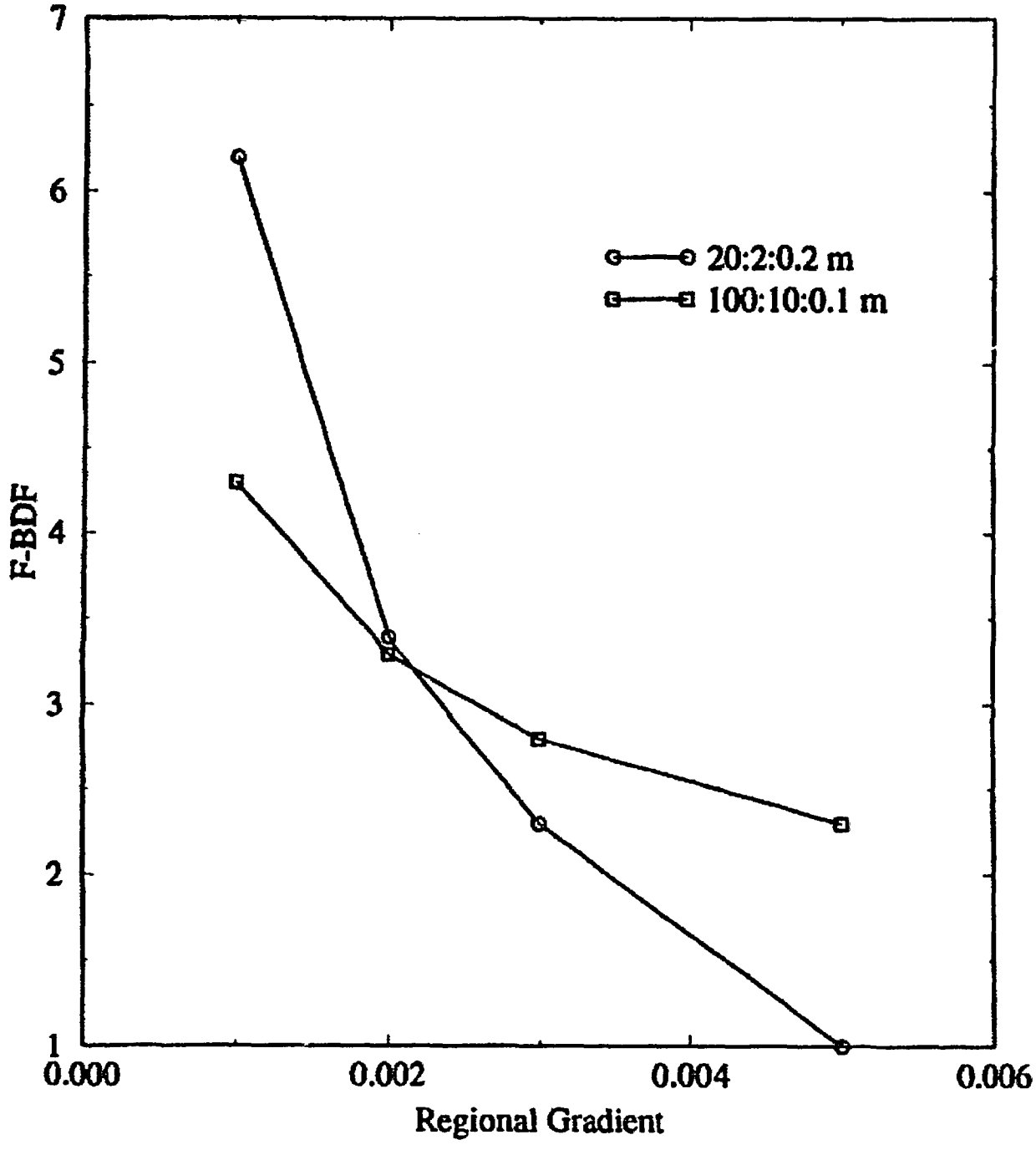

Figure 4-13. Effect of regional hydraulic gradient (0.001 to 0.0005) on dilution factors for irrigation-sized wells and a plume with 3D dispersion. Curves are plotted for two sets of dispersivity values.

dispersivity sets intersect due to the interplay between the thickness of the plume (the 20:2:0.2 plume is thicker) and the point where the entire plume is captured (the 100:10:0.1 plume is larger in area)

In summary, the effect of the plume size has the largest effect on the F-BDF. The values of the dilution factors are tabulated in appendix C. The shapes of plumes described above can be contrasted with the streamtubes used for the TPA (Baca et al., 1997; Manteufel et al., 1997). The plumes increase in size, and volumetric flow rate, with increasing distance from the source. The streamtubes have a fixed thickness and a variable width which depends on the streamlines. The width may increase or decrease for diverging converging, flow fields, respectively, but the volumetric flux does not change.

4.4 BOREHOLE DILUTION FACTORS BASED ON DISPERSIVE TRANSPORT

The F-BDF estimated in the previous section do not account for the concentration distribution of a migrating plume. Kessler and McGuire (1996) accounted for dispersion during plume migration by assuming the dilution factor was the ratio of the source concentration to the centerline concentration. Implicit in their assumption is that the plume has a uniform concentration equal to the centerline value that they justify as a conservative choice in terms of eventual dose to a critical group. This section will address the effect on borehole dilution of a concentration distribution within a plume.

The transport dispersion-based borehole dilution factor (T-BDF) was calculated by integrating the concentration distribution across the area of the portion of the plume which is captured by a pumping well. Portions of the plume not captured by the well do not contribute radionuclide mass to the well. The T-BDF was estimated by numerical integration of the concentration distribution in the area of the plume which was captured. The total borehole dilution factor can be estimated by linear combination of the F-BDF and T-BDF. The effect of domestic and irrigation wells on T-BDF varies significantly due to the thickness of the capture area and will be presented separately.

4.4.1 Domestic Wells

Figures 4-14 and 4-15 illustrate the effect of the concentration distribution within a plume on the T-BDF for two different plume configurations; a thin plume (25-m) with no vertical dispersion and a 3D dispersion plume. The T-BDF for the thin plume is nearly constant and its value is close to that of the P-DF (1.8) for pumping rates in the range of domestic and quasi-municipal wells (figure 4-14). The T-BDF for the plume with 3D dispersion vary from 9 to 18, increasing as the pumping rate increases. The larger values of T-BDF indicate the significance of pumping from less concentrated portions of the plume as compared to the centerline.

T-BDF is inversely proportional to the transmissivity (figure 4-15) with values ranging from 12 to 9 as transmissivity increases. Smaller transmissivity values lead to larger capture areas thus drawing water from portions of the plume with lower concentration. The effect of hydraulic gradient is similar to that of transmissivity.

4.4.2 Irrigation Wells

Figures 4-16 and 4-17 illustrate the effect of the concentration distribution on borehole dilution for irrigation wells. For the plume configuration with 3D dispersion, the T-BDF are as much as five

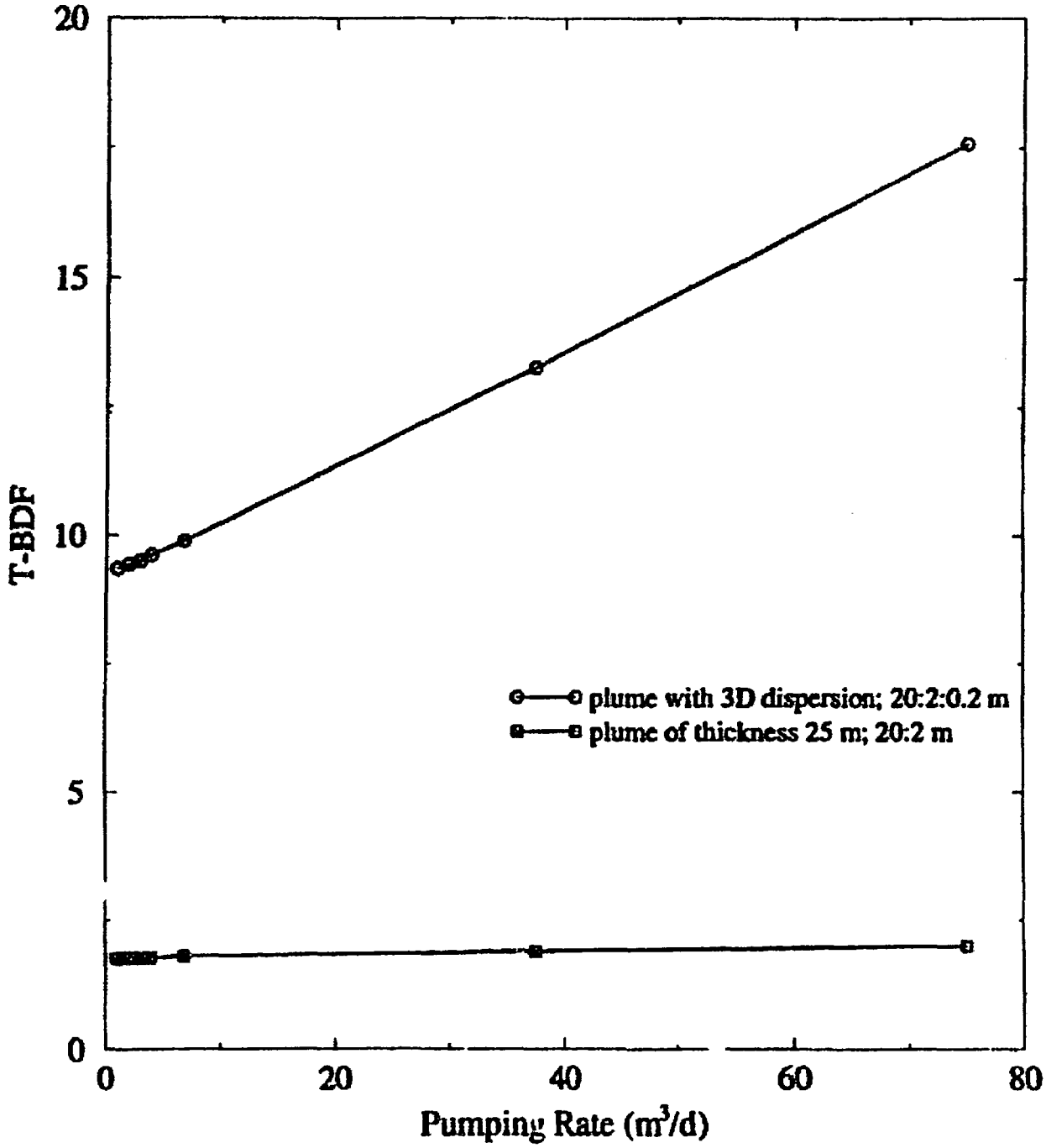

Figure 4-14. Effect of pumping rate (1-75 m^3/d) for domestic wells on transport dispersion-based borehole dilution factor for two different plume configurations: a thin plume with no vertical dispersion and a 3D dispersion plume both with dispersivity ratios as noted in the plot.

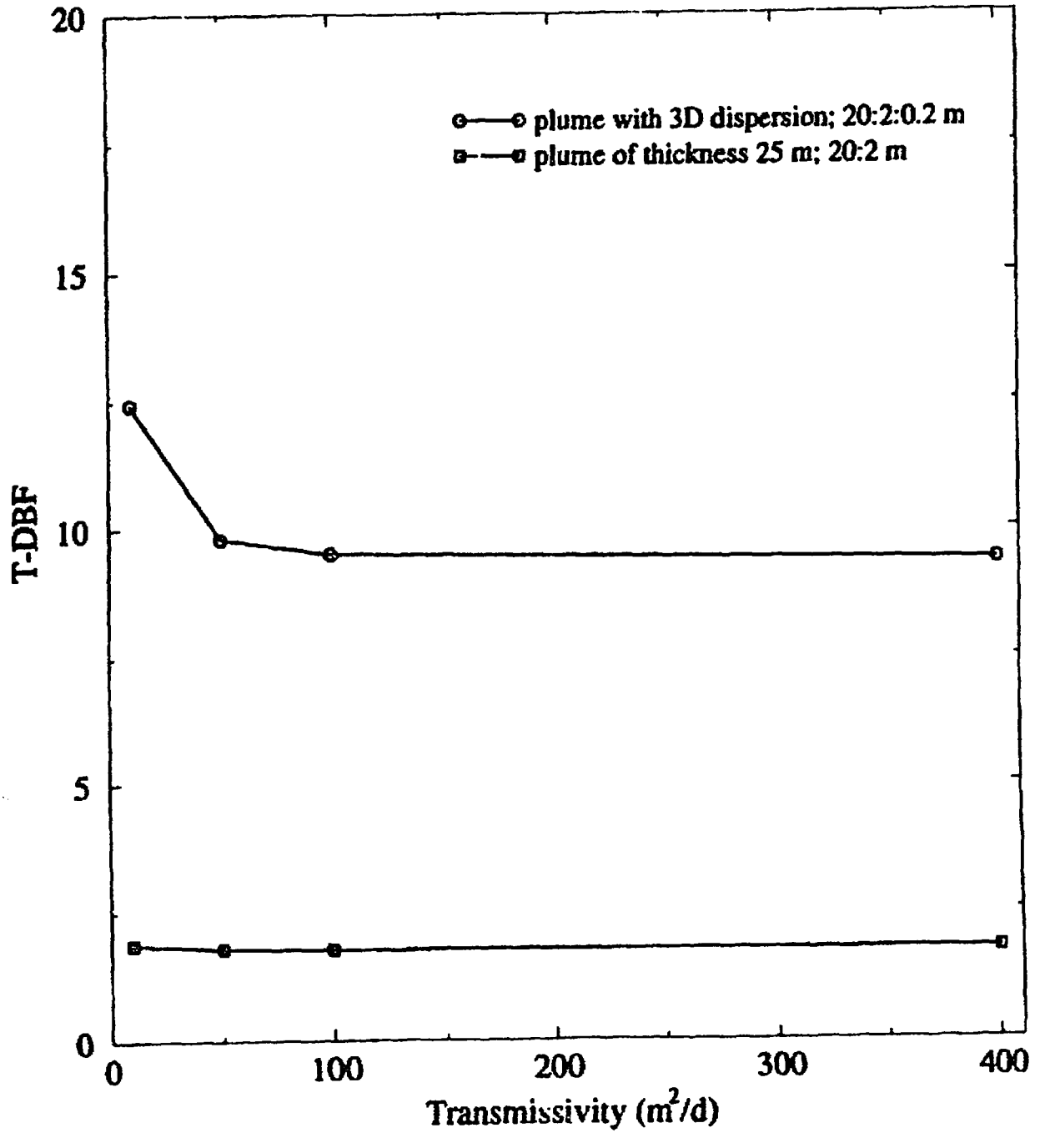

Figure 4-15. Effect of transmissivity (10–400 m^2/d) for domestic wells ($Q = 3\ m^3/d$) on transport dispersion-based borehole dilution factor for two different plume configurations: a thin plume with no vertical dispersion and a 3D dispersion plume, both with dispersivity ratios as noted in the plot.

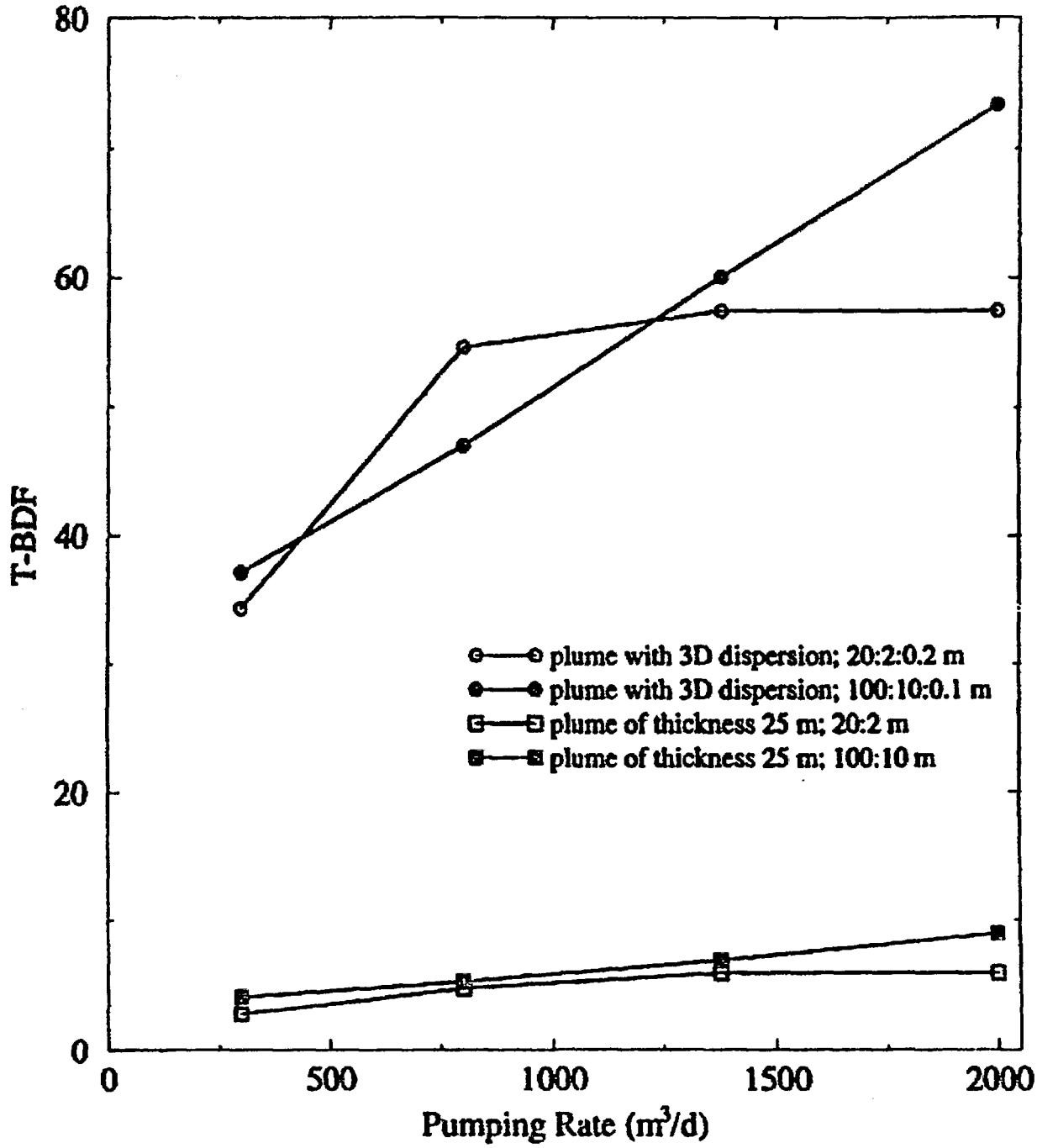

Figure 4-16. Effect of pumping rate (300–2,000 m^3/d) for irrigation wells on transport dispersion-based borehole dilution factor for four different plume configurations: two thin plumes with no vertical dispersion and two 3D dispersion plumes, all with dispersivity ratios as noted in the plot.

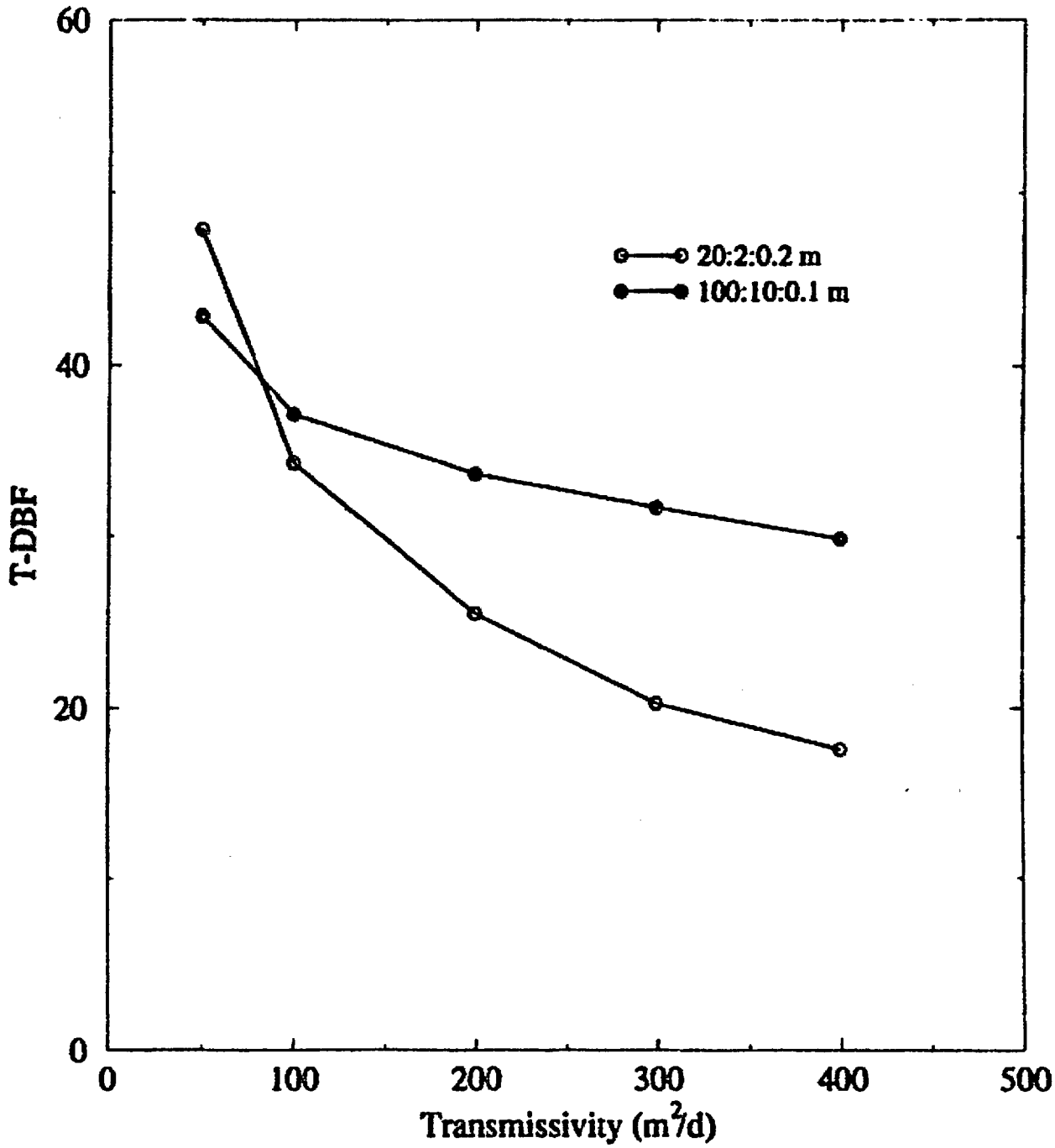

Figure 4-17. Effect of transmissivity (50–400 m^2/d) for large irrigation wells ($Q=2116\ m^3/d$) on transport dispersion-based borehole dilution factor for two different plume configurations: two 3D dispersion plumes with dispersivity ratios as noted in the plot.

times larger (figures 4-14 and 4-16) than those for the domestic wells due to the large thickness of the irrigation capture area drawing in portions of the plume with low concentrations. As with the domestic wells, the T-BDF for thin plumes with no vertical dispersion are near the value of the inverse of the normalized concentration. The straight line increase in T-BDF for the plume with 3D dispersion and dispersivity ratio of 100:10:0.1 m reflects the large size of the plume relative to the capture areas (figure 4-16). The plateau in the curve for the 3D plume with dispersivity ratio of 20:2:0.2 m at the larger pumping rates is due to the entire plume being captured.

For transmissivity increases from 50 to 400 m^2/d, the T-BDF decreases from 48 to 18 for the 3D plume with dispersivity ratio of 20:2:0.2 m and from 43 to 30 for the 3D plume with dispersivity ratio of 100:10:0.1 m. Effects due to hydraulic gradient are similar to those of the transmissivity (appendix C).

5 CONCLUSIONS

The approach used in this report to estimate borehole dilution is to separate it into two components: volumetric flux-based and dispersion transport-based components. The method used to estimate F-BDF in the Amargosa Farms region is to compare the capture area of a pumping well to the cross-sectional area of the portion of the plume which is captured. Borehole dilution factors presented in this report are calculated using the cross-sectional areas normal to the principal direction of regional flow. The method used to estimate the component of borehole dilution due to dispersion during transport is to numerically calculate an areal average for the portion of the plume captured by a pumping well. Since this report is a scoping analysis, the F-BDF and T-BDF have been kept separate in order to better delineate sensitive parameters.

Different configurations for the plume and the capture area were evaluated. For domestic wells, the capture area is generally much smaller than the cross-sectional area of a plume that has undergone horizontal and vertical transverse spreading due to macro-dispersion during transport along a 20- to 30-km pathway as shown in figure 4-1. Thus, as expected, F-BDF was minimal when the domestic well was aligned with the center of the plume. Any borehole dilution that might occur would be solely due to vertical gradients in the plume concentration and would be reflected in the T-BDF. For irrigation wells, or any high-discharge wells, the capture area is generally thicker than the plume, while the capture zone may be wider or narrower than the contaminant plume depending on the particular scenario.

To simulate the case in which stratification of the porous medium minimizes the vertical transverse dispersion and thus confines the plume to a thin layer near the water table, a 2D areal advection-dispersion equation was solved for which a fixed plume thickness was assumed. Based on field observations summarized by Gelhar et al. (1992), this non-vertically dispersing plume closely simulates the behavior of many contaminant plumes characterized in the field, and provides a worst-case scenario in terms of high resident concentrations. The position of the plume relative to the capture area affects the dilution factor.

Several conclusions can be drawn from this study. First, as defined in this study, F-BDF for individual wells are relatively small, ranging from 1 to 5 for an irrigation well extracting contaminant from a 3D plume, from 18 to 40 for an irrigation well extracting contaminant from a thin plume that does not disperse vertically, and from 3 to 18 for a domestic well extracting contaminant from a thin plume that does not disperse vertically. However, one must be careful when comparing F-BDF for different contaminant plume configurations since actual borehole concentrations depend on the mass of radionuclides captured and the volume of water pumped, not the area of the plume that is captured. On the one hand, a high-capacity well may capture the entire mass of radionuclides in a large plume, have an apparent dilution factor of only 1, yet still produce a low borehole concentration because the large plume would have a corresponding low mean resident concentration. On the other hand, a low-capacity domestic well may capture the entire mass of radionuclides in a very small plume, have a dilution factor of 10, yet produce a very high borehole concentration because the plume has a very high mean resident concentration.

The T-BDF account for the low or high mean resident concentrations in the different plume scenarios. T-BDF for domestic wells are generally low and approach the P-DF, whereas T-BDF for irrigation wells are up to two orders of magnitude depending on the plume scenario. The P-DF would be a poor estimate for the effect due to dispersion during transport for irrigation wells.

A second, and perhaps obvious, conclusion can be drawn from this study. Specifically, for a thin wide plume of specified dimensions, a low-capacity well screened over a thick section of the aquifer, may produce a higher dilution factor than a larger capacity well screened over a shorter vertical interval. Indeed, extremes in the individual borehole concentrations within a critical group will be greater if the contaminant plume is thin and borehole construction practices are varied, than if the plume is very thick and borehole construction practices are uniform. These results suggest that attention should be paid to understanding vertical spreading in the saturated zone along the presumed transport pathway. Indirect field evidence (Gelhar et al., 1992; Bedient et al., 1994) suggests minimal vertical spreading in alluvial aquifers; however, vertical spreading may be substantial in the fractured tuff aquifer, especially where flow crosses normal faults across which there is significant offset in the conductive and non-conductive strata.

The dilution factors computed in this study cannot be used to estimate borehole concentrations unless the conceptual model of transport adopted by the user conforms to the following description. The solution to the steady state advection-dispersion equation is used to define a material surface that extends from radionuclide source to radionuclide receptor locations through which all radionuclides are transported. The shape of this material surface is best described as a duct or tube bounded on the top by the water table and having a half-elliptical cross-section that increases in area from source to receptor in proportion to the assigned transverse dispersivities. Although radionuclides do not cross the boundary of this tube, water does; the flow rate of water changes in direct proportion to the cross-sectional area of the tube. Hence, under the assumptions of steady state transport, the mean radionuclide concentration computed over the cross-sectional area of the tube at any point along its length must decrease from source to receptor. For the case where vertical transverse dispersion is neglected, the true shape of the tube is not easily described, but the cross-section may be approximated by a vertical rectangle of fixed height whose width increases in direct proportion to the horizontal transverse dispersivity.

The shapes of plumes described above can be contrasted with the streamtubes used in the study by (Baca et al., 1997). The streamtubes have a fixed thickness and a variable width which depends on the streamlines. The width may increase or decrease for diverging or converging flow fields, respectively, but the volumetric flux remains constant within a streamtube.

Further work on borehole dilution would benefit greatly from both a better delineation of a plume entering the Amargosa Farms region and large-scale modeling of multiple-well systems. This report has shown that the plume configuration is an important component. Modeling multiple-well systems is an extension of this work that would better define the pumping effect on groundwater flow patterns in the Amargosa Farms region. The single-well approach used here should only be compared with approaches where the largest volume used for the pumping input is as small as the pumping from a single well. This also assumes that infiltration through the repository or saturated zone mixing beneath the aquifer would both be smaller than the pumping from a single well.

6 REFERENCES

Akindunni, F.F., W.W. Gillham, B. Conant, Jr., and T. Franz. 1995. Modeling of contaminant movement near pumping wells: Saturated-Unsaturated flow with particle tracking. *Ground Water* 33(2): 264-274.

Baca, R.G. et al. 1997. *NRC High-Level Radioactive Waste Program Annual Progress Report: Fiscal Year 1996. Chapter 9—Activities Related to Development of The U.S. Environmental Protection Agency Yucca Mountain Standard.* NUREG/CR-6513, No. 1. Washington, DC: U.S. Nuclear Regulatory Commission.

Bair, E.S., and T.D. Lahm. 1996. Variations in capture-zone geometry of a partially penetrating pumping well in an unconfined aquifer. *Ground Water* 34(5): 842-852.

Bauer, E.M., and K.D. Cartier. 1995. *Reference Manual for Data Base on Nevada Well Logs.* U.S. Geological Survey Open-File Report 95-460. Washington, DC: U.S. Geological Survey.

Bedient, P.B., H.S. Rifai, and C.J. Newell. 1994. *Ground Water Contamination Transport and Remediation.* Englewood Cliffs, New Jersey: PTR Prentice Hall.

Bedinger, M.S., K.A. Sargent, and W.H. Langer. 1989. *Studies of Geology and Hydrology in the Basin and Range Province, Southwestern United States, for Isolation of High-level Radioactive Waste-characterization of the Death Valley Region, Nevada and California.* U.S. Geological Survey Professional Paper 1370-F. Washington, DC: U.S. Geological Survey.

Buqo, T.S. 1996. *Baseline Water Supply and Demand Evaluation of Southern Nye County, Nevada.* Consultants Report Prepared for the Nye County Nuclear Waste Repository Office, Nye County, Nevada.

Burchfiel, B.C. 1966. *Reconnaissance Geologic Map of the Lathrop Wells 15-Minute Quadrangle, Nye County, Nevada.* USGS Miscellaneous Geological Investigations Map I-474. Washington, DC: U.S. Geological Survey.

Chiang, C., G. Raven, and C. Dawson. 1995. The relationship between monitoring well and aquifer solute concentration. *Ground Water* 33(5): 718-726.

Czarnecki, J.B., and R.K. Waddell. 1984. *Finite-Element Simulations of Groundwater Flow in the Vicinity of Yucca Mountain, Nevada-California.* U.S. Geological Survey Water-Resources Investigations Report 84-4349. Denver, CO: U.S. Geological Survey.

D'Agnese, F.A. 1994. *Using scientific information systems for three-dimensional modeling of regional ground-water flow systems, Death Valley Region, Nevada and California.* Ph.D Dissertation, Colorado School of Mines.

D'Agnese, F.A., C.C. Faunt, A.K. Turner, and M.C. Hill. 1996. *Hydrogeologic Evaluation and Numerical Simulation of the Death Valley Regional Ground-water Flow System, Nevada and California, Using Geoscientific Information Systems*. Washington, DC: U.S. Geological Survey (Draft).

Denny, C.S., and H. Drewes. 1965. *Geology of the Ash Meadows Quadrangle, Nevada-California*. U.S. Geological Survey Bulletin 1181-L. Washington, DC: U.S. Geological Survey.

Domenico, P.A., and G.A. Robbins. 1985. A new method of contaminant plume analysis. *Ground Water* 23(4): 476-485.

Fabryka-Martin, J.F., P.R. Dixon, S. Levy, B. Liu, H.J. Turin, and A.V. Wolfsberg. 1996. *Summary Report of Chlorine-36 Studies: Systematic Sampling for Chlorine-36 in the Exploratory Studies Facility*. LA-UR-96-1384. Los Alamos, NM: Los Alamos National Laboratory.

Faybishenko, B.A., I. Javandel, and P.A. Witherspoon. 1995. Hydrodynamics of the capture zone of a partially penetrating well in a confined aquifer. *Water Resources Research* 31(4): 859–866.

Fischer, J.M. 1992. *Sediment properties and water movement through shallow unsaturated alluvium at an arid site for disposal of low-level radioactive waste near Beatty, Nye County, Nevada*. U.S. Geological Survey Water-Resources Investigations Report 92-4032. Washington, DC: U.S. Geological Survey.

Flint, A.L., and L.E. Flint. 1994. Spatial distribution of potential near surface moisture flux at Yucca Mountain. *High-Level Radioactive Waste Management: Proceedings of the Fifth International Conference, Las Vegas, Nevada, May 22-26, 1994*. La Grange Park, IL: American Nuclear Society: 2352-2358.

Gelhar, L.W., C. Welty, and K.R. Rehfeldt. 1992. A critical review of data on field-scale dispersion in aquifers. *Water Resources Research* 28(7): 1,955–1,974.

Grubb, S. 1993. Analytical model for estimation of steady-state capture zones of pumping wells in confined and unconfined aquifers. *Ground Water* 31(1): 27–32.

Haitjema, H.M. 1995. *Analytic Element Modeling of Groundwater Flow*. New York: Academic Press.

Hoover, D.L., W.C. Swadley, and A.J. Gordon. 1981. *Correlation Characteristics of Surficial Deposits With a Description of Surficial Stratigraphy in the Nevada Test Site Region*; USGS. Open-File Report 81-512. Washington, DC: U.S. Geological Survey.

Kessler, J., and R. McGuire. 1996. *Yucca Mountain Total System Performance Assessment, Phase 3*. EPRI TR-107191. Palo Alto, CA: Electric Power Research Institute.

Kilroy, K.C. 1991. *Ground-Water Conditions in Amargosa Desert, Nevada-California, 1952-87*. U.S. Geological Survey Water-Resources Investigations Report 89-4101. Washington, DC: U.S. Geological Survey.

Laczniak, R.J., J.C. Cole, D.A. Sawyer, and D.A. Trudeau. 1996. *Summary of Hydrologic Controls on Ground-Water Flow at the Nevada Test Site, Nye County, Nevada*. U.S. Geological Survey Water-Resources Investigations Report 96-4109. Washington, DC: U.S. Geological Survey.

Manteufel, R.D., R.G. Baca, S. Mohanty, M.S. Jarzemba, R.W. Janetzke, S.A. Stothoff, C.B. Connor, G.A. Cragnolino, A.H. Chowdhury, T.J. McCartin, and T.M. Ahn. 1997. *Total-system Performance Assessment (TPA) Version 3.0 Code: Module Descriptions and User's Guide*. San Antonio, TX: Center for Nuclear Waste Regulatory Analyses.

Mohanty, S., G.A. Cragnolino, T. Ahn, D.S. Dunn, P.C. Lichtner, R.D. Manteufel, N. Sridhar. 1997. *Engineered Barrier System Performance Assessment Code: EBSPAC Version 1.1: Technical Description and User's Manual*. San Antonio, TX: Center for Nuclear Waste Regulatory Analyses.

Naff, R.L. 1973. *Hydrogeology of the southern part of the Amargosa Desert in Nevada*. Master's Thesis: University of Nevada at Reno.

Nevada Division of Water Resources. 1997a. *Well Driller's Logs for Amargosa Desert Townships 15,16,17S and Ranges 47,48,49,50E from Nevada Division of Water Resources*. Carson City, NV: Nevada Division of Water Resources.

Nevada Division of Water Resources. 1997b. *Annual Estimates of Water Use for Hydrographic Basin 230, Amargosa Desert*. Carson City, NV: Nevada Division of Water Resources.

Nevada Division of Water Resources. 1997c. *Well Permit Database for Hydrographic Basin 230, Amargosa Desert*. Carson City, NV: Nevada Division of Water Resources.

Nichols, W.D., and J.P. Akers. 1985. *Water-Level Declines in the Amargosa Valley area, Nye County, Nevada, 1962-84*. U.S.G.S. Water-Resources Investigations Report 85-4273. Washington, DC: U.S. Geological Survey

Nuclear Regulatory Commission. 1995. *NRC Iterative Performance Assessment Phase 2: Development of Capabilities for Review of a Performance Assessment for a High-Level Waste Repository*. NUREG-1464. Washington, DC: Nuclear Regulatory Commission.

Oatfield, W.J., and J.B. Czarnecki. 1991. Hydrogeologic inferences from drillers' logs and from gravity and resistivity surveys in the Amargosa Desert, southern Nevada. *Journal of Hydrology* 124: 131-158.

Osterkamp, W.R., L.J. Lane, and C.S. Savard. 1994. Recharge estimates using a geomorphic/distributed-parameter simulation approach, Amargosa River Basin. *Water Resources Bulletin* 30(3): 493-507.

Plume, R.W. 1996. *Hydrogeologic Framework of the Great Basin Region of Nevada, Utah, and Adjacent States*. U.S. Geological Survey Professional Paper 1409-B. Washington, DC: U.S. Geological Survey.

Reilly, T.E., O.L. Franke, and G.D. Bennett. 1989. Bias in groundwater samples caused by wellbore flow. *Journal of Hydraulic Engineering* 115(2): 270–276.

Savard, C.S. 1995. *Selected Hydrologic Data from Fortymile Wash in the Yucca Mountain Area, Nevada, Water Year 1992*. U.S. Geological Survey Open-File Report 94-317. Washington, DC: U.S. Geological Survey.

Schafer, D.C. 1996. Determining 3D capture zones in homogeneous, anisotropic aquifers. *Ground Water* 34(4): 628–639.

Stothoff, S.A. 1997. Sensitivity of long-term bare soil infiltration simulations to hydraulic properties in an arid environment. *Water Resources Research* 33(4): 547–558.

Strack, O.D.L. 1989. *Groundwater Mechanics*. Englewood Cliffs, NJ: Prentice-Hall.

Swadley, W.C. 1983. *Map Showing Surficial Geology of the Lathrop Wells Quadrangle, Nye County, Nevada*. USGS Misc. Invest. Series I-1361. Washington, DC: U.S. Geological Survey

Swadley, W.C., and W.J. Carr. 1980. *Geologic Map of the Quaternary and Tertiary deposits of the Big Dune Quadrangle, Nye County, Nevada, and Inyo County, California*. USGS Misc. Invest. Series I-1361. Washington, DC: U.S. Geological Survey.

TRW Environmental Safety Systems, Inc. 1995. *Total System Performance Assessment-1995: An Evaluation of the Potential Yucca Mountain Repository*. B00000000-01717-2200-00136. Las Vegas, NV: TRW Environmental Safety Systems, Inc.

U.S. Department of Energy. 1988. *Site Characterization Plan: Yucca Mountain Site, Nevada Research and Development Area, Nevada, Volume II, Part A*. Oak Ridge, TN: U.S. Department of Energy, Office of Civilian Radioactive Management.

U.S. Geological Survey. 1989. *National Water Information System User's Manual Volume 2, Chapter 4. Ground-Water Site Inventory System*. U.S. Geological Survey Open-File Report 89-587. Washington, DC: U.S. Geological Survey.

Walker, G.E., and T.E. Eakin. 1963. *Geology and Ground Water of Amargosa Desert, Nevada-California*. Nevada Department of Conservation and Natural Resources, Ground-Water Resources-Reconnaissance Series Report 14. Carson City, NV: Nevada Department of Conservation and Natural Resources.

Wexler, E.J. 1992. Analytical solutions for one-, two-, and three-dimensional solute transport in ground-water systems with uniform flow. *Techniques of Water-Resources Investigations of the U.S. Geological Survey*, Chapter B7, Book 3 of Applications of Hydraulics. Washington, DC: U.S. Geological Survey.

Wilson, M.L., J.H. Gauthier, R.W. Barnard, G.E. Barr, H.A. Dockery, F. Dunn, R.R. Eaton, D.C. Guerin, N. Lu, M.J. Martinez, R. Nilson, C.A. Rautman, T.H. Robey, B. Ross, E.E. Ryder, A.R. Schenker, S.A. Shannon, L.H. Skinner, W.G. Halsey, J.D. Gansemer, L.C. Lewis, A.D. Lamont, I.R. Triay, A. Meijer, and D.E. Morris. 1994. *Total-System Performance Assessment for Yucca Mountain - SNL Second Iteration (TSPA-1993) - Volume 1.* Sandia Report SAND93-2675. Albuquerque, NM: Sandia National Laboratories.

Winograd, I.J., and W. Thordarson. 1975. *Hydrogeologic and Hydrochemical Framework, South-Central Great Basin, Nevada-California, with Special Reference to the Nevada Test Site.* U.S. Geological Survey Professional Paper 712-C. Washington, DC: U.S. Geological Survey.

APPENDIX A

DETAILED WATER USE TABLES FOR 1983, 1985-1996

Table A-1. Annual water use estimates (acre-ft) from NDWR (1997b); qq = quarter-quarter section, qtr = quarter section, sec = section, twn = township, rng = range, xx = not recorded, com = commercial, mm = mining, irr = irrigation, qm = quasi-municipal.

qq qtr sec twn rng	Use	1996	1995	1994	1993	1992	1991	1990	1989	1988	1987	1986	1985	1983
se se 13 15 49	com	0.5	—	—	—	—	—	—	—	—	—	—	—	—
se se 16 16 48	com	2	—	—	—	—	—	—	—	—	—	—	—	—
se se 14 16 49	com	0.1	—	—	—	—	—	—	—	—	—	—	—	—
se sw 12 17 48	mm	272	349	340	232	347.5	335	383	525	569	298	284	110	255
se sw 25 18 50	com	—	—	—	—	—	—	—	—	0.5	0.5	0.6	—	—
xx se 35 16 49	com	1.0	—	—	—	—	—	—	—	—	—	—	—	—
xx sw 36 17 49	com	746.5	431	377	512	306	115	503.1	888	427	4	266	840	—
sw se 10 17 49	com	50	—	—	—	—	—	—	—	—	—	—	—	—
se sw 10 16 48	irr	—	300	60	—	—	—	—	—	385	385	385	375	400
se sw 8 16 48	irr	—	—	—	—	—	—	—	—	—	—	—	—	150
se se 16 16 48	irr	125	400	280	290	600	400	400	50	700	100	600	400	—
sw sw 7 16 48	irr	92.5	185	185	185	37	37	—	—	—	—	—	—	—
xx xx 36 16 48	irr	799.5	864.5	1,170	1,170	994.5	1170	25	—	—	860	864.5	864.5	625
sw sw 18 16 48	irr	400	400	480	200	—	—	—	—	200	—	600	300	—
se se 14 16 48	irr	175	175	175	175	—	—	—	—	—	—	—	—	—
se se 23 16 48	irr	625	625	625	668.8	625	800	—	—	—	—	—	325	625
se sw 25 16 48	irr	—	—	—	—	625	—	—	—	—	—	—	625	625
sw se 17 16 48	irr	—	—	50	—	—	—	—	—	—	—	—	128.9	75
se sw 15 16 48	irr	5	12.5	15	2	2	—	10	—	—	—	—	—	—
se sw 15 16 48	irr	7.5	2.5	2.5	1	4	—	—	—	6.3	—	—	—	—
se se 8 16 48	irr	5	90	75	90	—	—	—	—	50	—	195	—	—
sw sw 20 16 48	irr	17.5	17.5	10	20	40	20	—	—	—	—	—	—	300

Table A-1. Annual water use estimates (acre-ft) from NDWR (1997b); qq = quarter-quarter section, qtr = quarter section, sec = section, twn = township, rng = range, xx = not recorded, com = commercial, mm = mining, irr = irrigation, qm = quasi-municipal (cont'd).

qq qtr sec twn rng	Use	1996	1995	1994	1993	1992	1991	1990	1989	1988	1987	1986	1985	1983
ne ne 24 16 48	irr	227.5	300	200	175	175	175	150	175	175	175	—	—	—
ne se 24 16 48	irr	625	625	625	—	200	200	—	—	—	—	—	—	—
ne ne 36 16 48	irr	25	50	50	190	16	—	25	25	—	—	—	—	—
se sw 10 16 48	irr	—	400	—	200	—	—	—	—	—	—	—	—	—
se nw 18 16 48	irr	657.5	683	540.8	328.5	—	—	—	—	47.2	—	777.25	656.25	—
se sw 10 16 48	irr	5	5	—	—	—	—	—	—	—	—	—	—	—
nw sw 10 16 48	irr	17.5	17.5	17.5	17.5	17.5	—	5	5	2.5	2.5	2.5	—	—
nw sw 10 16 48	irr	11.25	—	—	—	—	—	—	—	—	—	—	—	—
nw sw 10 16 48	irr	—	—	—	—	1	—	22.5	—	—	—	—	—	—
sw se 8 16	irr	24	99	99	54	—	—	—	—	5	—	—	—	60
nw nw 15 16 48	irr	12.5	10	10	2	6	—	—	—	—	—	—	—	20
se nw 26 16 481	irr	583.5	583.5	223.34	250	—	—	250	- -	—	583.5	583.5	583.5	584
se ne 26 16 48	irr	233.4	233.4	—	—	—	—	583.5	—	—	583.5	583.5	583.5	584
sw se 8 16 48	irr	70.7	75	60	30	—	—	—	—	—	—	—	—	—
sw nw 24 16 48	irr	583.5	583.5	583.5	583.4	—	—	583.35	—	—	583.35	538.35	583.35	—
sw nw 15 16 48	irr	10	10	20.65	6	6	—	—	—	34.4	—	—	25	—
nw nw 15 16 48	irr	12.5	—	—	—	—	—	—	—	—	—	—	—	—
ne nw 15 16 48	irr	5	—	—	—	—	—	—	—	—	—	—	—	—
ne nw 15 16 48	irr	1	—	—	—	—	—	—	—	—	—	—	—	—
nw nw 15 16 48	irr	5	—	—	—	—	—	—	—	—	—	—	—	—
ne nw 15 16 48	irr	1	—	—	—	—	—	—	—	—	—	—	—	—

Table A-1. Annual water use estimates (acre-ft) from NDWR (1997b); qq = quarter-quarter section, qtr = quarter section, sec = section, twn = township, rng = range, xx = not recorded, com = commercial, min = mining, irr = irrigation, qm = quasi-municipal (cont'd).

qq qtr sec twn rng	Use	1996	1995	1994	1993	1992	1991	1990	1989	1988	1987	1986	1985	1983
ne ne 28 16 49	irr	183.4	183.4	183.4	183.4	183.4	—	75	73	183.4	183.4	183.4	109.9	210
ne sw 9 16 49	irr	—	—	—	—	—	—	—	—	—	—	—	—	5
ne se 32 16 49	irr	—	—	—	—	—	—	139.5	—	—	—	—	—	—
ne ne 14 16 49	irr	—	—	—	55	55	—	—	—	—	—	—	—	—
ne nw 30 16 49	irr	665	665	665	665	—	—	677.5	—	—	266	—	—	—
ne nw 35 16 49	irr	—	—	—	2	2	—	—	—	—	—	—	—	—
ne se 19 16 49	irr	625	625	625	625	625	625	400	250	—	—	—	—	—
se sw 9 16 49	irr	105	118.75	50	118.3	118.75	—	118.75	118.8	75	75	75	50	118.8
ne ne 8 16 49	irr	27.5	90	15	10	10	—	25	25	—	—	—	—	98.5
sw se 5 16 49	irr	—	—	1	—	—	—	—	—	—	—	—	—	—
ne se 8 16 49	irr	5	2	—	4	4	—	—	—	—	—	—	—	—
se nw 35 16 49	irr	26.28	26.2	18.2	18.2	18.24	—	—	—	—	—	—	—	—
se sw 9 16 49	irr	25	25	25	25	25	25	25	25	25	25	25	25	25
ne se 23 16 49	irr	625	625	625	625	625	625	—	—	—	—	—	—	625
nw ne 8 16 49	irr	—	—	—	13.9	—	—	—	—	—	—	—	—	—
se sw 9 16 49	irr	25	25	25	25	25	25	25	—	25	25	25	25	25
se se 23 16 49	irr	5	—	35	47.7	—	—	15	15	10	10	—	22.7	—
se ne 12 17 48	irr	—	—	—	—	—	—	—	—	—	—	—	—	25
se nw 12 17 48	irr	65	65	65	65	65	65	65	65	45	45	45	75	—
ne nw 9 17 49	irr	—	—	—	690	540	550	790	400	300	200	—	—	—
ne ne 9 17 49	irr	700	700	700	—	—	—	—	—	—	—	—	—	—

Table A-1. Annual water use estimates (acre-ft) from NDWR (1997b); qq = quarter-quarter section, qtr = quarter section, sec = section, twn = township, rng = range, xx = not recorded, com = commercial, mm = mining, irr = irrigation, qm = quasi-municipal (cont'd).

qq qtr sec twn rng	Use	1996	1995	1994	1993	1992	1991	1990	1989	1988	1987	1986	1985	1983
ne nw 15 17 49	irr	25	25	20	16	16	—	12	12	12	12	—	25	—
se se 8 17 49	irr	—	118.3	—	—	—	—	181.1	—	—	—	—	—	—
ne ne 9 17 49	irr	170	170	—	—	—	—	—	—	—	—	—	—	—
se ne 9 17 49	irr	628	628	312.5	628	—	—	—	—	—	—	—	—	—
xx sw 4 16 48	irr	—	—	—	—	—	—	—	—	375	—	—	—	—
xx nw 23 16 48	irr	—	—	—	—	—	—	—	—	—	—	—	—	625
xx sw 25 16 48	irr	—	—	—	—	—	—	—	—	—	—	—	—	625
nw nw 15 16 48	irr	7.5	—	—	—	—	—	—	—	—	—	—	—	—
xx nw 25 16 48	irr	625	625	625	—	—	—	—	—	—	—	—	625	—
xx sw 25 16 48	irr	625	625	—	—	—	—	—	—	—	—	—	—	—
ne nw 17 16 48	irr	—	60	60	—	—	—	—	—	—	—	—	240	—
sw se 32 16 49	irr	—	—	100	100	—	175	175	175	—	—	—		—
ne ne 28 16 49	irr	—	—	—	—	—	—	—	—	—	—	—	10	—
nw se 1 17 48	irr	—	—	—	—	—	—	—	—	—	—	—	—	625
se nw 12 17 48	irr	—	—	—	—	—	—	—	—	—	—	—	—	300
ne se 12 17 48	irr	50	50	50	50	50	50	125	125	—	—	—	—	—
xx se 1 17 48	irr	40	40	—	—	—	—	—	—	—	375	375	375	—
sw ne 9 17 49	irr	40	40	—	—	—	—	—	—	—	—	—	—	—
se se 9 17 49	irr	40	40	—	—	—	—	—	—	—	—	—	—	—
xx se 7 17 49	irr	—	—	—	—	—	—	—	—	—	200	—	625	—
xx sw 7 17 49	irr	625	625	—	—	—	—	50	—	312.5	625	625	25	—

Table A-1. Annual water use estimates (acre-ft) from NDWR (1997b); qq = quarter-quarter section, qtr = quarter section, sec = section, twn = township, rng = range, xx = not recorded, com = commercial, min = mining, irr = irrigation, qm = quasi-municipal (cont'd).

qq qtr sec twn rng	Use	1996	1995	1994	1993	1992	1991	1990	1989	1988	1987	1986	1985	1983
ne sw 9 17 49	irr	200	200	00	—	—	—	—	—	—	—	—	—	—
nw sw 9 17 49	irr	200	200	50	—	—	—	—	—	—	—	—	—	—
nw se 7 17 49	irr	—	—	—	—	—	—	—	—	—	—	—	—	625
nw sw 7 17 49	irr	—	—	—	—	—	—	—	—	—	—	—	—	312.5
nw ne 24 15 49	qm	8	—	—	—	—	—	—	—	—	—	—	—	—
ne nw 27 16 49	qm	3.4	—	—	—	—	—	—	—	—	—	—	—	—
sw se 31 16 49	qm	10.5	—	—	—	—	—	—	—	—	—	—	—	—
se se 26 16 49	qm	0.1	—	—	—	—	—	—	—	—	—	—	—	—
nw ne 16 16 49	qm	20	—	—	—	—	—	—	—	—	—	—	—	—
se sw 1 17 48	qm	7.5	—	—	—	—	—	—	—	—	—	—	—	—
se sw 2 17 49	qm	10	—	—	—	—	—	—	—	—	—	—	—	—
se sw 2 18 49	qm	16	—	—	—	—	—	—	—	—	—	—	—	—
sw sw 2 18 49	qm	50	—	—	—	—	—	—	—	—	—	—	—	—
nw ne 3 18 50	qm	2	—	—	—	—	—	—	—	—	—	—	—	—

APPENDIX B

CAPTURE ZONE DELINEATION TABLE

Table B-1. Calculated capture zone widths and thicknesses. Screen elevation based on 1,000-m-thick aquifer.

ID	Screen Elevation (m)	Pump Rate (m^3/d)	Gradient	Transmissivity (m^2/d)	Width (m)	Thickness (m)	Net Captured on Top (m)
1	940-1,000	1	0.005	100	29	73	–
2	940-1,000	2	0.005	100	54	82	–
3	940-1,000	3	0.005	100	76	88	–
4	940-1,000	4	0.005	100	97	96	–
5	940-1,000	6.815	0.005	100	146	113	–
6	940-1,000	37.5	0.005	100	418	224	–
7	940-1,000	75	0.005	100	607	309	–
8	940-1,000	300	0.005	100	1292	575	–
9	940-1,000	800	0.005	100	2330	825	–
10	940-1,000	1380	0.005	100	3382	941	–
11	940-1,000	2000	0.005	100	4450	985	–
12	940-1,000	3	0.005	10	369	203	–
13	940-1,000	3	0.005	50	133	108	–
14	940-1,000	3	0.005	100	76	88	–
15	940-1,000	3	0.005	400	22	70	–
16	940-1,000	3	0.001	100	248	151	–
17	940-1,000	3	0.0025	100	133	108	–
18	940-1,000	3	0.005	100	76	88	–
19	940-1,000	3	0.05	100	41	78	–
20	940-1,000	3	0.005	100	76	88	–

Table B-1. Table of calculated capture zone widths and thicknesses. Screen elevation based on 1,000-m-thick aquifer (cont'd).

ID	Screen Elevation (m)	Pump Rate (m^3/d)	Gradient	Transmissivity (m^2/d)	Width (m)	Thickness (m)	Not Captured on Top (m)
21	930-990	3	0.005	100	69	98	0.2
22	920-980	3	0.005	100	67	107	5
23	900-960	3	0.005	100	68	127	21
24	980-1,000	3	0.005	100	115	65	–
25	940-1,000	3	0.005	100	76	88	–
26	900-1,000	3	0.005	100	51	122	–
27	0-1,000	300	0.005	100	574	1000	–
28	500-1,000	300	0.005	100	940	752	–
29	810-1,000	300	0.005	100	1238	601	–
30	940-1,000	300	0.005	100	1292	575	–
31	940-1,000	300	0.005	50	1944	751	–
32	940-1,000	300	0.005	100	1292	575	–
33	940-1,000	300	0.005	200	876	424	–
34	940-1,000	300	0.005	300	705	352	–
35	940-1,000	300	0.005	400	607	369	–
36	940-1,000	2116	0.005	200	2810	859	–
37	940-1,000	2116	0.005	300	2146	793	–
38	940-1,000	2116	0.005	400	1798	719	–
39	940-1,000	2116	0.001	100	5596	1000	–
40	940-1,000	2116	0.002	100	3282	934	–

Table B-1. Table of calculated capture zone widths and thicknesses. Screen elevation based on 1,000-m-thick aquifer (cont'd).

ID	Screen Elevation (m)	Pump Rate (m^3/d)	Gradient	Transmissivity (m^2/d)	Width (m)	Thickness (m)	Not Captured on Top (m)
41	940-1,000	2116	0.003	100	2486	850	--
42	940-1,000	2116	0.005	100	1798	719	--

APPENDIX C

TABLE OF BOREHOLE DILUTION FACTORS

Table C-1. Calculated dilution factors for combinations of plume scenarios and capture zones at 25 km. Capture #ID in column No. 2 are in reference to table in appendix B; Q = pumping rate (m^3/d), T = transmissivity (m^2/d), grad = regional gradient. The dilution factors are V-BDF (volumetric flux-based borehole dilution factor), P-DF (point dilution factor based on centerline concentration), and T-BDF (dispersion during transport-based borehole dilution factor). Additional significant figures are reported to illustrate relative differences only.

Plume Description	Capture Description	V-BDF	P-DF	T-BDF
3D plume 1				
20:2:0.2 m	#8, Q = 300	1.4	9.1	34
20:2:0.2 m	#9, Q = 800	2.6	9.1	55
20:2:0.2 m	#10, Q = 1,380	3.5	9.1	57
20:2:0.2 m	#11, Q = 2,000	4.8	9.1	57
Small irrigation well, 3D plume 1				
20:2:0.2 m	#31, T = 50	2.6	9.1	48
20:2:0.2 m	#32, T = 100	1.8	9.1	34
20:2:0.2 m	#33, T = 200	1.4	9.1	26
20:2:0.2 m	#34, T = 300	1.0	9.1	20
20:2:0.2 m	#35, T = 400	1.0	9.1	18
Large irrigation well, 3D plume 1				
20:2:0.2 m	#36, T = 200	2.8	9.1	57
20:2:0.2 m	#37, T = 300	3.0	9.1	52
20:2:0.2 m	#38, T = 400	2.4	9.1	45
20:2:0.2 m	#39, grad = 0.001	6.2	9.1	57.5
20:2:0.2 m	#40, grad = 0.002	3.4	9.1	57.5
20:2:0.2 m	#41, grad = 0.003	2.3	9.1	56.6
20:2:0.2 m	#42, grad = 0.005	1.0	9.1	45
Domestic wells, 3D plume 1				
20:2:0.2m	#21, 940-1,000	9.1	9.5	1
20:2:0.2 m	#22, 930-990	9.1	9.7	1
20:2:0.2 m	#23, 920-980	9.1	9.9	1
20:2:0.2 m	#24, 900-960	9.1	10.4	1
20:2:0.2 m	#1, Q = 1	9.1	9.36	1

Table C-1. Calculated dilution factors for combinations of plume scenarios and capture zones at 25 km. Capture #ID in column No. 2 are in reference to table in appendix B; Q = pumping rate (m^3/d), T = transmissivity (m^2/d), grad = regional gradient. The dilution factors are V-BDF (volumetric flux-based borehole dilution factor), P-DF (point dilution factor based on centerline concentration), and T-BDF (dispersion during transport-based borehole dilution factor). Additional significant figures are reported to illustrate relative differences only (cont'd).

Plume Description	Capture Description	V-BDF	P-DF	T-BDF
20:2:0.2 m	#2, Q = 2	9.1	9.44	1
20:2:0.2 m	#3, Q = 3	9.1	9.5	1
20:2:0.2 m	#4, Q = 4	9.1	9.6	1
20:2:0.2 m	#5, Q = 6.8	9.1	9.9	1
20:2:0.2 m	#6, Q = 37.5	9.1	13	1
20:2:0.2 m	#7, Q = 75	9.1	18	1
20:2:0.2 m	#12, T = 10	9.1	[illegible]	1
20:2:0.2 m	#13, T = 50	9.1	[illegible]	1
20:2:0.2 m	#14, T = 100	9.1	9.5	1
20:2:0.2 m	#15, T = 400	9.1	9.3	1
20:2:0.2 m	#16, grad = 0.001	9.1	11	1
20:2:0.2 m	#17, grad = 0.0025	9.1	9.8	1
20:2:0.2 m	#18, grad = 0.005	9.1	9.5	1
20:2:0.2 m	#19, grad = 0.01	9.1	9.4	1
3D plume 2				
100:10:0.1 m	#8, Q = 300	1.9	14	37
100:10:0.1 m	#9, Q = 800	2.7	14	47
100:10:0.1 m	#10, Q = 1,380	3.3	14	60
100:10:0.1 m	#11, Q = 2,000	4.1	14	73
Small irrigation well, 3D plume 2				
100:10:0.1 m	#31, T = 50	3.2	14	43
100:10:0.1 m	#32, T = 100	2.4	14	37
100:10:0.1 m	#33, T = 200	1.8	14	34
100:10:0.1 m	#34, T = 300	1.6	14	32
100:10:0.1 m	#35, T = 400	1.5	14	30

Table C-1. Calculated dilution factors for combinations of plume scenarios and capture zones at 25 km. Capture #ID in column No. 2 are in reference to table in appendix B; Q = pumping rate (m^3/d), T = transmissivity (m^2/d), grad = regional gradient. The dilution factors are V-BDF (volumetric flux-based borehole dilution factor), P-DF (point dilution factor based on centerline concentration), and T-BDF (dispersion during transport-based borehole dilution factor). Additional significant figures are reported to illustrate relative differences only (cont'd).

Plume Description	Capture Description	V-BDF	P-DF	T-BDF
Large irrigation well, plume 2				
100:10:0.1 m	#36, T = 200	3.0	14	53
100:10:0.1 m	#37, T = 300	2.6	14	45
100:10:0.1 m	#38, T = 400	2.3	14	41
100:10:0.1 m	#39, grad = 0.001	4.3	14	—
100:10:0.1 m	#40, grad = 0.002	3.3	14	59
100:10:0.1 m	#41, grad = 0.003	2.8	14	49
100:10:0.1 m	#42, grad = 0.005	2.3	14	41
Thin plumes, Domestic wells at 25 km, 20:2 m dispersivity ratio				
25 m thick; 20:2 m	#21, 940-1,000	3.3	1.8	1.78
25 m thick; 20:2 m	#22, 930-990	4.3	1.8	1.77
25 m thick; 20:2 m	#23, 920-980	5.4	1.8	1.77
25 m thick; 20:2 m	#24, 900-960	43	1.8	1.76
10 m thick; 20:2 m	#21, S = 940-1,000	8.2	1.8	1.78
10 m thick; 20:2 m	#22, S = 930-990	10.3	1.8	1.77
10 m thick; 20:2 m	#23, S = 920-980	26	1.8	1.70
10 m thick; 20:2 m	#24, S = 900-960	N/A	1.8	N/A
25 m thick; 20:2 m	#1, Q = 1	2.8	1.8	1.76
25 m thick; 20:2 m	#2, Q = 2	3.1	1.8	1.77
25 m thick; 20:2 m	#3, Q = 3	3.3	1.8	1.78
25 m thick; 20:2 m	#4, Q = 4	3.5	1.8	1.78
25 m thick; 20:2 m	#5, Q = 6.8	4.0	1.8	1.80
25 m thick; 20:2 m	#6, Q = 37.5	7.6	1.8	1.90
25 m thick; 20:2 m	#7, Q = 75	10.2	1.8	2.01
10 m thick; 20:2 m	#1, Q = 1	7.0	1.8	1.76

Table C-1. Calculated dilution factors for combinations of plume scenarios and capture zones at 25 km. Capture #ID in column No. 2 are in reference to table in appendix B; Q = pumping rate (m^3/d), T = transmissivity (m^2/d), grad = regional gradient. The dilution factors are V-BDF (volumetric flux-based borehole dilution factor), P-DF (point dilution factor based on centerline concentration), and T-BDF (dispersion during transport-based borehole dilution factor). Additional significant figures are reported to illustrate relative differences only (cont'd).

Plume Description	Capture Description	V-BDF	P-DF	T-BDF
10 m thick; 20:2 m	#2, Q = 2	7.7	1.8	1.77
10 m thick; 20:2 m	#3, Q = 3	8.2	1.8	1.78
10 m thick; 20:2 m	#4, Q = 4	8.8	1.8	1.78
10 m thick; 20:2 m	#5, Q = 6.8	10.1	1.8	1.80
10 m thick; 20:2 m	#6, Q = 37.5	19	1.8	1.90
10 m thick; 20:2 m	#7, Q = 75	26	1.8	2.01
25 m thick; 20:2 m	#12, T = 10	6.9	1.8	1.88
25 m thick; 20:2 m	#13, T = 50	3.9	1.8	1.80
25 m thick; 20:2 m	#14, T = 100	3.3	1.8	1.78
25 m thick; 20:2 m	#15, T = 400	2.7	1.8	1.76
25 m thick; 20:2 m	#16, grad = 0.001	5.3	1.8	1.84
25 m thick; 20:2 m	#17, grad = 0.0025	3.9	1.8	1.80
25 m thick; 20:2 m	#18, grad = 0.005	3.3	1.8	1.78
25 m thick; 20:2 m	#19, grad = 0.01	2.9	1.8	1.77
10 m thick; 20:2 m	#12, T = 10	17	1.8	1.88
10 m thick; 20:2 m	#13, T = 50	9.8	1.8	1.80
10 m thick; 20:2 m	#14, T = 100	8.2	1.8	1.78
10 m thick; 20:2 m	#15, T = 400	6.8	1.8	1.76
10 m thick; 20:2 m	#16, grad = 0.001	13.2	1.8	1.84
10 m thick; 20:2 m	#17, grad = 0.0025	9.8	1.8	1.80
10 m thick; 20:2 m	#18, grad = 0.005	8.2	1.8	1.78
10 m thick; 20:2 m	#19, grad = 0.01	7.4	1.8	1.77
Thin plumes irrigation wells @ 25 km				
25m thick; 20:2 m	#8, Q = 300	19	1.8	2.8
25m thick; 20:2 m	#9, Q = 800	26	1.8	4.8

Table C-1. Calculated dilution factors for combinations of plume scenarios and capture zones at 25 km. Capture #ID in column No. 2 are in reference to table in appendix B; Q = pumping rate (m^3/d), T = transmissivity (m^2/d), grad = regional gradient. The dilution factors are V-BDF (volumetric flux-based borehole dilution factor), P-DF (point dilution factor based on centerline concentration), and T-BDF (dispersion during transport-based borehole dilution factor). Additional significant figures are reported to illustrate relative differences only (cont'd).

Plume Description	Capture Description	V-BDF	P-DF	T-BDF
25m thick; 20:2 m	#10, Q = 1,380	36	1.8	5.9
25m thick; 20:2 m	#11, Q = 2,000	49	1.8	5.9
25m thick; 50:5 m	#8, Q = 300	19	2.6	3.3
25m thick, 50:5 m	#9, Q = 800	26	2.6	4.8
25m thick; 50:5 m	#10, Q = 1,380	30	2.6	6.8
25m thick; 50:5 m	#11, Q = 2,000	33	2.6	8.8
25m thick; 100:10 m	#8, Q = 300	19	3.6	4.1
25m thick; 100:10 m	#9, Q = 800	26	3.6	5.2
25m thick; 100:10 m	#10, Q = 1,380	30	3.6	6.9
25m thick; 100:10 m	#11, Q = 2,000	32	3.6	8.9

ATTACHMENT C
MATRIX DIFFUSION SUMMARY REPORT

MATRIX DIFFUSION SUMMARY REPORT

Prepared for

Nuclear Regulatory Commission
Contract NRC-02-97-009

Prepared by

James Winterle

Center for Nuclear Waste Regulatory Analyses
San Antonio, Texas

February 1998

ABSTRACT

Matrix diffusion is the migration of dissolved solutes from flowing macropores or fractures into the more-or-less stagnant pores of adjacent rock matrix. This report provides a review of matrix diffusion transport model theory, assumptions, and practical aspects with a goal of assessing the appropriateness of incorporating matrix diffusion into performance assessment (PA) models of the proposed nuclear waste repository at Yucca Mountain (YM), Nevada. Scoping calculations indicate that matrix diffusion model assumptions are reasonable for the low-permeability, fractured tuffs in the saturated zone beneath YM. However, in the unsaturated zone, evidence suggests that diffusive solute transport is either limited or dominated by other transport processes and, as such, the matrix diffusion model is not appropriate for the YM unsaturated zone. Comparisons between first-order kinetic and matrix diffusion solute transport models indicate that first-order kinetic models provide a reasonable approximation of the matrix diffusion process for the cases considered. This last finding is of particular importance because the PA model currently used by the U.S. Nuclear Regulatory Commission already includes a first-order kinetic transport model for radionuclide transport. Future field, laboratory, and modeling investigations are suggested to more accurately constrain matrix diffusion model parameters for PA.

CONTENTS

Section Page

FIGURES vii
TABLES ix
ACKNOWLEDGMENTS xi

1 INTRODUCTION 1-1

2 BACKGROUND 2-1
2.1 CONCEPTUAL MODELS FOR FRACTURE-MATRIX INTERACTION 2-1
2.2 FRACTURE-MATRIX INTERACTION PERFORMANCE ASSESSMENT MODELS 2-2

3 MATRIX DIFFUSION TRANSPORT MODELS 3-1
3.1 DIFFUSION THEORY 3-1
3.2 MATRIX DIFFUSION TRANSPORT MODEL 3-1
3.3 TRANSPORT MODEL SENSITIVITY 3-3
3.3.1 Limiting Cases 3-6
3.3.2 Sensitivity to γ 3-7
3.3.3 Sensitivity to R 3-9
3.3.4 Sensitivity to β 3-10
3.3.5 Sensitivity to P 3-11
3.4 FIRST-ORDER APPROXIMATION OF MATRIX DIFFUSION 3-12
3.5 APPLICABILITY OF MATRIX DIFFUSION MODEL ASSUMPTIONS 3-13
3.5.1 Existence of an Immobile Region 3-14
3.5.2 Uniform Flow through Uniform Fractures 3-15
3.5.3 Uniform Diffusion in the Immobile Region 3-16
3.5.4 No Mechanical Dispersion 3-16
3.5.5 Finite versus Infinite Immobile Region 3-17

4 LABORATORY AND FIELD STUDIES 4-1
4.1 LABORATORY STUDIES 4-1
4.1.1 Existing Data 4-1
4.1.2 Future Laboratory Studies 4-3
4.1.3 Applicability of Laboratory Measurements to Field Conditions 4-3
4.2 FIELD STUDIES 4-4
4.2.1 C-Hole Tracer Tests 4-4
4.2.2 Implications of ^{36}Cl in the Exploratory Studies Facility 4-5
4.3 EVIDENCE FOR LIMITED MATRIX DIFFUSION 4-6
4.3.1 Unsaturated Zone 4-6
4.3.2 Saturated Zone 4-6

5 NEEDS FOR FURTHER TESTING 5-1

CONTENTS (cont'd)

Section Page

5.1 LABORATORY STUDIES 5-1
5.2 FIELD TESTING 5-1
5.3 TRANSPORT MODELING 5-2

6 CONCLUSIONS 6-1

7 REFERENCES 7-1

APPENDIX A ANALYTICAL SOLUTION USE FOR SENSITIVITY ANALYSES

FIGURES

Figure		Page
3-1	Immobile transport regions can consist of an assortment of microfractures, dead-end fractures, and matrix that has varying degrees of cementation and alteration. The result is that diffusive transport is seldom uniform throughout the immobile region. In practice, however, it is often sufficient to use "effective" diffusion coefficients.	3-2
3-2	Schematic representation of a model for solute transport in a system of parallel fractures.	3-4
3-3	Breakthrough curves show arrival times for a nonsorbing tracer for the two extreme cases where matrix diffusion does not occur; in the first case (dotted), effective porosity is equal to fracture porosity; in the second case (solid) all porosity is considered mobile.	3-8
3-4	Breakthrough curves show arrival times for a nonsorbing tracer under various assumed matrix diffusion scenarios. As matrix diffusion occurs more rapidly, the shape of the breakthrough curve approaches that of the case with all mobile porosity.	3-9
3-5	Increases in the retardation factor from the base case result in significant attenuation of solute the concentration. In the plots shown here, it is assumed that an increase in R implies a proportional increase in R_m. Thus, the value of γ decreases with increasing R.	3-10
3-6	Breakthrough curves show the effects of different fractions of mobile porosity (β). For the γ value used in this analysis, decreases in the value of β below about 0.1 had no significant effect on curve shape or arrival time.	3-11
3-7	Breakthrough curves show the effect of mechanical dispersion on the arrival time of a nonsorbing tracer..	3-13
3-8	Breakthrough curves show a comparison of matrix diffusion models (solid lines) and their first-order approximations (dashed lines)..	3-14

TABLES

Table		Page
3-1	Analytical solutions for transport in fractured rock with matrix diffusion	3-5
3-2	Parameters used for matrix diffusion model sensitivity analyses	3-7

ACKNOWLEDGMENTS

This report was prepared to document work performed by the Center for Nuclear Waste Regulatory Analyses (CNWRA) for the Nuclear Regulatory Commission (NRC) under Contract No. NRC-02-97-009. The activities reported here were performed on behalf of the NRC Office of Nuclear Material Safety and Safeguards (NMSS), Division of Waste Management (DWM). The report is an independent product of the CNWRA and does not necessarily reflect the views or regulatory position of the NRC.

QUALITY OF DATA, ANALYSES, AND CODE DEVELOPMENT

DATA: No CNWRA original data was generated in this report. Sources for other data should be consulted for determining the level of quality for those data.

ANALYSES AND CODES: A computer code was written to generate the breakthrough curves shown in this report. Although the code is not sufficiently developed to be placed under the CNWRA Configuration Management System, test cases showed that code output is in agreement with published breakthrough curves with the same input parameters.

1 INTRODUCTION

Yucca Mountain (YM), Nevada is the site of a proposed geologic repository for the disposal of high-level radioactive waste (HLW). Performance assessment (PA) models, which will be used to assess the long-term safety of this candidate repository are being developed by both the U.S. Department of Energy (DOE) and the Nuclear Regulatory Commission (NRC).

It is widely recognized that groundwater transport through both unsaturated and saturated zones is one of the most likely means of radionuclide migration from a geologic HLW repository. As such, improvements to PA models will depend on knowledge of the following issues: (i) rates and patterns of groundwater flow; (ii) maximum concentrations of radionuclides that might be mobilized by water in dissolved form, as colloids, or as particulates; (iii) the sorptive capacity of the rock through which radionuclides might travel; and (iv) the degree to which transport of dissolved radionuclides can be delayed by interaction between flowing macropores and the more-or-less stagnant groundwater that occupies the pore space of adjacent low-permeability matrix (Grisak et al., 1988). The focus of this paper is on issue (iv), often referred to as matrix diffusion which, as this report will show, is inextricably dependent upon the other three issues.

At YM, the process of matrix diffusion may impact repository performance because flow occurs primarily in fractures, which account for only a small fraction of total formation porosity. In such hydrologic systems, matrix diffusion can attenuate migration of radionuclides in two ways: (i) it can spread them physically from the flowing fractures into stagnant pore water, and (ii) rock matrix can provide a vast increase in mineral surface available for geochemical surface reactions (e.g., sorption) as compared to fracture surfaces alone.

Although matrix diffusion has long been recognized as potentially important to repository performance, to date, matrix diffusion has not been abstracted in PA models in ways tied closely to the physics of the system. Several other conceptual models for fracture-matrix interaction have been incorporated into PA codes, however, none of these models are based on known physical processes. Currently, there is no consensus on which conceptual model is most appropriate for the YM hydrologic system.

The purpose of this report is to provide a summary of relevant literature and theory regarding matrix diffusion processes in fractured-rock hydrologic systems. This summary is designed to support the NRC evaluations of conceptual models for matrix diffusion YM PA models. This report includes discussions of the following topics.

- Background: available conceptual models for matrix diffusion and treatment in previous PA codes for YM
- Matrix diffusion transport models: theory, sensitivity, and validity of assumptions
- Matrix diffusion experiments and field testing at YM
- Evidence for limited matrix diffusion
- Needs for further experiments, tests, or modeling

2 BACKGROUND

2.1 CONCEPTUAL MODELS FOR FRACTURE-MATRIX INTERACTION

Available conceptual models for flow and solute transport in fractured rock include. (i) discrete-feature models; (ii) equivalent continuum-models; (iii) multiple-continuum models; and (iv) hybrid models (Sagar, 1996). Discrete-feature models are those in which individual fractures and matrix blocks are explicitly represented in a numerical grid. This approach is sufficient for small scales where fracture geometry and hydraulic properties are known, and the necessary fine-scale numerical grid does not result in unreasonable computation times. For repository-scale modeling, these models are generally not practical due to lack of knowledge about fracture properties, and excessive computation time. In the equivalent-continuum approach, the bulk properties of the fractured medium are approximated by defining effective properties of a single equivalent continuum based on some observable behavior (e.g., tracer transport) associated with the actual medium. This approach does not explicitly treat the time-dependent interaction of solutes between fractures and matrix. Thus it is only reasonable for modeling single-solute transport at the scale and flow rate on which the equivalent continuum is based. When modeling transport of multiple solutes that may migrate between fractures and matrix at different rates, or when changing flow rates or transport distances result in different time scales for fracture-matrix interaction, equivalent continuum properties must be defined for each solute and for each transport distance and flow rate under consideration. Generally, this is not a practical approach for PA modeling of YM.

Multiple-continuum models treat the composite medium as a superposition of several media of different properties. In the context of fracture-matrix interaction, discussion is limited to dual-continuum models which treat rock matrix and fractures as separate continua that occupy the same computational domain and may or may not be coupled by some type of exchange term. For purposes of this report, dual-continuum models can be divided into two subcategories: dual-permeability models and dual-models. Dual-permeability models allow for advective transport in both rock matrix and fractures. In dual porosity models, it is assumed advective transport occurs only in fractures; water within rock matrix pores is assumed immobile but solutes can transition between the mobile and immobile regions, thus retarding solute migration. Because of the assumed mobile and immobile regions, dual-porosity models are often referred to as "two-region" models (e.g., van Genuchten et al., 1984, van Genuchten 1985). Both dual-permeability and dual-porosity models can be further subdivided according to the method used to couple solute transfer between fracture and matrix continua. These coupling methods may include: no transfer, rate-limited transfer, random transfer, and instantaneous equilibrium.

Hybrid models (e.g., Sagar, 1996) combine some of the properties of both the equivalent-continuum and dual-continuum conceptual models. Each cell in a numerical grid is assigned properties of both fractures and rock matrix. During each time step, solute concentration in a cell is assumed to be in equilibrium between the fracture and matrix. The mass of solute that is exchanged with adjacent cells is the combination of both fracture and matrix components of mass flux, driven by the local hydraulic gradient. Typically much more mass is transported in the fracture component than in the matrix component because of higher fracture permeability. At the end of the time step, the total solute mass in a cell is again assumed to be evenly distributed between fractures and matrix, regardless of whether the majority of solute initially entered the cell through a fracture. This conceptual model is equivalent to a dual-permeability model with instantaneous equilibrium between matrix and fractures, but it is computationally more efficient. A drawback to this type of conceptual model is that there is no clear physical basis for the assumed solute equilibrium between fractures and matrix. It is unclear how well

hybrid models can represent cases where the majority of flow occurs in widely spaced preferential flow paths.

All of the above model types have been used to simulate the process of matrix diffusion, and thus can be characterized as matrix diffusion models, even though many have little to do with the physical process of diffusion. Physically based matrix diffusion models are most commonly treated using a dual-porosity approach with rate-limited solute exchange (e.g., Neretnieks, 1980; Tang et al., 1981; Sudicky and Frind, 1986); the rate of transport into or out of the immobile rock matrix is limited by a Fickian diffusion process wherein diffusive flux is proportional to the solute concentration gradient across the fracture-matrix interface. For purposes of this report, the term "matrix diffusion model" refers to this type of dual-porosity model. Another commonly used dual-porosity approach is the first-order-kinetic model (e.g., van Genuchten and Wierenga, 1976) which treats fluid in the immobile region as well-mixed and of uniform concentration; the rate of solute transfer across the fracture-matrix interface is proportional to the concentration difference between the two regions. Although it is seldom the case that water within rock matrix is well-mixed, the first-order-kinetic model is often used to approximate the matrix diffusion model because it has a simpler analytical solution. Both the matrix diffusion model and the first-order-kinetic model are predicated on the assumption that water in the rock matrix pores is immobile. The applicability of this assumption to YM is discussed in section 3.5.1 of this report

2.2 FRACTURE-MATRIX INTERACTION PERFORMANCE ASSESSMENT MODELS

Previous attempts to incorporate fracture-matrix interactions into YM PA models have been based on the dual-permeability approach. For example, the 1995 DOE Total System Performance Assessment (TSPA-1995) (TRW Environmental Safety Systems, Inc., 1995) employed a Markov Transition Model algorithm (Golder Associates, Inc., 1994) to abstract the effects of fracture-matrix interaction during radionuclide transport through the unsaturated zone. This algorithm assumes that radionuclides transition between fracture and matrix after traveling some random distance as determined by a Poisson-process transition rate coefficient. This algorithm predicted significant radionuclide retardation due to fracture-matrix interaction. This method was criticized by the NRC (Codell, 1996) because it assumes rapid transition between fracture and matrix which is inconsistent with the observed lack of chemical equilibrium between fractures and matrix in the unsaturated zone at YM (e.g., Fabryka-Martin et al., 1996; Murphy, 1995).

The NRC Iterative Performance Assessment (IPA), Phase 2 (Nuclear Regulatory Commission, 1995) employed NEFTRAN II (Olague, et al., 1991) to simulate radionuclide transport in saturated and unsaturated zones. Although NEFTRAN II has the capability to model fracture-matrix interaction, this capability was not used for IPA Phase 2. Instead, a preprocessor, FLOWMOD, was used to divide radionuclide transport into fracture and matrix pathways for each hydrogeologic layer. Based on this approach, flow through a single layer can take one of two possible transport paths—fracture or matrix—with the probability of each based on respective permeability. At the end of each layer, the process is repeated for the next layer. In this manner, FLOWMOD calculates average transport velocities for 2^n pathways, where n is the number of layers. This hybrid approach allows interaction between fracture and matrix, and it accounts for the different travel times and fluxes in fracture and matrix. However, there is no physical basis for the resulting fracture-matrix interaction.

Both the NRC and DOE are investigating alternative methods for including the effects of matrix diffusion in their PA codes. For example, at recent technical exchanges DOE technical staff members have suggested the possibility of calculating an increased effective porosity based on various flow and

transport properties (e.g., Robinson, 1997; Zyvolski, 1997) Such a method would fall under the category of equivalent-continuum approaches, and would be subject to the limitations previously described in section 2.1. That is, an effective porosity would have to be calculated for each solute and each flow rate and model scale under consideration. Additionally, the effective porosity approach may not provide a good approximation of solute breakthrough behavior at an assumed point of exposure. The effects of effective porosity and matrix diffusion on solute breakthrough are discussed in section 3.3 of this report.

As previously mentioned, the NRC PA model incorporates NEFTRAN II (Olague et al., 1991) which can simulate fracture matrix interaction based on the first-order-kinetic model. NRC staff are currently considering the use of this option in future PA models[1]. A comparison of matrix diffusion and first-order-kinetic models can be found in section 3.4 of this report.

[1]T. McCartin, 1997, Nuclear Regulatory Commission, personal communication.

3 MATRIX DIFFUSION TRANSPORT MODELS

3.1 DIFFUSION THEORY

Matrix diffusion transport models are based on the assumption that solute transport occurs in two types of porosity—mobile and immobile. Conceptually, mobile porosity includes networks of connected fractures and macropores through which water and contaminants are transported by both advective and dispersive processes. The immobile porosity is that in which transport of contaminants occurs through diffusion only; it may include dead-end fractures and pore space, microfractures, and intergranular porosity. The concept of all flow occurring in fractures, and all matrix pores being stagnant imposes some conceptual limitations because not all fractures conduct fluid flow and not all matrix water is stagnant. For this reason, it is best to discuss the matrix diffusion process simply in terms of mobile and immobile porosity—designated by the subscripts m and im, respectively. Figure 3-1 illustrates this concept of matrix diffusion and highlights the fact that rock matrix is not a single homogenous domain, but rather is a complex system that may contain microfractures, mineral grains, porous fracture coatings, and altered zones.

In the classic Fickian approach, movement of contaminants from the mobile porosity domain into the immobile domain can be described by

$$J = -\theta_{im} D_{eff} \frac{\partial C_p}{\partial z} \Big|_{z=0}, \tag{3-1}$$

where J is the mass flux rate into the matrix per unit surface area of mobile-immobile interface; θ_{im} is immobile water-filled volumetric water content; D_{eff} is the effective diffusion coefficient; C_p is the local concentration in the immobile pore water; and z is distance from the mobile-immobile interface. The value of D_{eff} is a function of solute and solution molecular properties, temperature, and pore geometry. It can be calculated from the formula

$$D_{eff} = \frac{c}{\tau^2} D_w, \tag{3-2}$$

where, c is the matrix constrictivity factor ($0 \le c \le 1$), τ is the matrix tortuosity factor ($\tau \ge 1$), and D_w is the free water diffusion coefficient of the solute.

3.2 MATRIX DIFFUSION TRANSPORT MODEL

The general equation describing two-region solute transport with linear reversible sorption, and first-order decay of an aqueous solute in 1D form is

$$\theta_{im} R_{im} \frac{\partial C_{im}}{\partial t} + \theta_m R_m \frac{\partial C_m}{\partial t} = \theta_m D_m \frac{\partial^2 C_m}{\partial x^2} - \theta_m v_m \frac{\partial C_m}{\partial x} - \lambda(\theta_m C_m + \theta_{im} C_{im}), \tag{3-3}$$

where θ_m and θ_{im} are the volumetric water contents attributable to the mobile and immobile regions, such that $\theta_m + \theta_{im} = \theta$, where θ is the total system water-filled porosity. R_m and R_{im} are retardation

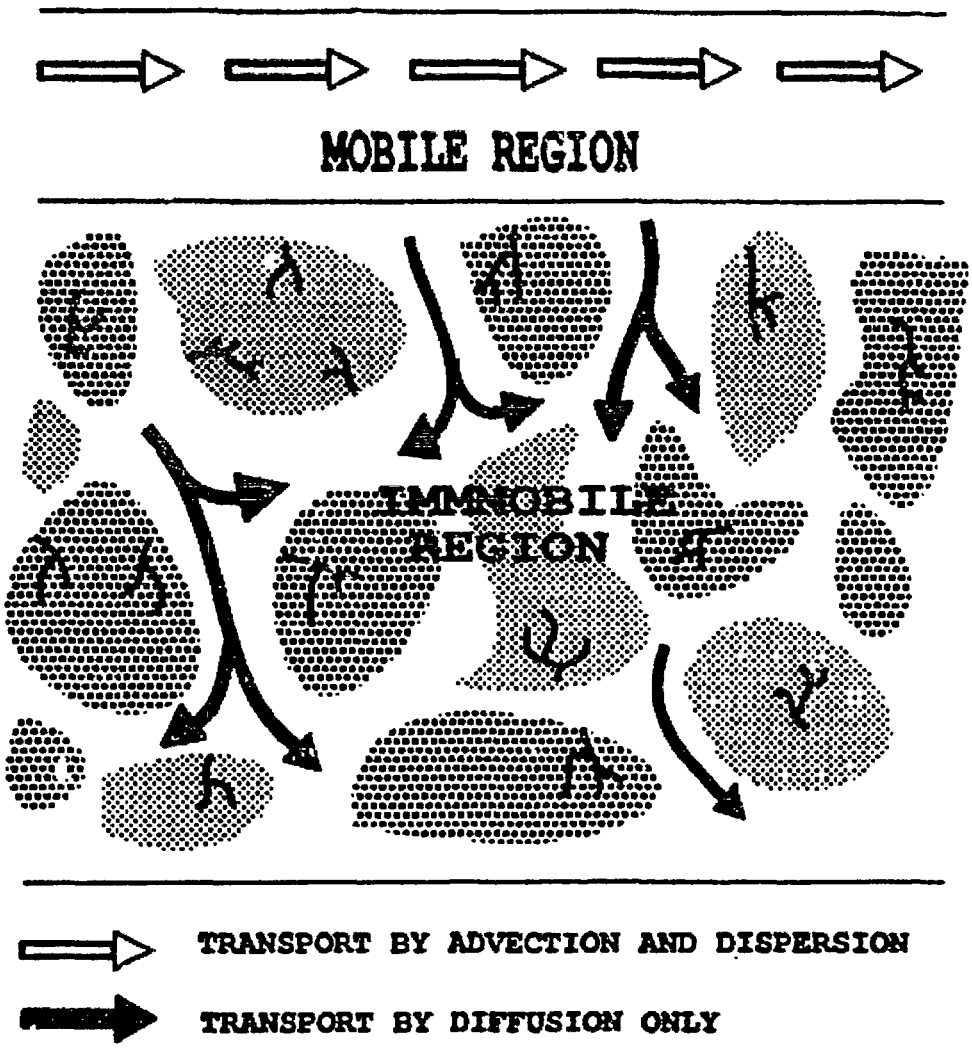

Figure 3-1. Immobile transport regions can consist of an assortment of microfractures, dead-end fractures, and matrix that has varying degrees of cementation and alteration. The result is that diffusive transport is seldom uniform throughout the immobile region. In practice, however, it is often sufficient to use "effective" diffusion coefficients.

factors of the two regions; C_m and C_{im} are the volume-averaged mobile and immobile solute concentrations; D_m and v_m are the macro-scale dispersion coefficient and advection velocity, respectively, for transport through the mobile region; x is distance in the direction of flow; t is time; and λ is a first-order radioactive decay coefficient. Coupling of this mass conservation equation to groundwater flow equations occurs through v_m and the groundwater-velocity-dependent D_m.

The first term on the left-hand side of Eq. (3-3) represents the time rate-of-change of solute mass per unit volume of immobile region. This term may be coupled to either a first-order kinetic rate model, or a diffusion rate model. Here, we discuss only the diffusion rate model. Coupling of Eq. (3-3) to the diffusion rate model requires the introduction of two additional equations. The coupling equations used are dependent upon system geometry, but for fracture-matrix systems, matrix is commonly represented

as planar sheets of thickness $2a$, separated by evenly spaced, constant aperture, parallel fractures of width $2b$, as shown in figure 3-2. For this type of rectangular system geometry, the coupling equations are

$$C_{im} = \frac{1}{a} \int_0^a C_s(x,z,t)\,dz \tag{3-4}$$

and

$$R_{im} \frac{\partial C_s}{\partial t} = D_{im} \frac{\partial^2 C_s}{\partial z^2} - \lambda C_s \tag{3-5}$$

where the immobile diffusion coefficient, D_{im}, is equal to the product $\theta_{im}\ D_{eff}$, and C_s is the local solute concentration in the immobile region.

Table 3-1 lists references for several well-known analytical solutions to variations of this transport model. This list illustrates some of the key differences between the various solutions. These differences include treatment of boundary conditions, dispersion, radionuclide decay, and system geometry.

Analytical solutions are limited in their application to homogenous mobile and immobile regions. In reality, however, fractures are not evenly-spaced and of constant aperture; matrix blocks differ in size and have zones of differing porosity, tortuosity, and sorptive properties. Recent studies (e.g., Hsieh, et al., 1997; Tidwell et al., 1997) have illustrated this point by showing that better model fits to laboratory diffusion experiments are obtained when matrix is divided into multiple domains—each with its respective diffusion coefficient. In practice however, it is often sufficient to assume average or effective matrix properties. Such assumptions are discussed in the following sections.

3.3 TRANSPORT MODEL SENSITIVITY

Breakthrough curves provide a useful means to demonstrate the sensitivity of matrix diffusion transport models to the variables in Eqs. (3-3) through (3-5). Breakthrough curves are plots of predicted concentration versus time for a sorbing or nonsorbing tracer at a given distance from the tracer source. These curves may be generated with using any of the models listed in table 3-1. However, for purposes of this report, it is convenient to use the analytical solution of Rasmuson and Neretnieks (1980) adapted for flow through rectangular voids (van Genuchten, 1985). The complete analytical solution is shown in appendix A. This 1D solution assumes evenly spaced parallel fractures, and a constant concentration source, no decay of the migrating solute is considered. Model variables are lumped into four dimensionless input parameters—P, R, γ, and β—that define the shape of the breakthrough curve. Examination of these dimensionless parameters is useful for understanding the interdependence of the variables in Eqs. (3-3)–(3-5). They are defined as follows:

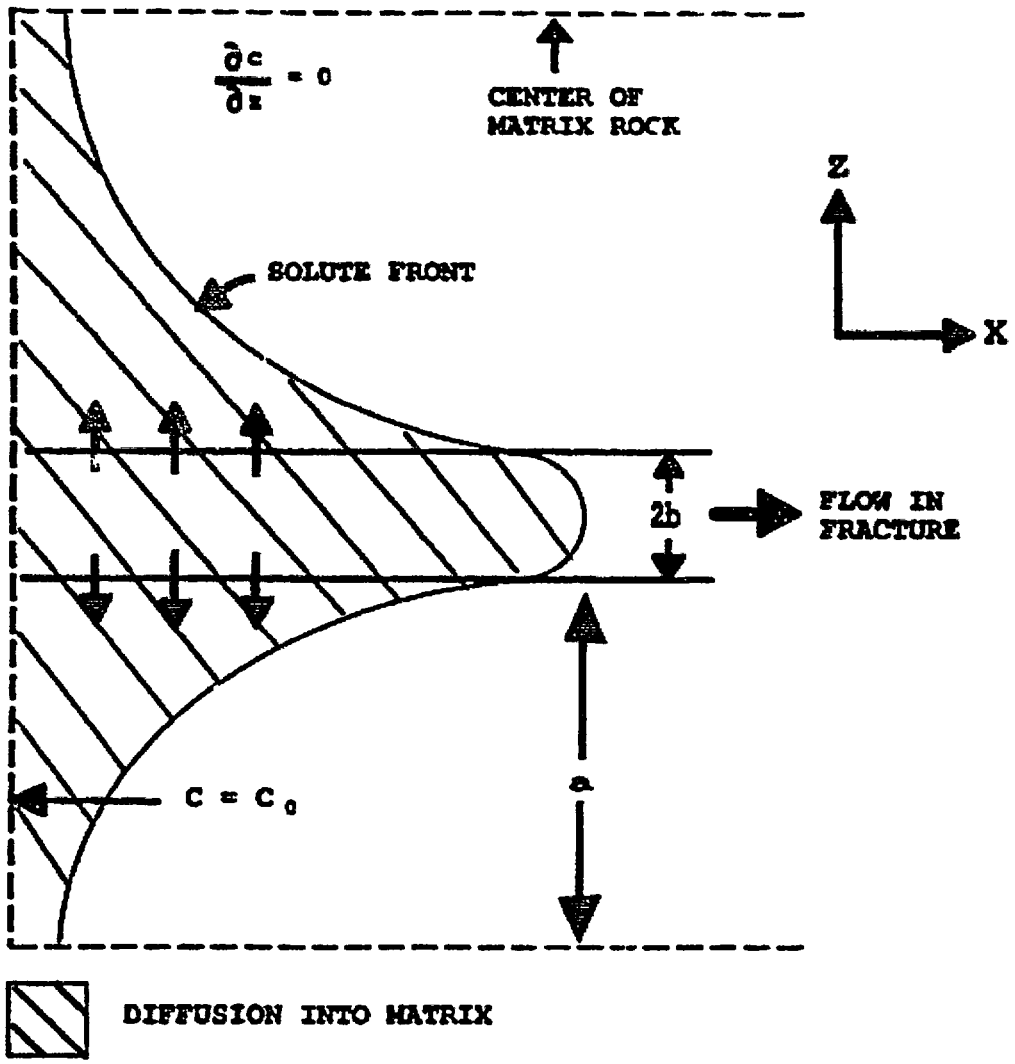

Figure 3-2. Schematic representation of a model for solute transport in a system of parallel fractures.

$$\gamma = \frac{D_{im}\,\theta\,L}{a^2\,q\,R_{im}}\,, \tag{3-6}$$

$$R = \frac{\theta_{im}\,R_{im} + \theta_m\,R_m}{\theta}\,, \tag{3-7}$$

$$\beta = \frac{\theta_m\,R_m}{\theta R}\,, \tag{3-8}$$

and

Table 3-1. Analytical solutions for transport in fractured rock with matrix diffusion.

Reference/Model	Flow Geometry and Boundary Conditions	Treatment of Source	Treatment of Radionuclide Decay	Treatment of Mechanical Dispersion
Neretnieks, 1980	1D flow in a single planar fracture with fixed aperture; infinite immobile region. Model solves for aqueous concentration in mobile region.	Allows for exponential decay.	Single decaying species; no decay chains.	No
Tang et al., 1981	1D flow in a single planar fracture with fixed aperture; infinite immobile region. Model solves for aqueous concentration in mobile region.	Allows for exponential decay.	Single decaying species; no decay chains.	Yes
Sudicky and Frind, 1982	1D flow in evenly spaced parallel fractures with fixed aperture; finite matrix domain. Model solves for aqueous concentration in mobile region.	Constant concentration.	Single decaying species; no decay chains.	No (approximate solution); Yes (exact solution)
van Genuchten et al., 1984; (see also: Rasmuson and Neretnieks, 1986)	1D flow in cylindrical macropore of constant radius; approximate solution for infinite cylindrical immobile region; exact solution for finite immobile region.	Allows for exponential decay.	Single decaying species; no decay chains.	No (approximate solution); Yes (exact solution)
Gureghian, 1987/ FRACFLO	2D fracture in x-y plane of fixed aperture; 2D infinite matrix in x-z plane. Model solves for aqueous concentration in both immobile and mobile regions.	Allows for exponential decay. Solutions for single and multiple patch sources, and Gaussian distributed source.	Single decaying species; no decay chains.	No
Gureghian, 1992/ MULTFRAC	1D flow in a single planar fracture; allows for layers, normal to flow, with variable fracture aperture and diffusion properties; infinite immobile region. Model solves for aqueous concentration in both immobile and mobile regions.	Allows for exponential decay, and periodically fluctuating source with exponential decay. Step and band release modes.	Single decaying species; no decay chains	No
Gureghian et al., 1994/ FRAC_SSI	1D flow in a single planar fracture with fixed aperture; infinite immobile region;	Allows for exponential decay. Step and band release modes.	Single parent species; allows user-specified decay chain. Only parent species decays in immobile region.	No

$$P = \frac{v_m L}{D_m} \approx \frac{L}{\alpha_L} \tag{3-9}$$

where L is distance from the source to the point of observation; α_L is longitudinal dispersion length; q is area-averaged fluid flux into the system; R_m and R_{im} are mobile region and matrix retardation factors, respectively.

Now that the model parameters have been introduced, the next order of business is to investigate how each parameter affects the prediction of solute transport through fractured rock when varied relative to a base case. The base case represents a "best guess" of conditions at YM, based on properties of the Prow-Pass Bullfrog interval of the C-Hole complex (Geldon, 1996; Flint, 1996), the range of laboratory-determined diffusion coefficients (e.g., Triay et al., 1996), and local hydraulic gradients, (e.g., Luckey et al., 1996). Table 3-2 lists the values for fixed and base case variables used in these analyses. For simplification, R_m and R_{im} are assumed to equal 1 as in the case of a nonsorbing solute. For sorbing solutes, R_{im} is likely to be much higher than R_m because of the increased surface area available for sorption within the rock matrix.

3.3.1 Limiting Cases

In section 2.2 it was noted that DOE is has proposed the use of an increased effective mobile porosity to account for the effects of matrix diffusion in their PA model without actually having to solve a matrix diffusion model. Presumably, the effective mobile porosity would increase with more rapid matrix diffusion. For this reason, it is useful to examine two limiting cases: (i) flow only in fractures with no matrix diffusion, and (ii) all mobile porosity with no matrix diffusion. Because no matrix diffusion is occurring, a simple equilibrium transport model is used to generate breakthrough curves for these two scenarios. The effective porosity is equal to fracture porosity for the first case ($\theta = 0.0015$), and equal to total porosity for the second case ($\theta = 0.15$).

Figure 3-3 shows the resulting breakthrough curves for these two cases. Note that all breakthrough curves shown in this report represent relative concentration at an observation point 1000 m downstream from a constant-concentration source with an area-averaged fluid flux of 0.15 m/yr. In the first case, when fluid flux occurs only in fractures and there is no matrix diffusion, the average fluid velocity is 100 m/yr resulting in a breakthrough time of 10 yr, with the earliest contaminants arriving in less than 5 yr. In the second case, when the total porosity (i.e., fracture and matrix) is available for fluid flow, average fluid velocity is only 1 m/yr resulting in a breakthrough time of 1,000 yr and arrival of the earliest contaminants at around 500 yr.

It is interesting to note that a breakthrough curve for the matrix diffusion model will approach the curve for the first case when matrix diffusion is very slow ($\gamma \rightarrow 0$) and it will approach the curve for the second case when matrix diffusion is very fast ($\gamma \rightarrow \infty$). This is likely the rationale behind DOE's suggested use of an increased effective porosity to simulate the effects of matrix diffusion. However, for the conditions used to generate the breakthrough curves in figure 3-3, the entire spectrum of breakthrough curves that can be generated by changing the effective porosity must fall within the area bounded by the two limiting cases shown. Conversely, the shapes of the breakthrough curves for the matrix diffusion model are not so constrained, as will be shown in the following section. This fact should be taken into consideration when evaluating the appropriateness of DOE's increased-effective-porosity approach.

Table 3-2. Parameters used for matrix diffusion model sensitivity analysis.

Area-averaged Flux (q)	0.15 m/yr	fixed for all scenarios
Total Porosity (θ)	0.15	fixed for all scenarios
Length Scale (L)	1,000 m	fixed for all scenarios
Retardation Factor ($R_m = R_{im}$)	1.0	base case value
Dispersion Length (α_L)	50 m	base case value
Matrix Block Half-Width (a)	0.5 m	base case value
Fracture Porosity (θ_m)	0.0015	base case value
Immobile Diffusion Coefficient (D_{im})	10^{-11} m²/s	base case value
Resulting Base case Model Parameters	—	—
γ	1.3	base case value
β	0.01	base case value
P	20	base case value

3.3.2 Sensitivity to γ

The parameter γ is central to this discussion because it is the only parameter that contains the immobile diffusion coefficient, D_{im}. It is useful to think of γ as a measure of the importance of matrix diffusion compared to the advective flux of solutes through the system. A higher γ-value implies more rapid diffusion into the matrix; when γ approaches zero, then very little matrix diffusion occurs and solutes remain in the mobile region where they can travel through convection and diffusion. Notice in Eq. (3-6) that, in addition to the diffusion coefficient, the value of γ is also proportional to the length-scale of the problem and the total porosity; it is inversely proportional to the liquid flux rate, the immobile region retardation factor, and the square of a.

Figure 3-4 includes the breakthrough curves for the two limiting effective porosity cases where no matrix diffusion occurs. Three additional curves show how changes in γ affect the arrival time of a nonsorbing tracer. The base case curve is the result of input parameters listed in table 3-2. Two additional curves are for slow and rapid diffusion cases: they have γ values based on a D_{im} that is one-tenth, and ten-times as great as that of the base case, respectively. Notice that slow diffusion moves the shape of the breakthrough curve from the base case toward the shape of the fracture-flow-only curve; fast diffusion causes the breakthrough curve to move toward the shape of the all-mobile-porosity curve.

Effective matrix block width determines the value of a. Because γ is inversely proportional to the square of a, the matrix diffusion model is more sensitive to matrix block size (i.e., spacing between flowing fractures) than it is to the value of D_{im}. At YM, distances between flowing fractures are not

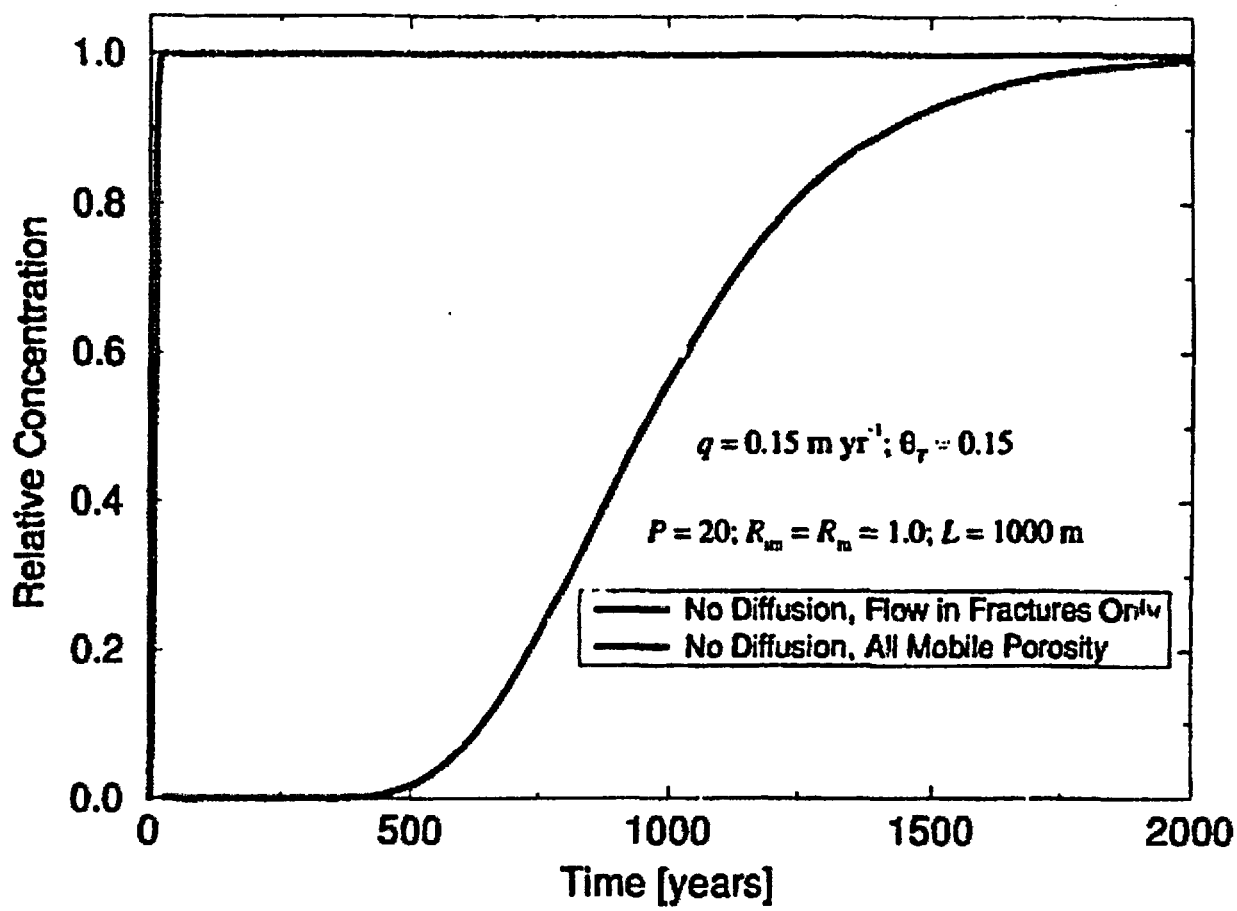

Figure 3-3. Breakthrough curves show arrival times for a nonsorbing tracer for two extreme cases where matrix diffusion does not occur; in the first case (dotted) effective porosity is equal to fracture porosity; in the second case (solid) all porosity is considered mobile.

well-characterized. This causes considerable uncertainty in estimating a range of possible values for a at YM, and is arguably the greatest source of uncertainty in estimating values for γ.

Because the value of γ is inversely proportional to R_{im}, increases in R_{im} result in smaller γ-values. Upon examining the model sensitivity to γ in figure 3-4, one might conclude that an increase in R_{im} could actually result in *earlier* solute arrival times. However, this counterintuitive behavior is only possible if R_{im} could increase without an accompanying increase in the overall retardation factor, R (i.e., an increase in θ_{im} R_{im} with an offsetting decrease in θ_m R_m). Generally, this would not be the case Sensitivity of the matrix diffusion model to R is discussed in the following section.

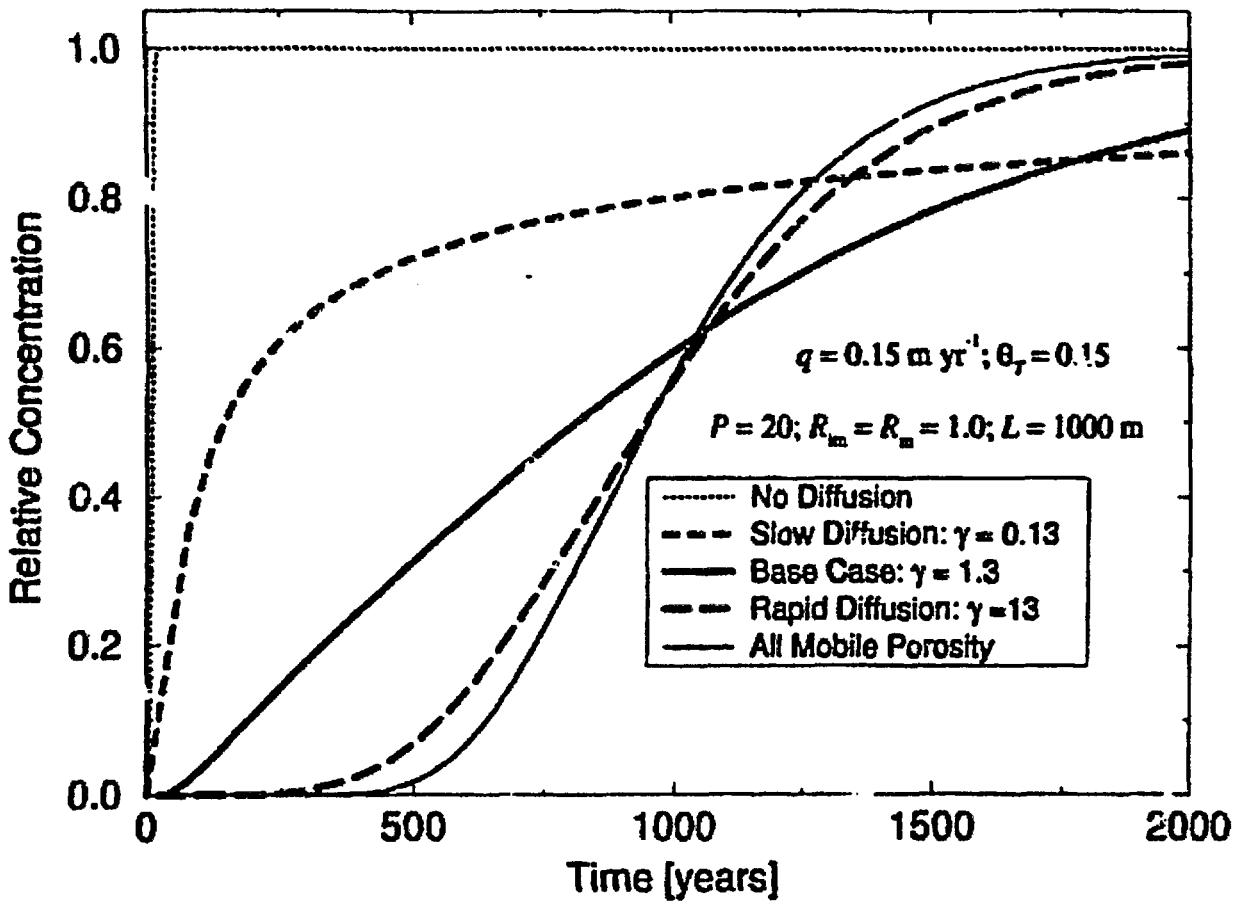

Figure 3-4. Breakthrough curves show arrival times for a nonsorbing tracer under various assumed matrix diffusion scenarios. As matrix diffusion occurs more rapidly, the shape of the breakthrough curve approaches that of the case with all mobile porosity.

3.3.3 Sensitivity to *R*

Figure 3-5 demonstrates the effect of an increased overall retardation factor on the base case scenario. For these analyses, it is assumed that R_{im} remains equal to R_m. Therefore, an increase in the value of R is accompanied by a proportional decrease in the value of γ. Notice that the earliest solute arrival time is not significantly affected, however the solute concentrations are attenuated considerably. This effect of increased R on the matrix diffusion transport model is quite different from the effect on an equilibrium model, where breakthrough curves retain their exact shape but arrival times are delayed.

Depending on host rock mineralogy and water chemistry, retardation factors for many sorbing radionuclides (e.g., Cs, Pu, Am, Sr, Ba) can be much higher than the $R = 10$ shown in figure 3-5 (e.g., Triay et al., 1996). Hence, matrix diffusion could result in considerable attenuation of sorbing radionuclides over periods on tens of thousands of years, given the scale and flow characteristics of the base case.

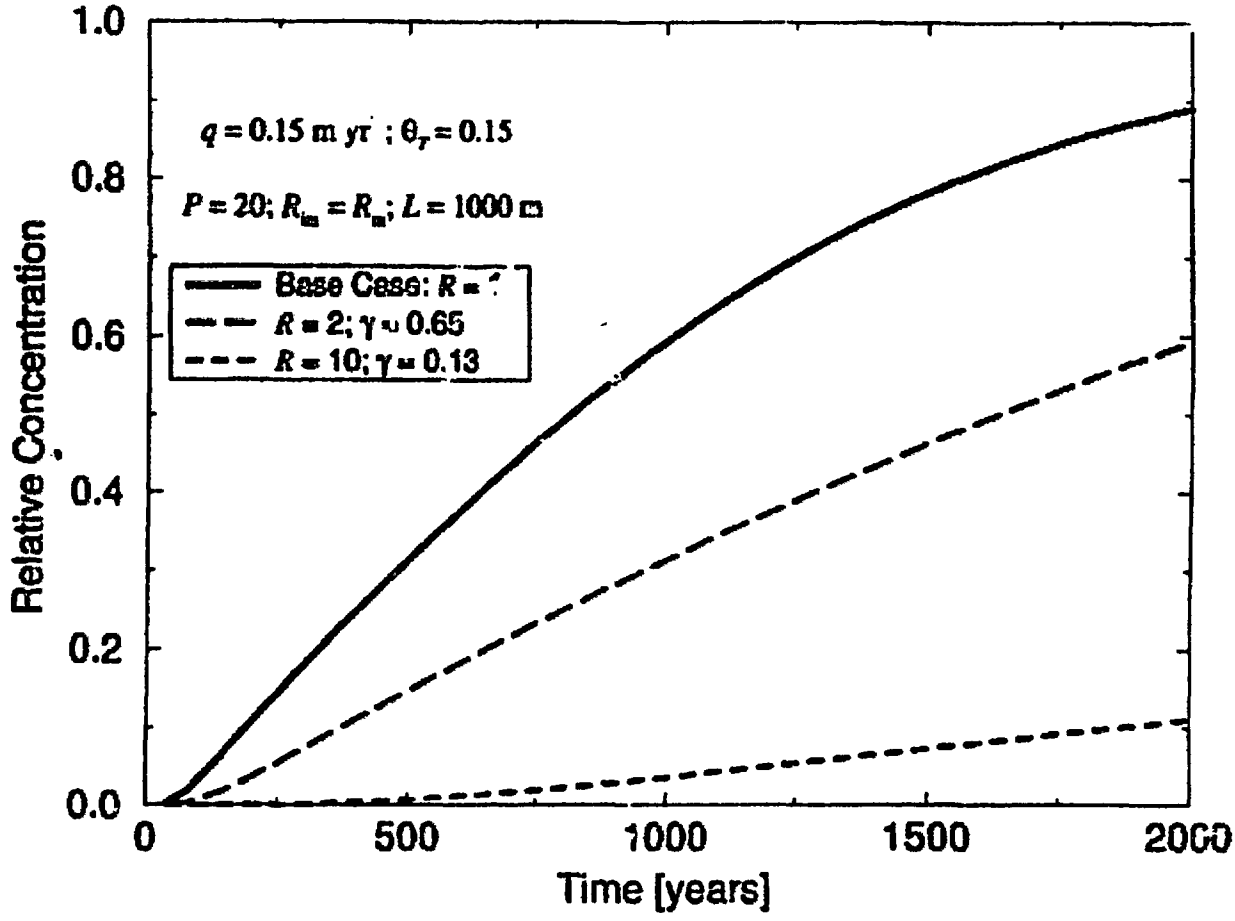

Figure 3-5. Increases in the retardation factor from the base case result in significant attenuation of solute the concentration. In the plots shown here, it is assumed that an increase in R implies a proportional increase in R_{im}. Thus, the value of γ decreases with increasing R.

3.3.4 Sensitivity to β

The β parameter can be thought of as the fraction of the total storage capacity due to the fracture. If the retardation coefficients in the fracture and matrix are equal, then β is simply the fraction of mobile porosity. If β is equal to one, then all porosity is mobile and matrix diffusion becomes irrelevant. Figure 3-6 illustrates the effect of increasing β relative to the base case scenario. With the γ parameter held constant, an increase in β could represent either a greater fraction of mobile porosity (e.g., increased fracture aperture), or more sorption in the mobile region.

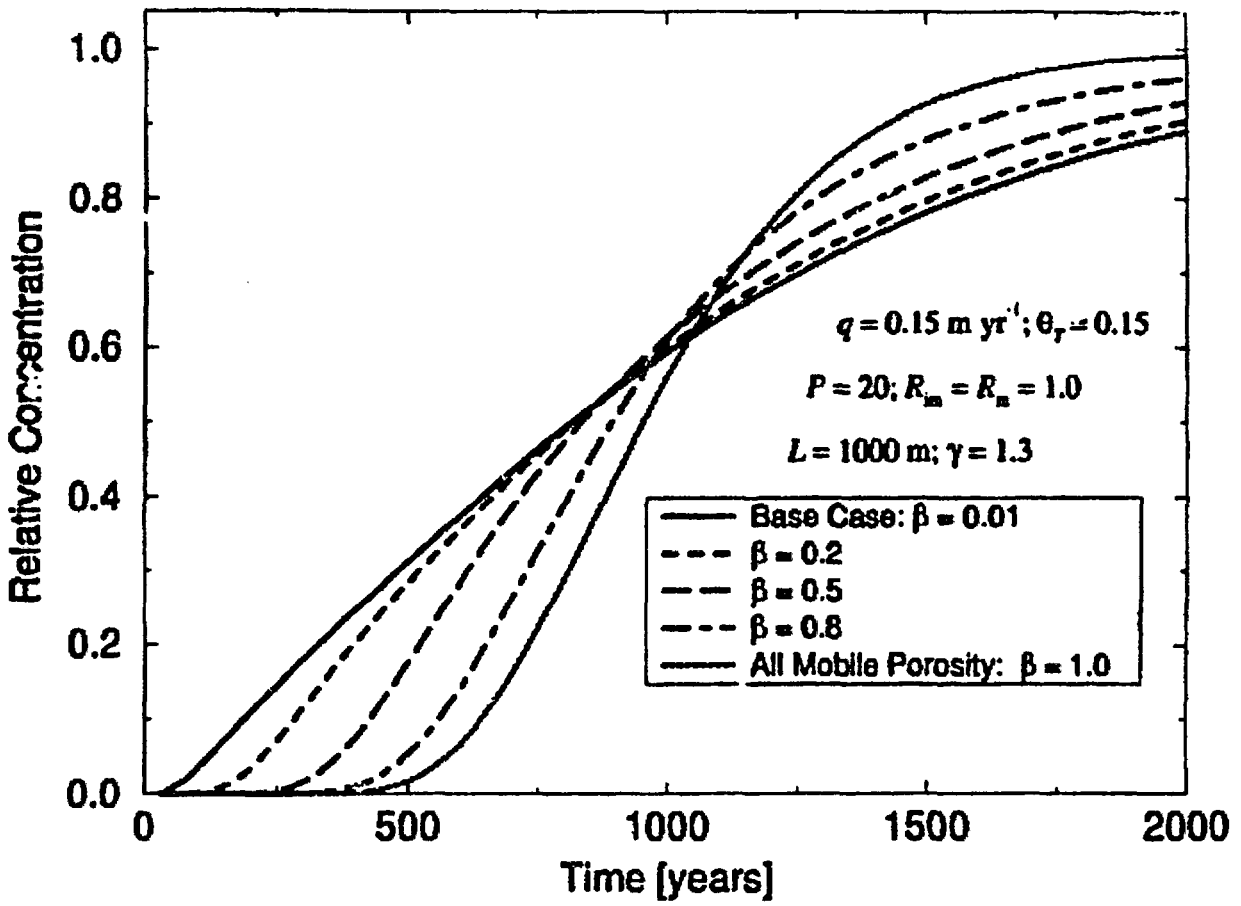

Figure 3-6. Breakthrough curves show the effects of different fractions of mobile porosity (β). For the γ-value used in this analysis, decreases in the value of β below about 0.1 had no significant effect on curve shape or arrival time.

As the value of β is increased, the effects of matrix diffusion become less distinguishable from the case where all porosity is mobile. For the conditions assumed for this analysis, a value of β as low as 0.0001 was not discernibly different from the base case. This latter observation is important because, with the assumed low fracture porosities at YM, the value of β is likely to be low—especially if the immobile region retardation factor is high relative to that of the mobile region. Because the model is less sensitive to β when β is low, it may be sufficient for PA purposes to simply estimate a lower bounding value.

3.3.5 Sensitivity to *P*

Many of the model solutions listed in table 3-1 are based on a simplifying assumption that the effects of mechanical dispersion in the mobile region are negligible compared to the effects of matrix diffusion. This assumption can be tested by examining model sensitivity to the parameter P. Defined by Eq. (3-9), P is the Peclet number for the mobile region; it represents the ratio of the average advection

velocity to the time scale for mechanical dispersion. Higher values of P infer less mechanical dispersion in the mobile region.

Figure 3-7 shows the effect of the value of P on the shape of the breakthrough curve. For the cased considered, P-values of 2.0 and 2,000 correspond to dispersion lengths of 500 m and 0.5 m, respectively, whereas the base case P value corresponds to a dispersion length of 50 m. This range of dispersion lengths conservatively brackets the range of observed dispersion lengths for the length scale under consideration (Gelhar et al., 1992). When there is very little mechanical dispersion (P = 2,000), results are not significantly different from the base case. However, when there is a great deal of mechanical dispersion (P = 2.0), tracer arrival occurs somewhat earlier.

3.4 FIRST-ORDER APPROXIMATION OF MATRIX DIFFUSION

The PA model currently used by the NRC incorporates NEFTRAN II (Olague et al., 1991), which uses a first-order kinetic model as an approximation of the matrix diffusion model. In first-order kinetic transport models, Eqs. (3-4) and (3-5) are replaced by a single equation:

$$R_{im}\theta_{im}\frac{\partial C_{im}}{\partial t} = \alpha\left(C_m - C_{im}\right) , \tag{3-10}$$

where α is an empirical rate coefficient that depends in some way on matrix block size and the immobile diffusion coefficient. A key assumption of first-order models is that solute concentration is uniform throughout the entire matrix block. This implies a uniform solute concentration within each matrix block. In other words, once a solute molecule is transported across the mobile-immobile interface, it is instantaneously well mixed within the immobile pore water. Of course, this is not true; however, depending on diffusion rates and matrix block size, it is often a reasonable approximation. A method for estimating α from matrix block and diffusion properties was developed by van Genuchten (1985) and has the form

$$\alpha = \frac{\theta_{im} D_{im}}{\mathrm{f}\, a^2} , \tag{3-11}$$

where f is a geometry-dependent shape factor. For flow through parallel fractures, as in the base case, f is equal to 0.28.

When the first-order approximation is used, the model parameter γ [Eq. (3-6)] is replaced by another dimensionless parameter, ω, where

$$\omega = \frac{\alpha L}{q} = \frac{\theta_{im} D_{im} L}{\mathrm{f} q a^2} . \tag{3-12}$$

Figure 3-8 compares breakthrough curves for two matrix diffusion scenarios with their associated first-order approximations calculated from the matrix diffusion parameters using Eq. (3-12). When the value of γ is increased (e.g., fast diffusion, low immobile sorption, or small matrix blocks), the

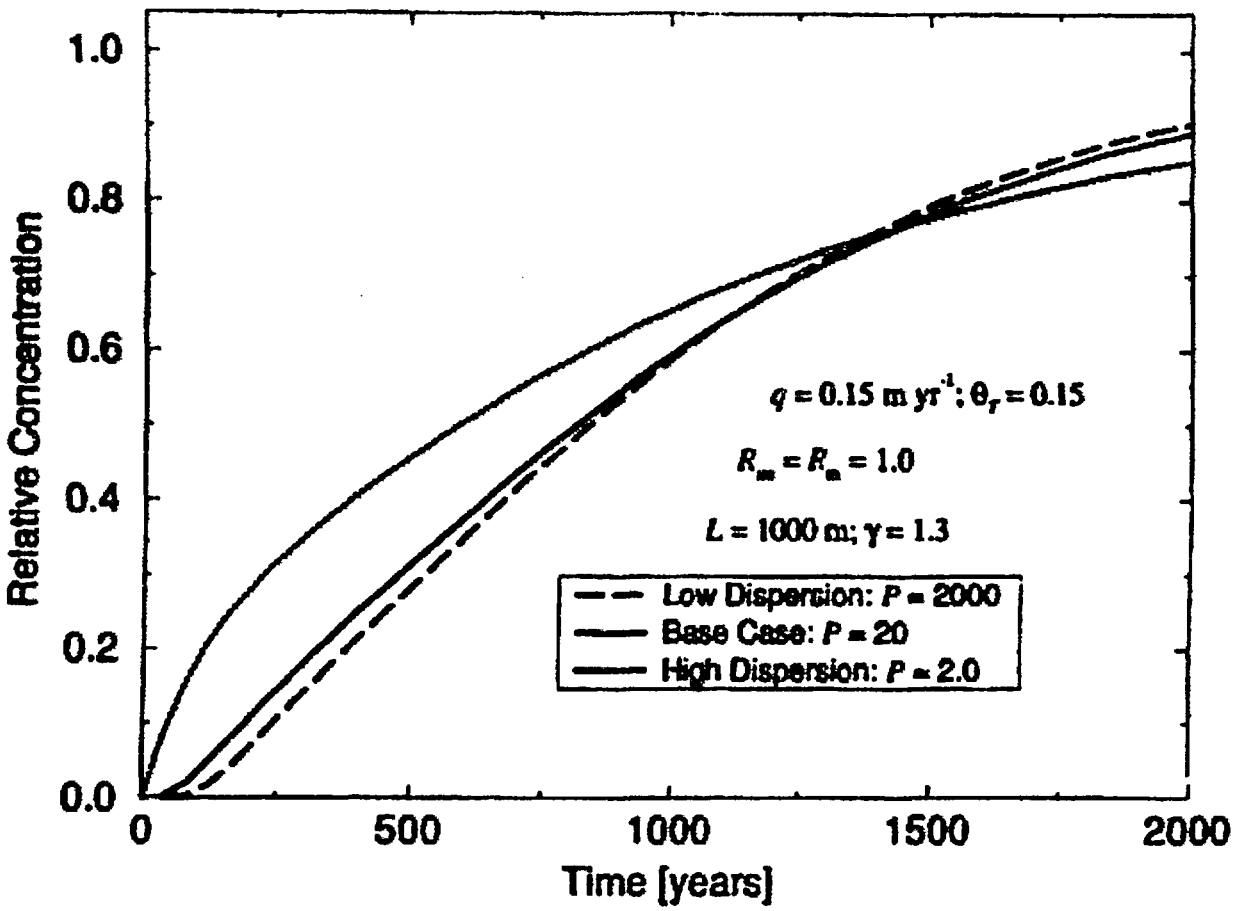

Figure 3-7. Breakthrough curves show the effect of mechanical dispersion on the arrival time of a nonsorbing tracer. The case with low dispersion has a slightly later arrival time than the base case. The high-dispersion case has an earlier arrival time and a faster increase in concentration than the base case.

agreement between the two models improves, and is quite good for the base case scenario. For small values of γ, the first-order approximation tends to overestimate solute concentrations at early times, and overestimate them at late times; however, the early overestimation is likely to be a conservative error, and the late underestimation is within about 10-percent of the matrix diffusion model.

3.5 APPLICABILITY OF MATRIX DIFFUSION MODEL ASSUMPTIONS

The use of a matrix diffusion model to describe transport through saturated and unsaturated geologic media is only as valid as the assumptions upon which it is based. These assumptions include

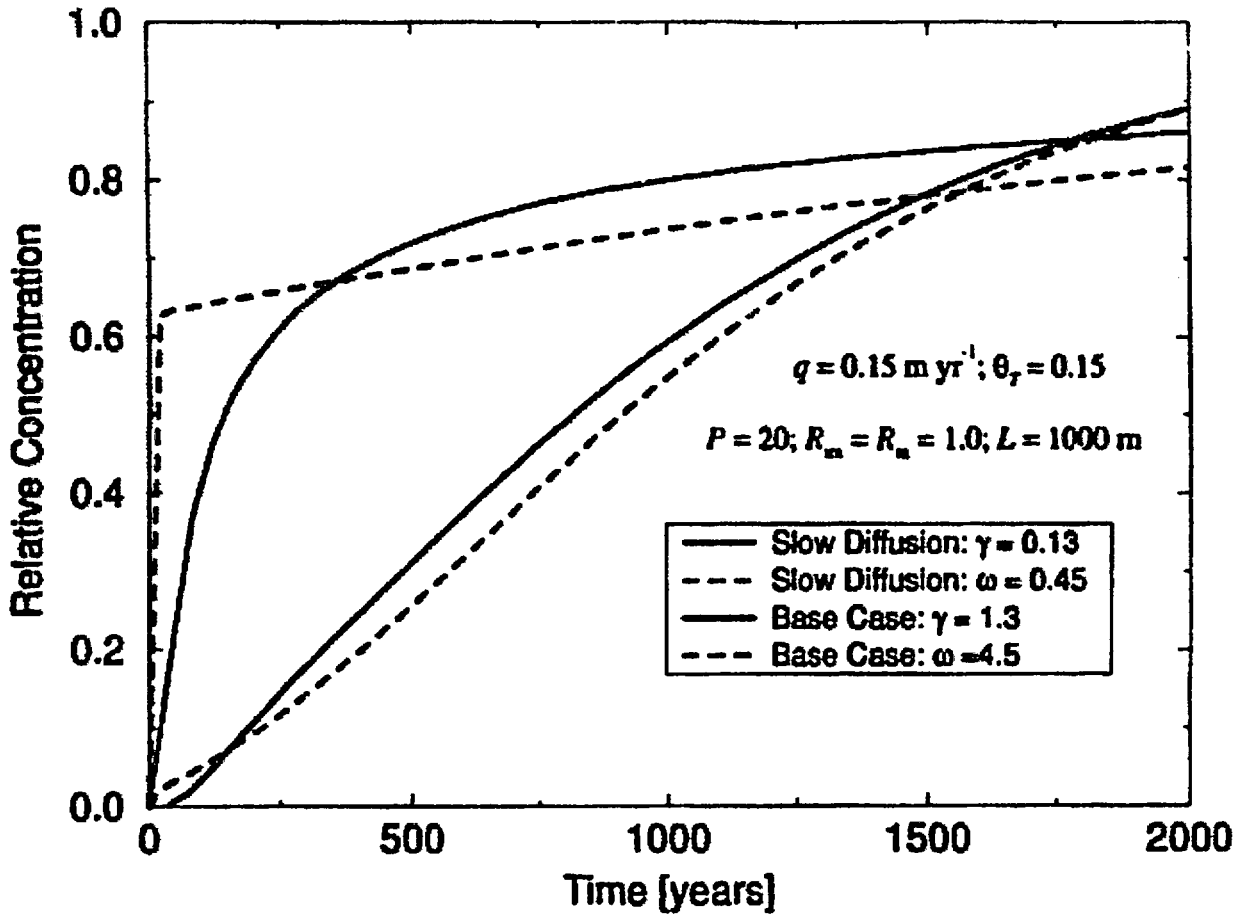

Figure 3-8. Breakthrough curves show a comparison of matrix diffusion models (solid lines) and their first-order approximations (dashed lines).

(i) the existence of mobile and immobile transport domains; (ii) uniform flow through uniform fractures, and (iii) uniform diffusion in the immobile region. Additional assumptions are introduced in the various analytical solutions to the matrix diffusion model—for example, the assumption that dispersion in the mobile region is negligible. Another common assumption used in analytical solutions is that flow occurs in either a single fracture (infinite immobile region) or in evenly spaced parallel fractures (finite immobile region). The applicability of these assumptions is discussed in the following subsections.

3.5.1 Existence of an Immobile Region

The coupling of Eqs. (3-3) and (3-5) is based on the existence of mobile and immobile transport domains. This implies an assumption that advective mass transport into the rock matrix is negligible compared to diffusive mass transport. However, even the most densely welded rocks found at YM have greater-than-zero matrix permeability. As such, under a hydraulic gradient, the advection through matrix pore water must also be greater than zero. The assumption of negligible matrix advection can be tested

by examining the ratio (B) of the time scale for advective transport within rock matrix to the time scale for diffusive transport. Assuming a cube-shaped matrix block of width 2a, and diffusion into the matrix from a planar fracture occurs normal to the direction of advection, this ratio can be express as

$$B = \frac{v_r a}{D_{im}} \tag{3-13}$$

where v is advection velocity within the rock matrix, and a is the matrix block half-width in the direction of diffusion. If B is much less than one, then diffusion is the dominant transport mechanism.

For rocks in the saturated zone beneath YM, a range for v can be estimated from a hydraulic gradient range of 0.0001 to 0.0003 (TRW Environmental Safety Systems, Inc., 1997), and a matrix hydraulic conductivity range of about 10^{-11} to 10^{-9} m s^{-1} (Flint, 1996). Laboratory-measured values of D_{im} for rocks at YM range from about 10^{-11} to 10^{-10} m^2 s^{-1} (Triay et al., 1996). Typical values for a range from about 0.2 to 0.8 m, based on a fracture spacing survey in the Exploratory Studies Facility (ESF) at YM (Anna, 1997). These numbers yield a range of values for B from 2×10^{-6} to 0.024. This range suggests that the assumption of negligible advection in the matrix is valid in areas of highly-fractured low-permeability rock layers at YM. It should be noted that some thin layers of high matrix permeability exist in the saturated zone beneath the proposed repository (e.g., Calico Hills vitric, Bedded Tuff). Flow in these layers is not dominated by fractures, so matrix diffusion is not an issue.

3.5.2 Uniform Flow through Uniform Fractures

Fractures are seldom of uniform aperture and many fractures are "dead-end" fractures that are not interconnected to a continuous fracture network. The result of variability in fracture properties is the formation of multiple preferential flow paths and considerable variation in advection velocities. This has three implications for the use of a matrix diffusion model: (i) multiple preferential transport pathways challenge the assumption of a uniform mobile continuum, (ii) mobile porosity cannot be estimated from total fracture porosity, and (iii) not all matrix block surface area is available for advected solutes to diffuse into.

Fortunately, in the case of item (i), if the scale of a transport model is larger than the scale of heterogeneity in fracture flow velocity and path length, then the effect of the multiple preferential flow paths can be treated as simple mechanical dispersion. There are two reasons for this: first, characteristics of the multiple flow paths tend to be averaged out; second, more flow paths are taken into consideration and their individual effects tend to be smoothed out. Thus, as long as the scale of the transport problem under consideration is sufficiently large, it should be reasonable to treat heterogenous flow patterns as part of the mechanical dispersion process.

Mobile porosity cannot be estimated from fracture porosity because, quite simply, many fractures do not transmit significant quantities of water. Additionally, as previously mentioned, not all matrix porosity is stagnant. For these reasons, the concepts of mobile and immobile porosity are preferable to fracture and matrix porosity in this context. Estimates of effective mobile porosity can be obtained by fitting a flow and transport model (e.g., Moench, 1995) to early breakthrough curve data from nonsorbing tracer tests. For example, Geldon et al. (1997) used conservative tracer data to estimate

a mobile porosity of 0.086 for the Bullfrog-Tram interval of the C-Hole Complex at YM. This mobile porosity estimate is much higher than fracture porosity. Given the ranges of fracture frequency and aperture measured in the near YM (Anna, 1997), fracture porosities should range from about 10^{-6} to 10^{-3}. It is not clear why the mobile porosity estimated from this tracer test is so much higher than the estimated range of fracture porosity. One reason may be that the Tram interval of the C-Holes is intersected by a zone of fault breccia which would have a higher-than-usual mobile porosity. Additionally, one cannot discount the possibility that mobile porosity estimates from tracer tests are biased by the assumption of an ideal flow velocity field.

Even if effective mobile porosity can be determined with confidence, the effect of preferential flow pathways on the system geometry must be taken into consideration. When contaminants are transported in isolated channels, not all of the fracture-matrix interface is contacted by the contaminant. Rasmuson and Neretnieks (1986) proposed that such preferential flow paths were analogous to flow in cylindrical channels and they developed an analytical solution for flow in such a system. This solution is listed in table 3-1.

The previous discussion highlights the important role that fracture properties play in development of dual-porosity models to describe solute transport through fractured rock. Unfortunately, it is rarely possible to fully characterize fracture network properties that might result in preferential flow pathways.

3.5.3 Uniform Diffusion in the Immobile Region

Most analytical solutions to dual-porosity transport models assume uniform diffusion properties throughout the immobile region. In reality, the immobile region may contain such heterogenous features as dead-end macro-pores, surface coatings and altered surfaces, microfractures within the matrix, and different degrees of matrix cementation. The result is that contaminants diffuse at different rates in different areas of the immobile region. Tidwell and others (1997) and used x-ray tomography techniques on core samples of Culebra Dolomite to verify that a brine tracer did indeed diffuse through the samples at different rates. Hsieh et al. (1997) were able to obtain better model fits to breakthrough curves when multiple diffusion coefficients were used instead of a single diffusion coefficient.

The importance of considering multiple diffusion rates for larger-scale transport is not clear. On the scale of inter-well tracer tests, it is often difficult to show that matrix diffusion is occurring at all. Trying to elucidate multiple diffusion rates from these tracer tests may not be a productive endeavor because of the potential for nonunique solutions. Future modeling studies could be useful for determining whether there is a need to consider multiple diffusion rates.

3.5.4 No Mechanical Dispersion

Model solutions that neglect macro dispersion in the mobile region (e.g., Neretnieks, 1980; Gureghian, 1990, 1994; Gureghian et al., 1992)—zero-dispersion models—can be expected to give results similar to the $P = 2{,}000$ scenario (figure 3-6), which is not significantly different from the base case. Thus, if mechanical dispersion at YM can be bounded as being "average" or low (e.g., $P \geq 10$), as the base case scenario is assumed to be, neglecting dispersion should not significantly bias transport predictions. Peclet numbers estimated from nonsorbing tracer tests at the C-Hole complex are estimated to be in the range of 11 to 15 (Geldon et al., 1997). On very large scales, Peclet numbers are likely to

be somewhat higher, because the dispersion length eventually reaches an asymptotic value as the length scale continues to increase. Therefore, zero-dispersion matrix diffusion models may be sufficient for transport predictions in the saturated zone at YM. In the unsaturated zone, however, the nature and magnitude of mechanical dispersion is highly uncertain due to the intermittent nature of infiltration.

3.5.5 Finite versus Infinite Immobile Region

Many analytical solutions to the matrix diffusion model are based on an assumed infinite immobile region (e.g., Neretnieks, 1980; Tang et al., 1981). An infinite immobile region is analogous to flow in a single fracture that bisects an infinite matrix block; hence, diffusing solutes are unhindered by boundary effects. These solutions have the advantage of being less computationally intensive because they require less numerical integration; however, the assumption of an infinite immobile region is only reasonable when values of γ are less than about 0.1 (Gureghian, 1990). Therefore the assumption of an infinite immobile region would be unreasonable for the base case, which has a γ-value of 1.3. However, for solutes that are strongly sorbed, the value of γ would be much smaller than it is for the nonsorbing base case scenario.

4 LABORATORY AND FIELD STUDIES

4.1 LABORATORY STUDIES

In order to effectively model solute transport through fractured rock, it is important to have reasonable estimates of diffusion coefficients for each radionuclide of concern and for each rock type modeled. In this section, laboratory methods and results of several YM studies are reviewed. Plans for future laboratory work and applicability to field conditions are also discussed.

4.1.1 Existing Data

Some of the earliest measurements of solute diffusion in rocks from YM were conducted by Walter (1982, 1985) who used a diffusion cell method. A diffusion cell is basically two chambers, separated by a rock sample. A known concentration of a solute is added to one chamber, and solute-free water is added to the opposite chamber; the rate of solute migration from one chamber to the other is then fit to a diffusion model. Based on these experiments, Walter concluded that Eq. (3-2) holds true for tuffaceous rocks from YM. That is, effective diffusion coefficients were proportional to free-water diffusion coefficients. He calculated a range of values for D_{eff} from 2×10^{-11} to 1.7×10^{-10} m²/s for nonsorbing sodium halides and sodium pentaflourobenzoate (PFBA). Total porosity was found to be the principal factor accounting for variation in D_{eff}. The lumped parameter c/τ^2, which ranged from 0.1 to 0.3, had a fair correlation with median pore diameter, as measured by mercury intrusion.

Additional investigations conducted by Walter include: osmosis experiments, assessment of multicomponent effects on diffusion, and a bench-scale fracture flow experiment. Osmosis experiments with YM tuff revealed pressure drops across samples that increased with increasing concentration gradient. Osmotic pressure results when water molecules can travel more freely through a porous media than ionic species that are dissolved in it. Ionic species are restricted when negatively charged mineral surfaces repell anions, thus effectively reducing the pore diameter from the perspective of an anion. This anion-exclusion process could significantly inhibit the diffusion of large anions.

The computed correlation matrix for various tracers revealed that, although there is coupling of diffusion fluxes between all ionic species, multi-component diffusion is a second-order effect that did not significantly affect experiment results.

Results of a bench-scale fracture flow experiment led Walter (1985) to conclude that the transport of ionic tracers was affected by diffusion into the tuff matrix, whereas the transport of a particulate tracer did not appear to be affected by diffusion.

More recently, Triay et al. (1996) performed laboratory diffusion experiments on tuff samples from YM for a variety of radionuclides. Two types of diffusion experiments were conducted: diffusion cell experiments and rock beaker experiments. Rock beaker experiments are similar to diffusion cell experiments, except the solute chamber is formed by the rock itself which is machined into a cup shape. Rock beakers were pre-saturated with solute-free water, tracer was added to the cup, and the observed dilution of solute in the cup was fit to a diffusion model. Because of the radial geometry of the rock beakers, Triay and others used a numerical model to solve for the diffusion coefficient. An analytical solution was used for the diffusion cell experiments. Batch sorption experiments were also conducted to determine distribution coefficients for the sorbing radionuclides.

Nonsorbing radionuclides used in the rock beaker experiments were tritiated water (HTO), and pertechnetate (TcO_4^-), a large anion. The sorbing species used in the experiments were Np, Am, Sr, Cs, and Ba. Estimated values of D_{eff} ranged from 1×10^{-10} to 3.5×10^{-10} m^2/s for HTO, and from 1×10^{-11} to 4.9×10^{-11} for TcO_4^-. The order of magnitude difference between these nonsorbing tracers was attributed to the effects of anion exclusion and the fact that TcO_4 is a much larger molecule than HTO.

Diffusion coefficients were not estimated for the sorbing species. Instead, observed dilution curves were compared to dilution curves calculated based on the average D_{eff} for HTO of 2×10^{-10}, and measured distribution coefficients. It was found that observed dilution of the sorbing species in the rock beakers was always faster than the calculated dilution, and therefore, use of the HTO diffusion coefficient for sorbing radionuclides was thought to be a conservative assumption (i.e., the assumption will predict slower matrix diffusion).

Diffusion cell experiments of Triay et al., (1996) used nonsorbing HTO and TcO_4, and variably sorbing, U(VI), Np(V), and Pu(V). Following are several of their key findings:

- Diffusion occurred at slower rates in devitrified tuff than in zeolitized tuff.
- The large anion TcO_4^- always diffused slower than HTO
- Pu migration was so dominated by sorption that it never reached the opposite side of the diffusion cell.
- Np(V) and U(VI) diffusion was affected by tuff type and water chemistry (i.e., variable sorption).
- In cases where Np(V) did not sorb, it diffused at a rate comparable to that of TcO_4^-

An important conclusion of Triay et al. (1996) was that observed diffusion of sorbing radionuclides was consistent with a conceptual model in which diffusion occurs in two stages. For example, solutes diffuse first through larger intercrystalline pores or microfractures before they diffuse into the narrower intracrystalline pores. It is not clear whether this proposed two stage diffusion process can be approximated with a single effective diffusion coefficient. It is also unclear why the nonsorbing solutes did not exhibit this two-stage-diffusion behavior. One possible explanation could be that the first stage of diffusion in the rock beaker experiments occurred along discrete pathways (e.g., fingering). This would cause relatively small surface sorption in the matrix, but the surface area of the interior cup wall would be large. The result would be an initially rapid dilution of sorbing solutes that would not be seen in nonsorbing solutes. This may also explain why dilution of sorbing radionuclides occurred faster than was predicted using the D_{eff} for HTO.

Multiple-rate diffusion was observed directly in experiments conducted by Tidwell et al. (1997), who used γ-ray tomography to visualize diffusion of a brine solution through low-permeability, low-porosity dolomite. They observed that variability of solute migration into a rock sample was associated with variability in porosity and the presence of microfractures For samples that exhibited multiple-rate diffusion, the diffusion coefficients used to fit observed solute migration data varied by about a factor of two, depending on whether a better fit was desired for early time or late time data. From a visual examination of the model fits obtained by Tidwell et al., it appears that a single diffusion coefficient could give a reasonable fit to the overall migration data. It should be noted that the

experiments of Tidwell et al have yet to undergo peer review and their data were not collected under a qualified quality assurance program

4.1.2 Future Laboratory Studies

According to Triay et al. (1996), the YM Study Plan calls for diffusion experiments on unsaturated tuffs. The Plan proposes a method in which tracers are allowed to diffuse into unsaturated samples for a given time. The samples would then be frozen and cut into sections; the sections would be analyzed for tracer concentration, and these data would be fit to a diffusion model to elucidate diffusion rates. These planned experiments are critically reviewed by Triay et al. who point out the great lengths of time it would take to obtain significant diffusive transport into an unsaturated rock matrix. They propose a much simpler indirect method of measuring electrical conductivity in a potentiostatic or galvanostatic mode, coupled with the Nernst-Einstein relationship, which provides reliable diffusion coefficients in electrolyte solutions.

Electrical conductivity and resistivity methods are well established for use in saturated samples (e.g., Miller 1972). In fact, resistivity measurements were used by Walter (1982) for saturated samples from the vicinity of YM. Electrical conductivity is related to diffusive migration of ions because, like diffusivity, it is related to the mean cross-sectional wetted area and tortuosity of the path through the porous media.

Because use of this method for unsaturated rocks is not well-referenced, additional confidence may be gained if the method is verified by a more direct measurement. For example, the method outlined in the YM Study Plan could be used on a few samples for verification. Another potential method of verification is the use of tomography techniques such as those used by Tidwell et al. (1997). Tomography allows for near-real-time observation of diffusion. Because the NRC will ultimately be tasked with reviewing DOE characterization of matrix diffusion in the unsaturated zone, NRC staff may wish to pursue development of such verification techniques. However, resources should only be expended in this area if DOE plans to use a matrix diffusion model for the unsaturated zone.

4.1.3 Applicability of Laboratory Measurements to Field Conditions

It is not clear whether diffusion coefficients determined in the laboratory are truly representative of field conditions because differences in temperature, pore geometry, and matrix surface alteration may result in significant differences in rates of diffusive mass transfer.

The effect of temperature on D_w, and thus D_{eff}, can be seen in the Stokes-Einstein equation

$$D_w = \frac{kT}{6\pi\mu r} \tag{4-1}$$

where k is the Boltzman constant, T is absolute temperature, μ is the temperature-dependent kinematic viscosity of water, and r is effective molecular radius of the solute. Using Eq. (4-1), it can be shown that, for any given solute, the value of D_w should approximately double due to a temperature change from 15 to 50 °C; most of this doubling effect is due to the decrease in the viscosity of water over this temperature range. Most laboratory measurements are conducted within this temperature range, typically

at 25 °C. When temperature profiles of transport flow paths are not known, diffusion coefficients should be conservatively estimated using the lowest temperature the solute is likely to encounter.

Matrix porosity and pore geometry may also differ between laboratory and field conditions. The combined effect of porosity and pore geometry can be treated as a lumped parameter called a formation factor (F) where

$$F = \theta_{im} \frac{c}{\tau^2}. \tag{4-2}$$

Archie (1942) suggested an empirical relationship whereby F varies in proportion to θ_{im}^{n}, where n has values of between 1.3 and 2.5 for various rock types. Dullien (1992) derived a physically based equation relating F to the range of pore throat diameters. Such relationships illustrate the important effect of porosity and pore geometry on the effective diffusion coefficient. Now, consider the fact that *in-situ* rock can be subjected to overburden pressure that could act to reduce both effective porosity and pore throat necks sizes from that encountered under laboratory conditions. Grisak et al. (1988) suggest that rates of solute diffusion through porous rock will diminish rapidly with depth due to overburden pressure; however, they provide no laboratory or field evidence for this assertion. Ohlsson and Neretnieks (1995) have also expressed concern over the fact that laboratory samples have been "de-stressed". Another matter that could influence laboratory results is the mechanical stress of sample collection and preparation which may alter pore structure or produce new fissures and result in higher diffusion rates in laboratory experiments.

It is also unclear whether results of laboratory diffusion experiments are valid when used to infer diffusion rates into natural fracture surfaces. Natural fracture surfaces have generally undergone some degree of chemical or mechanical alteration, and may be covered with a fracture coating. In their literature survey of matrix diffusion, Ohlsson and Neretnieks (1995) report that both diffusivities and sorption coefficients have been found to be the same order of magnitude or larger in most fracture coating materials compared to unaltered rock.

4.2 FIELD STUDIES

Field studies of the effects of matrix diffusion at YM discussed in this report are limited to discussions of tracer tests conducted at the C-Hole complex near YM, and the implications of bomb-pulse Chlorine-36 (^{36}Cl) found in fracture zones of the ESF.

4.2.1 C-Hole Tracer Tests

Tracer tests began at the C-Hole complex in February, 1996 and have continued intermittently until the present. The C-Hole complex consists of three wells (UE25c#1, UE25c#2, and UE25c#3), that are located approximately 2 km southeast of the proposed repository footprint. Each well penetrates about 900 m below land surface, and 500 m below the static water level (Geldon, 1996). The tracer tests discussed here were all conducted in a packed-off 90-m interval of the of the lower Bullfrog member of the Crater Flat Formation. This interval contains the most transmissive intervals in all three wells, and the high bulk-to-matrix permeability contrast is indicative of fracture-dominated flow.

Ideal tracer tests for shedding light on the issue of matrix diffusion are those performed under nearly identical conditions with the only significant difference being the diffusive properties of the tracers used in the test. One such test was initiated on October 9, 1996, and results were interpreted by Reimus and Turin (1997); a summary of their methods and interpretation follows.

Tracers used for the October 9, 1996 test were: (i) lithium ion, (ii) bromide ion, (iii) pentafluorobenzoate (PFBA), and (iv) carboxylate-modified latex polystyrene microspheres with a 0.36-μm diameter. Tracers were injected simultaneously into well c#2 and recovered from well c#3 with partial recirculation. The two wells are about 30 m apart at the surface. Bromide and PFBA served as nonsorbing solutes with free water diffusion coefficients differing by about a factor of two (D_w ~ 1.5×10^{-10} and 0.75×10^{-10} m^2/s, respectively). Thus, if matrix diffusion occurs, the bromide ion would be expected to diffuse more readily, and would be attenuated relative to PFBA. Conversely, if no matrix diffusion occurs, the two tracers would behave identically. The polystyrene microspheres served as large, low diffusivity tracers that should be excluded from the rock matrix and hence provide an indication of true fracture flow in the system without the effects of matrix diffusion. The lithium ion was used to investigate sorptive properties rather than diffusive properties and is not discussed further.

Tracer measurements in the recovery well show a double-peaked behavior. The PFBA and bromide responses showed qualitative evidence of matrix diffusion, as normalized concentrations are higher for PFBA at both peaks, and the second bromide peak appeared delayed relative to PFBA. These features are interpreted by Reimus and Turin (1997) to be indicative of matrix diffusion. The microsphere tracer results were ambiguous, with the only clear conclusion being that they indicate the potential for colloid transport over tens of meters with significant filtration.

The observed attenuation and delayed second peak of bromide relative to PFBA represents a small difference which may be attributed to small biases in measurement techniques. A similar test, conducted either on a larger scale or at a lower flow rate, could help to verify these preliminary interpretations of Reimus and Turin. For example, one could expect to see even greater attenuation of bromide relative to PFBA at a slower flow rate because there is more time for diffusion.

Reimus and Turin (1997) also attempted to determine diffusion properties by fitting a diffusion model to the tracer test data. Perhaps their most important conclusion in this regard is that, although it is possible to estimate an upper limit to the diffusion coefficient (constrained by the fact that the mass fraction of tracer cannot exceed 1), reasonably good fits to the data could also be obtained by assuming no matrix diffusion at all.

4.2.2 Implications of ^{36}Cl in the Exploratory Studies Facility

Elevated atmospheric ^{36}Cl occurred in the 1950s to 1960s as a result of above ground nuclear weapons testing. Elevated ^{36}Cl detected in the ESF is thought to be a result of this "bomb-pulse;" hence, the bomb-pulse ^{36}Cl must have been transported to the ESF in a time frame of less than approximately 40 yr. This bomb-pulse ^{36}Cl is generally associated with fracture zones which ostensibly represent fast flow pathways.

Actually, there is a paradox to the ^{36}Cl observations: ^{36}Cl is sampled in the ESF from matrix pore water in fractured zones, which means it somehow migrated into the matrix; on the other hand if ^{36}Cl diffuses significantly into the matrix, such rapid travel times would not be expected. This paradox

can be settled by the a conceptual model of limited matrix diffusion that only occurs in relatively wet fracture zones where matrix is broken into small pieces and hence has a large surface area for diffusion.

This view of limited matrix diffusion in the unsaturated zone indicates that application of diffusion models that work in saturated laboratory studies and in saturated zone field studies are not appropriate for the unsaturated zone at YM. For example, based on laboratory-determined diffusion coefficients, chloride can diffuse tens of centimeters into rock matrix on a time scale of several months to a few years. Yet this is not observed with ^{36}Cl near fracture zones in the ESF. Additionally, episodic fast flows and capillary-driven imbibition add further uncertainty to the significance of matrix diffusion in the unsaturated zone.

4.3 EVIDENCE FOR LIMITED MATRIX DIFFUSION

It is clear from laboratory studies that significant matrix diffusion can occur in low-porosity, low-permeability rocks. Still, uncertainty remains as to whether laboratory studies are directly applicable to field conditions. In this section, several field observations are discussed that suggest a limited role of matrix diffusion

4.3.1 Unsaturated Zone

As already discussed, ^{36}Cl data from the ESF provided evidence for limited matrix diffusion in the unsaturated zone. This argument against matrix diffusion in the unsaturated zone is strengthened by White et al. (1980) and Murphy and Pabalan (1994), who point out significant differences between the geochemical signatures of fracture water and matrix pore water in the unsaturated zones near YM and at Rainier Mesa. Murphy and Pabalan also pointed out similarities between fracture water at Rainier Mesa, and YM saturated zone water. Yang et al. (1996) presented YM data showing marked differences in the geochemical signatures of unsaturated zone pore waters and saturated zone well water, and similarities between perched zone water at YM and saturated zone water.

In addition to geochemical evidence, natural analog studies have been used to suggest limited matrix diffusion in the unsaturated zone. For example, investigations of the Nopal I uranium deposit (Pearcy et al., 1995) in the Peña Blanca mining district of Mexico revealed that occurrence of uranium in unfractured tuff matrix was limited to distances less than 1 mm from uranium enriched fracture filling minerals. Many other natural analog studies suggest limited matrix diffusion: for example, Ohlsson and Nerenieks (1995), after reviewing several natural analog studies, concluded that matrix diffusion seems to be limited to weathered or altered zones. One problem with natural analog studies, however, is that unknown initial and boundary conditions, as well as other possible transport mechanisms (e.g., imbibition, evaporation), make it difficult to draw unambiguous conclusions regarding matrix diffusion.

4.3.2 Saturated Zone

Murphy (1995) pointed out the common occurrence of calcite in rocks below the water table in the vicinity of YM, and the fact that saturated zone water at YM is undersaturated with respect to calcite. These observations are an indication that groundwater flow is channelized and that portions of rock that contain calcite are effectively isolated from present water circulation. Murphy (1995) also suggested that the presence of undissolved calcite and undersaturated water implies that matrix diffusion between channelized groundwater and rock matrix water is limited, perhaps over time scales of millions

of years. However, this conclusion may be premature, because no serious attempt has been made to estimate time scales for dissolution of calcite minerals from rock matrix by diffusion alone. It is possible that solute transport by matrix diffusion could occur rapidly enough to warrant inclusion into PA models, yet be too slow to dissolve calcite locked deep within matrix blocks—even over millions of years. It is therefore recommended that modeling be conducted to assess whether the observations pointed out by Murphy (1995) can be used to infer limited matrix diffusion in the saturated zone.

Geochemical data of the type used as evidence against matrix diffusion in the unsaturated zone would be useful for determining the potential for matrix diffusion in the saturated zone. Unfortunately, there is a lack of geochemical data for rock matrix pore water in the saturated zone.

5 NEEDS FOR FURTHER TESTING

Although much is known about the process of matrix diffusion in rocks at YM, there is still a considerable amount of uncertainty regarding the impact this process might have on overall repository performance. Much of this uncertainty lies in our understanding of matrix diffusion in the unsaturated zone. Although matrix diffusion in saturated zones is well understood, the ability to abstract matrix diffusion into PA models is limited by the lack of knowledge regarding preferential flow pathways and flow system geometry. In this section, areas of research that could improve our ability to develop an effective PA abstraction of the matrix diffusion process are discussed. Discussion is focused on laboratory studies, field testing, and transport modeling. It should be noted that no in depth scoping analyses have been performed to evaluate the feasibility or the utility of the following proposals; the intent of this discussion is merely to identify potential research areas for further discussion.

5.1 LABORATORY STUDIES

The electrical conductivity methods proposed by Triay et al. (1996), discussed in section 4.1.1, could provide significant insight into matrix diffusion in unsaturated rock. However, because this proposed method is an indirect measurement of diffusion properties, confidence in results could be improved by conducting some additional experiments for verification of results. Such additional experiments might include:

- Use of tomography methods to visualize migration of brine solution into unsaturated rock matrix (e.g., Tidwell et al., 1997)

- Conducting electrical conductivity measurements during wetting and drying cycles to examine the possibility of hysteretic diffusion properties

Although matrix diffusion under saturated conditions is fairly well understood, a few mysteries still exist. For example, diffusion of sorbing cations in the rock beaker experiments of Triay et al. (1996) occurred much more rapidly than expected. It is unclear whether this is a commonly observed phenomenon; however, if this observation could be attributed to some physical process, it could bode well for PA predictions of repository performance. An additional area of uncertainty in saturated matrix diffusion is the effect of overburden pressure on pore geometry and, hence, on diffusion. A laboratory experiment that might be helpful in this regard is measurement of the electrical conductivity response to stress on a saturated rock sample.

5.2 FIELD TESTING

Ongoing tracer studies at the C-Hole complex are expected to continue to shedding light on the process of matrix diffusion in the saturated zone beneath YM. The CNWRA and the NRC are currently conducting independent interpretations of these C-Hole tests. Tracer tests conducted over greater distances would prove useful for verifying the encouraging—though not conclusive—results of earlier tracer studies. Tracer tests over greater distances could improve the ability to observe matrix diffusion in two ways. First, the time scale would increase, allowing more time for solutes to diffuse. Second, when the scale of the tracer tests is greater than the scale of heterogeneities, the approximation of a homogeneous continuum is less likely to bias results.

A major obstacle to effective interpretation of tracer tests is a lack of understanding of the flow geometry in the saturated zone beneath YM. Because the matrix diffusion transport model is sensitive to the spacing between the fracture-dominated preferential flow paths, additional characterization in this regard would prove extremely useful to both tracer test interpretation and abstraction of matrix diffusion into PA models. Because resources available for drilling of additional boreholes are limited, innovative approaches are needed in order to obtain a better understanding of the YM groundwater flow system. Data and core samples from existing boreholes may hold clues that are as yet undiscovered. For example, as Murphy (1995) pointed out, the existence of undissolved calcite in saturated zone rock matrix is evidence for the existence of channelized groundwater flow. If so, then an analysis of the spacial distribution of such undissolved calcite from existing boreholes may help to place bounds on the likely spacing between preferential flow paths.

5.3 TRANSPORT MODELING

Additional transport modeling is recommended to gain a better understanding of the mechanisms that are important for consideration in future PA codes. Modeling studies could prove useful in the following ways.

- The importance of considering multiple rates of diffusion that occur within rock matrix could be evaluated.

- Various conceptual models for flow geometries and patterns could be tested. For example, it would be useful to compare results from the following scenarios: flow in narrow, highly fractured zones bounded by relatively unfractured rock (e.g., faults); flow that occurs in many discrete finger-type pathways; and flow that is relatively uniform.

- Results from matrix diffusion transport models could be compared to results from first-order-kinetic transport models. This would be useful in evaluating the reasonableness of using the first-order-kinetic model that is already incorporated into NEFTRAN II.

- A matrix diffusion transport model could be developed for the unsaturated zone in an attempt to identify unsaturated flow regimes that are consistent with observed bomb-pulse ^{36}Cl in the ESF.

- Modeling of time scales for dissolution of calcite minerals in the YM saturated zone should be performed to evaluate if their presence in waters that are undersaturated with calcite is an indication of limited matrix diffusion.

6 CONCLUSIONS

Previous PA models for YM relied on dual-permeability approaches to account for dilution of migrating solutes by interaction with near-stagnant water in adjacent rock matrix. The ability to abstract the process of matrix diffusion into PA models could provide a significant improvement over these dual-permeability approaches, which lack a sound physical basis.

Scoping calculations performed in this report indicate that the assumption of interacting mobile and immobile solute transport domains is reasonable for saturated, low-permeability, fractured tuffs at YM. Sensitivity analyses reveal that matrix diffusion models are strongly affected by the value of the effective matrix block size, the effective diffusion coefficient, the retardation coefficient for the assumed mobile and immobile regions, the fluid flux through the system, the total porosity, and the length scale under consideration. These sensitivity analyses also demonstrate that the conventional concept of retardation factors is not appropriate for predicting solute transport times when matrix diffusion occurs.

Evidence of limited matrix diffusion in the unsaturated zone suggests that conventional matrix diffusion models are not appropriate for unsaturated zone radionuclide transport. Additional laboratory work and modeling may help to gain insight into the possibility for radionuclide transport in the unsaturated zone. At present, however, the conservative approach is to treat matrix and fractures as separate and noninteracting.

Much more is known about saturated zone matrix diffusion processes. Results from field tracer studies—though not conclusive—lend support to the possibility of radionuclide attenuation due to matrix diffusion. Based on numerous laboratory investigations, there can be little doubt that matrix diffusion does indeed occur, however it is uncertain that it has any significant impact on radionuclide migration at YM. Although the impact of matrix diffusion is minor on the scale of tracer tests, the impact could be quite significant over the scale of several kilometers used in PA models.

7 REFERENCES

Anna, L.O. 1997. *Preliminary Three-Dimensional Discrete Fracture Model, Tiva Canyon Tuff, Yucca Mountain Area, Nye County Nevada*. Draft Water Resources Investigations Report. Denver, CO: U.S. Geological Survey.

Archie, G.E. 1942. *Transactions of the American Institute of Mechanical Engineers 146*: 54.

Codell, R.B. 1996. *Debunking the TSPA-95 Markov Transitioning Model*. Internal Memorandum (June 13) to Rex Wescott, Tim McCartin, Norm Eisenberg, and Keith McConnell, Division of Waste Management, U.S. Nuclear Regulatory Commission. Washington, DC: Nuclear Regulatory Commission.

Dullien, F.A.L. 1992. *Porous Media. Fluid Transport and Pore Structure*. 2nd edition. San Diego CA: Academic Press, Inc.

Fabryka-Martin, J.T., P.R. Dixon, S. Levy, B. Liu, H.J. Turin, and A.V. Wolfsberg. 1996. *Summary Report of Chlorine-36 Studies: Systematic Sampling for Chlorine-36 in the Exploratory Studies Facility*. LA-UR-96-1384, Los Alamos, NM: Los Alamos National Laboratory.

Flint, L.E. 1996. *Matrix Properties of Hydrogeologic Units at Yucca Mountain, Nevada*. Draft. Denver, CO: U.S. Geological Survey.

Geldon, A.L. 1996. *Results and Interpretation of Preliminary Aquifer Tests in Boreholes UE-25c#1, UE25c#2, and UE25c#3, Yucca Mountain, Nevada*. Water Resources Investigations Report 94-4177. Denver, CO: U.S. Geological Survey.

Geldon, A.L., A.M.A. Umari, M.F. Fahy, J.D. Earle, J.M. Gemmel, and J. Darnell. 1997. *Results of Hydraulic and Conservative Tracer Tests in Miocene Tuffaceous Rocks at the C-Hole Complex, 1995 to 1997, Yucca Mountain, Nevada*. Milestone Report SP23PM3. Las Vegas, NV: U.S. Geological Survey.

Gelhar, L.W., C. Welty, and K. Rehfeldt. 1992. A critical review of data on field-scale dispersion in aquifers. *Water Resources Research* 28 (7): 1,955–1,974.

Golder Associates, Inc. 1994. *RIP Performance Assessment and Strategy and Evaluation Model: Theory Manual and Users Guide, Version 3.20*. Redmond, WA: Golder and Associates, Inc.

Grisak, G.E., M.R. Reeves, and J.G. Blencoe. 1988. *Matrix Diffusion in Rock/Groundwater Systems*. Oak Ridge, TN: Oak Ridge National Laboratory.

Gureghian, A.B. 1990. *FRACFLO: Analytical Solutions for Two-Dimensional Transport of a Decaying Species in a Discrete Planar Fracture and Equidistant Multiple Parallel Fractures with Rock Matrix Diffusion*. Technical Report BMI/OWDT-5. Willowbrook, IL. Battelle: Energy Systems Group, Office of Waste Technology.

Gureghian, A.B. 1994. *FRAC_SSI: Far-Field Transport of Radionuclide Decay Chains in a Fractured Rock (Analytical Solutions and Model User's Guide)*. San Antonio, TX. Center for Nuclear Waste Regulatory Analyses.

Gureghian, A.B., Y.T. Wu, B. Sagar, and R.B. Codell. 1992. *Sensitivity and Uncertainty Analyses Applied to One-Dimensional Radionuclide Transport in a Layered Fractured Rock. MULTFRAC - Analytic Solutions and Local Sensitivities*. NUREG/CR-5917, Vol. 1. Washington, DC: Nuclear Regulatory Commission.

Hsieh, H.T., G.O. Brown, and D.A. Lucero. 1997. Comparison of the in situ emission gama ray tomography imaging and the flow breakthrough curves in a fractured dolomite. *Eos Transactions: Proceedings of the 1997 American Geophysical Union Fall Meeting*.

Luckey, R.R., P. Tucci, C.C. Faunt, E.M. Ervin, W.C. Steinkampf et al. 1996. *Status of Understanding of the Saturated-Zone Ground-Water Flow System at Yucca Mountain, Nevada, as of 1995*. Water-Resources Investigations Report 96-4077. Denver, CO: U.S. Geological Survey.

Miller, D.G. 1972. *Estimation of Tracer Diffusion Coefficients of Ions in Aqueous Solution*. UCRL-53319. Livermore, CA: Lawrence Livermore National Laboratory.

Moench, A.F. 1995. Convergent radial dispersion of a double porosity aquifer with fracture skin: Analytical solution and application to a field experiment in fractured chalk. *Water Resources Research 31*(8): 1,823-1,835.

Murphy, W.M. 1995. Contributions of Thermodynamic and Mass Transport Modeling to Evaluation of Groundwater Flow and Groundwater Travel Time at Yucca Mountain. *Scientific Basis for Nuclear Waste Management XVIII*. Materials Research Society: Symposium Proceedings 353: 419-426.

Murphy, W.M. and R.T. Pabalan. 1994. *Geochemical Investigations Related to the Yucca Mountain Environment and Potential Nuclear Waste Repository*. NUREG/CR-6288. Washington, DC: U.S. Nuclear Regulatory Commission.

Neretnieks, I. 1980. Diffusion in the rock matrix: an important factor in radionuclide retardation? *Journal of Geophysical Research* 85(B8): 4,379-4,397.

Nuclear Regulatory Commission. 1995. *Iterative Performance Assessment, Phase 2*. NUREG-1464. Washington, DC: U.S. Nuclear Regulatory Commission.

Ohlsson, Y., and I. Neretnieks. 1995. *Literature Survey of Matrix Diffusion Theory and of Experiments and Data Including Natural Analogues*. SKB Technical Report 95-12. Stockholm, Sweden: Swedish Nuclear Fuel and Waste Management Company.

Olague, N.E., D.E. Longsine, J.E. Campbell, and C.D. Leigh. 1991. *User's Manual for the NEFTRAN II Computer Code*. NUREG/CR-5618. Washington DC: U.S. Nuclear Regulatory Commission.

Pearcy, E.C., J.D. Prikryl, and B. Leslie. 1995. Uranium transport through fractured silicic tuff and relative retention in areas with distinct fracture characteristics. *Applied Geochemistry, 10*: 685-704.

Rasmuson, A., and I. Neretnieks. 1980. Exact solution for diffusion in particles and longitudinal dispersion in packed beds. *American Institute of Chemical Engineering Journal* 26: 686-690.

Rasmuson, A., and I. Neretnieks. 1986. Radionuclide transport in fast channels in crystalline rock. *Water Resources Research* 22(8): 1,247-1,256.

Reimus, P.W., and H.J. Turin. 1997. *Results, Analyses, and Interpretation of Reactive Tracer Tests in the Lower Bullfrog Tuff at the C-Wells, Yucca Mountain, Nevada*. Yucca Mountain Site Characterization Project Milestone Report SP2370M4. Los Alamos, NM: Los Alamos National Laboratory.

Robinson, B. 1997. *Matrix Diffusion in the Saturated Zone: Field Evidence and Implications for PA*. Presentation given at DOE/NRC Technical Exchange on Total System Performance Assessment. Las Vegas, NV. November 7.

Sagar B. 1996. Flow modeling in heterogenous media in the context of geologic nuclear waste repositories. *Nuclear Science and Engineering* 123: 443-454.

Sudicky, E.A., and E.O. Frind. 1986. Contaminant transport in fractured porous media: analytical solutions for a system of parallel fractures. *Water Resources Research* 18(6): 1,634-1,642.

Tang, D.H., E.O. Frind, and E.A. Sudicky. 1981. Contaminant transport in fractured porous media: Analytical solution for a single fracture. *Water Resources Research* 17(3): 555-564.

Tidwell, V., L. Meigs, T. Christian-Frear, C. Boney. 1997. Visualizing, quantifying, and modeling matrix diffusion in heterogenous rock slabs. *Eos Transactions: Proceedings of the 1997 American Geophysical Union Fall Meeting*.

Triay, I.R., A. Meijer, J.L. Conca, K.S. Kung, R.S. Rundberg, and E.A. Strietelmeier. 1996. *Summary and Synthesis Report on Radionuclide Retardation for the Yucca Mountain Site Characterization Project*. Milestone 3784. Los Alamos New Mexico: Los Alamos National Laboratory.

TRW Environmental Safety Systems, Inc. 1995. *Total Performance Assessment - 1995: An Evaluation of the Potential Yucca Mountain Repository*. Civilian Radioactive Waste Management System. Management & Operating Contractor Report B00000000-01717-2200-00316, Revision 01. Las Vegas, NV: TRW Environmental Safety Systems, Inc.

TRW Environmental Safety Systems, Inc. 1997. *Total System Performance Assessment-Viability Assessment Methods and Assumptions*. Civilian Radioactive Waste Management System. Management & Operating Contractor Report B00000000-01717-2200-00193, Revision 01. Las Vegas, NV: TRW Environmental Safety Systems, Inc.

van Genuchten, M.T. 1985. A General Approach for Modeling Solute Transport in Structured Soils. *In: Hydrogeology of Rocks of Low Permeability, IAH Memorandum* 17(2): 513–526. Ottawa, Ontario: International Association of Hydrogeologists.

van Genuchten, M. T., D H. Tang, and R. Guennelon. 1984. Some exact and approximate solutions for solute transport through soils containing large cylindrical macropores. *Water Resources Research* 20: 335–346.

van Genuchten, M.T., and P.J. Wierenga. 1976. Mass transfer studies in sorbing porous media. *Journal of the Soil Science Society of America* 40: 473–480.

Walter, G.R. 1982. *Theoretical and Experimental Determination of Matrix Diffusion and Related Solute Transport Properties of Fractured Tuffs from the Nevada Test Site*. Los Alamos Report LA-9471-MS. Los Alamos, NM: Los Alamos National Laboratory.

Walter, G.R. 1985. *Effects of Molecular Diffusion on Groundwater Solute Transport through Fractured Tuff*. Ph.D, dissertation, The University of Arizona.

White, A.F., H.C. Claassen, and L.V. Benson. 1980. *The Effect of Dissolution of Volcanic Glass on the Water Chemistry in a Tuffaceous Aquifer, Rainier Mesa, Nevada*. Geological Survey Water Supply Paper 1535-Q. Denver, CO: U.S. Geological Survey.

Yang, I.C., G.W. Rattray, and P. Yu. 1996. *Interpretation of Chemical and Isotopic Data from Boreholes in the Unsaturated Zone at Yucca Mountain, Nevada*. Water-Resources Investigations Report 96-4058. Denver, CO: U.S. Geological Survey.

Zyvoloski, G. 1997. *Saturated Zone Radionuclide Transport at Yucca Mountain, Nevada*. Presentation given at: Field Testing and Associated Modeling of Potential High-Level Nuclear Waste Geologic Disposal Sites (FTAM) Workshop. Berkeley, CA. December 16.

ANALYTICAL SOLUTION USE FOR SENSITIVITY ANALYSES

APPENDIX A

The analytical solution for a two-region (dual-porosity) model with 1D advective and dispersive transport through evenly spaced parallel fractures with diffusive mass transfer into rock matrix was derived by van Genuchten (1985), based on earlier work by Rasmuson and Neretnieks (1980) who derived a similar solution for spherical aggregates. To predict effluent (breakthrough) curves for a finite system the following solution for the flux-averaged concentration (C_e) should be used:

$$C_e(T) = \frac{1}{2} + \frac{2}{\pi}\int_0^\infty \exp\left(\frac{P}{2} - z_p\right)\sin\left(2\gamma\lambda^2 T - z_m\right)\frac{d\lambda}{\lambda} \; . \qquad \text{(A-1)}$$

Here, λ is a dummy variable of integration, T is dimensionless time, given by

$$T = \frac{qt}{\theta L} \; ; \qquad \text{(A-2)}$$

and z_p and z_m are given by the following equations:

$$z_p = \left[\frac{1}{2}\left(r_p + \Omega_1\right)\right]^{\frac{1}{2}} \qquad \text{(A-3)}$$

$$z_m = \left[\frac{1}{2}\left(r_p - \Omega_1\right)\right]^{\frac{1}{2}} \qquad \text{(A-4)}$$

$$r_p = \left(\Omega_1^2 + \Omega_2^2\right)^{\frac{1}{2}} \qquad \text{(A-5)}$$

$$\Omega_1 = \frac{P^2}{4} + \gamma P(1-\beta)R\Psi_1 \qquad \text{(A-6)}$$

$$\Omega_2 = 2\gamma P\beta R\lambda^2 + \gamma P(1-\beta)R\Psi_2 \qquad \text{(A-7)}$$

$$\Psi_1 = \frac{3\lambda(\sinh 2\lambda + \sin 2\lambda)}{\cosh 2\lambda - \sin 2\lambda} - 3 \tag{A-8}$$

$$\Psi_2 = \frac{3\lambda(\sinh 2\lambda - \sin 2\lambda)}{\cosh 2\lambda - \cos 2\lambda} \; . \tag{A-9}$$

The parameters γ, β, θ, P, R, q, t, and L are defined in section 3.2 and 3.3 of this report.

ATTACHMENT D

DOE'S SATURATED ZONE FLOW AND TRANSPORT EXPERT ELICITATION PROJECT

DOE'S SATURATED ZONE FLOW AND TRANSPORT EXPERT ELICITATION PROJECT

This expert elicitation was conducted over a 6-month period, with the first of a series of meetings being held during June 4-6, 1997 (DOE, 1998) The expert panelists included Dr. R. Allan Freeze, Dr. Lynn W. Gelhar, Dr. Donald Langmuir, Dr. Shlomo P Neuman, and Dr. Chin-Fu Tsang. The panelists addressed 16 key issues for the saturated zone, including topics such as conceptual models of groundwater flow patterns, dilution mechanisms, estimates of advective flux, effects of future climate change, colloidal transport of radionuclides, and other topics (DOE, 1998, p. 3-17). They provided estimates of key parameters, and also gave recommendations about the kinds of work that could help to reduce uncertainties associated with predicting radionuclide transport in the saturated zone. References that had been distributed to the panelists are cited in Appendix B of DOE, 1998.

Each of the panelists commented on general groundwater flow patterns in the vicinity of the proposed Yucca Mountain site:

- A. Freeze noted that "It seems well established that [groundwater] flow is to the southeast and to the south. Likewise, it is nearly certain that flow comes up from the carbonate aquifer." He envisioned downgradient flow paths heading to the southeast from the repository and turning south at Fortymile Wash.

- L. Gelhar referred to the need for additional large-scale, multi-well hydraulic and tracer tests, stating that they "...should be conducted in the area SSE of the site (south of the C-wells) to gain information along the flow paths from the repository." Gelhar also observed that "The upward gradient inferred from the single carbonate aquifer well makes movement [of radionuclides] into that unit very unlikely under present conditions."

- S. Neuman stated that "The average horizontal gradient of water level elevations...suggests a southeasterly direction for mean groundwater flow." Neuman cited a paper by J. Bredehoeft (1997) that estimates the upward flow rate between the carbonate and tuffaceous aquifers, based on data from UE-25p#1. Bredehoeft has suggested two possible ways in which the present-day upward flow potential from the carbonate aquifer might be reversed in the future: (1) groundwater withdrawals from the carbonate aquifer; and (2) through future climatic change.

- D. Langmuir stated that "Potentiometric maps indicate that groundwater flow of radionuclide contaminants from the proposed repository likely would follow a pathway defined by a flow tube, southeast from Yucca Mountain to Fortymile Wash and then south to Amargosa Valley. Elevated heads in the underlying Paleozoic carbonate aquifer under Yucca Mountain probably preclude groundwater flow from the Tertiary volcanics into the carbonates "

- C-F Tsang did not explicitly refer to the direction of groundwater flow away from the site, but he estimated the advective flux for the Bullfrog unit of the Crater Fl tuffs He used a hydraulic gradient of 0 0003, which is the inferred horizontal gradient in a general southeasterly direction. Like the other panelists, he referred to evidence of upward flow from the carbonate aquifer to the volcanic units.

The panelists noted some important criticisms of DOE's saturated zone studies. For example, D. Langmuir stated that DOE's approach to radionuclide transport may include assumptions that are unnecessarily conservative, especially with regard to the radionuclide Neptunium-237. L. Gelhar considered (p. LG-6 of 25) that "Both the regional model and site-scale models in their present forms are not useful for predicting groundwater flux beneath the potential repository." He also found unconvincing DOE's claim that the C-well tracer tests demonstrate a matrix diffusion effect.

With respect to dilution, the panelists found few mechanisms that would lead to substantial mixing in the saturated zone beneath Yucca Mountain. They rejected a "stirred tank" model that assumes mixing at the water table. They generally concluded that there will be only small amounts of lateral and vertical dispersion along flow paths from the proposed repository up to 30 km from the site.

On the subject of disruptive events, some of the experts addressed the issue of water-table changes caused by earthquakes. They concluded that such changes would be neither significant nor long-lived.

The panelists estimated cumulative probability for the following parameters: (1) volcanic aquife hydraulic conductivity; (2) volcanic aquitard hydraulic conductivity; (3) carbonate aquifer hydraulic conductivity; (4) alluvium hydraulic conductivity; (5) volcanic aquifer specific discharge; and (6) dilution factor. Plots of these cumulative probability estimates are attached as Figures 1-6. The NRC staff cautions that the figures reproduced here from DOE (1998) are provided as a summary for the convenience of the reader. The information should not be interpreted without full consideration of the text within DOE's (1998) expert elicitation report, and especially the elicitation interview summaries for each of the five expert panelists.

Examples of recommendations made by the experts to reduce uncertainty are given below. All of the panelists recommendations are available in Appendix D of Geomatrix (1998):

- Further well-controlled field tests may help clarify the nature of dispersion, sorption, and matrix diffusion in the volcanic rocks. Laboratory K_d values need to be confirmed in situ.

- Careful construction of flow nets in the vicinity of the large hydraulic gradient, using all available head data in a 3D context, would aid in settling the controversy about this feature.

- Conduct additional multi-well hydraulic and tracer tests SSE of the site (south of the C-wells) to gain information along flow paths from the repository

- Conduct diffusion-cell lab tests on natural fracture surfaces.

- Drill an additional borehole strategically into the area of the large hydraulic gradient, then log and sample it thoroughly to confirm whether the large gradient is an artifact of perched conditions.

- Investigate the hydrogeology of the Timber Mountain area between Pahute Mesa and Yucca Mountain to better estimate advective fluxes beneath and downstream of the site.

- C-well tests should be run for longer times to evaluate the relative importance of matrix vs. fracture flow in the volcanic rocks.

- The large amount of ^{14}C groundwater data contained in the literature for this site should be corrected to provide an internally consistent set of data for the general area. Such data may be useful for computing groundwater travel times.

- Use the borehole temperature logs in the calibration of a 3D site- or subsite-scale model, especially to address the question of upward flow into the volcanic aquifer.

- Re-drill borehole G-2 and emplace packers to study relative changes in packed intervals to reduce uncertainty about the cause of the large hydraulic gradient.

The NRC staff is not bound by the conclusions of an elicitation *a priori* solely based on adherence to guidance provided by the staff. As noted in NUREG-1563 (NRC, 1996, p. 8), "...the use of a formal elicitation process, even when conducted in a manner consistent with guidance provided in this BTP [NRC, 1996], [does not] guarantee that specific technical conclusions will be accepted and adopted by the staff, a Licensing Board, the Commission itself, or any other party to a potential HLW licensing proceeding." This is consistent with views expressed by NRC's Advisory Committee on Nuclear Waste, which stated (ACNW, 1997, p. 17) that "...the applicant [DOE] should not conclude that following the guidance [in NRC, 1996] implies automatic acceptance of the results."

REFERENCES

ACNW (Advisory Committee on Nuclear Waste), *A Compilation of Reports of The Advisory Committee on Nuclear Waste*, July 1996-June 1997, NUREG-1423, Vol. 7, August, 1997, p. 65.

Bredehoeft, J. D., *Fault Permeability Near Yucca Mountain*, Water Resources Research, Vol. 33, No. 11, November 1997, pp. 2459-2463.

Geomatrix, *Saturated Zone Flow and Transport Expert Elicitation Project [for Yucca Mountain]*. WBW 1.2.5.7, prepared for U.S Dept of Energy by Geomatrix Consultants, Inc , San Francisco, CA, January 1998

NRC (U.S Nuclear Regulatory Commission), *Branch Technical Position on the Use of Expert Elicitation in the High-Level Radioactive Waste Program*, NUREG-1563, November 1996

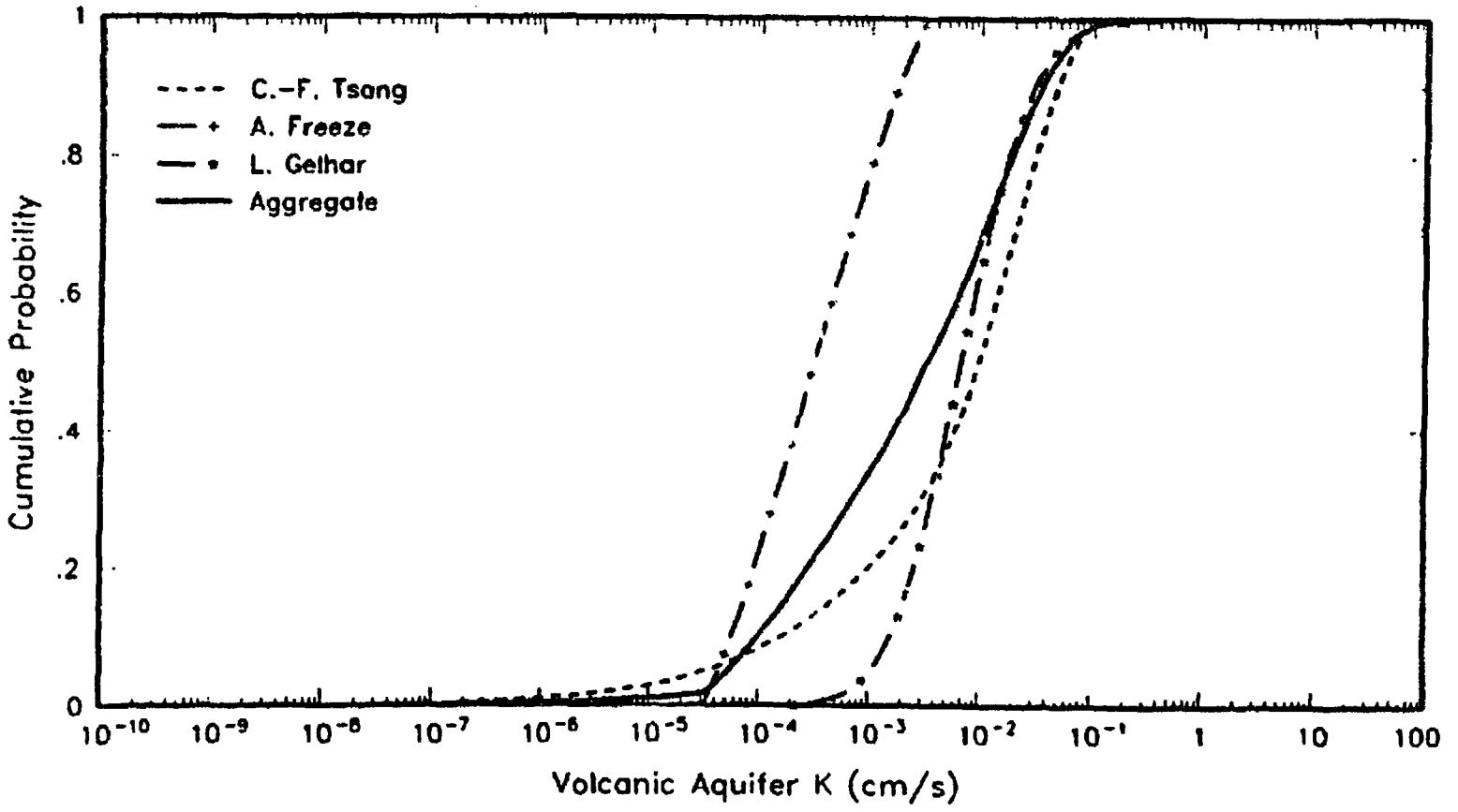

Figure 1. Individual and aggregate cumulative distributions for volcanic aquifer hydraulic conductivity

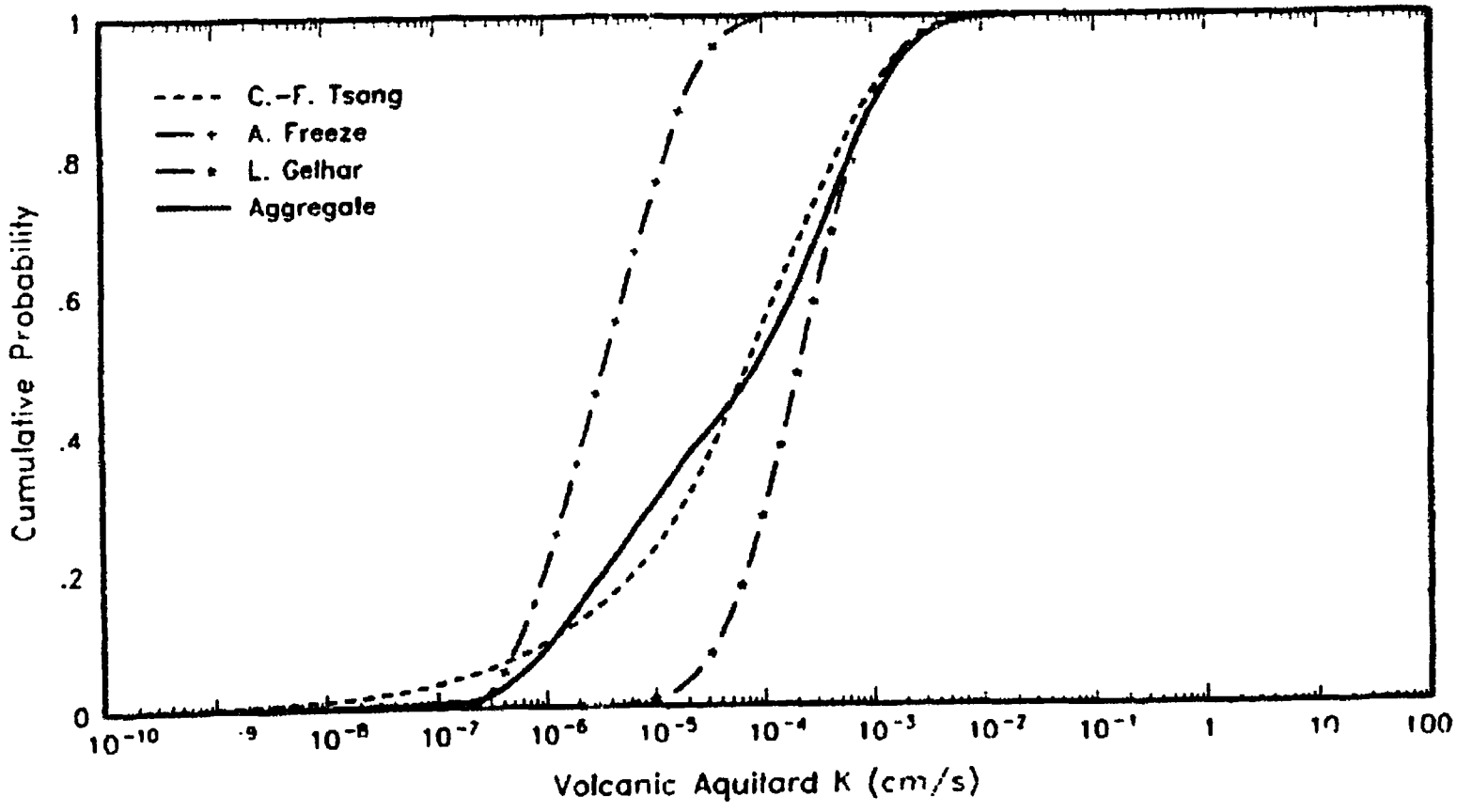

Figure 2. Individual and aggregate cumulative distributions for volcanic aquitard hydraulic conductivity

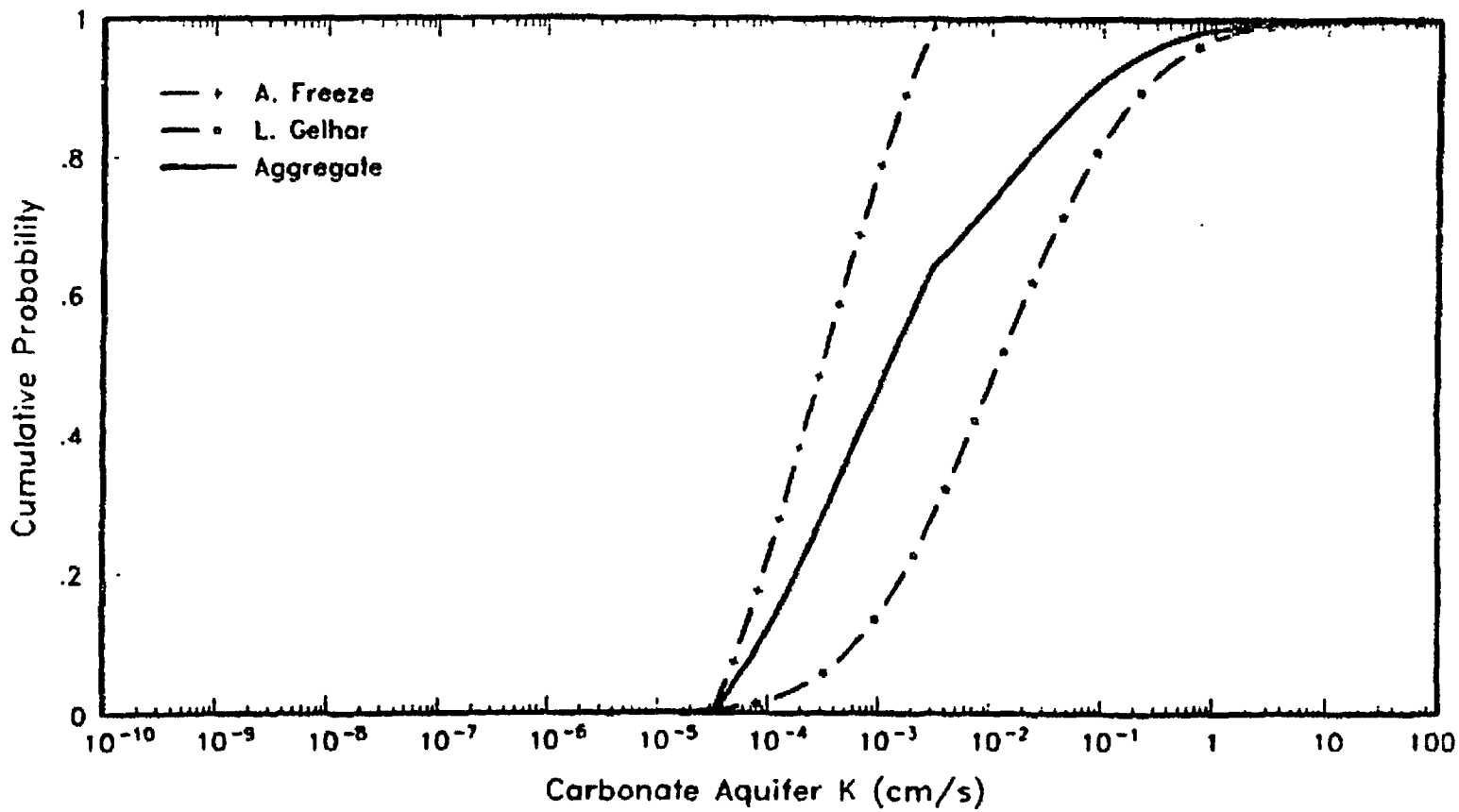

Figure 3. Individual and aggregate cumulative distributions for carbonate aquifer hydraulic

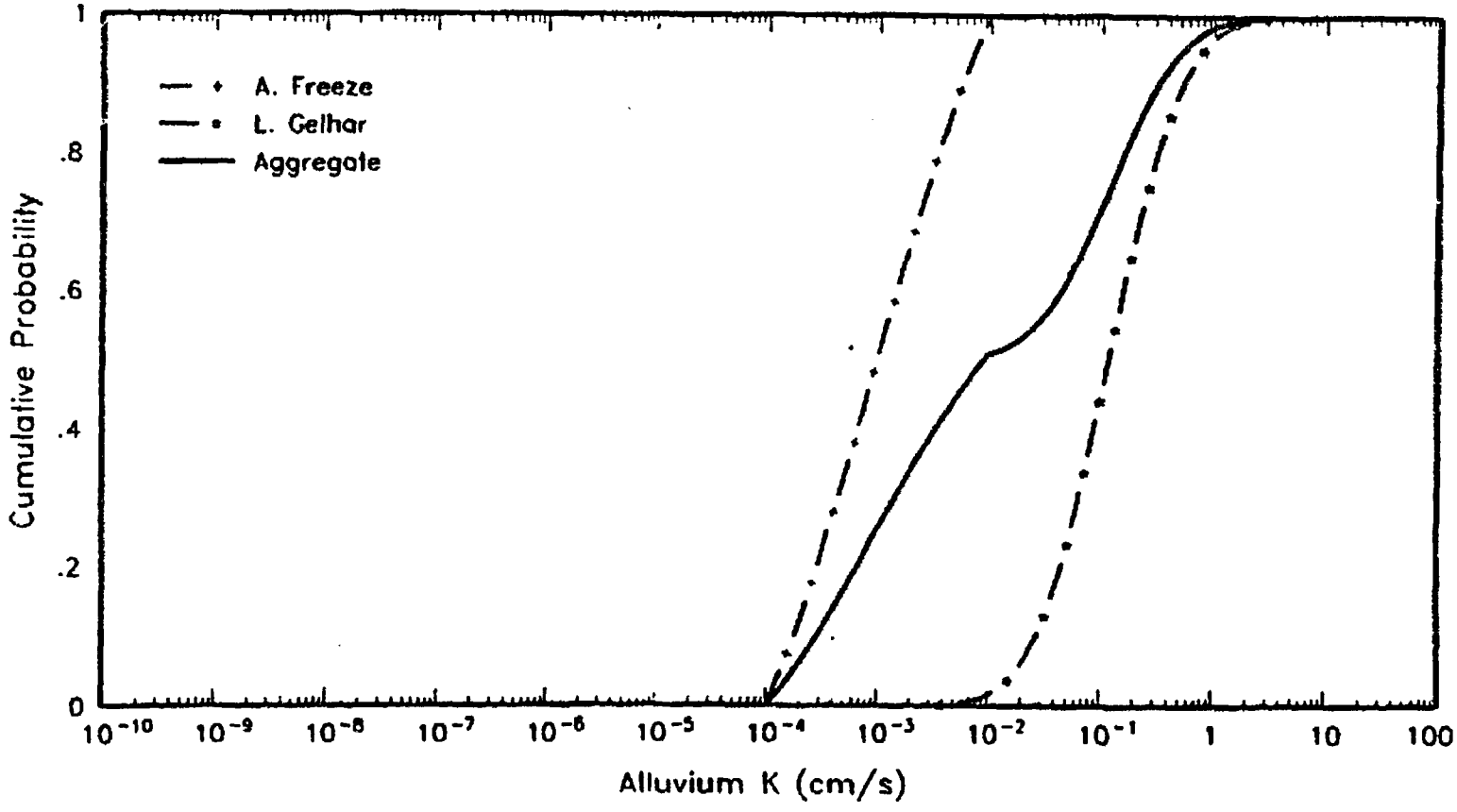

Figure 4. Individual and aggregate cumulative distributions for alluvium hydraulic conductivity

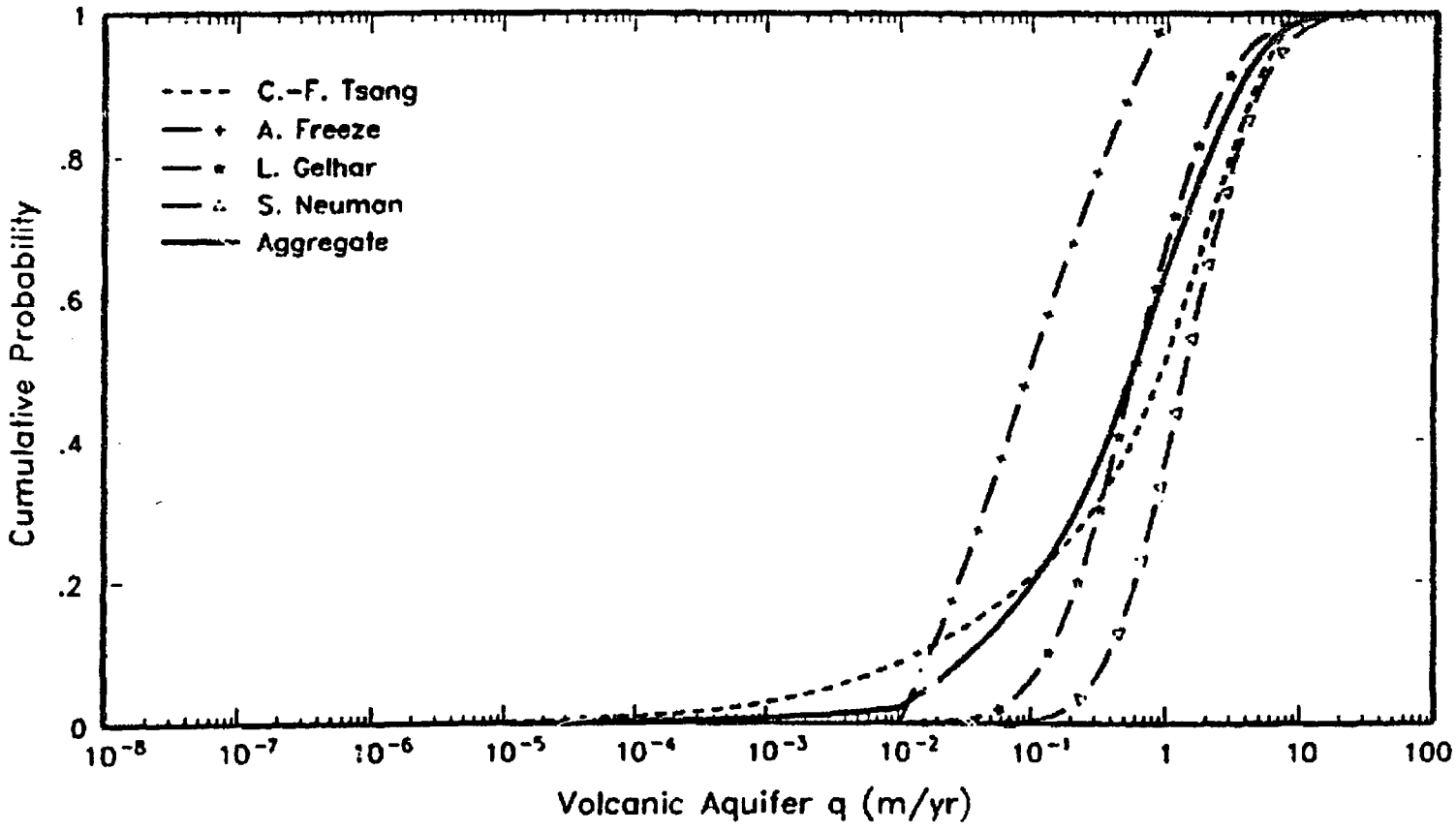

Figure 5. Individual and aggregate cumulative distributions for volcanic aquifer specific discharge

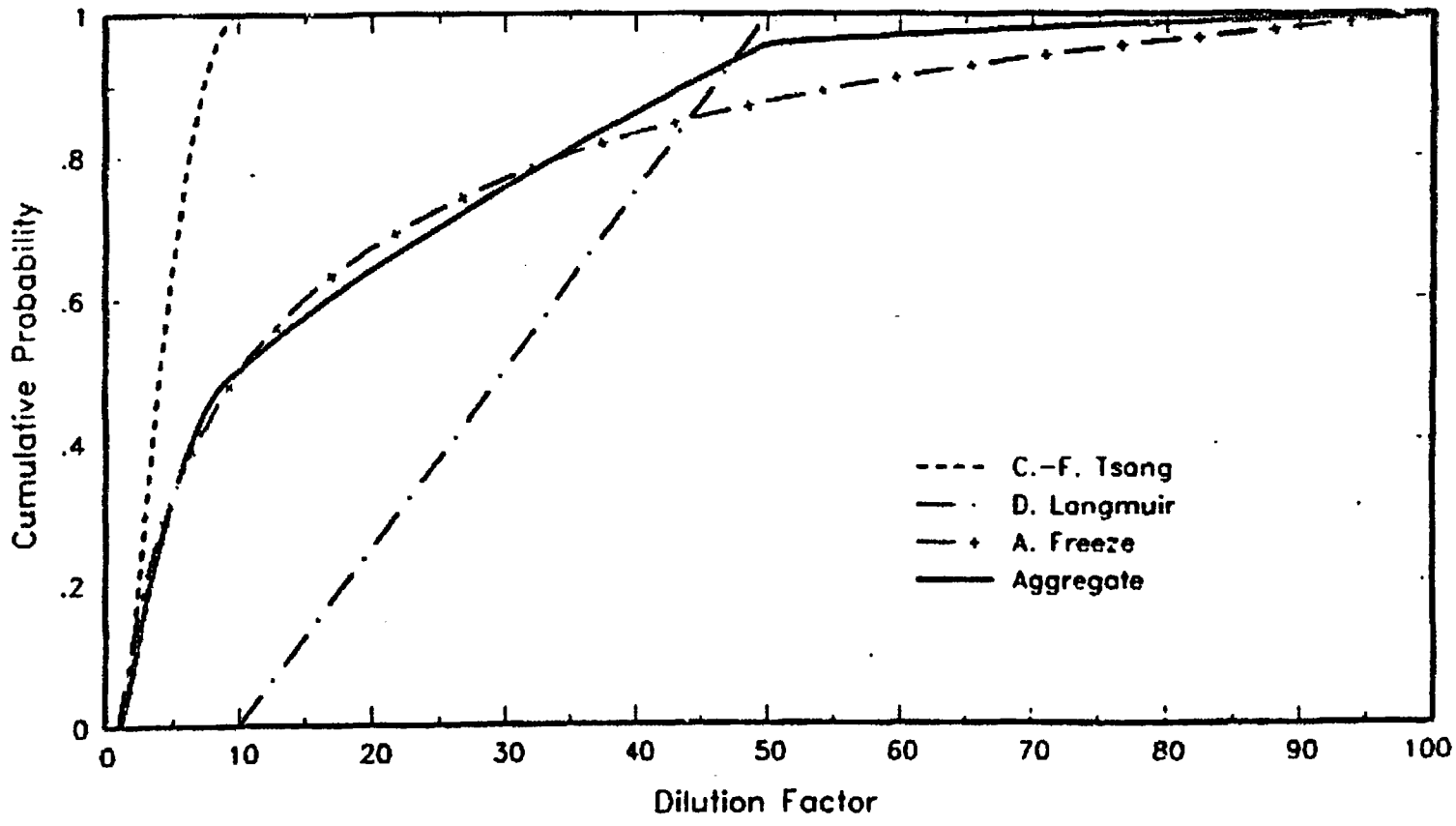

Figure 6. Individual and aggregate cumulative distributions for dilution factor

ATTACHMENT E

USFIC ISSUE RESOLUTION STATUS REPORT
(Climate Subissues)

June 30, 1997

ISSUE RESOLUTION STATUS REPORT ON METHODS TO EVALUATE CLIMATE CHANGE AND ASSOCIATED EFFECTS AT YUCCA MOUNTAIN

(KEY TECHNICAL ISSUE: UNSATURATED AND SATURATED FLOW UNDER ISOTHERMAL CONDITIONS)

Prepared by

Staff of the Division of
Waste Management
Office of Nuclear Material
Safety & Safeguards
U.S. Nuclear Regulatory Commission

June 1997

1.0 INTRODUCTION

One of the primary objectives of the Nuclear Regulatory Commission's (NRC's) refocused prelicensing program is to focus all its activities on resolving the 10 key technical issues (KTIs) it considers to be most important to repository performance. This approach is summarized in Chapter 1 of the staff's annual progress reports (e.g., NUREG/CR-6513, Center for Nuclear Waste Regulatory Analyses, 1996). Other chapters address each of the 10 KTIs by describing the scope of the issue and subissues, path to resolution, and progress achieved during fiscal year (FY) 1996.

Consistent with 10 CFR Part 60 requirements and a 1992 agreement with DOE, staff-level issue resolution can be achieved during the prelicensing consultation period; however, such resolution at the staff level would not preclude the issue being raised and considered during the licensing proceedings. Issue resolution at the staff level during prelicensing is achieved when the staff has no further questions or comments (i.e., open items) at a point in time, regarding how the DOE program is addressing an issue. There may be some cases where resolution at the staff level may be limited to documenting a common understanding regarding differences in the NRC and the DOE points of view. Pertinent additional information could raise new questions or comments regarding a previously resolved issue.

An important step in the staff's approach to issue resolution is to provide DOE with feedback regarding issue resolution, before the viability assessment. Issue Resolution Status Reports (IRSRs) are the primary mechanism that the staff will use to provide DOE feedback on the subissues making up the KTIs. IRSRs comprise 1) acceptance criteria which will be used by the staff to review the DOE license application and prelicensing submittals, as well as indicating the basis for resolution of the subissue, and 2) the status of resolution including where the staff currently has no comments or questions as well as where it does. Feedback is also contained in the staff's annual progress report, which summarizes the significant technical work toward resolution of all KTIs during the preceding FY. Finally, open meetings and technical exchanges with DOE provide opportunities to discuss issue resolution, identify areas of agreement and disagreement, and develop plans to resolve such disagreements.

In addition to providing feedback, the IRSRs will be guidance for the staff's review of information in DOE's viability assessment. The staff also plans to use the IRSRs in the future to develop the Standard Review Plan (SRP) for the repository license application.

Each IRSR contains five sections, including this introduction in Section 1.0. Section 2.0 defines the KTI, all the related subissues, and the scope of the particular subissue that is the subject of the IRSR. Section 3.0 discusses the importance of the subissue to repository performance, including: 1) qualitative descriptions, 2) reference to a total system performance flowdown diagram, 3) results of available sensitivity analyses, and 4) relationship to DOE's Waste Containment and Isolation Strategy (i.e., the approach to its safety case). Section 4.0 provides the staff's review methods and acceptance criteria that will be used to evaluate DOE's prelicensing and licensing submittals. These acceptance criteria are guidance for the staff and indirectly for DOE as well. The staff's technical basis for its acceptance criteria will also be included to further document the rationale for the staff's decisions. Section 5.0 concludes the report with the status of resolution indicating those items resolved at the staff level or those items remaining open. These open items will be tracked by the staff and resolution will be documented in future IRSRs.

2.0 ISSUE/SUBISSUE STATEMENT

This IRSR addresses two subissues of the KTI on Unsaturated and Saturated Flow under Isothermal conditions. The primary objective of this KTI is to assess all aspects of the ambient hydrogeologic regime of Yucca Mountain (YM) that have the potential to compromise the performance of the proposed repository. The secondary objective of this KTI is to develop review procedures and to conduct technical investigations to assess the adequacy of DOE's characterization of key site- and regional-scale hydrogeologic processes and features that may adversely affect performance. Subissues deemed important to the resolution of this KTI have been identified, and are framed as questions:

(i) What is the likely range of future climates at YM?

(ii) What are the likely hydrologic effects of climate change?

(iii) What is the estimated amount and what is the spatial distribution of present-day shallow groundwater infiltration?

(iv) What is the estimated amount and what is the spatial distribution of present-day groundwater percolation through the proposed repository horizon?

(v) What is the estimated amount and what is the spatial distribution of groundwater percolation through the proposed repository horizon during the period of repository performance?

(vi) What are the ambient flow conditions in the saturated zone?

This IRSR addresses subissues (i) and (ii) above. It focuses on methods for estimating future climate change at YM and its associated hydrologic effects. Climate itself is defined by the prevailing meteorological conditions, including temperature, precipitation, and wind. These factors, along with local geologic conditions and plant communities, control the rates of infiltration, deep percolation, and groundwater seepage through a geologic repository located in an unsaturated environment.

This report summarizes the pertinent conclusions of numerous climate-related publications that are relevant to YM. Based on the extensive scientific literature, the NRC staff concludes that reasonable methods exist to bound the range of future climate change and the resulting consequences. Enough information is currently available to reasonably estimate the range of future climates and water-table rise at YM. A procedure and acceptance criteria are provided for reviewing DOE's evaluations of climate change and related topics, and how they will be used to assess the performance of a high-level waste (HLW) repository.

3.0 IMPORTANCE OF SUBISSUES TO REPOSITORY PERFORMANCE

The Earth's climate could change significantly during the time that nuclear wastes will remain hazardous. Climate controls the range of precipitation, which, in part, controls the rates of infiltration, deep percolation, and groundwater flux through a geologic repository located in an unsaturated environment. Changes in groundwater recharge will likely induce other changes, such as regional fluctuations in the elevation of the water table. Water-table rise would reduce the thickness

of the unsaturated zone barrier. Therefore, future changes in climate could significantly influence the ability of a repository to isolate waste.

The importance of groundwater flux as the key parameter for repository performance in an unsaturated zone is well known, and has been further emphasized by DOE's most recent report (DOE, 1995) on total system performance assessment (TSPA). On page ES-30 of that report it is stated that " ... in the overall TSPA analyses, an over-arching theme comes back again and again as being the driving factor impacting the predicted results. Simply stated, it is the amount of water present in the natural and engineered systems and the magnitude of aqueous flux through these systems that controls the overall predicted performance.... Therefore, information on...[this topic]...remains the key need to enhance the representativeness of future iterations of TSPA." Sensitivity studies clearly showed the predominance of percolation flux in estimating cumulative radionuclide releases and peak radiation doses over a 10-kyr (1 kyr = 1000 years) period (see DOE, 1995, pp. 10-6 and 10-7).

DOE's "Waste Containment and Isolation Strategy" (DOE, 1996, p. 5) likewise states that "performance assessments have shown that seepage into the emplacement drifts is the most important determinant of the ability of the site to contain and isolate waste." The importance of infiltration as a hydrologic parameter was recognized by the staff in its Iterative Performance Assessment Phase 2. NRC (1995, p. 10-4) states that "Although the flux of liquid water through the repository depends on...infiltration, hydraulic conductivity, and porosity, performance correlates most strongly to infiltration." Finally, Figure 1 (CNWRA, 1994) shows that climate-related matters have been important factors in recent performance assessments.

Water flow through a geologic repository and its environs depends on both surface processes (precipitation, evapotranspiration, overland flow, and infiltration) and subsurface processes (deep percolation, moisture recirculation, and lateral flow). To evaluate the significance of climate change to repository performance, bounds can be determined for either: (i) climate change (and by inference the importance of surface processes), or (ii) the subsurface processes such as shallow infiltration and deep percolation based on geohydrologic parameters, or (iii) both. Obtaining bounds of water flow from both the climate change and from geohydrologic parameters will most likely provide reasonable assurance that water flow has been appropriately incorporated within the TSPA for the repository.

At YM, cooler and wetter conditions would increase infiltration and could also significantly affect future human populations in the region, leading to changes in patterns of groundwater and land use. These changes should be considered to a reasonable extent in estimating future doses to the critical group identified for the repository.

The staff is developing a strategy for assessing the performance of a proposed repository at YM. As currently visualized by the staff, key elements of this strategy are defined by those elements necessary to demonstrate repository performance. These elements are illustrated in draft figure A-1 in Appendix A. Acceptance criteria for abstracting each of these elements into a demonstration of compliance are under development. Climate change, as defined by long term changes in temperature and precipitation, is an important factor in repository performance because it can alter groundwater infiltration, deep percolation, near-field hydrology, and far-field dilution and transport rates. Climate is also a factor in assumptions about the characteristics of a critical group and reference biosphere.
Therefore, the acceptance criteria for the treatment of climate are subsidiary to and designed to complement the broader-level acceptance criteria for the abstraction of the key elements.

For DOE to adequately demonstrate and quantify in its TSPA the effects that climate change might have on repository performance, it must consider how these effects interplay with the other factors within and between key elements in the engineered and natural subsystems of the repository. As highlighted in Figure A-1, climate change and its effects are important factors that need to be abstracted into four of the key elements of the engineered and natural subsystems. (1) Quantity and Chemistry of Water Contacting Waste Forms (includes consideration of deep percolation); (2) Spatial Distribution of Flow (includes consideration of infiltration), (3) Volumetric Flow in Production Zones (includes dilution and transport rates); and (4) Location and Lifestyle of Critical Group (includes consideration of water-table rise).

4.0 REVIEW METHODS AND ACCEPTANCE CRITERIA

The NRC staff has determined that methods based on paleohydrologic, paleoclimatic, and geochemical information can be used to gain an adequate understanding of the range of past climates in the YM region. These insights can then be used to estimate the range of future climate variability, information that is needed to conduct meaningful performance assessments for a potential repository at YM. Multiple sources of data are needed to help reconstruct past environmental conditions. These include information from: paleodischarge sites; packrat (*Neotoma*) middens; pollen studies· paleolake levels and sediments; groundwater isotopic data; soil properties; tree rings; erosion studies; . nd other sources.

Paleoclimatic and paleohydrologic data can serve as "windows" to the past. They can provide "snapshots" of climatic conditions at various time intervals. To provide meaningful results, data sources must provide paleoclimate and paleoenvironmental indicators, along with materials that can be dated with radioisotopes or fossils.

Some data sources are relatively continuous and represent averaged or regional conditions. Ice cores from Greenland and Antarctica have been used to reconstruct high-latitude climate conditions over tens to hundreds of thousands of years. An example from the Great Basin is the 500-kyr temperature proxy record from Devils Hole, which is now recognized as one of the longest and best paleorecords on Earth. This record can be used to directly compare ancient climates of the Great Basin to proxy records from around the world. The Devils Hole site shows how aquifers can serve as "archives" of ancient climatic conditions.

Tree rings provide a relatively continuous record over a shorter time interval, ranging from decades to as much as several millennia for long-lived species. Some paleo data are discontinuous and representative of highly localized conditions. For example, ancient packrat middens preserve plant remains and pollens that can be used to identify local paleo-assemblages of plants. The limited foraging radius of < 50 m (< 164 ft) of modern packrats requires that plant fragments found in ancient middens came from the immediate vicinity. Numerous ancient middens have been found throughout the Great Basin, including a number near YM.

Paleodischarge sites, like the Lathrop Wells Diatomites near YM, are especially powerful sources of information. If they can be dated and verified as having been produced by discharge from the regional water table, then they can establish times of increased groundwater recharge. The data can be used to help understand the response of the hydrologic system to the range of late Pleistocene

	Climate Change
U S. Nuclear Regulatory Commission, Phase 1 (NRC, 1992)	• Increased Infiltration • Water-Table Rise
U.S. Nuclear Regulatory Commission, Phase 2 (NRC, 1995)	• Increased Infiltration • Water-Table Rise
Sandia National Laboratories, TSPA 1991 (SNL, 1992)	• Increased Infiltration
Pacific Northwest Laboratory (PNL, 1993)	• Increased Infiltration
Electric Power Research Institute, Phase 1 (EPRI, 1990)	• Increased Infiltration
Electric Power Research Institute, Phase 2 (EPRI, 1992)	• Increased Infiltration - Current - Greenhouse - Micropluvials • Water-Table Rise

Figure 1. Comparison of implementations of climate scenarios for Yucca Mountain. (after CNWRA, 1994, p. 7-4)

climatic conditions. The past extent of pluvial lakes in the Great Basin also reflects enhanced recharge conditions on a regional scale.

The staff's technical review of DOE's treatment of future climate will be based on professional judgments regarding the completeness and applicability of the data and evaluations presented by DOE. It is expected that DOE will summarize or document the results of all significant paleo-studies that have been conducted in the YM region. The staff will determine whether DOE has reasonably complied with the Acceptance Criteria in sections 4.1 and 4.2 below.

4.1 Climate Change

It will be necessary for DOE to develop assumptions about future climate change at YM. Staff will review DOE's assumptions to determine whether they are consistent with known trends of past climatic variation. The following *Acceptance Criteria* apply:

- Climate projections based primarily on paleoclimate data are acceptable for use in performance assessments of the YM site. During its review, the staff should determine whether DOE has made a reasonably complete search of paleoclimate data that are available for the YM site and region, and has satisfactorily documented the results. Staff should determine that, at a minimum, DOE has considered information contained in Forester, et al. (1996); Winograd, et al. (1992); Szabo, et al. (1994); and other reports that may become available.

- DOE's projections of long-term climate change are acceptable if these projected changes are consistent with evidence from the paleoclimate data. Specifically, staff should determine whether DOE has evaluated long-term climate change based on known patterns of climatic cycles during the Quaternary, especially the last 500 kyr. The current analysis indicates that these cycles included roughly 100-kyr cycles of glacial/interglacial climates, with interglacials lasting about 20 kyr. Current information also suggests that past climate conditions were cooler and wetter than today, about 60 to 80 percent of the time.

- The staff will not require climate modeling to estimate the range of future climates. If DOE uses numerical climate models, determine whether such models were calibrated with paleoclimate data before they were used for projection of future climate, and that their use suitably simulates the historical record.

- Values for climatic parameters (time(s) of onset of climate change; mean annual precipitation (MAP); mean annual temperature (MAT); etc.) to be used in DOE's safety case must be adequately justified. Determine whether appropriate scientific data were used, reasonably interpreted, and appropriately synthesized into parameters such as MAP, MAT, and long-term climate variability. The current knowledge about these parameters, coupled with past climate change, will require that, as a bounding condition, a return to full pluvial climate (higher precipitation and lower temperatures) be considered for at least a part of the 10-kyr period (current information does not support persistence of present-day climate for a duration of 10 kyr or more). The current interpretations of paleoclimate data indicate an increase in MAP by a factor of 2 to 3 and a lowering of MAT of 5-10 °C (9-18 °F) during the pluvial climate episodes.

- If DOE uses expert elicitation to arrive at values of climate parameters, determine whether the guidance in the Branch Technical Position on Expert Elicitation (NRC, 1996a) was followed by DOE.

4.1.1 Technical Bases for Review Procedures and Acceptance Criteria (Climate Change)

- Overview of Climate Change

Climate change is one of the most important factors that can influence the isolation of HLW in a geologic repository. Therefore, it is necessary for DOE to estimate the range of future climatic conditions to provide inputs to performance assessments. The study of climate change seems a formidable task because it involves both natural and anthropogenic components. Long-term natural variations in climate are clearly seen in the paleoclimatic record of the last 500 kyr. Five glacial/interglacial cycles occurred during that interval, each lasting roughly 100 kyr.

Climate has been changing since the world began, billions of years ago. Earth's early atmosphere was probably dominated by carbon dioxide (CO_2), and it took billions of years for algae in the world's oceans to remove most of that gas and replace it with enough oxygen to sustain life on the continer The sheer mass of carbonate sedimentary rocks on Earth shows the effectiveness with which biol[illegible]cal and chemical mechanisms have gradually removed carbon from the atmosphere (see Krauskopf, 1967, Table 21-2).

The causes of climate change are receiving close scrutiny from the scientific community. Natural variations in the Earth's orbital parameters (Milankovitch hypothesis) must play a significant role. But exactly how long-term climate shifts occur is unclear because complex, non-linear, feedback mechanisms probably exist within the atmosphere-hydrosphere-cryosphere system. Plate tectonics also plays a role by controlling the distribution of land masses and major topographic features.

Human influences on the climate are very recent, providing no long-term history of human influences that could help to project future anthropogenic changes or the manner in which natural cycles may be altered. Only unreliable speculation is available to predict the manner and degree to which future human activities would affect climate over many thousands of years. Human activities could, under various circumstances, delay or even advance a transition to the next glacial stage. But there is general agreement that the chief concern is the addition of greenhouse gases to the atmosphere caused by combustion of fossil fuels. The average temperature at the Earth's surface is thought to have risen by about 0.5 °C (0.9 °F) in the last century, and sea level along the U.S. coast is estimated to be rising 2.5-3.0 mm/yr (0.10-0.12 in/yr). But these changes cannot yet unambiguously be labeled as results of greenhouse warming. One reason for this is that recent ice core data have revealed natural oscillations in climate on a scale of 10-10[illegible] years. Also, during the last interglacial (circa 125 kyr ago), sea level stood for a time about 6 m (2[illegible]) above the present level. This was caused by natural variation because there were no significa[illegible] influences on climate at that time.

Substantial reserves of fossil fuels [illegible]ist on Earth, but most of the remaining resources will probably be depleted on a time scale of centuries rather than millennia. The question then remains. How long will the legacy of an enhanced greenhouse effect continue after fossil fuels are gone? The answer to this question is uncertain, although it is possible that centuries will pass before excess CO_2 concentrations in the atmosphere could return to pre-industrial levels. The complex oceanic and

terrestrial mechanisms that remove carbon from the atmosphere continue to be the foci of extensive research. General circulation models have been applied to these problems, but the data required to greatly improve general circulation modeling are not yet available. General circulation models themselves have limitations, as do all numerical models.

It has been argued that the next 200 years of anthropogenic climate change may create conditions unprecedented in human history. There are predictions of drought-induced famines, the spread of tropical diseases, coastal flooding from sea-level rise, a dramatic increase in the numbers and intensities of hurricanes, and even "run-away" greenhouse effects with drastic biological consequences. The scientific literature includes examples of heated debate about the rate of atmospheric change and the national and international actions that should be taken. Recent assessments of climate change have scaled back the estimated rate of greenhouse warming, one reason being that oceanic and terrestrial carbon sinks may be more effective than previously thought. The climate is still susceptible to so-called "abrupt transitions," which have occurred naturally on time scales of decades or less even during the Holocene. Chaotic changes in ocean currents may be partly responsible for this. Fortunately, on a global scale there is a built-in resistance to drastic climate change, mainly because of the enormous heat capacity of the hydrosphere. This fact is undoubtedly responsible for the long-term evolution and abundance of life on Earth. The complex interactions between the atmosphere, cryosphere, and the hydrosphere provide mechanisms that help to buffer global climate shifts.

Given the realities outlined above, and the need to proceed with reasonable performance assessments, the staff recommends a pragmatic approach to address climate change and its effects. The staff has determined that anthropogenic changes to the atmosphere are detectible and likely to increase with time. The effects of global, enhanced, greenhouse warming will be presumed to last no more than several thousand years, and that, about 3 kyr in the future, the climate at YM will resume or continue the global cooling predicted by the Milankovitch orbital theory of climate. Staff will postulate that full pluvial (cooler and wetter) conditions will dominate at least several thousand years of the next 10 kyr. In other words, anthropogenic effects will be assumed to delay but not prevent an inevitable return to pluvial conditions at YM. Pluvial conditions of higher effective moisture would be reasonably challenging to repository performance, providing conservatism for NRC's safety analysis.

- Natural Variations in Climate

Lamb (1972, 1977) provides a detailed overview of the many mechanisms and phenomena that contribute to climate variability and change. The present-day global climate is part of a sequence that began about 2 million years ago, the beginning of the Quaternary Period. The Quaternary itself is divided into the Pleistocene and Holocene epochs. The Holocene began about 10 kyr B.P. The Quaternary differs climatically from the earlier, generally warmer Tertiary Period because the glaciations were more severe and extensive than those of the late Tertiary. The Tertiary and Quaternary periods comprise the Cenozoic era. The Pleistocene glacial/interglacial cycles were most pronounced in the past million years, during which ten cycles are thought to have occurred. The best long-term records of this climate variability are provided by ice cores, cores from vein calcites, and samples from deep ocean sediments (Dansgaard, et al., 1993; Winograd, et al., 1992; Lamb, 1977).

The reasons for the climate cooling of the late Cenozoic are unknown, but an interesting hypothesis involves plate tectonics. Raymo and Ruddiman (1992, p. 119) propose that

> ...late Cenozoic uplift of the Himalayan region and Tibetan plateau would have resulted in regionally, and hence globally, higher chemical erosion rates, causing a drawdown of atmospheric CO_2 and global cooling. The timing of this tectonically driven CO_2 decrease should be post-Eocene, coincident with the formation of the Tibetan plateau and in agreement with geological evidence for when global cooling was most rapid.

If this tectonic uplift hypothesis is ever verified, it would demonstrate the sensitivity of global climates to relatively small changes in atmospheric composition. Other events that may have helped lead to cooler climates include the occupation of the south polar region by Antarctica and creation of a nearly enclosed Arctic Ocean fringed by mountainous lands (Lamb, 1972, p. 38). However, Raymo and Ruddiman (1992) state that these events cannot account for the observed magnitude of Cenozoic global cooling.

It seems likely that more than one mechanism must be responsible for the Tertiary/Quaternary climate shift. Broecker (1997) points out that water vapor is in fact the principal greenhouse gas in the Earth's atmosphere. He speculates that climate shifts could be caused by changes in the water-vapor budget for the atmosphere, perhaps caused by chaotic changes in global ocean currents, which play a major role in the transfer of heat from the tropics to the poles (Broecker, 1995 and 1997). The potential for climate to be influenced by changes in the energy output of the sun was investigated by Wigley and Raper (1990). They used solar irradiance reconstructions back to 1874 to estimate the effects on global-mean temperatures. Modeled temperature changes were shown to be relatively insensitive to model uncertainties. They concluded that the direct effects of irradiance changes on global-mean temperature are likely to be very small. However, given limitations of available data, the question of low-frequency solar effects on climate remains open (Wigley and Raper, 1990, p. 2171) and can only be addressed by decades of additional data collection. More recent work suggests that low-frequency solar effects are reflected in global temperatures (Lean and Rind, 1994; Kerr, 1996).

The astronomical theory of Milankovitch is a widely accepted model for the stimulus of long-term, natural climate change. Crowley (1996, p. 5) states that the "...onset and recovery from Ice Age conditions is [are] now attributed to slow changes in the Earth's orbit -- the so-called Milankovitch effect -- that modify the seasonal cycle of solar radiation at the Earth's surface." Lamb (1972, p. 30) compared the Milankovitch effect with the effects of solar variations.

> Much greater variations of the Earth's annual radiation budget must occur through very long-term, periodic changes in the Earth's orbit, the tilt of its rotation axis and the seasonal variation of the Earth's distance from the sun characteristic of epochs defined by the orbital situation. Such epochs commonly change their character only slowly, over some thousands of years. But the changes are big, and some effects on climate appear inescapable, probably including the causation of the alternation of ice ages and warm interglacial periods during the Quaternary era...when the large-scale geography has been much as now.

Changes in insolation caused by precessional variations of the earth's orbit and varying tilt of the Earth's rotation axis (Milankovitch model) are known to correlate to some degree with past variations in global ice volumes. Tilt varies with an average period of 41 kyr and precession with an average period of 21 kyr (Kominz and Pisias, 1979). The periodicity of variations in the eccentricity of the earth's orbit is about 100 kyr. Kominz and Pisias (1979) found that, based on simple linear models, less than 25 percent of the variation in global ice volume during the last 730 kyr is related to tilt and

precession. They concluded that Pleistocene glacial variations are largely stochastic in nature. No evidence was found for a linear relationship between eccentricity and ice volume, but Kominz and Pisias did note the existence of a dominant 100-kyr cycle of climatic change. Although tilt and precession are not strongly correlated to global ice volume, they evidently have the potential to trigger or enhance climatic shifts.

Lamb (1977, p. 312) found that the periodicity seen in paleoclimate data was "...so close to the periods of the Earth's orbital variables as to constitute a remarkable vindication of Milankovitch's ...hypothesis regarding the origin of the Quaternary glacial-interglacial cycles.... It is only curious that the 100,000-year time scale is always more prominent than the theory suggests." Historical proof of the gradually changing tilt of the Earth's axis may be found in the monuments throughout the world that mark former latitudes of the Tropic of Cancer and the Tropic of Capricorn (Chao, 1996). The Tropic of Cancer will continue to move south another 90 km (56 mi) before it reverses in about 9300 years and migrates northward.

In a milestone paper, Hays, et al. (1976, p. 1131) likewise concluded that "...changes in the earth's orbital geometry are the fundamental cause of the succession of Quaternary ice ages." Their conclusion was based on analyses of long-term (> 20 kyr) variations in paleoclimate data compared with predictable orbital and insolation changes. They noted that an explanation of the correlation between the dominant 100-kyr climate cycle and orbital eccentricity probably requires an assumption of nonlinearity. At variance with Hays, et al., Winograd, et al. (1992, p. 259) concluded that the paleoclimate record from the carbonate aquifer at Devils Hole was

> ...inconsistent with the Milankovitch hypothesis that orbitally controlled variations in solar insolation play a direct role in Pleistocene climate change. The hypothesis fails to predict the timing of deglaciations during the period 500 to 100 ka [kyr]. During the middle-to-late Pleistocene the increase in the duration of glacial cycles from about 80,000 to 130,000 years suggests that climate shifts were aperiodic. Interglacial climates lasted on the order of 20,000 years.

Winograd, et al. (1992, p. 258) did note that "Obliquity and precession periodicities are evident in the DH-11 record [based on a 36 cm (14 in) core of vein calcite from Devils Hole]. Such periodicities suggest that although solar insolation may not be the primary determinant of the onset of glacial-interglacial shifts, astronomical geometry could still be one of several factors contributing to Pleistocene paleoclimate changes." An independent confirmation of two samples from the Devils Hole chronology has been provided by Edwards, et al., 1997. They used a dating technique based on protactinium-231 to check both the Devils Hole record and records of sea-level change in Barbados corals. Compared with previous dating methods, the Devils Hole samples yielded consistent dates. Therefore, if the samples are representative, the record is accurate. The Barbados data support the astronomical theory of climate change. Differences found in the Devils Hole record are apparently real, but may represent local climatic events (Edwards, et al., 1997; Kerr, 1997).

Regardless of the actual causes of the Pleistocene climates, four glacial stages have occurred in the last 400 kyr. Forester (1996) considers that a full glacial "mega cycle" lasts about 400 kyr and contains glacial/interglacial subcycles of roughly 100 kyr. Forester believes that the Devils Hole record shows that the southern Nevada climate responds to solar insolation on a millennial time scale.

The present Holocene climate has remained relatively stable, even in view of intervals like the so-called "Little Ice Age" that occurred during the period from about 1450 to 1890 (Crowley, 1996). However, Dansgaard, et al. (1993) raised the question of whether the Holocene will remain stable despite anthropogenic effects. They reported evidence for general instability of past climate based on ratios of stable oxygen isotopes in Greenland ice cores. Their high-resolution data suggest that, except for the Holocene, the North Atlantic region has been relatively unstable during the last 230 kyr. Their conclusions apply even to the two previous interglacial stages.

Following the report by Dansgaard, et al. (1993), the previous interglacial has been studied extensively to gain insights about climate variability during warmer intervals (see *Quaternary Research*, Vol. 43, No. 2, March 1995). The last interglacial (oxygen isotope substage 5e) occurred from about 133 to 114 kyr B.P. (before present), based on Greenland ice core data (Dansgaard, et al., 1993). In North America this interglacial is known as the Sangamon; in Europe it is called the Eemian or Eem. For a time during the Sangamon, sea level stood about 6+ m (20 ft) higher than today (Muhs, et al., 1994; Brigham-Grette and Hopkins, 1995; Neumann and Hearty, 1996). This higher sea level corresponded to a significant reduction in global ice, equivalent to a large percentage of the ice volume in present-day Greenland. There were no significant anthropogenic effects on climate during the Sangamon. It is therefore interesting that a natural sea-level rise occurred that is similar in magnitude to that predicted by some future scenarios of enhanced greenhouse warming. Even higher sea-level rises have occurred in the geologic past. For example, global sea level may have been 25 to 35 m (82 to 115 ft) above present-day sea level during the Pliocene (Cronin and Dowsett, 1993).

- Comments on Anthropogenic Climate Change

Karl, et al. (1997) present an excellent summary of the possible causes and consequences of human-induced climate changes. Because of the complex interactions of the Earth's hydrosphere, atmosphere, and cryosphere, the long-term effects of anthropogenic changes to the atmosphere and to the earth's surface (e.g., increase of greenhouse gases, deforestation, abundance of jet contrails, etc.) are still unclear. They could, under various circumstances, delay or even advance a transition to the next glacial stage. Miller and de Vernal (1992) outline conditions in which increased concentrations of greenhouse gases in the atmosphere might lead to ice-sheet growth and an accompanying drop in sea level. It is even possible that reductions in fossil fuel emissions could cause some global warming because of the rapidity with which sulfate aerosols, which are thought to exert a cooling effect, are removed from the atmosphere (Wigley, 1991).

Many of the current concepts regarding anthropogenic changes to climate are predicated on increasing atmospheric CO_2 caused by the use of fossil fuels and biomass burning. Such practices are likely to change as fossil fuels are consumed. Anthropogenic activities also release other greenhouse gases, such as methane and nitrous oxide. Large supplies of fossil fuels still exist on Earth, but the remaining resources will likely last for centuries rather than millennia. Proven energy reserves do not represent total resources, but do provide the best picture of readily available fossil fuels. Proven commercial energy reserves of coal, oil, and natural gas for the world have been estimated at 34.6 x 10^6 petajoules (3.28 x 10^{19} BTUs) (WRI, 1994). Coal is by far the most abundant fossil fuel, and proven world reserves could sustain current production rates for 209 years (WRI, 1994, Table 9.2). Proven reserves of oil and gas could sustain current production for 45 and 52 years, respectively. Crowley (1996) claims that only about 5 percent of the available fossil fuel reservoir has been

consumed to date, but his estimate may not have considered the recent decline in estimated coal reserves in China (WRI, 1994).

As evidence of global warming, investigators have examined whether subtle, long-term changes exist in the temperature record. A report by the Forum on Global Change Modeling (Barron, 1995) gives consensus conclusions about climate change, and specifically temperature. The report found that average global surface air temperatures are about 0.5 °C (0.9 °F) higher than in the last century. However, the change "...cannot yet be unambiguously ascribed to increased concentrations of greenhouse gases." Based on the assumption that greenhouse gases will increase, the report found that it is very probable that mean precipitation will increase, northern sea ice will decrease, and sea level will rise at an increasing rate. If atmospheric CO_2 doubles, global mean surface temperatures will increase by 1.5 to 4.5 °C (2.7 to 8.1 °F), with 2.5 °C (4.5 °F) considered most likely. Mean surface temperatures are estimated to rise 0.5 to 2 °C (0.9 to 3.6 °F) by 2050. But there is also an estimated 10 percent chance that temperatures will rise by over 4 °C (7 °F) by 2100 (Carlowicz, 1995). Carlowicz noted other research that supports the view that even minor changes in global temperature are amplified in the polar regions.

In addition to temperature change, another key variable in tracking global warming is sea-level rise. Titus and Narayanan (1995) reported that sea level is currently rising 2.5 to 3.0 mm/yr (0.10 to 0.12 in/yr). In a detailed report, they assessed the probability of future sea-level rise. Their study consisted of two phases. In the first phase they developed a simplified model for estimating sea level rise as a function of 35 major uncertainties. The report by Titus and Narayanan (1995, p. 1 of summary)

> develops probability-based projections that can be added to local tide-gauge trends to estimate future sea level at particular locations. It uses the same models employed by previous assessments of sea level rise. The key coefficients in those models are based on subjective probability distributions supplied by a cross section of climatologists, oceanographers, and glaciologists. The experts who assisted this effort were mostly authors of previous assessments by the National Academy of Sciences and the Intergovernmental Panel on Climate Change (IPCC).

In phase two the results were documented in a draft report that was circulated to a panel of experts. Feedback from the experts was then used to revise the analyses. Titus and Narayanan (1995, p. 2 of summary) concluded that "Global warming is most likely to raise sea level 15 cm by the year 2050 and 34 cm by the year 2100. There is also a 10% chance that climate change will contribute 30 cm by 2050 and 65 cm by 2100. These estimates do not include sea level rise caused by factors other than greenhouse warming."

Overall, Titus and Narayanan (1995) concluded that sea level is likely to rise less than estimated by earlier studies. The lower estimates reportedly result from a downward revision of future temperatures, and growing consensus that Antarctica will probably not add to sea-level rise in the next one hundred years. Also, recent revisions in carbon cycle models have lowered estimates of CO_2 concentrations. Carbon "sinks" continue to be the subjects of intensive research. For example, Sabine, et al. (1997) estimated that the oceans remove about 37 percent of the CO_2 produced each year from the burning of fossil fuels. This estimate is being improved by a program of direct measurements of carbon in seawater. The oceans naturally contain much more carbon than the atmosphere, mostly in the form of bicarbonate ions (Sabine, et al., 1977).

DeWispelare, et al. (1993) reported the results of an expert elicitation study on future climate in the YM region. Three of five climate experts believed that the principal greenhouse warming effects might last about 3-5 kyr. The other two experts believed that anthropogenic effects could last significantly longer. In fact, one researcher stated (DeWispelare, et al., 1993, p. H-63) that "Human induced atmospheric and surface changes (e.g., greenhouse gas changes, land surface alterations including increased agriculture, and absolute human population growth) will lead to such dramatic climate changes that the paleoclimate record will not be the key to the distant future."

The staff recognizes that, in the end, predictions about the manner and degree to which human activities would affect climate in the distant future will remain highly uncertain. Anthropogenic effects could significantly influence world climates during the next several thousand years. However, realistically, there are limits on how long greenhouse warming can last. After fossil fuels are depleted the natural carbon sinks will gradually remove excess amounts of CO_2. Therefore, the staff's current view is that there is no reason to presume that anthropogenic effects will be of sufficient magnitude and duration to indefinitely postpone a new glacial cycle. More importantly, with respect to a safety analysis of YM, it would not be conservative to presume that present-day conditions will persist for 10 kyr or longer. Instead, the presumption that cooler and wetter conditions will return promotes analyses that are more challenging to repository performance. These kinds of analyses are needed to provide confidence in the results of a HLW safety analysis.

In summary, predictions about the magnitude and duration of future anthropogenic changes in world climates are expected to remain highly uncertain. However, for purposes of evaluating repository performance, it is both pragmatic and conservative to postulate that such changes will be relatively short (several thousand years at most) and that global cooling will return, gradually leading to the next glacial stage. That would lead to pluvial climatic conditions at YM which, as in the past, would be generally cooler and wetter than today's climate.

- Climate Models and High-Level Waste

Various national and international efforts, such as those of the World Climate Research Programme, are analyzing climate change through the development of general circulation or global climate models (GCMs), intercomparison of model results, and the acquisition of paleoclimatic data. For example, 29 atmospheric GCMs participated in the Atmospheric Model Intercomparison Project (Gates, 1992). GCMs have considerable societal value in studying the potential effects of deforestation and burning of fossil fuels, etc., on global and regional climate patterns. Possible benefits of global warming will not be addressed here. Global warming could have various adverse consequences, such as increasing the prevalence of drought conditions in grain-producing regions or increasing the numbers and intensities of tropical storms. Over the next several centuries sea level may rise enough to inundate coral atolls and low-lying continental coasts and cities around the world. Portentous as these possibilities are, they are not relevant to potential HLW disposal at YM unless they would indirectly lead to higher rates of groundwater infiltration.

Timbal, et al. (1997) describe a continuing multi-phase project that seeks to improve GCM results by better integrating land-surface and atmospheric models. Nonetheless, attempts to use GCMs to predict climatic changes over tens of thousands of years would almost certainly remain controversial, leading to debate over the competence of one model and data set vs. another. Heated debates have even arisen over studies of present-day anthropogenic effects on climate (Risbey, et al., 1991a,b; Schlesinger and Jiang, 1991a,b,c; Bolin, 1992; Harvey, 1992; Oeschger, 1992; Schlesinger, 1992;

Feder, 1996). A staff concern is that GCM results could be used to suggest that greenhouse warming might postpone the return of pluvial conditions at YM for more than 10 kyr. The staff considers GCM predictions inadequate to support such a claim. Efforts to validate GCMs will likely result in continual model calibration. These difficulties, along with known limitations of GCMs (Stone and Risbey, 1990), have led the staff to conclude that climate modeling will not be required to support HLW licensing. Instead, a more direct approach is available.

- Representation of Future Climate at YM

With respect to a HLW repository, the staff considers that it is adequate to forecast and bound future hydrologic conditions by studying conditions during past pluvial climates (Coleman, et al., 1996). This kind of work has included the collection and interpretation of regional and global paleoclimatic data to better understand the past range of climates at YM. The data include information from paleodischarge sites, packrat (*Neotoma*) middens, pollen studies, paleolake levels and sediments, groundwater isotopic data, soil properties, tree rings, erosion studies, and other sources. These data are often used to calibrate GCMs, but they can be used directly to bound past climates.

Given the difficulties and realities outlined above, and the need to proceed with realistic performance assessments, the staff recommends a pragmatic approach to address climate change and its effects. Current information does not support an assumption that the present-day climatic regime at YM will persist unchanged for 10 kyr or more. Therefore, it will be presumed, based partly on the results of a climate expert elicitation that the staff sponsored, that an enhanced greenhouse warming will last at most several thousand years, and that about 3 kyr in the future the climate at YM will resume or continue the global cooling predicted by the Milankovitch orbital theory of climate. In other words, anthropogenic effects will be assumed to delay but not prevent an inevitable return to pluvial conditions at YM.

To ensure realism in its safety analysis, staff will postulate that full pluvial (cooler and wetter) conditions will dominate at least several thousand years of the next 10 kyr. Such conditions would be reasonably challenging to repository performance because groundwater fluxes through a repository are expected to be higher during pluvial episodes. The staff's presumption is somewhat conservative if, as appears to be the case, full pluvial conditions at YM are associated with the onset, duration, and waning of glacial maxima in the northern hemisphere. In reality the paleorecord shows that much more than 10 kyr are needed for glacial stages to reach their maxima. There is another safety benefit that accrues by presuming full pluvial conditions will recur. It recognizes the possibility that unforeseen human effects or the natural recovery of global climate from these effects could cause cooler and wetter conditions at YM than otherwise expected. And finally, any safety analysis that covers time periods longer than 10 kyr into the future should simulate climate change using 100 kyr cycles of glacial/interglacial stages, similar to those seen in the paleoclimate record.

This approach to climate representation is consistent with the findings of Dansgaard, et al. (1993), who reported evidence for general instability of past climate based on ratios of stable oxygen isotopes in Greenland ice cores. They raised the question of whether the Holocene will remain stable despite anthropogenic effects. No other period during the last 250 kyr has apparently enjoyed such a stable climate. This climate approach is also consistent with Milankovitch cycles, because a minimum in northern-hemispheric summer insolation will occur during the next 10-15 kyr, based on the solar insolation curves of Vernekar (1968, 1972) as reproduced in part by Lamb (1977). A summer insolation high equivalent to the one centered around 11-kyr B.P. will not recur at northern latitudes

>45° during the next 105 kyr (Lamb, 1977, pp. 314-315). The next substantial peak in summer insolation at these latitudes is predicted to occur about 65-75 kyr in the future. Updated solar insolation calculations have been performed by A. Berger and others, and these should be used to evaluate time periods greater than 50-100 kyr after present (AP), if necessary (see references in Winograd, et al., 1992, note 22).

The assumption that pluvial conditions will return to YM during the next 10 kyr has the advantage that useful estimates of future climate can be obtained even though the scientific debate about the causes of climate change continues unabated. This approach clearly demonstrates that conditions challenging to repository performance will be considered in performance assessments because these conditions would invoke higher rates of precipitation and groundwater infiltration than are occurring at the site today. Such an approach is consistent with conclusions reached by the National Research Council (1995, p. 9), which concluded that the probabilities and consequences of climate change (and other processes) are sufficiently boundable that these factors can be included in performance assessments that extend over a time frame of 10^6 years.

- Comments by the U. S. Nuclear Waste Technical Review Board (NWTRB)

The NWTRB discussed climate issues in a report to the U.S. Congress and the Secretary of Energy (NWTRB, 1993). Chapter 3 of that report was entitled "Resolving Difficult Issues - Future Climates." They stated (p. 55) that

> While there is no guarantee that future climatic and hydrologic states will be similar to those in the past, the Board believes that it is appropriate to assume that the paleoclimatic and paleohydrologic data base (to the extent that it is both sufficiently accurate and complete) can serve as an excellent foundation for predicting the range of these future states at Yucca Mountain...however, this assumption falls short when trying to assess the impacts of modern industrial society on future climate.

The NWTRB report also states (p. 57) that "Past analogues of future greenhouse-gas-changed climate have not been found. Thus while paleoclimates can assist in building confidence by hindcasting, they cannot yet be used as predictions of regional climate change due to future increases in greenhouse gases." With respect to GCMs, the report states that (p. 57)

> ...it is unclear at what time in the future climate models will be sufficiently mature to provide confident detailed long-term predictions of climate at regional and local scales, such as those associated with the Yucca Mountain site. Climate models could, however, provide valuable insights as to the processes affecting future climate, the likelihood of past climate states occurring in the future, and, perhaps, most importantly, the occurrence of climate states such as the enhanced greenhouse effect, which are not reflected in the paleoclimate data base.

One of the NWTRB's (1993, p. 59) recommendations was that "Future climate states should be estimated primarily through the use of paleoclimatic and paleohydrologic data. Numerical modeling can play a supplementary, but important, role in overcoming the limitations of the paleoclimate data and estimating the likelihood of adverse climate states." The NWTRB also states (p. 58) that DOE will have to "...decide when it has reached the point of diminishing returns with respect to its climate-related studies.... The key element in this decision should not be the ability to predict future climate

at Yucca Mountain, but rather the ability to determine, with sufficient confidence, whether future climate states will or will not cause the repository to fail."

The staff generally agrees with the NWTRB (1993) report, although it believes that enough information is already available to reasonably estimate the range of future climates at YM and to analyze their effects on repository performance. DOE's current use of climate modeling can provide additional information, but the staff will not require such work to estimate the range of future climatic conditions at YM over many thousands of years.

4.2 Effects of Climate Change

It will be necessary for DOE to develop one or more representations of future climate, to estimate the ranges of future precipitation, temperature, and water-table rise at YM. Water-table rise would clearly be an "effect" of the climate changing to cooler and wetter conditions. Changes in precipitation and temperature will be discussed as though they were also "effects" of climate change, but the staff recognizes that climate itself is largely defined by prevailing conditions of precipitation and temperature. Staff will review DOE's future climate representations to determine whether they are consistent with known trends of past climatic variation. The following *Acceptance Criteria* apply:

- Bounding values of climate-induced effects (for example water-table rise) based primarily on paleoclimate data will be acceptable. Staff should determine whether DOE has made a reasonably complete search of paleoclimate data pertinent to water-table rise and other effects (for example, changes in precipitation and geochemistry) of climate change that are available for the YM site and region, and has satisfactorily documented the results. In evaluating DOE's analyses, staff should determine whether, at a minimum, DOE has fully considered information contained in Paces, et al. (1996), Szabo, et al. (1994), Forester, et al. (1996), and other reports that may become available.

- It will be acceptable for DOE to use regional and sub-regional models for the saturated zone to predict climate-induced consequences if these models are calibrated with the paleohydrology data. Staff should determine whether DOE's models of the consequences of climate change are consistent with evidence from the extensive paleoclimate data base. Specifically, climate-induced water-table rise is expected to occur in response to elevated precipitation during future pluvial climate episodes, and the staff should determine whether DOE's estimates of climate-induced water-table rise are consistent with the paleoclimate data. The currently known estimate of water-table rise during the late Pleistocene is 120 m (394 ft). Staff should determine whether DOE's assumptions about climate-induced water-table rise over 10 kyr, if different from 120 m (394 ft), are adequately justified.

- Based on staff judgment and analysis, determine whether DOE has adequately incorporated future climate changes and associated effects in its performance assessments. Current information does not support an assumption that present-day climate will persist unchanged for 10 kyr or more. The staff should keep in mind that the consequences of climate change may be coupled to other events and processes and therefore the projections of water-table rise that are used in total system performance may be different from those based solely on climate change.

4.2.1 Technical Bases for Review Procedures and Acceptance Criteria (Climate Change - Futur Precipitation and Temperature)

Recent published work suggests that future pluvial climates could experience an MAP upper threshold that is significantly greater than present-day MAP. Various researchers have used paleoecological methods to estimate the range of MAP and MAT during the late Quaternary in the Great Basin. Forester (1994, p. 2750) stated that "Preliminary estimates from fossil plant and animal records sugges that during the last glacial (14 to 25 ka [kyr]) mean annual precipitation may have been as much as five times modern, while mean annual temperatures were 8-10 °C lower than today." Forester and Smith (1994) studied fossil ostracodes from deposits in the upper Las Vegas Valley. They concluded (p. 2560) that "...during the late Pleistocene average climate conditions in southern Nevada may have beer about four times wetter than today and perhaps as much as 10 °C colder." In a presentation to the U.S. Nuclear Waste Technical Review Board, Forester (1996, p. 18) stated that "During the last glacia within 100 miles of YM, MAP likely varied from about 15 to more than 20 inches at some localities between 5 and 6 k feet with as yet unknown standard deviation and regional variability." This estimated range of MAP (380-510+ mm, or 15.0-20.1 in) is roughly two to three times the present-day MAP of 150-160 mm (5.90-6.30 in)(DOE, 1988b, p. 5-17).

Morrison (1996) forecasts that, consistent with the last interglacial/glacial transition, the coming transitional period will consist of repeated extreme changes in global climate. He concludes that the southern Great Basin will experience frequent episodes with order-of-magnitude increases in effective precipitation, flood magnitudes, and erosion rates. Based on a discussion with staff, Morrison defines effective precipitation as effective moisture, which is the residual precipitation (not lost to evapotranspiration) that contributes to surface-water runoff and groundwater recharge.

Mifflin and Wheat (1979) noted that there is evidence for 53 pluvial lakes of Wisconsin age in Nevada. They studied the variability of modern climates and hydrologic regimes in the Great Basin to infer what conditions were like during past pluvials. Mifflin and Wheat (1979, p. 5) concluded that "...the observed pluvial lake paleohydrology could have been maintained by: a) mean annual temperatures approximately 5 °F lower than those of today; b) by corresponding pluvial mean annual precipitation averaging 68 percent over modern precipitation; c) by mean annual pluvial lake evaporation averaging 10 percent less than mean annual modern lake evaporation." Mifflin and Wheat (1979) also summarized conclusions of earlier, pioneering researchers who studied paleoclimates in the Great Basin.

Mifflin (1990) described the regional hydrologic effects of past pluvial climates in the YM region. Based on the extent of former pluvial lakes in the Great Basin, effective moisture (runoff and recharge) was elevated by about an order of magnitude over modern conditions, and regional water tables rose as much as several hundred feet. That would be consistent with the findings of Oviatt (1997) who described climatic fluctuations of Lake Bonneville for the period from 30 to 10 kyr B.P. This period includes the Wisconsin glacial maximum. Lake Bonneville was the largest of the late Pleistocene pluvial lakes, located in northern Utah in the northeastern portion of the Great Basin.

Spaulding (1985, p. 50) estimated departures of MAT and MAP for various intervals from 45 to 10 kyr B.P. He estimated that MAP during the Wisconsin glacial maximum (around 18 kyr B.P.) was 30 to 40 percent greater than modern. Spaulding (1990) described contrasts between Middle and Late Wisconsin fossil records. He found that mesophytic species (plants needing moderate amounts of moisture) appear to have been more abundant during the Middle Wisconsin, while steppe shrubs

appear dominant during the Late Wisconsin. Spaulding concluded that effective moisture and temperature may therefore have been lower during the late Wisconsin, especially during the glacial maximum ca. 18 kyr B.P. Referring to the glacial maximum, Spaulding (1990, p. 1255) concluded that "An estimated increase in average annual precipitation (Pa) of 40% is all that is required to account for the paleobiotic record in this [YM] region. With the fossil record dominated by xerophytic species [plants tolerant of dry habitats] it is difficult to see how the increase could have been greater."

Spaulding (1995) summarized past climatic conditions at YM based on paleoecological data accumulated to date.

- In the YM region, maximum recharge occurs during warmer climatic intervals (interstadials). The last occurred between ca. 14 kyr and 8 kyr B.P. and was characterized by long-term increases in MAP of up to 100 percent. Short-term (decadal to century) departures of MAP may have approached 400 percent of modern values.

- The Wisconsin glacial maximum (ca. 18 kyr B.P.) was cold and dry, with a decline in MAT of about 7 °C (13 °F) and an increase in MAP of about 40 percent.

- The period ending around 23 kyr B.P. (unit D time) had higher MAP (and recharge) than later periods. This period was characterized by more common deep-water environments in valley bottoms, and early episodes with poorly constrained ages were as wet or wetter.

Wigand, et al. (1994) documented late Holocene climate shifts at various sites in the Great Basin. Their main conclusion was that shifts to times of higher effective moisture were not accompanied by rapid shifts in plant communities. The result was a lag time during which there was less competition for water and greater opportunities for groundwater recharge. There was more competition for moisture and less recharge after plant communities adjusted to the wetter conditions. Wigand, et al. (1994, Figure 2) also presented evidence from Tule Springs (upper Las Vegas Valley) and from various mountain sites that suggests MAP was 2-3 times higher than today from 18 kyr to >23 kyr B.P.

An NRC-sponsored study elicited the opinions of five experts regarding climate change over the next 10 kyr (DeWispelare, et al., 1993). In the next 10 kyr, one expert predicted a doubling of precipitation; one foresaw 15 percent less precipitation; and three others ranged from no change in precipitation to 30-40 percent increases over the present. The experts believed that the montane rain shadow that dominates the Great Basin climate would continue to exert a strong regional influence. A discussion of the rain shadow and its long-term effect is given by Winograd and Szabo (1988).

The milestone report produced by Forester, et al. (1996, p. 33) provides estimates of MAP for 8 intervals over the period from 12 kyr to 35 kyr B.P. They draw several conclusions with respect to past precipitation and effective moisture (p. 65).

> Effective moisture throughout the last glacial was greater than present, but the reasons for its increase differed. In the cool wet periods, gains in MAP probably played as important a role as those [declines] in MAT. During the cold dry periods substantial depressions in MAT with

only modest gains in MAP probably explain the greater levels of effective moisture. Average gains in MAP appear to be about 1.5X to 2X modern, with an unknown standard deviation. Present MAP standard deviations are about fifty percent of the mean value, which, if applicable to the past, would place typical MAP in a range from modern-like to about 3X present MAP. The white fir episodes likely had higher mean MAP. Depressions in MAT appear to range from about 5 to perhaps more than 10 °C below modern. Refinement of past MAP and MAT estimates in both time and space and determining the standard deviations about those means remains a key item to be completed.

These MAT and MAP conditions representing a pluvial climate at YM are similar to the present-day climate in northern Nevada and eastern Oregon, based on data from the U. S. Geological Survey (USGS) (1970). The following table summarizes the precipitation increases during past pluvials as estimated by various workers:

Forester, et al., 1996	YM region	Average gains in MAP appear to be about 1.5X to 2X modern, with unknown standard deviation (range from modern-like to about 3X modern).
Forester, 1996	Area within 100 miles (161 km) of YM	Roughly two to three times modern MAP during last glacial.
Morrison, 1996	Southern Great Basin	Order of magnitude increase in recharge [effective moisture] - implies at least 100 percent increase in MAP.
Spaulding, 1995	YM region	Latest Wisconsin to early Holocene: up to 100 percent increase in MAP (short-term increases in MAP near 400 percent of modern). Glacial maximum: about 40 percent increase in MAP. Middle Wisconsin: greater MAP and recharge than later periods.
Forester, 1994	YM area	Up to five times modern MAP.
Wigand, et al., 1994	Various Great Basin sites	MAP 2-3 times higher than modern (from 18 kyr to >23 kyr B.P.).
Forester and Smith, 1994	Upper Las Vegas Valley	Late Pleistocene average conditions about four times modern MAP.
DeWispelare, et al., 1993 (elicitation of five expert opinions)	Vicinity of YM	For 10 kyr future period, one estimate was 15 percent less precipitation; three estimates were for no change or 30-40 percent increase; and one expert foresaw doubling of precipitation.

Mifflin, 1990	YM region	Order of magnitude increase in effective moisture (runoff and recharge) compared with present-day climate
Spaulding, 1985	YM region	Over the period from 39 to 10 kyr B P, MAP increases ranged from 10 to as much as 40 percent higher than modern.
Mifflin & Wheat, 1979	Basin areas of former paleolakes	About 70 percent increase over modern MAP.

The staff have noted an apparent convergence of professional opinions regarding precipitation during past pluvials. For example, higher estimates of MAP have been revised downward, from about 5 times modern MAP (Forester, 1994) to a factor of 2 to 3 (Forester, 1996; Forester, et al., 1996). Lower estimates have been revised upward (Spaulding, 1985; Spaulding, 1995). The revised MAP estimates approach that by Wigand, et al. (1994) and are more consistent with the estimates provided by other workers. The staff has determined that MAP during past pluvials at YM is the best indicator of what to expect during future pluvial climates. This kind of information can be used to estimate a range for future pluvial MAP, which can further be used to estimate rates of infiltration and deep percolation

Compared with Wisconsin conditions, groundwater recharge has been significantly reduced during the Holocene interglacial. This is best illustrated by the disappearance or dramatic reduction in size of pluvial lakes. There is no reason to believe that future pluvial climates will not be similar to those of the Wisconsin glacial stage. Since glacial stages last longer than interglacials, future climates at YM will be wetter than today most of the time. Based on currently available information, the NRC staff has determined that the potentiometric data from Brown's Room in Devils Hole provide the best available indicators of the duration of higher recharge conditions in the Great Basin during the Wisconsin (Szabo, et al., 1994).

4.2.2 Technical Bases for Review Procedures and Acceptance Criteria (Effect of Climate Change - Water-Table Rise)

There are various lines of evidence that bear on past water-table stands at YM. Taken as a whole they can be used to define a reasonable upper limit to which the water table may rise in response to increased recharge under future pluvial conditions.

- Location and nature of paleospring deposits known as the Lathrop Wells diatomites

Quade (1994) and Quade, et al. (1995) studied fossil spring deposits over a large part of the southern Great Basin. From their survey of fine-grained sediments in this region, they concluded that the deposits were associated with elevated water tables and increased groundwater discharge at various times during the Pleistocene. At various locations inferred water-level changes since late Wisconsin time vary from as little as 15 m (49 ft) to as much as 95-115 m (312-377 ft). One set of paleospring deposits is located only 20 km (12 mi) SW of YM in the southern part of Crater Flat. The nature and position of these diatomites suggests that the water table may have been as much as 115 m (377 ft) higher during the Pleistocene. The water table may have been at or near ground level as recently as

12 kyr ago. The deposits contain mudstones and diatomites, and have been informally named the Lathrop Wells diatomites by Quade, et al. (1995).

Previously, Paces, et al. (1993) estimated ages for several of the Lathrop Wells Diatomites. Using uranium-series disequilibrium, they determined that the deposits represent active springs at 18 ± 1, 30 ± 3, 45 ± 4, and > 70 kyr. They found that two samples from different sites yielded identical ages, suggesting that the springs may have been contemporaneous and were likely part of the same hydrodynamic system. Uranium isotopic compositions suggested that groundwater from the regional Tertiary-volcanic aquifer was the source of the spring flow, and that the water table had formerly risen 80-115 m (262-377 ft) above present levels and may have fluctuated repeatedly. Forester (1996), in a presentation to the NWTRB, noted that analysis of the diatomite deposits (Horsetooth Site) suggests groundwater discharge from the regional aquifer and from a perched flow system.

Stuckless (1994) discussed dating of the diatomite deposits in a presentation to NRC's Advisory Committee on Nuclear Wastes (ACNW). The apparent ages of one deposit range from 16 kyr to 133 kyr, with six sample ages occurring in the interval of the last glacial maximum, broadly 15 to 21 kyr B.P. Another deposit yielded dates of 12 kyr to 28 kyr B.P. The two youngest dates represent the latest Wisconsin. Stuckless caveated the data as preliminary and predecisional.

Additional details about the Lathrop Wells Diatomites and their estimated ages were described by Paces, et al., 1996. They found evidence that the deposits were formed during two distinct periods, from about 15 to 60 kyr and an older episode of 90 to 180 kyr. They report that isotope and paleontological data rule out a surface-water source for the deposits. Drainage from perched-water systems was also discounted as a source. Paces, et al. (1996, p. 1) found that

> ...regional, saturated-zone ground water most likely supplied discharge during pluvial episodes. This conclusion requires the regional water table to fluctuate up to about 100 to 120 m between pluvial and interpluvial periods. Fluctuations of the same magnitude occurred over the last two glacial cycles...much of the late Pleistocene was characterized by higher water tables (as much as 60 to 80% of the last 200 ka [kyr]). Therefore...it is anticipated that this hydrologic state will recur in the future.

The staff recognizes that the exposed setting of the Lathrop Wells Diatomites could cause geochemical open-system behavior, an adverse factor in radiometric dating. However, parts of these deposits are certainly Pleistocene in age, as suggested by radiometric dating, because fossil remains of mammoth (*Mammuthus*) have been found there (Quade, et al., 1995).

Modern-day groundwater is about 115 m (377 ft) lower than the paleospring deposits. Consistent with Paces, et al. (1993), Quade (1994) and Quade, et al. (1995) noted that if water table gradients were similar to modern-day gradients, then a 115-m (377 ft) rise could be extrapolated to YM. This degree of rise could possibly be used to define a reasonable upper limit for rise of the water table at YM during future pluvial climates. Such a rise would significantly reduce the thickness of the unsaturated zone barrier at YM, but it would not saturate a hypothetical repository in the Topopah Spring tuff. A water-table rise of this magnitude would generate spring flow in areas south of YM, which would provide surface drainage outlets for groundwater and perhaps reduce the potential for greater rise.

The staff recognizes that there is continuing discussion about the nature and age of the Lathrop Wells Diatomites. However, they should be interpreted as evidence of former water-table rise unless compelling evidence becomes available to prove that the deposits resulted entirely from the surface discharge of perched water. It is remotely possible that similar, undiscovered deposits may exist at higher altitudes and closer to YM. However, it seems unlikely that such deposits would have escaped the notice of geologists and soil scientists who have extensively mapped the region.

- Strontium isotopic evidence for calcites in the unsaturated zone

Marshall, et al. (1993) compared strontium isotope ratios for five different types of samples, including the paleospring sites, pedogenic (or near-surface) calcites, fracture-fill calcites from the unsaturated and saturated zones, and groundwater from the Tertiary aquifer. The fracture calcite samples came from five boreholes at YM. The calcites in the unsaturated zone have strontium ratios almost identical to the pedogenic calcites, suggesting that they have a similar origin. The only exceptions are four samples from fractures about 85 m (280 ft) above the water table in hole G-2. These four samples have strontium ratios that suggest a significant non-pedogenic component as a source for their strontium. Their strontium ratios are similar to those found in groundwater from the Tertiary tuff aquifer. Based on this, Marshall, et al. (1993) concluded that the water table may have been about 85 m (280 ft) higher than now. This amount of suspected water table rise is of similar magnitude to and corroborates that estimated from the paleosprings to the south (Paces, et al., 1996). Marshall, et al. (1993) also noted that fracture-filling calcites from above and below the water table show different colors under ultraviolet light. Unsaturated zone calcites have a white to purplish fluorescence, whereas those from the saturated zone fluoresce from pink to orange.

- Glassy nonwelded material thins and disappears where the basal Topopah Spring occurs close to the water table

Bish and Vaniman (1985) used X-ray diffraction methods to study mineral distributions in tuffs at YM. They prepared cross-sections to show the distribution of minerals and glassy, or vitric, material. Their work was updated a few years later by Bish and Chipera (1989). An interesting pattern was found in the disappearance of vitric material in the tuffs. Below the dark layer of volcanic glass that forms the basal vitrophyre of the Topopah Spring is the Calico Hills non-welded tuff. The top of the Calico Hills contains abundant pumice and glassy shards in voids. This vitric zone occurs just below the vitrophyre. However, closer to the water table the glassy material mostly disappears. Bish and Vaniman state that the glassy material has been progressively altered to zeolites where the zone is closer to the water table. Based on the data from Bish and Vaniman (1985) and Bish and Chipera (1989), it appears that the base of the glassy (vitric) tuff is about 80-100 m (262-330 ft) above the current water table. This suggests to the staff that the water table was previously higher than now for extended periods, especially since the alteration process may have required thousands of years. The data do not indicate when the water table was higher, but do suggest that the water table may have risen no more than about 100 m (330 ft) higher than at present.

Levy (1991) further discussed the use of geochemical indicators in nonwelded tuffs to interpret paleohydrology. She notes that most zeolites in these tuffs appear to be products of diagenetic alteration in which zeolites were precipitated when the original glassy material dissolved at ambient temperatures in a water-rich environment. Levy suggests that zeolitization may require time periods on the order of 10 kyr, and that much of the zeolitization may have occurred long ago. The static

water level (SWL) is presently about 100 m (330 ft) below the glassy-zeolitic boundary, a stratigraphic transition zone that is about 10 m (33 ft) thick. Levy (1991) states (p. 482) that

> .. the vitric-zeolitic transition in the central-eastern part of Yucca Mountain probably marks the highest SWL established at the mountain during the last 12.8 myr. The SWL remained at its highest position no more than 1.2 myr. Subsequent water levels may have existed at higher elevations than the present SWL (about 120 m below the zeolitic transition in [well] G-4), but have not been any higher than 16 m below the zeolitic transition and perhaps no higher than 59 m below the transition (adding the 43-m thickness of the devitrified zone in H-6 to the 16-m depth of glassy tuff below the transition).

Levy also stated that, compared to mineralogic changes, features such as paleospring mounds are more direct indicators of former hydraulic conditions because they were formed by aqueous transport and deposition. Levy (1991) concluded that the highest groundwater levels were reached and receded downward 11.6 to 12.8 million years ago, and since that time the water level at YM has probably not risen more than about 60 m (200 ft) above present levels. DOE (1992, p. 2-66) cites Levy's (1991, p. 2-66) estimate that the water table has probably not been higher than 60 m (200 ft) above its present level for prolonged periods. However, Levy's work occurred before more recent studies of the Lathrop Wells Diatomites that suggest higher potential rises of the water table.

- Other geochemical evidence

Quade and Cerling (1990, p. 1549), writing in the journal Science, reached the following conclusions:

> Comparison of the stable carbon and oxygen isotopic compositions of the fracture carbonates with those of modern soil carbonates in the area shows that the fracture carbonates are pedogenic in origin and that they likely formed in the presence of vegetation and rainfall typical of a glacial climate. Their isotopic composition differs markedly from that of carbonate associated with nearby springs. The regional water table therefore remained below the level of Trench 14 [located on the eastern side of YM] during the time that the carbonates and silica precipitated, a period probably covering parts of at least the last 300,000 years.

- Presence of a perennial paleodischarge site in Fortymile Wash

To the northeast of YM there is paleoecological evidence of higher recharge and precipitation in the past. A perennial discharge site existed in Fortymile Canyon about 50 kyr ago. Spaulding (1994) and others have studied ancient packrat nests, or middens, in the region. Modern-day packrats have a foraging radius of < 50 m (164 ft), and materials preserved in the fossilized nests of their ancient ancestors can help identify local assemblages of prehistoric plants.

Spaulding and others (1994) found a set of ancient middens in northern Fortymile Canyon. They occur near the UE-29 boreholes about 12 km (7.4 mi) northeast of YM. Most of these ancient middens have carbon isotope ages of 13 to 22 kyr and contain no evidence of water-loving plants. But one midden was much more ancient, about 50 kyr or older (at the limit of radiocarbon dating), and contained remains of willows (*Salix*), knotweed (*Polygonum*), and wild rose (*Rosa*). These plants must have constantly damp soil or proximity to the water table to survive and reproduce (see the description of indicator plant species described by the National Research Council, 1992, p. 208-211). Spaulding (1994) refers to this older midden site as FMC-7, or Fortymile Canyon sample #7. It is on

water level (SWL) is presently about 100 m (330 ft) below the glassy-zeolitic boundary, a stratigraphic transition zone that is about 10 m (33 ft) thick. Levy (1991) states (p. 482) that

> ...the vitric-zeolitic transition in the central-eastern part of Yucca Mountain probably marks the highest SWL established at the mountain during the last 12.8 myr. The SWL remained at its highest position no more than 1.2 myr. Subsequent water levels may have existed at higher elevations than the present SWL (about 120 m below the zeolitic transition in [well] G-4), but have not been any higher than 16 m below the zeolitic transition and perhaps no higher than 59 m below the transition (adding the 43-m thickness of the devitrified zone in H-6 to the 16-m depth of glassy tuff below the transition).

Levy also stated that, compared to mineralogic changes, features such as paleospring mounds are more direct indicators of former hydraulic conditions because they were formed by aqueous transport and deposition. Levy (1991) concluded that the highest groundwater levels were reached and receded downward 11.6 to 12.8 million years ago, and since that time the water level at YM has probably not risen more than about 60 m (200 ft) above present levels. DOE (1992, p. 2-66) cites Levy's (1991, p. 2-66) estimate that the water table has probably not been higher than 60 m (200 ft) above its present level for prolonged periods. However, Levy's work occurred before more recent studies of the Lathrop Wells Diatomites that suggest higher potential rises of the water table.

- Other geochemical evidence

Quade and Cerling (1990, p. 1549), writing in the journal Science, reached the following conclusions:

> Comparison of the stable carbon and oxygen isotopic compositions of the fracture carbonates with those of modern soil carbonates in the area shows that the fracture carbonates are pedogenic in origin and that they likely formed in the presence of vegetation and rainfall typical of a glacial climate. Their isotopic composition differs markedly from that of carbonate associated with nearby springs. The regional water table therefore remained below the level of Trench 14 [located on the eastern side of YM] during the time that the carbonates and silica precipitated, a period probably covering parts of at least the last 300,000 years.

- Presence of a perennial paleodischarge site in Fortymile Wash

To the northeast of YM there is paleoecological evidence of higher recharge and precipitation in the past. A perennial discharge site existed in Fortymile Canyon about 50 kyr ago. Spaulding (1994) and others have studied ancient packrat nests, or middens, in the region. Modern-day packrats have a foraging radius of < 50 m (164 ft), and materials preserved in the fossilized nests of their ancient ancestors can help identify local assemblages of prehistoric plants.

Spaulding and others (1994) found a set of ancient middens in northern Fortymile Canyon. They occur near the U[illegible]-29 boreholes about 12 km (7.4 mi) northeast of YM. Most of these ancient middens have carbon isotope ages of 13 to 22 kyr and contain no evidence of water-loving plants. But one midden was much more ancient, about 50 kyr or older (at the limit of radiocarbon dating), and contained remains of willows (*Salix*), knotweed (*Polygonum*), and wild rose (*Rosa*). These plants must have constantly damp soil or proximity to the water table to survive and reproduce (see the description of indicator plant species described by the National Research Council, 1992, p. 208-211). Spaulding (1994) refers to this oldest midden site as FMC-7, or Fortymile Canyon sample #7. It is on

the eastern flank of Fortymile Wash about 60 m (200 ft) above the Canyon floor. The site is about 460 m (1510 ft) north of wellsite UE-29. At this location the water table is presently more than 400 m (1310 ft) higher than at YM. The water table at UE-29 is shallow, only 27 m (88 ft) deep, because this area is north of the so-called zone of high hydraulic gradient. At this canyon site a modest water table rise of less than 30 m (100 ft) could generate spring flow in Fortymile Wash. Based on the location of FMC-7, inferred erosion rates, present-day groundwater elevations, and fossil plants, Spaulding (1994) concluded that the water table was 75 to 95 m (246 to 312 ft) higher during the period from 73 kyr to 47 kyr B.P.

- Inferences based on the extent of paleolakes

Mifflin (1990) described the regional hydrologic effects of past pluvial climates in the YM region. Based on the extent of former pluvial lakes in the Great Basin, effective moisture (runoff and recharge) was elevated by about an order of magnitude over modern conditions, and regional water tables rose as much as several hundred feet.

- Timing in changes of potentiometric levels of the carbonate aquifer at Devils Hole

Winograd and Szabo (1988, p. 151-152) stated that "...the continuing uplift of the Sierra Nevada...and Transverse Ranges, and lowering of Death Valley...relative to surrounding regions, should result in a continued progressive decline of the regional water table in the next 100,000 to 1 million yr (and beyond?) in response to increasing aridity and to lowering of ground-water base level." However, Winograd and Szabo (1988, p. 151) noted that their suggestion of a long-term lowering of the regional water table does not preclude relatively rapid fluctuations in response to pluvial climates of the Pleistocene, as indicated by data from Devils Hole in the Amargosa Desert.

There is solid evidence from Devils Hole of a Wisconsin-age rise of potentiometric levels in the Paleozoic carbonate aquifer. Szabo, et al. (1994) reported a record of water-table fluctuations in Brown's Room at Devils Hole. Their data are extensive enough to suggest that the water table may have been more than 4 m (13 ft) higher than present-day levels throughout the Wisconsin. They specifically conclude that the paleo-water table stayed more than 5 m (16 ft) above present levels between about 116 kyr and 53 kyr ago, that the level fluctuated between about +5 m (16 ft) and +9 m (+30 ft) from 44 kyr to 20 kyr ago, and then declined rapidly from about +9 m (+30 ft) to its present level during the last 20 kyr. Szabo, et al. (1994) considered climate change to be the main cause of the water-table fluctuations over the last 100 kyr.

The water-level changes at Devils Hole relate only to the Paleozoic carbonate aquifer within the Ash Meadows groundwater basin and cannot be used to determine water levels in other aquifers. But groundwater levels in this regional aquifer must exert a major control on water levels in overlying tuff and valley-fill aquifers. Because the Ash Meadows groundwater basin is very large, Szabo, et al. (1994, p. 68) suggested that the data from Brown's Room "may record the timing of regional hydrologic changes that occurred in the southern Great Basin." The staff agrees with this, and believes that the timing of significant water-level fluctuations at YM should correlate reasonably well with those at Devils Hole. This is reasonable even though YM and Devils Hole may exist in different subbasins of the regional Death Valley groundwater flow system (Laczniak, et al., 1996). The fact that the water table at YM may have risen [illegible] times higher than at Devils Hole would not be unusual, because of the proximity of YM to areas of higher elevation where recharge would have been

enhanced. Higher transmissivities in the Paleozoic carbonate aquifer would also result in smaller fluctuations of the potentiometric surface at Devils Hole.

The staff's views about water-table rise are strongly influenced by the fact that paleoclimatic indicators throughout the Great Basin are reasonably consistent. For example, the Wisconsin-age high stands measured at Devils Hole are consistent with a long-duration high stand of Searles Lake, and with the reported dates of paleospring flow at the Lathrop Wells Diatomites. Likewise, there is reasonable correlation between proxy paleoclimatic records for Searles Lake, Las Vegas Valley, Grand Canyon travertine, south-central Nevada plant records, and Brown's Room at Devils Hole (Szabo, et al., 1994). A high stand of Lake Manley in Death Valley (Li, et al., 1996, Fig. 16) also coincides with the general timing of high stands of Searles, Lahontan, and Bonneville Lakes, and with a high groundwater stand in Devils Hole. Long-term records of paleolake levels in particular show important differences that must be related to local hydrologic conditions. For example, Lake Manly was the last in a chain of "overflow" lakes, and it therefore did not always receive a substantial surface-water influx.

Szabo, et al. (1994) and other investigators have noted inconsistencies in the paleoclimatic data that have yet to be explained. But in general, except for the temperature proxy data from Devils Hole, the paleoclimatic data are discontinuous and only provide "snapshots" of prevailing conditions at various sites and times. The well-dated, relatively continuous 500-kyr record of paleotemperatures from Devils Hole (Winograd, et al., 1992) is one of the best paleoclimate records in existence and has been used to link past climate change in the Great Basin to changes elsewhere. The staff has determined that this and other paleoclimate records could reasonably be used to estimate the likely range of future climate variability at YM.

- Inferences from hydrologic modeling of the saturated zone flow system

Czarnecki (1985) used a finite-element model to simulate the effects of a future increase in precipitation and recharge on water levels. He concluded that a doubling of precipitation could lead to a 15-fold increase in recharge and a water-table rise of 130 m (426 ft) beneath YM. Although Czarnecki's (1985) work suggests that water-table rises greater than 120 m (394 ft) are not impossible, the preponderance of field evidence suggests that the water table has not risen more than 120 m (394 ft) above present levels for extended periods since the deposition of the volcanic tuffs. The Paintbrush and Calico Hills tuffs were deposited more than 10 million years ago (DOE, 1988a, p. 1-56).

Ahola and Sagar (1992) developed a regional flow model and analyzed various phenomena that could influence the regional water table. They estimated that a water-table rise of about 75-100 m (246-330 ft) could occur in response to a 10-fold increase in groundwater recharge. This particular analysis included a zone of enhanced recharge that represented Fortymile Wash. They concluded that the water table near Yucca Mountain is relatively sensitive to variations in recharge along this wash.

The following table briefly summarizes the degree of former water-table rise that has been estimated by various workers:

Forester, et al., 1996	YM and southern Nevada	Up to 100-120 m (330-394 ft) at various times during the last two glacial cycles.
Paces, et al., 1996	Lathrop Wells Diatomites, SW of YM	100-120 m (330-394 ft) (data suggest elevated regional water tables as much as 60-80 percent of the last 700 kyr).
Quade, Mifflin, et al., 1995; Quade, 1994	Lathrop Wells Diatomites, 20 km (12 mi) SW of YM	< 115 m (377 ft)
Szabo, et al., 1994	Brown's Room, Devils Hole (Ash Meadows - Paleozoic carbonate aquifer)	up to +9 m (30 ft)
Spaulding, 1994	Fortymile Canyon NE of YM (FMC-7 packrat midden site)	75-95 m (246-312 ft)
Paces, et al., 1993	Lathrop Wells Diatomites, SW of YM	80-115 m (262-377 ft)
Marshall, et al., 1993	YM boreholes	< 85 m (280 ft)
Ahola & Sagar, 1992	YM (regional groundwater model)	75-100 m 246-330 ft)
Levy, 1991	YM boreholes	< 60 m (200 ft)
Mifflin, 1990	YM region	Less than 100 m (up to several hundred feet in the YM region).
Bish & Vaniman, 1985; Bish & Chipera, 1989	YM boreholes	< 100 m (330 ft) (inferred by NRC staff)
Czarnecki, 1985	YM (regional groundwater model)	< 130 m (426 ft)

This status report has focused on the effects of past climate change on the regional water table and what may reasonably be expected in the future. Wisconsin-age water-table rise occurred under natural conditions uninfluenced by humans. Future human activities will undoubtedly have a major influence on the regional flow system. The most recent water-supply forecast for southern Nye County (Nevada) is presented by Buqo (1997). Despite access to Lake Mead, the city of Las Vegas is experiencing water supply problems. Las Vegas continues to be one of the fastest growing cities in the United States. WRMI (1992) reported that, even if responsible water conservation is imposed, all available water resources would be fully used by the year 2006, and after that time additional water sources would be needed. Groundwater is the most likely new source of water supplies for Las Vegas Valley, and given the very low rates of groundwater recharge in southern Nevada it will be

necessary to adopt a regional approach to groundwater development to prevent local potentiometric drawdowns from becoming extreme. This means that a large region will have to be developed for groundwater supplies, including areas to the north and west. The YM site and the Amargosa Desert occur in this extended region northwest of Las Vegas Valley.

Tectonic and volcanic events could also possibly influence the regional water table. These mechanisms, along with future human activities, will be discussed in some detail in an IRSR dedicated to saturated zone topics. DOE may consider that human activities could cause future water-table rise to be less than occurred in the past. However, DOE's safety analysis should assume that the climate-related component of future water-table rise will be at least as great as has occurred in the past. It is DOE's responsibility to reasonably demonstrate that future water-table conditions are consistent with postulated dose scenarios, which may include groundwater pumping, irrigation, and other activities.

5.0 STATUS OF SUBISSUE RESOLUTION AT THE STAFF LEVEL

The staff has identified no open items solely related to future climate change and associated hydrologic effects. Accordingly, the staff has no further questions at this time on methods to estimate future climate variability, or regarding methods to estimate hydrologic effects of climate change (e.g., future precipitation and water-table rise).

6.0 REFERENCES

Ahola, M. and B. Sagar, "Regional Groundwater Modeling of the Saturated Zone in the Vicinity of Yucca Mountain, Nevada: Iterative Performance Assessment - Phase 2," NUREG/CR-5890, October, 1992.

Barron, E. J., "Global Change Researchers Assess Projections of Climate Change," Eos Trans. AGU, Vol. 76, No. 18, May 2, 1995, pp. 185-190.

Bish, D. L. and S. J. Chipera, "Revised Mineralogic Summary of Yucca Mountain, Nevada," LA-11497-MS, Los Alamos National Laboratory, Los Alamos, New Mexico, 1989.

Bish, D. L. and D. T. Vaniman, "Mineralogic Summary of Yucca Mountain, Nevada," LA-10543-MS, Los Alamos National Laboratory, Los Alamos, New Mexico, 1985.

Bolin, B., "The Use of Scenarios in the Greenhouse Debate," Eos Trans. AGU, Vol. 73, No. 30, July 28, 1992, pp. 324-325.

Brigham-Grette, J. and D. M. Hopkins, "Emergent Marine Record and Paleoclimate of the Last Interglaciation along the Northwest Alaskan Coast," Quaternary Research, Vol. 43, No. 2, 1995, pp. 159-173.

Broecker, W. S., "Chaotic Climate," Scientific American, November 1995, pp. 62-68.

Broecker, W. S., "Will Our Ride into the Greenhouse Future be a Smooth One?" GSA Today, Vol. 7, No. 5, May 1997, pp. 1-7.

Buqo, T. S., "Baseline Water Supply and Demand Evaluation of Southern Nye County, Nevada," prepared for Nye County Nuclear Waste Repository Office (undated: received at NRC 5/97), 45 pp.

Carlowicz, M., "Global Warming Picture Remains Clouded," Editorial in Eos Trans. AGU, Vol. 76, No. 45, November 7, 1995, p. 452.

Chao, B. F., "'Concrete' Testimony to Milankovitch Cycle in Earth's Changing Obliquity," Eos Trans. AGU, Vol. 77, No. 44, October 29, 1996, p. 433.

CNWRA (Center for Nuclear Waste Regulatory Analyses), "NRC High-Level Radioactive Waste Research at CNWRA, July - December, 1993," CNWRA 93-02S, February 1994.

CNWRA (Center for Nuclear Waste Regulatory Analyses), "NRC High-Level Radioactive Waste Program Annual Progress Report, Fiscal Year 1996," NUREG/CR-6513, No. 1, November 1996.

Coleman, N., N. Eisenberg, and D. Brooks, "Regulatory Perspective on Future Climates at Yucca Mountain," in Proceedings of the Seventh Annual International Conference on High Level Radioactive Waste Management, Las Vegas, Nevada, April 29-May 3, 1996.

Cronin, T. M. and H. J. Dowsett, "PRISM - Warm climates of the Pliocene," Geotimes, November, 1993, pp. 17-19.

Crowley, T. J., "Remembrance of Things Past: Greenhouse Lessons from the Geologic Record," by Thomas J. Crowley of the Dept. of Oceanography, Texas A & M University; this 1996 document is available at the following internet web site: http://www.pbs.org/wgbh/pages/nova/ice/resources.html.

Czarnecki, J. B., "Simulated Effects of Increased Recharge on the Ground-Water Flow System of Yucca Mountain and Vicinity, Nevada-California," U. S. Geological Survey, Water Resources Investigations Report 84-4344, 1985, 33 pp.

Dansgaard, W., S. J. Johnsen, et al., "Evidence for General Instability of Past Climate from a 250-kyr Ice-Core Record," Nature, Vol. 364, July 1993, pp. 218-220.

DeWispelare, A. R., L. T. Herren, M. P. Miklas, and R. T. Clemen, "Expert Elicitation of Future Climate in the Yucca Mountain Vicinity," CNWRA 93-016, Prepared for the U.S. Nuclear Regulatory Commission by the Center for Nuclear Waste Regulatory Analyses, San Antonio, Texas, 1993.

DOE (U.S. Department of Energy), "Site Characterization Plan - Yucca Mountain Site, Nevada Research and Development Area, Nevada," DOE/RW-0199, Office of Civilian Radioactive Waste Management, Vol. I, Part A, December 1988a.

DOE (U.S. Department of Energy), "Site Characterization Plan - Yucca Mountain Site, Nevada Research and Development Area, Nevada," DOE/RW-0199, Office of Civilian Radioactive Waste Management, Vol. II, Part A, December 1988b.

DOE (U.S. Department of Energy), "Report of Early Site Suitability Evaluation of the Potential Repository Site at Yucca Mountain, Nevada," SAIC-91/8000, Prepared by Science Applications International Corp. for U.S. Dept. of Energy, January 1992.

DOE (U.S. Department of Energy), "Total System Performance Assessment - 1995: An Evaluation of the Potential Yucca Mountain Repository," Prepared by TRW Environmental Safety Systems, Inc. for U.S. Dept. of Energy, Office of Civilian Radioactive Waste Management, B00000000-01717-2200-00136, Rev. 01, November 1995.

DOE (U.S. Department of Energy), "[Draft] Highlights of the U.S. Department of Energy's Updated Waste Containment and Isolation Strategy for the Yucca Mountain Site," enclosure to a letter from S. J. Brocoum, U.S. Department of Energy, to M. V. Federline, U.S. Nuclear Regulatory Commission, dated July 19, 1996.

Edwards, R. L., H. Cheng, M. T. Murrell, and S. J. Goldstein, "Protactinium-231 Dating of Carbonates by Thermal Ionization Mass Spectrometry: Implications for Quaternary Climate Change," Science, Vol. 276, May 2, 1997, pp. 782-786.

EPRI (Electric Power Research Institute), "Demonstration of a Risk-Based Approach to High-Level Waste Repository Evaluation," EPRI NP-7057, Palo Alto, CA, 1990.

EPRI (Electric Power Research Institute), "Demonstration of a Risk-Based Approach to High-Level Waste Repository Evaluation: Phase 2," EPRI TR-100384, Palo Alto, CA, 1992.

Feder, T., "Attacks on IPCC Report Heat Controversy Over Global Warming," Physics Today, August 1996, p. 55-57.

Forester, R. M., "Late Glacial to Modern Climate Near Yucca Mountain Nevada," in Proceedings of the Fifth Annual International Conference on High Level Radioactive Waste Management, Las Vegas, Nevada, May 22-26, 1994, Vol. 4, pp. 2750-2754.

Forester, R. M., "Paleoclimate Records - Implications for Future Climate Change," Presentation to U.S. Nuclear Waste Technical Review board, Denver, Colorado, July 9-10, 1996, 18 pp.

Forester, R. M. and A. J. Smith, "Late Glacial Climate Estimates for Southern Nevada - The Ostracode Fossil Record," in Proceedings of the Fifth Annual International Conference on High Level Radioactive Waste Management, Las Vegas, Nevada, May 22-26, 1994, Vol. 4, pp. 2553-2561.

Forester, R. M., et al., "Synthesis of Quaternary Response of the Yucca Mountain Unsaturated and Saturated Zone Hydrology to Climate Change," 1996 Milestone Report 3GCA102M, U.S. Geological Survey, Yucca Mountain Project Branch, 1996, 110 pp.

Gates, W. L., "AMIP: The Atmospheric Model Intercomparison Project," Bulletin of the American Meteorological Society, Vol. 73, 1992, pp. 1962-1970.

Harvey, L. D. D., "Comments on the Greenhouse Debate," Eos Tran. AGU, Vol. 73, No. 30, July 28, 1992, p. 325.

Hays, J. D., J. Imbrie, and N. J. Shackleton, "Variations in the Earth's Orbit: Pacemaker of the Ice Ages," Science, Vol. 194, No. 4270, December 10, 1976, pp. 1121-1132.

Karl, T. R., N. Nicholls, and J. Gregory, "The Coming Climate," Scientific American, May 1997, pp. 78-83.

Kerr, R. A., "A New Dawn for Sun-Climate Links?" Science, Vol. 271, March 8, 1996, pp. 1360-1361.

Kerr, R. A., "Second Clock Supports Orbital Pacing of the Ice Ages," Science, Vol. 276, May 2, 1997, pp. 680-681.

Kominz, M. A. and N. G. Pisias, "Pleistocene Climate: Deterministic or Stochastic?" Science, Vol. 204, April 1979, pp. 171-173.

Krauskopf, K. B., "Introduction to Geochemistry," McGraw-Hill Book Company, New York, New York, 1967.

Lamb, H. H., "Climate - Present, Past and Future, Vol. 1, Fundamentals and Climate Now," Barnes and Noble, 1972.

Lamb, H. H., "Climate - Present, Past and Future, Vol. 2, Climatic History and the Future," Barnes & Noble, New York, 1977.

Laczniak, R. J., J. C. Cole, D. A. Sawyer, and D. A. Trudeau, "Summary of Hydrogeologic Controls on Ground-Water Flow at the Nevada Test Site, Nye County, Nevada," U.S. Geological Survey Water-Resources Investigations Report 96-4109, 1996, 59 pp.

Lean, J. and D. Rind, "Solar Variability: Implications for Global Change," Eos Trans. AGU, Vol. 75, No. 1, January 4, 1994, pp. 1-7.

Levy, S., "Mineralogic Alteration History and Paleohydrology at Yucca Mountain, Nevada," in Proceedings of the Second Annual International Conference on High-Level Radioactive Waste Management, Vol. 1, Las Vegas, Nevada, April 28-May 3, 1991, pp. 477-485.

Li, J., et al., "A 100 ka Record of Water Tables and Paleoclimates from Salt Cores, Death Valley, California," Palaeogeography, Palaeoclimatology, Palaeoecology, Vol. 123, 1996, pp. 179-203.

Marshall, B. D., Z. E. Peterman, and J. S. Stuckless, "Strontium Isotopic Evidence for a Higher Water Table at Yucca Mountain," in Proceedings of the Fourth Annual International Conference on High-Level Radioactive Waste Management, Vol. 2, Las Vegas, Nevada, April 26-30, 1993, pp. 1948-1952.

Mifflin, M. D., "Effects of Past Pluvial Climates on Regional Hydrology," Briefing to the National Academy of Sciences Panel on Coupled Hydrologic/Tectonic/Hydrothermal Systems at Yucca Mountain, Menlo Park, California, May 30, 1990, 20 pp.

Mifflin, M. D. and M. M. Wheat, "Pluvial Lakes and Estimated Pluvial Climates of Nevada," Nevada Bureau of Mines and Geology, Bulletin 94, 1979, 57 pp.

Miller, G. H. and A. de Vernal, "Will Greenhouse Warming Lead to Northern Hemisphere Ice-Sheet Growth?" Nature, Vol. 355, January 16, 1992, pp. 244-246.

Morrison, R. B., "Quaternary and Pliocene Geology of Tecopa Valley, California: A Multi-Million-Year Stratigraphic, Tectonic, Climatic, Erosion, and Hydrogeologic Record and its Relevance to the Proposed Nuclear-Waste Repository at Yucca Mountain, Nevada," draft in review for publication by the Geological Society of America; distributed to those who attended the Summer 1996 Meeting of the U.S. Nuclear Waste Technical Review Board, in Denver, CO, 76 pp.

Muhs, D. R., G. L. Kennedy, and T. K. Rockwell, "Uranium-Series Ages of Marine Terrace Corals from the Pacific Coast of North America and Implications for Last-Interglacial Sea Level History," Quaternary Research, Vol. 42, 1994, pp. 72-87.

National Research Council, "Ground Water at Yucca Mountain - How High Can It Rise?" Final report of the Panel on Coupled Hydrologic/Tectonic/Hydrothermal Systems at Yucca Mountain, Board on Radioactive Waste Management, National Academy Press, Washington, DC, 1992.

National Research Council, "Technical Bases for Yucca Mountain Standards," Committee on Technical Bases for Yucca Mountain Standards, Board on Radioactive Waste Management, Commission on Geosciences, Environment, and Resources, National Research Council, National Academy Press, Washington, DC, 1995.

Neumann, A. C. and P. J Hearty, "Rapid Sea-Level Changes at the Close of the Last Interglacial (Substage 5e) Recorded in Bahamian Island Geology," Geology, Vol. 24, No. 9, September 1996, pp. 775-778.

NRC (U.S. Nuclear Regulatory Commission), "Initial Demonstration of the NRC's Capability to Conduct a Performance Assessment for a High-Level Waste Repository," NUREG-1327, Washington, D.C., 1992.

NRC (U.S. Nuclear Regulatory Commission), "NRC Iterative Performance Assessment Phase 2 - Development of Capabilities for Review of a Performance Assessment for a High-Level Waste Repository," NUREG-1464, October 1995.

NRC (U.S. Nuclear Regulatory Commission), "Branch Technical Position on the Use of Expert Elicitation in the High-Level Radioactive Waste Program," NUREG-1563, November 1996a.

NRC, (U.S. Nuclear Regulatory Commission), "Total System Performance Assessment 1995 Audit Review," Letter and attachment dated November 5, 1996 to R. Milner, U. S. Department of Energy, from J. Austin, U. S. Nuclear Regulatory Commission, 1996b.

NWTRB (U.S. Nuclear Waste Technical Review Board), "Resolving Difficult Issues - Future Climates," Chapter 3 in NWTRB Report to the U.S. Congress and the Secretary of Energy, January to December, 1993, pp. 51-59.

Oeschger, H., "Urgency of CO_2 Emission Control," Eos Tran. AGU, Vol. 73, No. 30, July 28, 1992, pp. 321 and 324.

Oviatt, C. G., "Lake Bonneville Fluctuations and Global Climate Change," Geology, Vol. 25, No. 2, February 1997, pp. 155-158.

Paces, J. B., E. M. Taylor, and C. Bush, "Late Quaternary History and Uranium Isotopic Compositions of Ground Water Discharge Deposits, Crater Flat, Nevada," in Proceedings of the Fourth Annual International Conference on High-Level Radioactive Waste Management, Vol. 2: American Nuclear Society, Las Vegas, Nevada, April 1993, pp. 1573-1580.

Paces, J. B., et al., "Synthesis of Ground-Water Discharge Deposits Near Yucca Mountain," Report 3GQH671M, U. S. Geological Survey, Final Version August 24, 1996, 75 pp.

PNL (Pacific Northwest Laboratory), "Preliminary Total-System Analysis of a Potential High-Level Nuclear Waste Repository at Yucca Mountain," PNL-8444, Richland, WA, 1993.

Quade, J., "Spring Deposits and Late Pleistocene Ground-Water Levels in Southern Nevada," in Proceedings of the Fifth Annual International Conference on High-Level Radioactive Waste Management, Vol. 4: American Nuclear Society, Las Vegas, Nevada, May 1994, pp. 2530-2537.

Quade, J. and T. E. Cerling, "Stable Isotopic Evidence for a Pedogenic Origin of Carbonates in Trench 14 near Yucca Mountain, Nevada," Science, Vol. 250, Dec. 14, 1990, pp. 1549-1552.

Quade, J., M. D. Mifflin, et al., "Fossil Spring Deposits in the Southern Great Basin and Their Implications for Changes in Water-Table Levels near Yucca Mountain, Nevada, During Quaternary Time," Geological Society of America Bulletin, Vol. 107, No. 2, Feb. 1995, pp. 213-230.

Raymo, M. E. and W. F. Ruddiman, "Tectonic Forcing of Late Cenozoic Climate," Nature, Vol. 359, September 1992, pp. 117-122.

Risbey, J. S., M. D. Handel, and P. H. Stone, "Should We Delay Responses to the Greenhouse Issue?" Eos Trans. AGU, Vol. 72, No. 53, 1991a, pp. 593-594.

Risbey, J. S., M. D. Handel, and P. H. Stone, "Do We Know What Difference A Delay Makes?" Eos Trans. AGU, Vol. 72, No. 53, 1991b, pp. 596-597.

SNL (Sandia National Laboratories), "TSPA 1991: An Initial Total-System Performance Assessment for Yucca Mountain," SAND91-2795, Albuquerque, NM. 1992.

Sabine, C. L., D. W. Wallace, and F. J. Millero, "Survey of CO_2 in the Oceans Reveals Clues about Global Carbon Cycle," Eos Trans. AGU, Vol. 78, No. 5, February 4, 1997, pp. 49-55.

Schlesinger, M. E. and X. Jiang, "Revised Projection of Future Greenhouse Warming," Nature, Vol. 350, 1991a, p. 219.

Schlesinger, M. E. and X. Jiang, "A Phased-In Approach to Greenhouse-Gas-Induced Climatic Change," Eos Trans. AGU, Vol. 72, No. 53, 1991b, pp. 594-596.

Schlesinger, M. E. and X. Jiang, "Climatic Responses to Increasing Greenhouse Gases," Eos Trans. AGU, Vol. 72, No. 53, 1991c, pp. 597-598.

Schlesinger, M. E., "Reply - Greenhouse Economics and Policy," Eos Tran. AGU, Vol. 73, No. 30, July 28, 1992, pp. 325-327.

Spaulding, W. G., "Vegetation and Climates of the Last 45,000 Years in the Vicinity of the Nevada Test Site, South-Central Nevada," U.S. Geological Survey Professional Paper 1329, 1985, 83 pp.

Spaulding, W. G., "Environments of the Last 50,000 Years in the Vicinity of Yucca Mountain, Central-Southern Nevada," in Proceedings of the First Annual International Conference on High-Level Radioactive Waste Management, Vol. 2: American Nuclear Society, Las Vegas, Nevada, April 8-12, 1990, pp. 1251-1258.

Spaulding, W. G., "Paleohydrologic Investigations in the Vicinity of Yucca Mountain: Late Quaternary Paleobotanical and Palynological Records," NWPO-TR-022-94, State of Nevada, Agency for Nuclear Projects, Nuclear Waste Project, October 5, 1994.

Spaulding, W. G., "Climate Change and Ground Water Conditions in the Vicinity of Yucca Mountain - General Considerations," Summary review of DOE's Technical Basis Report (MP/TBR-0001), Dames and Moore, Las Vegas, NV, 1995, 6 pp.

Stone, P. H. and J. S. Risbey, "On the Limitations of General Circulation Climate Models," Geophysical Research Letters, Vol. 17, No. 12, 1990, pp. 2173-2176.

Stuckless, J. S., "Status of Groundwater and Paleo-Groundwater Dating at the Proposed Yucca Mountain Site," presentation to NRC's Advisory Committee for Nuclear Wastes, Bethesda, MD, October 21, 1994.

Szabo, B. J., et al., "Paleoclimatic Inferences from a 120,000-Yr Calcite Record of Water-Table Fluctuation in Brown's Room of Devils Hole, Nevada," Quaternary Research, Vol. 41, 1994, pp. 59-69.

Timbal, B., et al., "Integrating Land-Surface and Atmospheric Models," Eos Trans. AGU, Vol. 78, No. 17, April 29, 1997, pp. 173-181.

USGS (U. S. Geological Survey), "The National Atlas of the United States of America," U. S. Department of Interior, Washington, DC, 1970.

Vernekar, A. D., "Research on the Theory of Climate, Vol. 2: Long-Period Global Variations of Incoming Solar Radiation," Hartford, CN, Travelers Research Center, Final Report of the U.S. Dept. of Commerce, Environmental Science Services Administration, Contract No. E22-137-67(N), 1968.

Vernekar, A. D., "Long-Period Global Variations of Incoming Solar Radiation," Met. Monogs, Vol. 12, No. 34, Boston, MS, American Meteorological Society, 1972.

Wigand, P. E., M. L. Hemphill, and S. Patra, "Late Holocene climate Derived from Vegetation History and Plant Cellulose Stable Isotope Records from the Great Basin of Western North America," in Proceedings of the Fifth Annual International Conference on High Level Radioactive Waste Management, Las Vegas, Nevada, May 22-26, 1994, Vol. 4, pp. 2574-252583.

Wigley, T. M. L., "Could Reducing Fossil-Fuel Emissions Cause Global Warming?" Nature, Vol. 349, February 1991, pp. 503-506.

Wigley, T. M. L. and S. C. B. Raper, "Climatic Change Due to Solar Irradiance Changes," Geophysical Research Letters, Vol. 17, No. 12, Nov. 1990, pp. 2169-2172.

Winograd, I. J., et al., "Continuous 500,000-Year Climate Record from Vein Calcite in Devils Hole, Nevada," Science, Vol. 258, Oct. 9, 1992, pp. 255-260.

Winograd, I. J. and B. J. Szabo, "Water Table Decline in the South Central Great Basin during the Quaternary Period: Implications for Toxic Waste Disposal," in M.D. Carr and J.C. Young (eds.) "Geologic and Hydrologic Investigations of a Potential Nuclear Waste Disposal Site at Yucca Mountain, Southern Nevada," U. S. Geological Survey Bulletin 1790, 1988, pp. 147-152.

Winograd, I. J., B. J. Szabo, T. B. Coplen, and A. C. Riggs "A 250,000-Year Climatic Record from Great Basin Vein Calcite: Implications for Milankovitch Theory," Science, Vol. 242, Dec. 2, 1988, pp. 1275-1280.

WRI (World Resources Institute). "World Resources: 1994-95," Report in collaboration with the United Nations Environment Programme and the United Nations Development Programme. Oxford University Press, New York.

WRMI (Water Resources Management, Inc.). "WRMI Process -- Water Supply Planning for the Las Vegas Region." WRMI, Columbia, Maryland, May 1992.

Appendix A

Draft Figure Illustrating Elements of the NRC Staff's Total System Performance Assessment

DRAFT

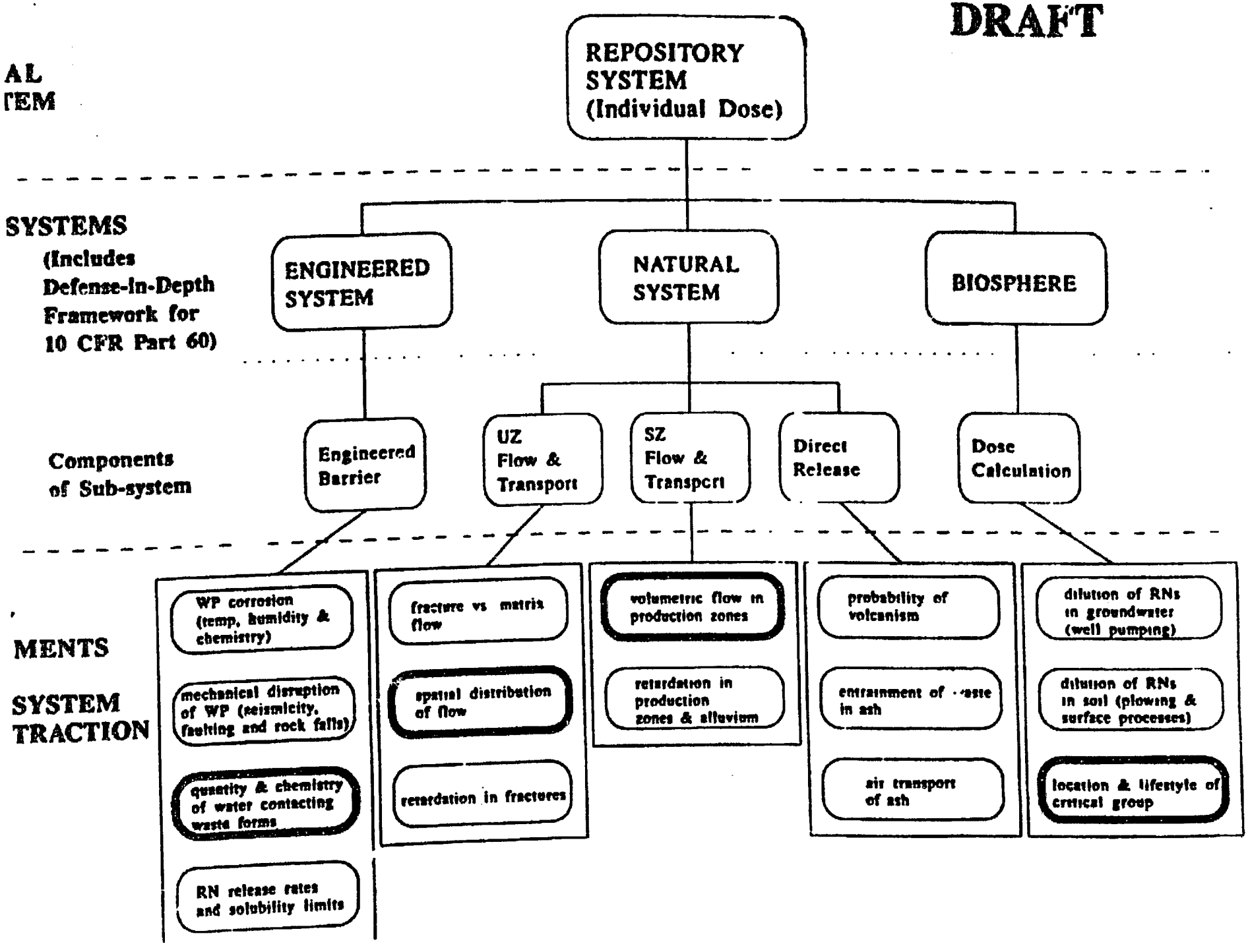
AL
TEM
REPOSITORY SYSTEM (Individual Dose)
SYSTEMS
(Includes Defense-In-Depth Framework for 10 CFR Part 60)
ENGINEERED SYSTEM
NATURAL SYSTEM
BIOSPHERE
Components of Sub-system
Engineered Barrier
UZ Flow & Transport
SZ Flow & Transport
Direct Release
Dose Calculation
MENTS
SYSTEM TRACTION
WP corrosion (temp, humidity & chemistry)
mechanical disruption of WP (seismicity, faulting and rock falls)
quantity & chemistry of water contacting waste forms
RN release rates and solubility limits
fracture vs matrix flow
spatial distribution of flow
retardation in fractures
volumetric flow in production zones
retardation in production zones & alluvium
probability of volcanism
entrainment of waste in ash
air transport of ash
dilution of RNs in groundwater (well pumping)
dilution of RNs in soil (plowing & surface processes)
location & lifestyle of critical group

ATTACHMENT F

USFIC ISSUE RESOLUTION STATUS REPORT
(Shallow Infiltration Subissue)

November 7, 1997

ISSUE RESOLUTION STATUS REPORT

KEY TECHNICAL ISSUE: UNSATURATED AND SATURATED FLOW UNDER ISOTHERMAL CONDITIONS

Division of Waste Management
Office of Nuclear Material
Safety & Safeguards
U.S. Nuclear Regulatory Commission

Revision 0

September 1997

TABLE OF CONTENTS

ACKNOWLEDGMENTS i

QUALITY OF DATA, ANALYSES, AND CODE DEVELOPMENT i

1.0 INTRODUCTION 1

2.0 ISSUE/SUBISSUE STATEMENT 2

3.0 IMPORTANCE OF SUBISSUES TO REPOSITORY PERFORMANCE 2
- 3.1 What is the likely range of future climates at Yucca Mountain (YM)? 2
- 3.2 What are the likely hydrologic effects of climate change? 3
- 3.3 What is the estimated amount and what is the spatial distribution of present-day shallow groundwater? 3
- 3.4 What is the estimated amount and what is the spatial distribution of present-day groundwater percolation through the proposed repository horizon? 5
- 3.5 What is the estimated amount and what is the spatial distribution of groundwater percolation through the proposed repository horizon during the period of repository performance? 5
- 3.6 What are the ambient flow conditions in the saturated zone? 5

4.0 REVIEW METHODS AND ACCEPTANCE CRITERIA 6
- 4.1 What is the likely range of future climates at YM? 6
- 4.2 What are the likely hydrologic effects of climate change? 6
- 4.3 What is the estimated amount and what is the spatial distribution of present-day shallow groundwater? 6
- 4.3.1 Acceptance Criteria 6
- 4.3.1 Technical Basis for Review Methods and Acceptance Criteria 6
  - Implications of Net Infiltration Characterization for Repository Performance . 8
  - Measurements and Modeling Related to Net Infiltration at YM 9
    - 1. Empirical Correlations 9
      - a. Recharge 9
      - b. Potential Evapotranspiration 10
    - 2. Estimates of Net Infiltration from Indirect Evidence 10
      - a. Fluxes Inferred from Neutron-Probe Data 10
      - b. Fluxes Inferred from Hydraulic Properties 11
      - c. Fluxes Inferred from Thermal Considerations 12
      - d. Fluxes Inferred from Natural and Anthropogenic Tracers 14
    - 3. Estimates of Net Infiltration from Water Balance Calculations 18
      - a. Precipitation Data 18
      - b. Evapotranspiration Data 19
      - c. Lateral-Moisture-Flow Data 19
      - d. Hydraulic-Property Data 20
      - e. Predictive Modeling of Net Infiltration 20
- 4.4 What is the estimated amount and what is the spatial distribution of present-day groundwater percolation through the proposed repository horizon? . . . 21

4.5 What is the estimated amount and what is the spatial distribution of groundwater percolation through the proposed repository horizon during the period of repository performance? 21
4.6 What are the ambient flow conditions in the saturated zone? 22

5.0 STATUS OF OPEN ITEMS AT THE STAFF LEVEL 22
5.1 What is the likely range of future climates at YM? 22
5.2 What are the likely hydrologic effects of climate change? 22
5.3 What is the estimated amount and what is the spatial distribution of present-day shallow groundwater? 22
5.3.1 Items Resolved at the Staff Level 22
5.4 What is the estimated amount and what is the spatial distribution of present-day groundwater percolation through the proposed repository horizon? 23
5.5 What is the estimated amount and what is the spatial distribution of groundwater percolation through the proposed repository horizon during the period of repository performance? 23
5.6 What are the ambient flow conditions in the saturated zone? 23
5.6.1 Item Resolved at the Staff Level 24
5.7 Other Technical Issues in Isothermal Hydrology 24
5.7.1 Items Resolved at the Staff Level 24

6.0 REFERENCES 26

APPENDIX A - DRAFT FIGURE ILLUSTRATING ELEMENTS OF THE NRC STAFF'S TOTAL SYSTEM PERFORMANCE ASSESSMENT

APPENDIX B - CONCEPTUAL MODEL OF INFILTRATION AT YUCCA MOUNTAIN

APPENDIX C - DOE'S UNSATURATED ZONE FLOW MODEL EXPERT ELICITATION PROJECT

APPENDIX D - OPEN KTI ITEMS UNRESOLVED AT THE STAFF LEVEL

ACKNOWLEDGMENTS

This report has been prepared jointly by staff from the NRC and the Center for Nuclear Waste Regulatory Analyses (CNWRA) Primary authors of the report are Neil Coleman (NRC), Stuart Stothoff (CNWRA), and William Murphy (CNWRA). The authors offer special thanks to Budhi Sagar (CNWRA), Gordon Wittmeyer (CNWRA), and David Brooks (NRC) for their excellent reviews. The report greatly benefitted from insights contributed by consultants David Groeneveld, Dani Or, and David Woolhiser.

QUALITY OF DATA, ANALYSES, AND CODE DEVELOPMENT

DATA: No NRC or CNWRA-generated original data are contained in this report. Sources for other data should be consulted for determining the level of quality of those data.

ANALYSES AND CODES: BREATH computational software was used to develop Figure B-2 (estimated net infiltration in the vicinity of the proposed repository footprint). BREATH is controlled under CNWRA Technical Operating Procedure-018, Development and Control of Scientific and Engineering Software. The calculations were checked as required by QAP-014, Documentation and Verification of Scientific and Engineering Calculation, and recorded in a scientific notebook.

1.0 INTRODUCTION

One of the primary objectives of the Nuclear Regulatory Commission's (NRC's) refocused prelicensing program is to focus all its activities on resolving the 10 key technical issues (KTIs) it considers to be most important to repository performance This approach is summarized in Chapter 1 of the staff's annual progress reports (e g., NUREG/CR-6513, Center for Nuclear Waste Regulatory Analyses, CNWRA, 1996). Other chapters address each of the 10 KTIs by describing the scope of the issue and subissues, path to resolution, and progress achieved during fiscal year (FY) 1996.

Consistent with 10 CFR Part 60 requirements and a 1992 agreement with the U.S. Department of Energy (DOE), staff-level issue resolution can be achieved during the prelicensing consultation period; however, such resolution at the staff level would not preclude the issue being raised and considered during the licensing proceedings. Issue resolution at the staff level during prelicensing is achieved when the staff has no further questions or comments (i.e., open items) at a point in time, regarding how the DOE program is addressing an issue. There may be some cases where resolution at the staff level may be limited to documenting a common understanding regarding differences in the NRC and the DOE points of view. Pertinent additional information could raise new questions or comments regarding a previously resolved issue.

An important step in the staff's approach to issue resolution is to provide DOE with feedback regarding issue resolution, before the viability assessment. Issue Resolution Status Reports (IRSRs) are the primary mechanism that the staff will use to provide DOE feedback on the subissues making up the KTIs. IRSRs comprise 1) acceptance criteria which will be used by the staff to review the DOE license application and prelicensing submittals, as well as indicating the basis for resolution of the subissue, and 2) the status of resolution including where the staff currently has no comments or questions as well as where it does. Feedback is also contained in the staff's annual progress report, which summarizes the significant technical work toward resolution of all KTIs during the preceding FY. Finally, open meetings and technical exchanges with DOE provide opportunities to discuss issue resolution, identify areas of agreement and disagreement, and develop plans to resolve such disagreements.

In addition to providing feedback, the IRSRs will be guidance for the staff's review of information in DOE's viability assessment. The staff also plans to use the IRSRs in the future to develop the Standard Review Plan (SRP) for the repository license application.

Each IRSR contains six sections, including this introduction in Section 1.0. Section 2.0 defines the KTI, all the related subissues, and the scope of the particular subissue that is the subject of the IRSR. Section 3.0 discusses the importance of the subissue to repository performance, including: 1) qualitative descriptions, 2) reference to a total system performance flowdown diagram, 3) results of available sensitivity analyses, and 4) relationship to DOE's Waste Containment and Isolation Strategy (i.e., the approach to its safety case). Section 4.0 provides the staff's review methods and acceptance criteria that will be used to evaluate DOE's prelicensing and licensing submittals. These acceptance criteria are guidance for the staff and indirectly for DOE as well. The staff's technical basis for its acceptance criteria will also be included to further document the rationale for the staff's decisions. Section 5.0 concludes the report with the status of resolution indicating those items resolved at the staff level or those items remaining open. These open items will be tracked by the staff and resolution will be documented in future IRSRs. Section 6.0 contains the references cited in the report.

2.0 ISSUE/SUBISSUE STATEMENT

The primary objective of this KTI is to assess all aspects of the ambient hydrogeologic regime at Yucca Mountain (YM) that have the potential to compromise the performance of the proposed repository The secondary objective of this KTI is to develop review procedures and to conduct technical investigations to assess the adequacy of DOE's characterization of key site- and regional-scale hydrogeologic processes and features that may adversely affect performance Subissues deemed important to the resolution of this KTI have been identified, and are framed as questions:

(i) What is the likely range of future climates at YM?

(ii) What are the likely hydrologic effects of climate change?

(iii) What is the estimated amount and what is the spatial distribution of present-day shallow groundwater infiltration?

(iv) What is the estimated amount and what is the spatial distribution of present-day groundwater percolation through the proposed repository horizon?

(v) What is the estimated amount and what is the spatial distribution of groundwater percolation through the proposed repository horizon during the period of repository performance?

(vi) What are the ambient flow conditions in the saturated zone?

Subissues (i) and (ii) have already been addressed in an issue resolution status report dated June 30, 1997 (NRC, 1997). This revision of the IRSR addresses subissue (iii) above, which focuses on methods to estimate present-day shallow groundwater infiltration at YM. Subissues (iv), (v), and (vi) will be treated in future IRSRs by the staff.

Prevailing meteorological conditions, along with local geologic conditions and plant communities, control the rates of infiltration, deep percolation, and groundwater seepage through a geologic repository located in an unsaturated environment. Reasonable estimates of present-day infiltration i.e., initial conditions, must be obtained so that projections can be made about future infiltration and deep percolation under conditions of climate change. This report summarizes the pertinent conclusions of numerous publications related to infiltration that are relevant to YM. Based on the extensive scientific literature, the NRC staff concludes that reasonable methods exist to bound the range of present-day shallow infiltration. Review methods and acceptance criteria are provided for reviewing DOE's evaluations of shallow infiltration, and how they will be used to assess the performance of a high-level waste (HLW) repository.

3.0 IMPORTANCE OF SUBISSUES TO REPOSITORY PERFORMANCE

3.1 What is the likely range of future climates at YM?

This information was provided in the pilot IRSR (see NRC, 1997). An EPA reference, Titus and Narayanan (1995), was omitted from the bibliography in NRC, 1997. Titus and Narayanan

(1995) is available via the internet (http //www gcrio org/EPA/sealevel/text html)

- **NRC/CNWRA Sensitivity Studies**

The range of future climates at YM is not being assessed in our sensitivity studies It is already well understood that repository performance can be significantly affected by climate change NRC (1997) describes the acceptance criteria that the staff will use to review DOE's treatment of climate change in performance assessments.

3.2 What are the likely hydrologic effects of climate change?

This information was provided in the pilot IRSR (see NRC, 1997).

- **NRC/CNWRA Sensitivity Studies**

These studies are currently underway. The sensitivity of hypothetical dose to variations in shallow groundwater infiltration will be documented in a separate report in FY98.

3.3 What is the estimated amount and what is the spatial distribution of present-day shallow groundwater infiltration?

Present-day shallow infiltration is a key hydrologic factor in the isolation of HLW within a proposed geologic repository at YM. It must be reasonably understood to provide initial conditions for projecting future hydrologic changes, because the Earth's climate could change significantly during the time that wastes will remain hazardous. Climate controls the range of precipitation, which, in part, controls the rates of infiltration, deep percolation, and groundwater flux through a geologic repository located in an unsaturated environment. Water flow through a geologic repository and its environs depends on both surface processes (precipitation, evapotranspiration, overland flow, and infiltration) and subsurface processes (deep percolation, moisture recirculation, and lateral flow). Changes in infiltration will likely induce other changes, such as regional fluctuations in the elevation of the water table. Water-table rise would reduce the thickness of the unsaturated zone barrier. Therefore, future changes in climate could alter infiltration from present-day rates and significantly influence the ability of a repository to isolate waste.

The importance of groundwater flux as the key parameter for repository performance in an unsaturated zone is well known, and has been further emphasized by DOE's most recent report (DOE, 1995) on total system performance assessment (TSPA). On page ES-30 of that report it is stated that

> ...in the overall TSPA analyses, an over-arching theme comes back again and again as being the driving factor impacting the predicted results. Simply stated, it is the amount of water present in the natural and engineered systems and the magnitude of aqueous flux through these systems that controls the overall predicted performance.... Therefore, information on...[this topic]...remains the key need to enhance the representativeness of future iterations of TSPA.

Sensitivity studies clearly showed the predominance of percolation flux in estimating cumulative radionuclide releases and peak radiation doses over a 10-kyr (1 kyr=1000 years) period (see DOE 1995, pp 10-6 and 10-7)

DOE's "Waste Containment and Isolation Strategy" (DOE, 1996, p 5) likewise states that "performance assessments have shown that seepage into the emplacement drifts is the most important determinant of the ability of the site to contain and isolate waste." The importance of infiltration as a hydrologic parameter was recognized by the staff in its Iterative Performance Assessment Phase 2. NRC (1995, p 10-4) states that "Although the flux of liquid water through the repository depends on...infiltration, hydraulic conductivity, and porosity, performance correlates most strongly to infiltration." Finally, Figure 1 (CNWRA, 1994) shows that infiltration-related matters have been important factors in recent performance assessments.

	Response to Climate Change
U S. Nuclear Regulatory Commission, Phase 1 (NRC, 1992)	• Increased Infiltration • Water-Table Rise
U S Nuclear Regulatory Commission, Phase 2 (NRC, 1995a)	• Increased Infiltration • Water-Table Rise
Sandia National Laboratories, TSPA 1991 (SNL, 1992)	• Increased Infiltration
Pacific Northwest Laboratory (PNL, 1993)	• Increased Infiltration
Electric Power Research Institute, Phase 1 (EPRI, 1990)	• Increased Infiltration
Electric Power Research Institute, Phase 2 (EPRI, 1992)	• Increased Infiltration - Current - Greenhouse - Micropluvials • Water-Table Rise

Figure 1. Comparison of implementations of infiltration scenarios for YM (after CNWRA, 1994, p. 7-4)

The staff is developing a strategy for assessing the performance of a proposed repository at YM. As currently visualized by the staff, key elements of this strategy are defined by those elements needed to demonstrate repository performance. These elements are illustrated in draft Figure A-1 in Appendix A. Acceptance criteria for abstracting each of these elements into a demonstration of compliance are under development. Present-day shallow infiltration is an important factor in repository performance because it must be reasonably understood to provide initial conditions for projecting future changes in infiltration, deep percolation, near-field

hydrology, and transport rates in the unsaturated zone Therefore the acceptance criteria for the treatment of infiltration are subsidiary to and designed to complement the broade.-level acceptance criteria for the abstraction of the key elements

For DOE to adequately demonstrate and quantify in its TSPA the effects that present-day infiltration might have on repository performance, it must consider how these effects interplay with the other factors within and between key elements in the engineered and natural subsystems of the repository As highlighted in draft Figure A-1, present-day shallow infiltration is an important factor that needs to be abstracted into three of the key elements of the engineered and natural subsystems. (1) Quantity and Chemistry of Water Contacting Waste Forms (includes consideration of shallow infiltration and deep percolation); (2) Fracture vs Matrix Flow (includes consideration of shallow infiltration); and (3) Spatial and Temporal Distribution of Flow (includes consideration of infiltration)

- **NRC/CNWRA Sensitivity Studies**

These studies are currently underway. The sensitivity of hypothetical dose to variations in shallow groundwater infiltration will be documented in a separate report in FY98

3.4 What is the estimated amount and what is the spatial distribution of present-day groundwater percolation through the proposed repository horizon?

See Section 3 3

- **NRC/CNWRA Sensitivity Studies**

These studies are currently underway. The sensitivity of hypothetical dose to variations in shallow infiltration, deep groundwater percolation, and unsaturated zone flow parameters will be documented in a separate report in FY98

3.5 What is the estimated amount and what is the spatial distribution of groundwater percolation through the proposed repository horizon during the period of repository performance?

See Section 3 3.

- **NRC/CNWRA Sensitivity Studies**

These studies are currently underway. The sensitivity of hypothetical dose to variations in shallow infiltration, deep groundwater percolation, and unsaturated zone flow parameters will be documented in a separate report in FY98.

3.6 What are the ambient flow conditions in the saturated zone?

This subissue is important to repository performance because saturated zone characteristics will influence how future societies may use groundwater resources in the YM region. In brief, the ambient flow conditions in the saturated zone must be considered to: (1) estimate volumetric

flow in well production zones. (2) estimate transport rates in the volcanic and alluvial aquifers (3) estimate retardation of radionuclides in production zones and alluvium. (4) estimate dilution of radionuclides during well pumping. and (5) determine the location and lifestyle of a critical population group These elements are shown in draft figure A-1 (see Appendix A)

- **NRC/CNWRA Sensitivity Studies**

These studies are currently underway The sensitivity of hypothetical dose to variations in saturated zone flow parameters and groundwater pumping scenarios will be documented in a separate report in FY98.

4.0 REVIEW METHODS AND ACCEPTANCE CRITERIA

4.1 What is the likely range of future climates at YM?

Review methods, acceptance criteria, and technical bases were provided in a previous version of this IRSR (see NRC, 1997) One additional acceptance criterion should be added to Section 4.1, p. 6 of NRC, 1997, as follows

- Data were collected and documented under acceptable quality assurance (QA) procedures Analyses were developed and documented under acceptable QA procedures.

4.2 What are the likely hydrologic effects of climate change?

Review methods, acceptance criteria, and technical bases were provided in a previous version of this IRSR (see NRC, 1997). One additional acceptance criterion should be added to Section 4.2, p. 16 of NRC, 1997, as follows

- Data were collected and documented under acceptable QA procedures. Analyses were developed and documented under acceptable QA procedures.

4.3 What is the estimated amount and what is the spatial distribution of present-day shallow groundwater infiltration?

The staff's technical review of DOE's treatment of present-day shallow infiltration will be based on an evaluation of the completeness and applicability of the data and evaluations presented by DOE. It is expected that DOE will summarize or document the results of all significant infiltration-related studies that have been conducted in the YM vicinity. The staff will determine whether DOE has reasonably complied with the Acceptance Criteria in section 4.3.1 below.

4.3.1 Acceptance Criteria

- DOE has estimated shallow infiltration for use in the performance assessment (PA) of YM using mathematical models that incorporate site-specific climatic, surface, and subsurface information. DOE has provided sufficient evidence that the mathematical models were reasonably verified with site data. These data would include measured infiltration data and indirect evidence such as geochemical and geothermal data. DOE may choose to

use a vertical one-dimensional (1D) model to simulate infiltration However in that case DOE must reasonably show that the fundamental effects of heterogeneities, time-varying boundary conditions, evapotranspiration depth of soil cover, and surface-water runoff have been considered in ways that do not underestimate infiltration

- DOE has (1) appropriately considered the spatial and temporal variability (2) has analyzed infiltration at appropriate time and space scales, and (3) has tested the abstracted model against more detailed models to assure that it produces reasonable results for shallow infiltration under conditions of interest. Recent studies by NRC (Stothoff, et al., 1996) and the DOE (Flint, et al., 1994, Flint and Flint, 1995; Flint, et al., 1996a) suggest that shallow infiltration is relatively high in areas where rocks are covered with shallow soils or channels and relatively low in areas where soil cover is deep. In addition, infiltration takes place episodically in time with areas having a shallow soil cover contributing more frequently.

- DOE has characterized shallow infiltration in the form of either probability distributions or deterministic upper-bound values for PA The DOE has provided sufficient data and analyses to justify the chosen probability distribution or bounding value. DOE's expert elicitation on unsaturated zone flow (DOE, 1997) resulted in various estimates of a related parameter, the groundwater percolation flux at the depth of the proposed repository (see Appendix C of this report, Table C-2) The estimated aggregate mean flux was approximately 10 mm/yr The panelists estimated the 95th-percentile percolation flux over a range from 10 to 50 mm/yr, with an aggregate estimate of 30 mm/yr An independent staff assessment of an upper bound for yearly shallow infiltration under present climatic conditions is about 25 mm, which is somewhat less than the aggregate 95th percentile flux estimated by the expert panel. Given the importance of infiltration in PA, and the degree to which estimates of this parameter have changed in recent years, the staff will continue to review infiltration at YM If needed, we will provide updates in future revisions of the IRSR

- DOE's estimates of the probability distribution or upper bound for present-day shallow infiltration need not be refined further if the DOE demonstrates through TSPA and associated sensitivity analyses that such refinements will not significantly alter the estimate of total-system performance.

- If used, expert elicitations were conducted and documented using the guidance in the Branch Technical Position on Expert Elicitation (NRC, 1996), or other acceptable approaches.

- Data were collected and documented under acceptable QA procedures Analyses were developed and documented under acceptable QA procedures.

4.3.2 Technical Basis for Review Methods and Acceptance Criteria

- **Implications of Net Infiltration Characterization for Repository Performance**

The behavior of deep percolation is of direct interest for characterizing repository performance, both for characterizing how liquid (the dominant vector of radionuclide release) contacts the waste packages and for characterizing how the released radionuclides migrate to the water table and to potential receptors. If flow is predominately within the matrix, the waste-emplacement drifts would tend to be protected through capillary-barrier effects and migration through the unsaturated zone would tend to be quite slow (e.g., assuming 1 mm/yr fluxes and 10 percent average moisture content, water travel times for 100 m would be 10^4 yr and sorption processes might further retard many radionuclides). As matrix flow in welded and nonwelded tuffs is strongly diffusive due to capillary forces, matrix flows would tend to be smoothly distributed in space and many drifts might be affected by matrix fluxes. On the other hand, if flow is predominantly through fractures, the drifts would be less well protected through capillary-barrier effects and travel times to the water table would be drastically reduced. Also, as permeabilities of the fractures are rather large, it is possible that relatively few fractures might carry the bulk of the water and only a few drifts would be contacted by a flowing fracture. Accordingly, it is important to characterize net infiltration in terms of the capacity for driving fracture flow at and below the repository horizon.

Net vertical infiltration from the ground surface is the predominant source of moisture for deep percolation with capillary rise from the water table and vapor redistribution due to the geothermal gradient both potentially contributing a small amount of water to deep percolation. Deep percolation patterns can be strongly dependent on the nature of infiltration due to the intermittent pattern of precipitation in arid and semiarid climates. For example, consider a homogeneous fractured welded tuff with a matrix saturated hydraulic conductivity K_{sat} of 10 mm/yr and a fracture K_{sat} of 10^4 mm/yr. If a source of water is applied at a steady rate of 5 mm/yr, then the fractures will not be active due to capillary effects. On the other hand, if the same total volume of water is due to an extreme precipitation event and applied over a short period, for example 1 month out of every 10 yr, the average flow during that month is 600 mm/yr and at best the matrix can carry 1.7 percent of the total flux, leaving the remainder to the fractures. Further, unless percolation-flux measurements are made at less than one-month intervals, the example episodic-flow event that dominates the hydraulic regime could be completely missed. High flux rates should not be unexpected, as a significant rainfall might be 1 cm over a period of a day (equivalent to 3,650 mm/yr under steady-state conditions). Accordingly, the episodicity of infiltration and the ability of the soil profile to attenuate the wetting pulses are issues that should be evaluated to appropriately characterize the behavior of deep percolation.

The spatial distribution of net shallow infiltration is a related issue with implications for deep percolation characterization. Consider the same homogeneous fractured welded tuff as before. If a steady 5 mm/yr source of water is applied uniformly over the surface of the tuff, the matrix should carry the entire flow and the fractures not participate. On the other hand, if the same steady total volume of water were concentrated in a small part of the area (i.e., channels in the study area considered by Flint, et al., 1996a), the local flux would be much larger and the fractures would carry most of the flow near the surface. Characterization of deep percolation behavior is dependent on the localization of shallow net infiltration.

The ability of shallow-infiltration characterization methods to predict shallow infiltration under climatic variation is a final issue that must be considered This issue is not addressed explicitly in this report Performance of the potential repository however must be assessed over periods of time long enough for climatic variation to be a factor And methods for characterizing shallow infiltration that are suitable for such long time periods are more useful for PA than methods that can only be applied for current climatic conditions Thus, methods explicitly reliant on climatic information would be expected to be more useful than methods that do not consider it

- **Measurements and Modeling Related to Net Infiltration at YM**

A wide variety of methods are used to estimate net infiltration and the components of a water-balance equation in semiand environments. Good overviews of advantages and disadvantages of some of the more common methods are presented by Allison, et al. (1994) and Gee and Hillel (1988).

A number of background papers discuss issues related to infiltration in and and semiand environments (Barnes, et al., 1994, French, et al., 1996, Gee, et al., 1994; Stephens, 1994) In such environments, particularly in deep alluvial covers, recharge is highly intermittent due to the need for one or several large storms to overcome the soil-moisture deficit arising from an excess of potential evapotranspiration over average annual precipitation. Timing of the precipitation is important, as a moderate rainfall when evapotranspiration is low may be more significant to net infiltration than a much larger event when evapotranspiration is high Distribution of extreme events is also important, as in some environments total precipitation over a month must be several times larger than the mean for that month for net infiltration to occur (Barnes et al 1994)

The literature generally does not discuss situations where shallow soils overlie fractured bedrock, common over much of the repository footprint. In such areas, there is relatively little storage volume to fill above fracture pathways that may conduct fluxes to depths below the evapotranspiration zone One might expect that net infiltration in shallow soils may occur with smaller, more frequent storms than discussed in the literature.

Each of the methods discussed below has been used at YM or the Nevada Test Site (NTS) to estimate infiltration or a component of the water-balance equation. Advantages and disadvantages of each method, and relevant predictions using the method, are discussed in each section.

1. Empirical Correlations

a. Recharge

An empirical correlation between elevation and recharge for Nevada groundwater basins was developed by Maxey and Eakin in the late 1940s and early 1950s (Maxey and Eakin, 1949; Eakin, et al., 1951). The relationship was based on estimating discharges from a basin and correlating the discharge to the percentage of the basin within each of several broad elevation classes. Each elevation class has an associated precipitation and percent of precipitation that becomes recharge, both increasing with elevation. Watson, et al. (1976) investigated the relationship in 63 of the 212 basins in Nevada that were characterized at the time, concluding

that the method is necessarily subjective reasonably robust but mainly useful as a first approximation

Using the method, one can estimate recharge anywhere within Nevada, however, the method is most reasonable on a regional scale and larger and is highly questionable at scales as small as the YM site scale The method is applicable to time scales comparable to the residence time within a basin. The method was developed under current climatic conditions and extending the method to consider climatic change is not straightforward A variety of investigators have used the Maxey-Eakin method or a variant of the method at or near YM (Malmberg and Eakin, 1962, Rush, 1970; Czarnecki and Waddell, 1984; Czarnecki, 1985; Hevesi and Flint, 1996), primarily in the context of regional scale hydrology or regional-scale flow simulators. Rush (1970) estimates maximum recharge for Crater Flat and Jackass Flats to be 3 percent of infiltration Czarnecki (1985) estimates areally distributed recharge for Crater Flat, Jackass Flats, and YM to be 0.5 mm/yr. In Czarnecki's model, Timber Mountain and the area northeast of YM were assigned a recharge value of 2 mm/yr; recharge along Fortymile Wash was estimated at 410 mm/yr (NRC, 1995a, p. I-10).

b. Potential Evapotranspiration

Evapotranspiration is a major component of the water balance equation commonly addressed through empirical relationships. Evapotranspiration is difficult to measure, particularly in areas with significant heterogeneity in vegetation or topography such as is common at YM In arid and semiarid environments, areal evapotranspiration estimates can be obtained readily by simply using the measured or estimated values for precipitation, as net infiltration is typically a small percentage of precipitation. This procedure is useless for estimating net infiltration, however

Potential evapotranspiration is the amount of evapotranspiration that would occur if soil moisture were not the limiting factor. An empirical relationship predicting potential evapotranspiration as a function of temperature and ground slope appropriate for Nevada was developed by Behnke and Maxey (1969). Shevenell (1996) provided a set of piecewise-linear regression relationships to approximate potential evapotranspiration in Nevada. Although potential annual evapotranspiration far exceeds annual precipitation at YM, potential evapotranspiration is quite low in the winter when most precipitation occurs.

2. Estimates of Net Infiltration Inferred from Indirect Evidence

a. Fluxes Inferred from Neutron-Probe Data

Neutron probes provide an estimate of the moisture content within a soil or rock mass, based on the percentage of neutrons reflected from the soil. The presence of water strongly mediates the return rate, thereby providing an estimate of the water content averaged over a volume with a radius somewhat larger than the borehole radius.

A total of 99 boreholes have been used to obtain neutron-probe data at YM (Flint and Flint, 1995) representative of different micro-environments. Yucca Crest, lower sideslopes, terraces, and channels are well represented, but no boreholes were drilled into upper or middle sideslopes due to the difficulty of drilling there. Flint, et al. (1994) discuss moisture contents from 34 of the boreholes. Every ridgetop and lower sideslope borehole is reported to have exhibited

moisture-content responses in the bedrock, while only 4 of 20 terrace or channel boreholes ha a response (each having a particularly shallow cover)

Hevesi and Flint (1993) used moisture contents from borehole N7 to calibrate a 1D numeric model. Borehole N7 is in the Pagany Wash channel and has 12.3 m of alluvium overlyin welded Tiva Canyon (TCw) bedrock (Flint and Flint, 1995) During the model calibration proces a root zone was imposed to a depth of 7 1 m to account for observed changes in moistur content, while a root zone of 2 m was considered reasonable for site vegetation Vapor flow i invoked as a possible explanation for the discrepancy. Hevesi, et al (1994) use N7, N8, an N9 (closely spaced boreholes across the wash cross-section) with an additional year of data t further refine the model. The root zone was extended farther, to bedrock, to simulate observe changes in moisture content, again arguing that this must account for vapor or lateral flow.

Examining moisture content history from the complete set of closely spaced boreholes in Pagan Wash (N2 through N9 and N63), one can indeed see indications of flow spreading from th channel. Although the model may be calibrated for this location, the generality of the calibratio is questionable, as the effects of plant uptake are not separated from the very special case c lateral spreading from the channel. In most other locations, it would be more appropriate to hav the vegetation represented using physically appropriate parameters.

b. Fluxes Inferred From Hydraulic Properties

As discussed by Nimmo, et al. (1994), one can estimate fluxes in a small sample when on knows the *in situ* moisture content. By adjusting the flow through the minimally disturbed sampl in the laboratory (e.g., using a centrifuge) until the moisture content is identical to the *in sit* moisture content, one can get a direct estimate of the flux passing through the sample in th field. If the *in situ* flux is steady state and vertical, an estimate of net infiltration is obtained. A less accurate way of estimating fluxes is to directly use Darcy's law with known *in situ* potentials and the unsaturated hydraulic conductivity appropriate for the potentials (Tyler, 1987)

Tyler (1987) and Tyler and Jacobson (1990) summarize several studies on the NTS where fluxes in deep alluvial soils were calculated using estimates of the hydraulic properties. The estimates range over 3 to 4 orders of magnitude, due to uncertainties in hydraulic gradient and hydraulic properties. The largest estimates from two deep-alluvium locations (Rock Valley and Frenchman Flat) are 0.12 and 2.6 mm/yr.

Several studies have attempted to estimate infiltration fluxes for YM bedrock while neglecting fractures. Waddell, et al. (1984) estimated the matrix flux to be 0.03 mm/yr in the weldec Topopah Spring (TSw) unit, based on measurements in borehole UE-25a1, noting that either ne infiltration is significantly less than in deep alluvium or fracture flow must be occurring Montazer, et al. (1988) performed a similar study on the TSw unit based on observations from borehole UZ-1, estimating net infiltration of 0.1 to 0.5 mm/yr. Flint, et al. (1993) calculated th response of UZ-1S to paleoclimatic change using 1D simulations with time variation based on $\delta^{18}O$ records from ocean sediments, concluding that current conditions may actually reflect long-term drying. Gauthier (1993) used steady-state 1D Monte-Carlo simulations to estimate the mos likely flux through H-1, neglecting fractures, and found that likely matrix fluxes are between 0 an 0.01 mm/yr. Fluxes of 0.1 and 0.5 mm/yr are rejected using statistical methods. Flint and Flin (1994) provided the first estimate of the spatial distribution of potential net infiltration b

assuming saturated hydraulic conductivity of the matrix was the maximum infiltration flux with net infiltration rates ranging from 0 02 to 13 4 mm/yr and with an areal average of 1 4 mm/yr

Brown, et al (1993) attempted to predict moisture contents in boreholes N53, N54, and N55 assuming matrix-only fluxes. A range of fluxes between 0 01 to 0 1 mm/yr provided the best match to observed moisture contents, but the distribution of moisture contents with depth was not well matched Considering fracture flow by using a dual-porosity model, Brown, et al (1993) demonstrated that the distribution of predicted matrix moisture contents was much better matched using the dual-porosity model with fluxes between 1 and 10 mm/yr and found that predicted matrix moisture contents were relatively insensitive to flux when fracture flow was accommodated.

Kwicklis, et al. (1993) attempted to calculate vertical fluxes in boreholes UZ-4, UZ-5, UZ-7, and UZ-13 using estimated hydraulic properties and potential gradients. The calculations were hampered by the lack of a consistent set of both properties and potentials for any borehole Estimates varied widely between boreholes, between layers within a borehole, and between results obtained using different assumptions for the same layer within a borehole. Locally, even the direction of flow may not have been consistent, suggesting that lateral flow may be occurring

In general, it appears that the direct determination of infiltration fluxes from unsaturated hydraulic conductivity may be credible for some well-controlled situations, where fluxes are steady and vertical. A deep alluvial column may satisfy these requirements. Estimates obtained from fractured welded tuffs are not credible because flowing fractures cannot be sampled The reliability of estimates from nonwelded units (typically having few fractures) cannot be rejected out of hand, but analyses assuming a unit hydraulic gradient in the matrix (without verification) are questionable, as significant variations of hydraulic properties may occur within a short vertical span so that capillary forces may cause significant flow.

c. Fluxes Inferred From Thermal Considerations

If the temperature and thermal conductivity profiles of a rock mass are known, one can calculate the energy flux due to conduction. If the actual energy flux through the rock mass differs from the conductive flux, it must be due to advection (i e energy transported through liquid or vapor fluxes). When a vertical column has smaller conductive fluxes than actual fluxes, it may be due to cool infiltrating water that warms while moving to depth or upward vapor transport with an associated large latent-heat transport. To estimate infiltration fluxes when moisture movement is predominantly vertical, one can use an analytic solution or a numerical simulator accounting for both conductive and advective fluxes, and adjust the infiltration flux until the measured temperature profile is obtained. Lachenbruch and Sass (1977) presented a relationship indicating that reduction in apparent heat flux is roughly proportional to volume of infiltrating water, thermal gradient, and distance considered. Typically it is assumed that vapor flux is negligible, although this assumption is not necessary if the vapor flux can be accounted for. Implicit in the approach is the assumption that liquid and rock remain in thermal equilibrium.

An advantage of the method is it is not necessary to know in detail how liquid moves within the rock. On the other hand, it is necessary to have an independent estimate for the thermal flux, which can be difficult to obtain. It is also essential to know thermal conductivities, but these are typically quite well constrained

Estimates of thermal and liquid fluxes throughout the NTS are presented by Sass, et al. (1980) and Sass and Lachenbruch (1982), with results summarized by Sass, et al. (1988). Sass, et al. (1988) analyzed a set of boreholes in the YM area with estimates of conductive and total heat fluxes from the saturated zone (SZ) into the unsaturated zone (UZ) of 40±9 and 49±8 mW/m^2 with an average heat flux in the UZ of about 41 mW/m^2. Sass, et al. (1988) contour conductive heat fluxes in the YM area (Figure 15 by Sass, et al., 1988), which indicates that conductive fluxes are 70 to 74 mW/m^2 southeast through southwest of YM, roughly 60 mW/m^2 in the southwest part of Midway Valley, roughly 50 mW/m^2 in and near Fortymile Wash, Dune Wash, Yucca Wash, and Solitario Canyon, and roughly 30 to 40 mW/m^2 over the repository footprint and north past Drillhole Wash. Sass, et al. (1988) suggest there may be an apparent reduction of heat flow from the SZ to the UZ of 5 to 10 mW/m^2 and calculate this apparent reduction of heat flow could be achieved by 2 to 5 mm/yr net infiltration. If 0.1 mm/yr of water were vaporized, about 8 mW/m^2 reduction would be achieved. Lateral flow in the shallow SZ is also considered a possible source of local anomalies. Sass, et al. (1988) also note (without further comment) that apparent heat flux is negatively correlated with elevation; one might infer that lateral diversion to lower topographic areas may be occurring, although the study by Rousseau, et al. (1996) discussed in another paragraph would suggest the opposite due to the insulating properties of alluvium.

An implication of the analysis by Sass, et al. (1988) is that at least locally over the repository block and Drillhole Wash deficits in the apparent heat flux that occur in the UZ may be as much as 20 mW/m^2 [assuming that 10 mW/m^2 is roughly equivalent to 5 mm/yr infiltration, as calculated by Sass, et al. (1988)], so that locally about 10 mm/yr infiltration might be estimated. When estimating infiltration, it may be better to estimate the vertical heat flux from boreholes that are unlikely to have significant infiltration. Infiltration fluxes in deep alluvium and not close to channels are likely to be quite small, so that the boreholes in Midway Valley and south of YM in deep alluvium may be more representative of regional vertical heat flux. If so, vertical heat flux could be as much as 60 to 75 mW/m^2 and local deficits at YM could be as much as 45 mW/m^2, implying that locally more than 20 mm/yr infiltration could be inferred from the thermal data. Assuming that the UZ heat flux is 60 mW/m^2, heat-flux deficits on the order of 15 to 30 mW/m^2 in the area of the repository block and Drillhole Wash could be justified, implying that local infiltration rates may be 7 through 15 mm/yr in this area.

Montazer, et al. (1988) discuss the installation of devices for monitoring temperature, air pressure, matric potential, and water potential in borehole UZ-1 as well as analysis of some of the data. Using the temperature and air-pressure information, Montazer, et al. (1988) estimated the maximum upward vapor flux to be 0.025 to 0.05 mm/yr, which would account for 2 to 4 mW/m^2 of the heat-flux anomaly discussed by Sass, et al. (1988).

Both Montazer, et al. (1988) and Sass, et al. (1988) present a set of temperature profiles for boreholes in Drillhole Wash (UZ-1, UE-25a5, and UE-25a7) that show cooling suddenly (within weeks or months) at depths of 50 to 150 m, consistent with transient moisture redistribution such as might occur from infiltration events. Sass, et al. (1988) calculate heat fluxes for these boreholes of 32 to 33 mW/m^2, among the lowest reported, consistent with an interpretation of locally high infiltration. Rapid redistribution of moisture to depth is consistent with an interpretation of significant fault-related flow.

Fridrich, et al. (1994) provide an alternative interpretation of the Drillhole Wash heat-flux low and generally low temperatures at the water table under the repository footprint as indicative of lateral flow in the SZ associated with the large hydraulic gradient. If significant flow is moving down the large hydraulic gradient, the temperature anomaly south of Drillhole Wash would be partially explained. On the other hand, later information gathered from borehole G-2 suggests that the large hydraulic gradient may represent a perched zone (Czarnecki, et al., 1994, Czarnecki, et al., 1995), in which case flow may be predominantly vertical.

The regional-scale analysis presented by Sass, et al. (1988) provided the independent energy flux required for site-scale analyses by Bodvarsson, et al. (1996). Both conduction-only and coupled conduction/convection models were investigated. Using an average heat flux of 50 mW/m^2 and temperature data from UZ-7a, NRG-6, NRG-7, and SD-12, infiltration fluxes of 10 mm/yr were calculated for UZ-7a (WT-2 Wash) and SD-12 (Antler Wash) and 7 mm/yr for NRG-6 and NRG-7a (Drillhole Wash, outside the fault zone). Using an average heat flux of 40 mW/m^2, the infiltration rates dropped to 6 and 2 mm/yr. The infiltration rates would increase to about 15 and 11 mm/yr if the heat flux is assumed to be about 60 mW/m^2.

Rousseau, et al. (1996) estimate net infiltration from thermal fluxes in Pagany Wash (UZ-4 and UZ-5). One- and two-dimensional (2D) combined conduction/convection simulations were used to estimate infiltration based on a heat flux of 36.5 mW/m^2 applied at the water table. It was found that significant 2D heat-flow variation may result due to the insulating properties of the alluvium in the wash, a 2D conduction-only simulation had a heat flux from the wash surface of about 2/3 of the flux at the water table, and a heat flux from the sideslope surface of about 5/3 of the flux at the water table. Based on 1D simulations of the temperature profiles in the boreholes, estimates of net infiltration were roughly 18 mm/yr in UZ-4 (channel) and 5 mm/yr UZ-5 (sideslope), although the 2D heat flow effects were interpreted as causing the UZ-4 estimate to be too high and the UZ-5 estimate to be too low. Note that the thermal flux used by Rousseau, et al. (1996) is quite low relative to estimates by Sass, et al. (1988); calculated infiltration fluxes with a thermal flux of 50 mW/m^2 would be larger by more than 5 mm/yr.

Not only are the estimates of infiltration based on heat-flux calculations insensitive to the precise manner in which water percolates in the fractured medium, but the estimates are on a particularly useful scale, considerably larger than the borehole, as heat conduction tends to quickly damp out temperature perturbations. Additional studies using site-scale simulations, such as the one by Finsterle, et al. (1996) should help delineate the impacts of coupled heat and moisture transport.

One significant advantage of the heat-flux method is that it can yield upper-bound estimates for infiltration rates. Assuming that the regional heat flux is 85 mW/m^2, neglecting all other sources of reduction in apparent heat flux such as lateral flow in the SZ and vapor fluxes, using a value of 35 mW/m^2 as the average apparent heat flux over the repository block and using the rule-of-thumb that 10 mW/m^2 reduction in apparent flux is equivalent to 5 mm/yr infiltration, one finds the maximum average infiltration over the repository block is about 25 mm/yr.

d. Fluxes Inferred From Natural and Anthropogenic Tracers

Both naturally occurring and anthropogenic (e.g., bomb-pulse related) tracers can be used to estimate infiltration, and methods based on tracers are considered particularly robust in arid

environments (Gee and Hillel 1988 Allison et al 1994) Tracer methods average flux over long periods of time a significant advantage in environments with highly sporadic infiltration events

Assuming that flows are perfectly vertical, that tracers do not mix (water moves as piston flow and dispersive processes are negligible) water-rock interaction is negligible, and that the age of a tracer can be accurately determined, one is able to directly infer the travel time as a function of depth within a borehole The time required for the tracer to reach a depth may be calculated by integrating the tracer mass to that depth (e g . the chloride mass balance method), calculating the ratio of a radioactive isotope to the stable isotope (e.g., the ratio of ^{36}Cl to Cl or ^{14}C to C), relating the variation with depth of stable-water-isotope compositions to known climatic variation, or calculating the ratio of daughter product to the parent radioactive isotope (e.g . ^{230}Th to ^{234}U). Further assumptions regarding moisture content are required to convert travel time into velocity, and velocity into flux.

There are several areas of uncertainty involved with tracer methods The inability to unambiguously achieve tracer mass balance is a primary uncertainty The time history of the tracer input must be known, which can be difficult to determine, particularly over geologic time scales For example, the cosmogenic production of ^{36}Cl is estimated to have increased by a factor of 2 over the last 500 ka (Fabryka-Martin, et al . 1996a) Deposition rates of bomb-pulse constituents (i e . ^{36}Cl, ^{14}C tritium) varied in both time and space, due to the influence of particular testing events and were not measured at YM Due to this uncertainty, tracer mass balance is uncertain and one may be unable to determine if fast pathways bypass sampled locations. On the other hand, if inputs are variable in time but known, one may be able to correlate the variability of the tracer with depth in terms of source variability, thus improving estimates of velocities.

Another cause of uncertainty arises from the various transport pathways that the tracers follow Each tracer may be transported somewhat differently causing uncertainties in interpretation Tritium is subject to vapor transport. Carbon-14 is partitioned into the gas phase as carbon dioxide. Chloride may move up to 20 percent faster than ambient water, perhaps because of anion exclusion in the soil (Gee and Hillel, 1988). A suite of tracers is often used to provide corroboratory interpretations

A further confounding uncertainty arises when waters of different ages or different chemistries mix, thereby yielding a composite age perhaps not representative of either pathway. Once two waters have mixed, one cannot extract the age of the input waters from the apparent age of the mixture, although one may constrain the ages somewhat. This uncertainty arises whenever more than one flow pathway exists (e.g., both matrix and fracture pathways) or when dispersive fluxes are significant and can make flux interpretations very difficult at depth in fractured rocks such as exist at YM. In each of the cases discussed by Phillips (1994) (all with soil or alluvium profiles), he asserts that piston flow appears to be closely approximated except at the shallowest soil depths with the implication that mixing may be minimal in many desert soils.

Even when the actual age of waters can be accurately calculated with depth, the actual flux history may not be uniquely determined; at best, a velocity history may be calculated under the assumption that fluxes are constant with depth even though varying in time. The flux history is less certain than the velocity history, due to the uncertainties associated with moisture conten

over time Often however the uncertainties associated with moisture content are small relative to other uncertainties

Phillips (1994) presents a comparison of data from tracer studies across the American Southwest (including two boreholes from the NTS) using ^{36}Cl, tritium, and chloride tracers and discusses various interpretations of the profiles. Phillips (1994) suggests that the 12 profiles he considered from west Nevada to west Texas, consistently support a 20-fold drop in net infiltration over the period of 16 to 13 ka, and further suggests that this drop is due partly to changing climatic conditions and perhaps partly due to a change in vegetation from mesic to xeric species

Tyler (1987) and Tyler and Jacobson (1990) review soil-moisture flux studies at the NTS, including those that examined bomb-pulse tritium. Velocities are estimated between 30 to 80 mm/yr, and as much as 200 mm/yr (with a calculated flux of 38 mm/yr) in the Yucca Flat playa where occasional ponding occurs. As discussed by Tyler and Walker (1994), net infiltration from bomb-pulse tracers may be seriously overpredicted if changing water velocities with depth in the root zone, due to plant uptake of soil water, is not accounted for. Tyler and Walker (1994) report discrepancies of tritium dating relative to the chloride mass balance approach that result in net-infiltration overpredictions of as much as 3 orders of magnitude The influence of the root zone on predicted travel times is negligible once the tracers have migrated deep into the profile so that the infiltration estimates most affected by the root zone may be those using bomb-pulse tracers

Tyler, et al. (1995) discuss dating of waters from three deep-alluvium boreholes in Frenchman Flat using ^{36}Cl, stable chloride, and stable isotopes. Tyler, et al. (1995) interpret the results as likely showing the effects of the last two glacial periods with one borehole receiving focussed runoff recharging to the water table in the last glacial period and the other two recording wetting pulses in the last two glacial periods that did not reach the water table No evidence of wetting pulses from even earlier glacial stages was detected Removal of tracers due to a higher water table is considered and dismissed by both Conrad (1993) and Tyler, et al. (1995) based on arguments by Jones (1982) and Winograd and Doty (1980) Conrad (1993) estimates average net infiltration for another Frenchman Flat deep-alluvium borehole of about 0.04 mm/yr using the chloride mass balance technique.

Using shallow bomb-pulse tritium profiles, Kwicklis, et al (1993) estimate net infiltration to be 35.1 mm/yr at UZ-4 (the channel of Pagany Wash) and 23.6 mm/yr at UZ-7 (the channel of Wren Wash). Using ^{14}C profiles, Kwicklis, et al. (1993) estimate net infiltration to be 20 mm/yr at UZ-4 and 4 mm/yr at UZ-5 (the sideslope of Pagany Wash, near UZ-4). Analyses based on heat-flux considerations suggest that net infiltration is less than 18 mm/yr at UZ-4 and more than 5 mm/yr at UZ-5 (Rousseau, et al., 1996), corroborating the estimates from near-surface tracer calculations. Estimates however, of percolation fluxes at depth in the UZ are significantly smaller. Using pore waters from the nonwelded Paintbrush tuff (PTn) unit obtained from UZ-4 and UZ-5, chloride mass balance calculations yield estimates of net infiltration of 1.1 and 1.5 to 2.5 mm/yr (Fabryka-Martin, et al., 1996b) apparently by assuming that precipitation, net infiltration, and chloride deposition rates have been constant for sufficient time to reach a steady state and further assuming that matrix and fracture waters have fully mixed.

The chloride mass balance technique, as applied by Fabryka-Martin, et al. (1996b), assumes that average Cl^- concentration multiplied by total flux is conserved. Knowing (1) the average

precipitation rate (2) Cl concentration corresponding to the average Cl deposition rate and (3) Cl concentration in a well-mixed reservoir at depth, the percolation flux at depth can be determined Yang, et al (1996) report Cl concentrations in perched water of 4 1 to 15 5 mg/L with 15 of the 17 reported values being no greater than 8 3 mg/L and a Cl concentration of 7 mg/L at NRG-7a (the nearest borehole to UZ-4 and UZ-5 with a reported perched-water sample) Using the same precipitation rate (170 mm/yr) and Cl concentration (0 62 mg/L) as Fabryka-Martin, et al. (1996b) and assuming that the perched water is well mixed with the matrix waters, calculated net infiltration is 25.7, 12 7, and 6 8 mm/yr for concentrations of 4 1, 8 3, and 15 5 mg/L, respectively An infiltration value of about 26 mm/yr would represent an upper bound based on the perched-water chloride data; if the matrix waters do not mix completely with the perched water, infiltration values may be lower The estimated infiltration values are more consistent with the shallow infiltration estimates than the estimates from the PTn, however, suggesting that a considerable portion of the infiltrating water may bypass the PTn matrix.

Fabryka-Martin, et al. (1996b) use the chloride mass balance approach to estimate net infiltration from alluvium profiles in the YM area, with estimates below the root zone generally less than 1 mm/yr and with some estimates as low as 0.015 mm/yr Norris, et al. (1987) estimate infiltration in Yucca Wash (apparently not in the channel) using the ratio of ^{36}Cl to Cl, arriving at a value of 1 8 mm/yr; however, the peak in ^{36}Cl/Cl is within the root zone and coincides with a change in soil properties

Paces, et al. (1996) provide a preliminary estimate of the percolation fluxes required to deposit calcite and opal in the form of fracture fillings and lithophysae coatings at YM. Assuming that the fracture characteristics and filling patterns observed in the Exploratory Studies Facility (ESF) are representative of the entire UZ, all cations are deposited within the UZ, and infiltrating water has the composition observed under current conditions, the average infiltration flux rate required to match the observed patterns is calculated to be 2 1 mm/yr for calcite and 0.3 mm/yr for opal. As noted by Paces, et al. (1996), these are minimum estimates, as almost certainly not all calcium and silica is deposited.

One can test conceptual models for shallow infiltration by observing the degree of compatibility with unambiguous bomb-pulse signatures. Fabryka-Martin, et al. (1996b) present ^{36}Cl data obtained from 23 boreholes. Areas with minimal soil depths (ridges, sideslopes) generally had unambiguous bomb-pulse signatures at depths tens of meters and more into the underlying TCw bedrock and locally into the underlying PTn, suggesting that wetting pulses in the last 50 yr have penetrated well below the zone of evapotranspiration. These deep bomb-pulse signatures are consistent with an interpretation of relatively high infiltration rates in areas with shallow soils. Areas with deeper soils tended not to have bomb-pulse signatures in the bedrock, consistent with relatively low infiltration rates. Recent modeling work that may aid in assessing consistency of conceptual models of deep percolation with ^{36}Cl data, thereby enabling estimates of net infiltration, are discussed by Wolfsberg, et al. (1996), Fabryka-Martin, et al. (1996a), Fairley and Sonnenthal (1996), and Robinson, et al. (1996).

Fabryka-Martin, et al. (1996b) describe studies of ^{36}Cl/Cl ratios in precipitation, subsurface waters, and packrat middens at YM. The work also included many rock samples from the ESF at YM, including samples from the proposed repository horizon in the Topopah Spring tuff Fabryka-Martin, et al. (1996b, p. 33) conclude that "the initial ^{36}Cl/Cl ratio in infiltrating water

could have been more than twice as high as its present ratio of 500 x 10^{-15} during the past several hundred thousand years " Also,

> ratios significantly higher than a threshold of 1500 x 10^{-15} are interpreted as being clearly elevated above meteoric background and most likely contain a component of bomb-pulse ^{36}Cl Samples with ratios ≤ 1500 x 10^{-15} may contain a component of bomb-pulse ^{36}Cl but may also contain Cl from old water recharged when the input ratio was higher.

Murphy (1997, p. 4), in a commentary on the ^{36}Cl studies in the ESF, concludes that "samples containing $^{36}Cl/Cl$ ratios greater than 900 x 10^{-15} to 1000 x 10^{-15} contain some bomb pulse ^{36}Cl " and that "...fast pathways for water flow from the surface to the ESF are fairly common Statistical analyses interpreting the data as the mixture of two normally distributed samples indicate that 20 to 25 percent of samples reported for the ESF show signs of bomb pulse contamination." Although the ^{36}Cl data provide unequivocal evidence of relatively fast flow paths from the surface down to the ESF, the corresponding magnitude of infiltration flux is unclear. Simulation of ^{36}Cl transport to the ESF by Fabryka-Martin, et al. (1996b) suggests that average recharge rates probably exceed 1 mm/yr.

The use of tracers to robustly estimate infiltration rates in the YM area would appear to be limited to deep alluvium profiles where lateral flow processes are not significant. Difficulties with estimating the impacts of vegetation, lateral flow, and multiple pathways would appear to limit their use over most of the repository footprint, where shallow soils overlie fractured bedrock Nevertheless, unambiguous bomb-pulse signatures observed at depth in the ESF, which are interpreted as occurring where high infiltration occurs over a zone having a fault that provides a fast pathway through the PTn unit (Levy, et al., 1997) were instrumental in demonstrating that fast pathways exist and, by implication, that at least locally there are areas where infiltration might be much higher than previously thought

Despite the limitations of tracer methods, the chloride mass balance technique does provide a means of estimating an upper bound for net infiltration. The upper-bound value obtained by chloride mass balance on perched water, 26 mm/yr, is remarkably consistent with the upper-bound value obtained by geothermal heat-flux calculations.

3. Estimates of Net Infiltration from Water Balance Calculations

Direct estimates of net infiltration are considered more robust than estimating infiltration from water balance considerations (Gee and Hillel, 1988; Allison, et al., 1994), as the magnitude of uncertainties in precipitation, runoff, and evapotranspiration may be considerably larger than the magnitude of net infiltration. Nevertheless, simulation methods based on water-balance calculations are likely to provide the basis for predictions of net infiltration used in PA. In order to quantify net infiltration under potential future climatic changes, it is necessary to be able to understand and predict the response of net infiltration under current conditions.

a. Precipitation Data

Precipitation is perhaps the best characterized of all components of the water balance, although the record is still too short to estimate frequencies of extreme events. There are numerous

stations where precipitation records have been obtained across southern Nevada and into California. Available data and interpretations are discussed by French (1983), Quiring (1983), French (1986), Nichols (1987), Hevesi, et al. (1992a), Hevesi, et al. (1992b), Hevesi, et al. (1994), Ambos, et al. (1995), Hevesi and Flint (1996) and Flint, et al. (1996a).

b. Evapotranspiration Data

Although evapotranspiration is the second-largest component of the hydrologic balance in the YM area, behind only precipitation, far less attention has been focussed on measuring evapotranspiration. Nichols (1987) discusses evaporation studies relevant to the low-level Beatty facility, and Czarnecki (1990) considers evapotranspiration at Franklin Lake playa (approximately 60 km downgradient of YM), but little attention has been paid to evaporation at YM in particular. Measurements of evaporation at YM over several years, using a class A pan, are found to exceed calculated potential evaporation by about a factor of 2 (Flint, et al., 1996a). Flint, et al. (1996b) reports that the most success in estimating evapotranspiration at YM has been using inverse modeling based on neutron-probe data, with numerous limitations.

Information is available on the types and distributions of vegetation on the NTS (Wallace and Romney 1972; Beatley 1974; Beatley 1976; O'Farrell and Emery 1976; O'Farrell and Collins 1983; EG&G 1991, and Hessing, et al., 1996). Most information, however, emphasizes vegetation description and habitat, rather than plant uptake patterns.

Leary (1990) directly measured plant water use, soil moisture evaporation, and soil moisture flux in 3 study plots (a wash, an alluvial fan, and a sideslope) 13 km northwest of the ESF north portal. The work emphasized measurement-technique evaluation, however rather than quantifying uptake patterns. Preliminary estimates of rooting depths, active months, and minimum xylem potential for some species common to YM are presented by Flint, et al. (1996a).

The relative lack of YM-specific attention is unfortunate, due to th act of desert vegetation uptake patterns, responses to precipitation, and life cycles on net infiltration. In particular, information on the impact of a fractured bedrock with shallow soil cover on plant uptake patterns has received very little attention, despite the ubiquity of shallow soils over the repository footprint.

c. Lateral-Moisture-Flow Data

According to Flint, et al. (1996a) episodic runoff has been observed at YM during the period from 1984 to 1995. Data quantifying some of the events are reported by Pabst, et al. (1993), Osterkamp, et al. (1994), and Savard (1994, 1995). Flint, et al. (1996a) discusses several overland-flow episodes in the period of 1984 to 1995, indicating that both short, intense convective events and extended winter storms can cause overland flow events. The largest runoff events occurred in the winter of 1994–95; unfortunately, neutron-probe data collection had already been discontinued, so that subsequent redistribution could not be monitored.

Little or no data has been collected quantifying shallow lateral flow. Anecdotal and suggestive evidence does exist, however. Flint, et al. (1996a) state that lateral flow has been observed to occur along the soil-bedrock interface. Norris, et al. (1987) suggest that lateral flow is probably the reason that ^{36}Cl and chloride profiles from a soil profile near the ESF North Portal showed

complex layering and that only 7 percent of estimated chloride deposition was found in the profile.

d. Hydraulic-Property Data

A large database of bedrock hydraulic properties has been collected, correlated to lithologic structure, and analyzed for spatial trends, using core samples collected from outcrops and from boreholes. (Peters, et al., 1984; Klavetter and Peters, 1986; Flint and Flint, 1990; Rautman and Flint, 1992; Flint and Flint, 1994; Istok et al., 1994; McKenna and Rautman, 1995; Rautman, et al., 1995; Schenker, et al., 1995; Flint, 1996; Flint, et al., 1996b; Moyer, et al., 1996; Rousseau, et al., 1996).

Hydraulic properties of soils are less well characterized, with estimated or measured properties reported by Nichols, 1987; Schmidt, 1989, Guertal, et al., 1994; Flint, et al., 1996a; and Stothoff and Winterle, 1997. A general agreement exists that the hydraulic properties of the soils are quite spatially uniform; *in situ* saturated hydraulic conductivities over the repository footprint measured by Stothoff and Winterle (1997) (using a ponded-head permeameter) are on the order of 10 to 18 cm/hr, while estimated values for soils in similar locations, based on textural characteristics, are about 2 cm/hr (Schmidt, 1989; Flint, et al., 1996a), suggesting that textural analysis may underpredict *in situ* values by up to an order of magnitude.

Surficial-cover classification is mapped by Lundstrom, et al. (1994, 1995, 1996) and Taylor (1995). Soil depths are qualitatively described by Flint, et al. (1996a). Quantitative soil-depth estimates are primarily available at boreholes and trenches. A modeling approach for estimating soil thickness is presented by Stothoff, et al. (1996) and Bagtzoglou, et al. (1996).

Hydraulic properties of bedrock fractures are poorly characterized. General descriptions of fracture hydraulic properties are presented by Flint, et al. (1994); approximate distributions of fracture apertures and percentage of filled fractures appropriate for each lithostratigraphic layer, for modeling purposes, are presented by Flint, et al. (1996a). Despite the relative lack of characterization, unpublished 1D simulations by Stothoff (1997) examining the impact of soil and fracture properties on net infiltration suggest that it is important to know if fractures are filled or not, but fracture densities are sufficiently high in many areas that net infiltration may be controlled by other factors, such as soil hydraulic properties and soil depths.

e. Predictive Modeling of Net Infiltration

A number of studies have attempted to estimate net infiltration using numerical simulations. By far the most common approach is to perform vertical 1D or quasi-1D (e.g., bucket, local 2D) water-balance simulations [Electric Power Research Institute (1990, 1992, 1996); Lane and Osterkamp, 1991; Hevesi and Flint, 1993; Long and Childs, 1993; Hevesi, et al., 1994; Hudson, et al., 1994; Fairley and Sonnenthal, 1996; Flint et al., 1996a; Stothoff, 1997]. The models treat processes such as moisture redistribution, energy, hydraulic properties, and evapotranspiration using differing approximations, but fundamentally all of the models consider vertical processes and neglect lateral redistribution (aside from allowing surface runoff to occur). Generally the 1D models agree that infiltration increases as soils become shallower, as precipitation increases (particularly in winter), and as temperatures decrease.

The appropriateness of a 1D simulation requires that net lateral flow is negligible so that areas with active lateral flow (e g . channels) are poorly approximated by 1D approaches Nevertheless, 1D simulations do provide estimates of the relative importance of various processes and features, and 1D simulations are much faster than 2D or 3D (three-dimensional) simulations

Stothoff (1997) analyzed the calculated response of net infiltration to hydraulic properties and climatic inputs, by performing a series of simulations that systematically varied one property or climatic input per simulation. Stothoff (1997) found that in cases where soil overlies a fractured bedrock with an impermeable matrix and unfilled fractures, net infiltration is much less when soil covers are deeper than a few tens of centimeters, due to the infrequent wetting pulses that breach the capillary barrier represented by an open fracture. Net infiltration was found to be somewhat sensitive to soil properties but insensitive to fracture properties.

Subsequent unpublished simulations suggest that net infiltration is somewhat different when carbonate-filled fractures are considered. The sensitivity of net infiltration to soil depth is muted for filled fractures. An order-of-magnitude change in bubbling pressure or saturated hydraulic conductivity for the fracture filling changes net infiltration by factors of about 3 and 2, respectively, in contrast to the open-fracture simulations. There are no published data on the bubbling pressure of the fillings found at YM, and only minimal information on saturated hydraulic conductivity is available (i e . Flint, et al (1996a)

Several researchers have made estimates of the spatial distribution of net infiltration based on independent 1D simulations, either on a pixel-by-pixel basis (Flint, et al., 1996a) or as a basis for abstraction (Stothoff, et al., 1996, Bagtzoglou, et al., 1996). Qualitatively the resulting maps are quite similar, and bear a remarkable qualitative similarity both to the map of vertical heat flux presented by Sass, et al. (1988) and to the maps of net infiltration based on regressions of neutron-probe data as presented by Hudson and Flint (1996). Estimated average infiltration fluxes over the repository block using the 1D simulations are generally within a factor of less than half an order of magnitude, remarkably in agreement considering the different physical processes considered in the simulations. Even the simulations presented by Electric Power Research Institute (1992, 1996) would provide qualitatively similar maps, although the calculated infiltration magnitudes would be somewhat lower than predicted by Flint, et al. (1996a) and Stothoff, et al (1996).

4.4 What is the estimated amount and what is the spatial distribution of present-day groundwater percolation through the proposed repository horizon?

Review methods, acceptance criteria, and technical bases will be provided in Revision 1 of this IRSR in FY98.

4.5 What is the estimated amount and what is the spatial distribution of groundwater percolation through the proposed repository horizon during the period of repository performance?

Review methods, acceptance criteria, and technical bases will be provided in Revision 1 of this IRSR in FY98.

4.6 What are the ambient flow conditions in the saturated zone?

Review methods, acceptance criteria, and technical bases will be provided in Revision 1 of th IRSR in FY98

5.0 STATUS OF OPEN ITEMS AT THE STAFF LEVEL

The staff has identified numerous SCA (Site Characterization Analysis; NRC, 1989), study plar and other open items related to this KTI As discussed below, a number of these open item can be resolved at the staff level. Others will be addressed in future updates of this KTI IRSF No new open items have been raised in this IRSR

Appendix D contains a list of open items related to this KTI. It is not yet clear whether thes may be resolved at the staff level. However, they will be further reviewed in future updates c this IRSR.

5.1 What is the likely range of future climates at YM?

The staff has identified no open items solely related to climate change. Accordingly, the stal has no further questions at this time on methods to estimate future climate variability (see NRC 1997).

5.2 What are the likely hydrologic effects of climate change?

The staff has identified no open items solely related to hydrologic effects related to climate change. Accordingly, the staff has no further questions at this time on methods to estimate the hydrologic effects of climate change (see NRC, 1997).

5.3 What is the estimated amount and what is the spatial distribution o present-day shallow groundwater infiltration?

The staff has identified a number of open items related to present-day shallow infiltration. As discussed below, some of these open items can be resolved at the staff level. Others will be addressed in future updates of this KTI IRSR. No new open items have been raised in this IRSF on the top c of present-day shallow infiltratior

5.3.1 Items Resolved at the Staff Level

The staff has reviewed the status of open items described in NRC, 1995b, many of which were first described in the staff's SCA for YM (NRC, 1989). Recent events in the DOE program provide a sufficient basis to resolve a number of open items at the staff level. The constructior of the ESF has produced a wealth of subsurface data that reflects on hydrologic properties, suc as evidence from Cl-36 for localized paths of groundwater flow and detailed information abou faults and fracture systems. The planned east-west drift will add even further to that informatior base. DOE is also planning to drill additional wells at the site. For example, WT-24 has alread begun and is located in an area favorable for analyzing the source of the so-called larg hydraulic gradient. Most importantly, DOE has developed a Waste Containment and Isolatio Strategy (WCIS) that identifies key site issues related to site performance (DOE, 1996). Sinc

development of the WCIS DOE has conducted a series of performance assessment abstraction workshops, on topics such as unsaturated zone flow and saturated zone flow and transport Subsequent expert elicitations have been held on the topics of unsaturated zone flow and saturated zone flow and transport Finally, the NRC staff has refocused its review program into a series of key technical issues that concentrate on issues most pertinent to performance The staff have reviewed DOE's most recent total system performance assessment and participated in an NRC/DOE workshop on performance assessment In summary, the staff believes that DOE now has in place a program that is effectively identifying and obtaining the information needed to support a license application

SCA (NRC, 1995b) comments 1, 10, and 18 address the need for a systematic, iterative approach to identify the information needed to support a license application They are summarized below. Based on the rationale given in the previous paragraph, they are considered resolved at the staff level.

SCA Comment 1· Although the SCP commits to a systematic iterative approach to identifying the information needed to support a license application (the Issue Resolution Strategy), the documentation in the SCP does not demonstrate that such a program is in place. While this comment includes several concerns not raised elsewhere, it also collects and summarizes concerns expressed in other comments, which collectively point to the absence of such a program

SCA Comment 10 No technical basis was provided for assessments of significance of hydrogeologic features, events and processes to design and performance measures and parameters

SCA Comment 18· DOE has given only partial consideration of all features, events or processes that may be essential for a valid mathematical representation of the hydrogeologic system for use in performance assessment analyses As a consequence, planned activities are insufficient to provide technical justification for initial modeling strategies.

5.4 What is the estimated amount and what is the spatial distribution of present-day groundwater percolation through the proposed repository horizon?

Under this topic, information on open items will be provided in a 1998 update of this IRSR

5.5 What is the estimated amount and what is the spatial distribution of groundwater percolation through the proposed repository horizon during the period of repository performance?

Under this topic, information on open items will be provided in a 1998 update of this IRSR

5.6 What are the ambient flow conditions in the saturated zone?

Under this topic, one open item can be resolved. Information on other open items will be provided in a 1998 update of this IRSR.

5.6.1 Item Resolved at the Staff Level

The following open item (study plan Question 4) can be resolved at the staff level It was developed during the staff review of DOE's study plan on Site Saturated-Zone Hydrologic System Synthesis and Modeling (DOE, 1993) The question is no longer relevant because it is a clarifying question about unclear language in a study plan that DOE has cancelled Therefore, question 4 is resolved at the staff level.

SP 831233 Question 4 - What is meant by "actual results should be bounded in a statistical sense by predicted results?"

5.7 Other Technical Issues in Isothermal Hydrology.

5.7.1 Items Resolved at the Staff Level

The following four open items were developed during the staff review of DOE's study plan on Characterization of the Yucca Mountain Regional Surface-Water Runoff and Streamflow (DOE, 1990). They are resolved at the staff level because we agree with the rationale presented in DOE's most recent progress report (DOE, 1997). On page A-8 of that report, it is stated that

> ..the data are not needed for the regional ground-water-flow model. Regional ground-water modeling .. did not require runoff data for model calibration because data describing a direct relationship between precipitation and ground-water recharge was used Because flooding and fluvial-debris transport were shown .. to pose little or no threat to the ESF the potential repository, or surface facilities at Yucca Mountain, studies to document transport of debris by severe runoff were terminated before being fully implemented.

The staff agrees that flooding is primarily a pre-closure concern, and we have determined that no open items exist with respect to flooding so long as portals to the ESF are sited above the probable maximum flood (PMF), as discussed by Coleman, et al., 1996. Previous DOE studies (Blanton, 1992; Bullard, 1992; Glancy, 1994) address flooding at Yucca Mountain and indicate that portals to the ESF are adequately sited above the PMF. DOE must also provide assurance in a possible license application that any facilities where HLW could temporarily be stored at a hypothetical repository would be sited above the PMF, or otherwise provide adequate justification that storage facilities are designed to safely withstand the effects of a PMF.

SP 831212 Comment 2 - The NRC staff recommended that regionalization methods be included in analyses of the probabilities of runoff magnitudes.

SP 831212 Question 1 - Have the field-tests of the surface runoff measurement devices, systems, and proposed techniques been completed? And if not, when will they be completed?

SP 831212 Question 2 - Has DOE considered any other instrumentation for measuring in-situ flow depth and velocity, especially for large ephemeral flows, such as sonar, pressure transducers, and induction probes?

SP 831212 Question 3 - Are there plans for taking sediment samples at the gaging stations?

The following open item (Question 3) was developed during staff review of DOE. 1992 This item is resolved at the staff level because we agree with the rationale provided by DOE in the most recent progress report (DOE, 1997). On page A-48 of that report, it is noted that "...precipitation-runoff models of modern surface-water conditions and basin characteristics were terminated because runoff occurs so infrequently that collecting data sets sufficient to calibrate the models was not feasible." We recognize that the calibration and validation of regional surface water models for an ephemeral surface drainage like Fortymile Wash is not attainable with existing data. Much more data are available for the Amargosa River, but that drainage has regional significance only and will not contribute to an understanding of repository performance at YM. Nonetheless, it is expected that DOE will estimate groundwater recharge along Fortymile Wash during the period of repository performance. This estimate should be based on available hydrologic information and reasonable climatic assumptions (see NRC, 1997)

SP 831522 Question 3 - How will surface water models for regional hydrology studies be calibrated and validated?

6.0 REFERENCES

Allison, G B., G.W Gee, and S.W Tyler, "Vadose-Zone Techniques for Estimating Groundwater Recharge in Arid and Semiarid Regions," *Soil Science Society of America Journal*, 58(1), 1994, pp. 6–14.

Ambos, D.S., A.L. Flint, and J A Hevesi, "Precipitation Data for Water Years 1992 and 1993 from a Network of Nonrecording Gages at Yucca Mountain, Nevada," Open-File Report 95-146, Denver, CO, U.S. Geological Survey, 1995.

Bagtzoglou, A.C., E.C. Pearcy, S.A. Stothoff, G.W. Wittmeyer, and N.M Coleman, "Unsaturated and Saturated Flow Under Isothermal Conditions," B. Sagar ed., NRC High-Level Radioactive Waste Program FY96 Annual Progress Report, Volume NUREG/CR-6513, No. 1, Washington, DC, U.S. Nuclear Regulatory Commission, 1996, pp. 10-1 through 10-28.

Barnes, C.J., G. Jacobson, and G.D. Smith, "The Distributed Recharge Mechanism in the Australian Arid Zone," *Soil Science Society of America Journal*, 58(1), 1994, pp. 31–40.

Beatley, J.C., "Phenological Events and Their Environmental Triggers in Mojave Desert Ecosystems," *Ecology*, 55, 1974, pp. 856–863.

Beatley, J.C., "Vascular Plants of the Nevada Test Site and Central-Southern Nevada: Ecological and Geographical Distributions," TID-26881, U S. Energy Research and Development Administration, 1976

Behnke, J.J., and G.B. Maxey, "An Empirical Method for Estimating Monthly Potential Evapotranspiration in Nevada," *Journal of Hydrology*, 8 1969, pp. 418–430.

Blanton, J.O., "Nevada Test Site Flood Inundation Study, Part of U.S. Geological Survey Flood Potential and Debris Hazard Study, Yucca Mountain Site," NNA.921125 0006, prepared by U S. Department of Interior, Bureau of Reclamation, for the U.S. Department of Energy, 1992

Bodvarsson, G.S., Y.S. Wu, and S. Finsterle, "Development and Calibration of the Three-Dimensional Site-Scale Unsaturated Zone Model of Yucca Mountain, Nevada. Temperature and Heat Flow Analysis," G. Bodvarsson, and T.M. Bandurraga, eds., LBNL-39315, Berkeley, CA, Lawrence Berkeley Laboratory, 1996, pp. 355–379.

Brown, T.P., L.L. Lehman, and J.L. Nieber, "Testing Conceptual Unsaturated Zone Flow Models for Yucca Mountain, Nye County, Nevada," *Proceedings of the Topical Meeting on Site Characterization and Model Validation: Focus '93*, La Grange Park, IL, American Nuclear Society, 1993, pp. 31–38.

Bullard, K.L., "Nevada Test Site Probable Maximum Flood Study, Part of U.S. Geological Survey Flood Potential and Debris Hazard Study, Yucca Mountain Site," NNA.921125.0006, prepared by U.S. Department of Interior, Bureau of Reclamation, for U.S. Department of Energy, 1992.

Cacas, et al., "Modeling Fracture Flow with a Stochastic Discrete Fracture Network: Calibration and Validation, 1. The Flow Model," *Water Resources Research*, 26(3), 1990, pp. 479-489.

CNWRA (Center for Nuclear Waste Regulatory Analyses) "NRC High-Level Radioactive Waste Research at CNWRA. July - December 1993" CNWRA 93-02S February 1994

CNWRA (Center for Nuclear Waste Regulatory Analyses). "NRC High-Level Radioactive Waste Program Annual Progress Report, Fiscal Year 1996." NUREG/CR-6513. No 1. November 1996

Coleman, N. M., R G. Wescott, and T L. Johnson, "Flooding of an Underground Facility at Yucca Mountain. A Summary of NRC Review Plans," *Proceedings of the Seventh Annual International Conference on High Level Radioactive Waste Management*, La Grange Park. IL, American Nuclear Society, 1996, pp. 205-207

Conrad, S.H., "Using Environmental Tracers to Estimate Recharge Through an Arid Basin," *Proceedings of the Fourth Annual High-Level Radioactive Waste Management*, La Grange Park, IL, American Nuclear Society, 1993, pp. 132–137

Czarnecki, J.B., "Simulated Effects of Increased Recharge on the Ground-Water Flow System of Yucca Mountain and Vicinity, Nevada-California," Water-Resources Investigations Report 84-4344, Denver, CO, U.S. Geological Survey, 1985

Czarnecki, J.B., "*Geohydrology and Evapotranspiration at Franklin Lake Playa, Inyo County, California*," USGS Open-File Report 90-356, Denver, CO, U.S. Geological Survey 1990

Czarnecki, J.B., and R.K. Waddell, "*Finite-Element Simulation of Groundwater Flow in the Vicinity of Yucca Mountain, Nevada-California*," Water-Resources Investigations Report 84-4349, Denver, CO, U.S. Geological Survey 1984

Czarnecki, J.B., et al., "Is There Perched Water Under Yucca Mountain in Borehole USW G-2," *Supplement to Eos, Transactions*, 75(44), Washington, DC, American Geophysical Union, 1994, pp. 249–250.

Czarnecki, J.B., P.H. Nelson, G.M. O'Brien, J.H. Sass, B. Thapa, Y. Matsumoto, and O. Murakami, "Testing in Borehole USW G-2 at Yucca Mountain: The Saga Continues," F190,F192, *In Supplement to Eos, Transactions*, 74(46), Washington, DC: American Geophysical Union, 1995.

DOE (U.S Department of Energy), "Study Plan for Characterization of the Yucca Mountain Regional Surface-Water Runoff and Streamflow," YMP-USGS-SP 8.3.1.2.1.2, Prepared by the U.S. Geological Survey for DOE, 1990.

DOE (U.S. Department of Energy), "Characterization of Future Regional Hydrology Due to Climate Changes," YMP-USGS-SP 8.3.1.5.2.2, Prepared by the U.S. Geological Survey for DOE, 1992.

DOE (U.S. Department of Energy), "Study Plan for Site Saturated-Zone Hydrologic System Synthesis and Modeling," YMP-USGS-SP 8.3 1 2.3.3, Prepared by the U.S. Geological Survey for DOE, 1993.

DOE (U S Department of Energy) "Total System Performance Assessment - 1995 A Evaluation of the Potential Yucca Mountain Repository " Prepared by TRW Environmental Safe Systems Inc for U S Dept of Energy Office of Civilian Radioactive Waste Managemen B00000000-01717-2200-00136 Rev 01 November 1995

DOE (U S Department of Energy) "[Draft] Highlights of the U S Department of Energy Updated Waste Containment and Isolation Strategy for the Yucca Mountain Site." Enclosure t a letter from S J Brocoum U S Department of Energy. to M V Federline. U S Nuclea Regulatory Commission. dated July 19. 1996

DOE (U.S Department of Energy). "Site Characterization Progress Report (No 15): Yucc Mountain, Nevada," DOE/RW-0498, April 1997

Eakin, T.E , G.B. Maxey, T.W. Robinson, J C. Fredericks. and O.J Loeltz, "Contributions to th Hydrology of Eastern Nevada," Bulletin 12, Carson City, NV Department of Conservation an Natural Resources, State of Nevada, 1951

EG&G, "Yucca Mountain Biological Resources Monitoring Program." Annual Report FY89 & FY90, 10617-2084, EG&G Energy Measurements, Goleta CA, 1991

EPRI (Electric Power Research Institute) "Demonstration of a Risk-Based Approach to High-Level Waste Repository Evaluation " EPRI NP-7057 Palo Alto, CA, 1990

EPRI (Electric Power Research Institute) "Demonstration of a Risk-Based Approach to High-Level Waste Repository Evaluation Phase 2," EPRI TR-100384 Palo Alto, CA, 1992

EPRI (Electric Power Research Institute), "Yucca Mountain Total System Performance Assessment, Phase 3," EPRI TR-107191, Palo Alto, CA, 1996

Fairley, J , and E. Sonnenthal, "Preliminary Conceptual Model of Flow Pathways Based on ^{36}Cl and Other Environmental Isotopes," G Bodvarsson, and T.M Bandurraga, eds., LBNL-39315, Berkeley, CA, Lawrence Berkeley Laboratory, 1996, pp 380–431

Fabryka-Martin, J.T , P R. Dixon, S Levy, B Liu, H J Turin, and A V. Wolfsberg, "Summary Report of Chlorine-36 Studies. Systematic Sampling for Chlorine-36 in the Exploratory Studies Facility," LA-UR-96-1384, Los Alamos, NM Los Alamos National Laboratory, 1996a.

Fabryka-Martin, J.T., H.J. Turin, A.V. Wolfsberg, D. Brenner, P.R. Dixon, and J.A. Musgrave, "Summary Report of Chlorine-36 Studies," LA-CST-TIP-96-003, Los Alamos, NM, Los Alamos National Laboratory, 1996b.

Finsterle, S., T.M. Bandurraga, C. Doughty, and G.S. Bodvarsson, "Simulation of Coupled Processes in a Two-Dimensional West-East Cross-Section of Yucca Mountain, Nevada," G Bodvarsson, and T.M. Bandurraga, eds., LBNL-39315, Berkeley, CA, Lawrence Berkeley Laboratory, 1996, pp. 463–495.

Flint, L.E., "Matrix Properties of Hydrogeologic Units at Yucca Mountain, Nevada," Open-File Report 96-xx [draft dated September 25, 1996], Denver, CO, U S. Geological Survey, 1996

Flint, L E and A L Flint "Preliminary Permeability and Water-Retention Data for Nonwelded and Bedded Tuff Samples Yucca Mountain Area Nye County Nevada " Open-File Report 90-569 Denver, CO U S Geological Survey 1990

Flint, A L , and L E Flint. "Spatial Distribution of Potential Near Surface Moisture Flux at Yucca Mountain." *Proceedings of the Fifth Annual International Conference on High-Level Radioactive Waste Management*. La Grange Park, IL. American Nuclear Society. 1994, pp 2 352–2,358

Flint, L E , and A L Flint. "Shallow Infiltration Processes at Yucca Mountain, Nevada—Neutron Logging Data 1984-93." Water-Resources Investigations Report 95-4035, Denver, CO, U S Geological Survey, 1995

Flint, A.L., L.E. Flint, and J A Hevesi, "The Influence of Long Term Climate Change on Net Infiltration at Yucca Mountain," *Proceedings of the Fourth Annual International Conference on High-Level Radioactive Waste Management*," La Grange Park, IL, American Nuclear Society, 1993, pp. 152–159

Flint, L.E , A L Flint, and J.A. Hevesi, "Shallow Infiltration Processes in And Watersheds at Yucca Mountain, Nevada," *Proceedings of the Fifth Annual International Conference on High-Level Radioactive Waste Management*. La Grange Park, IL. American Nuclear Society. 1994 pp. 2,315–2,322

Flint A.L , J.A. Hevesi, and L E Flint. "Conceptual and Numerical Model of Infiltration for the Yucca Mountain Area, Nevada." Water-Resources Investigations Report, Denver, CO, U S Geological Survey, 1996a

Flint, L.E., A.L Flint, C A Rautman, and J D Istok, "Physical and Hydrologic Properties of Rock Outcrop Samples at Yucca Mountain, Nevada," Open-File Report 95-280, Denver, CO. U S Geological Survey, 1996b

French, R.H., "Precipitation in Southern Nevada," *Journal of Hydraulic Engineering*, 109(7), 1983, pp 1,023–1,036

French, R.H., "Daily, Seasonal, and Annual Precipitation at the Nevada Test Site, Nevada," Publication No 45042, Reno, NV, Desert Research Institute, 1986.

French, R.H., R.L. Jacobson, and B F Lyles, "Threshold Precipitation Events and Potential Ground-Water Recharge," *Journal of Hydraulic Engineering*, 122(10), 1996, pp. 573–578.

Fridrich, C.J., W.W. Dudley, Jr., and J.S. Stuckless, "Hydrogeologic Analysis of the Saturated-Zone Ground-Water System Under Yucca Mountain, Nevada," *Journal of Hydrology*, 154, 1994, pp. 133–168.

Gauthier, J.H., "The Most Likely Groundwater Flux Through the Unsaturated Tuff Matrix at USW H-1," *Proceedings of the Fourth Annual International Conference on High Level Radioactive Waste Management*, La Grange Park, IL, American Nuclear Society, 1993, pp. 146–151

Gee, G.W., and D. Hillel, "Groundwater Recharge in Arid Regions: Review and Critique of Estimation Methods," *Hydrological Processes*, 2, 1988, pp. 255–266.

Gee, G.W., P.J. Wierenga, B.J. Andraski, M.H. Young, M.J. Fayer, and M.L. Rockhold, "Variations in Water Balance and Recharge Potential at Three Western Desert Sites," *Soil Science Society of America Journal*, 58(1), 1994, pp. 63–72.

Glancy, P.A., "Evidence of Prehistoric Flooding and the Potential for Future Extreme Flooding at Coyote Wash, Yucca Mountain, Nye County, Nevada," Open-File Report 92-458, Denver, CO, U.S. Geological Survey, 1994.

Guertal, W.R., A.L. Flint, L.L. Hofmann, and D.B. Hudson, "Characterization of a Desert Soil Sequence at Yucca Mountain, NV," *Proceedings of the Fifth Annual International Conference on High-Level Radioactive Waste Management*, La Grange Park, IL, American Nuclear Society, 1994, pp. 2,755–2763.

Hessing, M.B., G.E. Lyon, G.T. Sharp, W.K. Ostler, R.A. Green, and J.P. Angerer, "The Vegetation of Yucca Mountain: Description and Ecology," B00000000C-01717-5705-00030, Rev. 00, Las Vegas, NV, TRW Environmental Safety Systems Inc., 1996.

Hevesi, J.A., and A.L. Flint, "The Influence of Seasonal Climatic Variability on Shallow Infiltration at Yucca Mountain," *Proceedings of the Fourth Annual International Conference on High-Level Radioactive Waste Management*, La Grange Park, IL, American Nuclear Society, 1993, pp. 122–131.

Hevesi, J.A., and A.L. Flint, "Geostatistical Model for Estimating Precipitation and Recharge in the Yucca Mountain Region, Nevada—California," Water-Resources Investigations Report 96-4123, Denver, CO, U.S. Geological Survey, 1996 (in press).

Hevesi, J.A., D.S. Ambos, and A.L. Flint, "A Preliminary Characterization of the Spatial Variability of Precipitation at Yucca Mountain, Nevada," *Proceedings of the Fifth Annual International Conference on High-Level Radioac[illegible] Waste Management*, La Grange Park, IL, American Nuclear Society, 1994, pp. 2,520–2,529.

Hevesi, J.A., A.L. Flint, and J.D. Istok, "Precipitation Estimation in Mountainous Terrain Using Multivariate Geostatistics, Part II, Isohyetal Maps," *Journal of Applied Meteorology*, 31(7), 1992a, pp. 677–688.

Hevesi, J.A., J.D. Istok, and A.L. Flint, "Precipitation Estimation in Mountainous Terrain Using Multivariate Geostatistics, Part I, Structural Analysis," *Journal of Applied Meteorology* 31(7), 1992b, pp. 661–676.

Hevesi, J.A., A.L. Flint, and L.E. Flint, "Verification of a 1-Dimensional Model for Predicting Shallow Infiltration at Yucca Mountain," *Proceedings of the Fifth Annual International Conference on High-Level Radioactive Waste Management*, La Grange Park, IL, American Nuclear Society, 1994, pp. 2,323–2,332.

Hudson D B and A L Flint. "Estimation of Shallow Infiltration and Presence of Potential Fast Pathways for Shallow Infiltration in the Yucca Mountain Area Nevada Water-Resources Investigations Report 96 Denver CO U S Geological Survey 1996

Hudson, D B , A L Flint, and W R Guertal, "Modeling a Ponded Infiltration Experiment at Yucca Mountain, NV," *Proceedings of the Fifth Annual International Conference on High-Level Radioactive Waste Management*, La Grange Park, IL American Nuclear Society, 1994 pp 2,168–2,174

Istok, J.D., C A. Rautman, L E Flint, and A L Flint, "Spatial Variability in Hydrologic Properties of a Volcanic Tuff," *Ground Water*, 32(5), 1994, pp. 751–760

Jones, B.F., "Mineralogy of the Fine Grained Alluvium from Borehole U11g, Expl 1, Northern Frenchman Flat Area, Nevada Test Site," Open-File Report 82-765, Denver, CO, U S Geological Survey, 1982.

Klavetter, E.A , and R.R Peters, "Estimation of Hydrologic Properties of An Unsaturated, Fractured Rock Mass," SAND84-2642, Albuquerque, NM, Sandia National Laboratories, 1986

Kwicklis, E.M., A L Flint, and R W Healy, "Estimation of Unsaturated Zone Liquid Water Flux at Boreholes UZ#4, UZ #5, UZ #7, and UZ #13, Yucca Mountain, Nevada, from Saturation and Water Potential Profiles," *Proceedings of the Topical Meeting on Site Characterization and Model Validation: Focus '93*, La Grange Park, IL, American Nuclear Society, 1993, pp. 39–57

Lachenbruch, A H., and J H Sass, "Heat Flow in the United States and the Thermal Regime of the Crust," H G Heacock ed., *The Earth's Crust, Volume Geophysical Monograph 20*, Washington, DC, American Geophysical Union, 1977, pp. 626–675.

Lane, L J., and W.R. Osterkamp, "Estimating Upland Recharge in the Yucca Mountain Area," *Irrigation and Drainage Proceedings 1991*, American Society of Civil Engineers, 1991, pp 170–176.

Leary, K.D., "Analysis of Techniques for Estimating Potential Recharge and Shallow Unsaturated Zone Water Balance Near Yucca Mountain, Nevada," Ph D. thesis, Reno, NV, University of Nevada, 1990.

Levy, S.S., D.S. Sweetkind, J.T. Fabryka-Martin, P.R. Dixon, J.L. Roach, L.E. Wolfsberg, D. Elmore, and P. Sharma, "Investigations of Structural Controls and Mineralogic Associations of Chlorine-36 Fast Pathways in the ESF," LA-EES-1-TIP-97-004, Los Alamos, NM, Los Alamos National Laboratory, 1997.

Long, A., and S.W. Childs, "Rainfall and Net Infiltration Probabilities for Future Climate Conditions at Yucca Mountain," *Proceedings of the Fourth Annual International Conference on High-Level Radioactive Waste Management*, La Grange Park, IL, American Nuclear Society, 1993, pp. 112–121.

Lundstrom S C and E M Taylor. "Preliminary Surficial Deposits Map of the Southern Half of the Topopah Spring NW 7 5-Minute Quadrangle Scale 1 12.000." USGS Open-File Report 95-134, Denver, CO. U S Geological Survey. 1995

Lundstrom. S C S A Mahan. and J B Paces. "Preliminary Surficial Deposits Map of the Northwest Quarter of the Busted Butte 7 5-Minute Quadrangle. Scale 1 12 000." USGS Open-File Report 95-133, Denver, CO. U S Geological Survey 1996 (In press)

Lundstrom, S C , J R Wesling, E M Taylor, and J B Paces, "Preliminary Surficial Deposits Map of the Northeast Quarter of the Busted Butte 7 5-Minute Quadrangle. Scale 1.12,000." USGS Open-File Report 94-341, Denver, CO, U S. Geological Survey, 1994

Lundstrom, S.C., J.W. Whitney, J.B. Paces, S.A. Mahan, and K.R. Ludwig, "Preliminary Surficial Deposits Map of the Southern Half of the Busted Butte 7.5-Minute Quadrangle. Scale 1 12,000." USGS Open-File Report 95-131, Denver, CO, U.S. Geological Survey, 1995

Malmberg, G T., and T.E Eakin, "Hydrology of the Valley-Fill and Carbonate-Rock Reservoirs, Pahrump Valley, Nevada-California," Water-Supply Paper 1832, U.S Geological Survey, 1962

Maxey, G.B , and T.E Eakin, "Ground Water in White River Valley, White Pine, Nye, and Lincoln Counties, Nevada " Bulletin 8, Carson City NV. Department of Conservation and Natural Resources, State of Nevada, 1949

McKenna, S.A , and C A Rautman. "Summary Evaluation of Yucca Mountain Surface Transects with Implications for Downhole Sampling." SAND94-2038, Albuquerque NM. Sandia National Laboratories, 1995

Montazer, P., E P Weeks, F. Thamir, D Hammermeister, S.N. Yard, and P.B. Hofrichter. "Monitoring the Vadose Zone in Fractured Tuff." *Ground Water Monitoring Review* 8(2), 1988, pp. 72–88.

Moyer, T.C., J.K. Geslin, and L.E Flint, "Stratigraphic Relations and Hydrologic Properties of the Paintbrush Tuff Nonwelded (PTn) Hydrologic Unit, Yucca Mountain, Nevada," USGS Open-File Report 95-397, Denver, CO, U S Geological Survey, 1996.

Murphy, W. M., "Commentary on Studies of Cl-36 in the Exploratory Studies Facility at Yucca Mountain, Nevada," Center for Nuclear Waste Regulatory Analyses, San Antonio, TX, 1997.

Nichols, W.D , "Geohydrology of the Unsaturated Zone at the Burial Site for Low-Level Radioactive Waste Near Beatty, Nye County, Nevada," Water-Supply Paper 2312, Denver, CO, U.S.Geological Survey, 1987.

Nimmo, J R., D.A. Stonestrom, and K.C. Akstin, "The Feasibility of Recharge Rate Determinations Using the Steady-State Centrifuge Method," *Soil Science Society of America Journal*, 58(1), 1994, pp. 49–56.

Norris A E K Wolfsberg. S K Gifford H W Bentley and D Elmore "Infiltration at Yucca Mountain. Nevada. traced by ^{36}Cl." *Nuclear Instruments and Methods in Physics Research.* B29 1987 pp. 376–379

NRC (U.S. Nuclear Regulatory Commission). "NRC Staff Site Characterization Analysis of the Department of Energy's Site Characterization Plan. Yucca Mountain Site. Nevada," NUREG-1347. Division of High-Level Waste Management. Washington. DC. 1989

NRC (U S Nuclear Regulatory Commission). "Initial Demonstration of the NRC's Capability to Conduct a Performance Assessment for a High-Level Waste Repository," NUREG-1327, Division of Waste Management. Washington. D.C , 1992

NRC (U.S. Nuclear Regulatory Commission). "NRC Iterative Performance Assessment Phase 2 - Development of Capabilities for Review of a Performance Assessment for a High-Level Waste Repository," NUREG-1464, 1995a.

NRC (U.S. Nuclear Regulatory Commission). "[Draft] Open Item Status Report," Prepared for the U S Nuclear Regulatory Commission by the Center for Nuclear Waste Regulatory Analyses. San Antonio, TX. 1995b

NRC (U S Nuclear Regulatory Commission). "Branch Technical Position on the Use of Expert Elicitation in the High-Level Radioactive Waste Program," NUREG-1563 November 1996

NRC (U S. Nuclear Regulatory Commission) "Issue Resolution Status Report on Methods to Evaluate Climate Change and Associated Effects at Yucca Mountain." Attachment to a letter from N K. Stablein (NRC) to S Brocoum (DOE). dated June 30. 1997. 37 pp.

O'Farrell. T.P., and L A. Emery. "Ecology of the Nevada Test Site: A Narrative Summary and Annotated Bibliography," NVO-167. Boulder City. NV Desert Research Institute. 1976.

O'Farrell. T.P . and E. Collins. "1982 Biotic Studies of Yucca Mountain. Nevada Test Site. Nye County. Nevada," 10282-2004. Goleta. CA. EG&G Energy Measurements. 1983.

Osterkamp. W.R., L.J. Lane. and C S. Savard. "Recharge Estimates Using a Geomorphic/Distributed-Parameter Simulation Approach. Amargosa River Basin," *Water Resources Bulletin.* 30(3). 1994. pp. 493–507

Pabst. M.E., D.A. Beck. P.A Glancy. and J.A. Johnson. "Streamflow and Selected Precipitation Data for Yucca Mountain and Vicinity. Nye County. Nevada. Water Years 1983–85," USGS Open-File Report 93-438. Carson City. NV. U.S. Geological Survey. 1993.

Paces. J.B L.A. Neymark. B.D. Marshall. J.F. Whelan. and Z.E Peterman. "Ages and Origins of Subsurface Secondary Minerals in the Exploratory Studies Facility (ESF)," Report 3GQH450M. Denver. CO. U.S. Geological Survey. 1996

Peters. R.R., E.A. Klavetter. I.J. Hall. S C. Blair. P R. Heller. and G.W. Gee., "Fracture and Matrix Hydrologic Characteristics of Tuffaceous Materials from Yucca Mountain. Nye County. Nevada," SAND84-1471. Albuquerque. NM: Sandia National Laboratories. 1984

Phillips, F.M., "Environmental Tracers for Water Movement in Desert Soils of the American Southwest," *Soil Science Society of America Journal* 58(1) 1994, pp 15–24

PNL (Pacific Northwest Laboratory), "Preliminary Total-System Analysis of a Potential High-Level Nuclear Waste Repository at Yucca Mountain," PNL-8444, Richland WA, 1993

Quiring, R.F., "Precipitation Climatology of the Nevada Test Site," National Weather Service Report WSNSO 351-88, Asheville, NC, National Oceanic and Atmospheric Administration, 1983

Rautman, C.A., and A.L. Flint, "Deterministic Geologic Processes and Stochastic Modeling," SAND91-1925C, Albuquerque, NM, Sandia National Laboratories, 1992.

Rautman, C.A., L.E. Flint, A.L. Flint, and J.D. Istok, "Physical and Hydrologic Properties of Rock Outcrop Samples From a Nonwelded to Welded Tuff Transition, Yucca Mountain, Nevada," Water-Resources Investigations Report 95-4061, Denver, CO, U.S. Geological Survey, 1995.

Robinson, B.A., A.V. Robinson, C.W. Gable, and G.A. Zyvoloski, "An Unsaturated Zone Flow and Transport Model of Yucca Mountain," YMP Milestone 3468, Los Alamos, NM, Los Alamos National Laboratory, 1996

Rousseau, J.P., E.M. Kwicklis, and D.C. Gillies, eds., "Hydrogeology of the Unsaturated Zone, North Ramp Area of the Exploratory Studies Facility, Yucca Mountain, Nevada," Water-Resources Investigations Report, Denver, CO, U.S. Geological Survey, 1996.

Rush, F.E., "Regional Ground-Water Systems in the Nevada Test Site Area, Nye, Lincoln, and Clark Counties, Nevada," Water Resources Reconnaissance Series Report 54, Carson City, NV, Department of Conservation and Natural Resources, State of Nevada, 1970.

Sass, J.H., and A.H. Lachenbruch, "Preliminary Interpretations of Thermal Data from the Nevada Test Site," USGS Open-File Report 82-973, Reston, VA, U.S. Geological Survey, 1982.

Sass, J.H., A.H. Lachenbruch, and C.W. Mase, "Analysis of Thermal Data From Drill Holes UE25a-3 and UE25a-1, Calico Hills and Yucca Mountain, Nevada Test Site," USGS Open-File Report 80-826, Menlo Park, CA, U.S. Geological Survey, 1980.

Sass, J.H., A.H. Lachenbruch, W.W. Dudley, Jr., S.S. Priest, and R.J. Munroe, "Temperature, Thermal Conductivity, and Heat Flow Near Yucca Mountain, Nevada: Some Tectonic and Hydrologic Implications," USGS Open-File Report 87-649, Denver, CO, U.S. Geological Survey, 1988.

Savard, C.S., "Ground-Water Recharge in Fortymile Wash Near Yucca Mountain, Nevada, 1992–93," *Proceedings of the Fifth Annual International Conference on High-Level Radioactive Waste Management*, La Grange Park, IL, American Nuclear Society, 1994, pp. 1,805–1,813.

Savard, C.S., "Selected Hydrologic Data From Fortymile Wash in the Yucca Mountain Area, Nevada, Water Year 1992," USGS Open-File Report 94-317, Denver, CO, U.S. Geological Survey, 1995.

Schenker. A R D C Guenn T H Robey C A Rautman and R W Barnard "Stochastic Hydrogeologic Units and Hydrogeologic Properties Development for Total-System Performance Assessments." SAND94-0244. Albuquerque. NM Sandia National Laboratories 1995

Schmidt. M R . "Classification of Upland Soils by Geomorphic and Physical Properties Affecting Infiltration at Yucca Mountain. Nevada." Master s thesis. Colorado State University 1989

Shevenell, L . "Statewide Potential Evapotranspiration Maps for Nevada." Nevada Bureau of Mines and Geology. Report 48. University of Nevada. 1996

SNL (Sandia National Laboratories). "TSPA 1991 An Initial Total-System Performance Assessment for Yucca Mountain." SAND91-2795. Albuquerque. NM. 1992.

Stephens. D.B . "A Perspective on Diffuse Recharge Mechanisms in Areas of Low Precipitation." *Soil Science Society of Ameri... ...rnal*. 58(1). 1994. pp 40–48

Stotnoff. S A.. "Sensitivity of Long-Term Bare Soil Infiltration Simulations to Hydraulic Properties in an Arid Environment." *Water Resources Research*. 33(4). 1997. pp 547–558

Stothoff. S A.. H M Castellaw. and A C Bagtzoglou. "Simulating the Spatial Distribution of Infiltration at Yucca Mountain. Nevada." San Antonio. TX Center for Nuclear Waste Regulatory Analyses. sent under letter from E Pearcy (CNWRA) to N Coleman (NRC). dated July 3 1996

Stothoff. S.A. and J R Winterle. "Trip Report - Trip to Yucca Mountain for Hydrology Field Work " Documenting trip to Yucca Mountain (March 26-28 1997) by staff and contractors of the Center for Nuclear Waste Regulatory Analyses. San Antonio. TX. dated April 9. 1997. 6 pp

Titus. J. G. and V. K Narayanan. "The Probability of Sea Level Rise." The U.S. Global Change Research Information Office (GCRIO). U S EPA. 1995 [this U S. Environmental Protection Agency document is available at the following internet web site http //www gcrio org/EPA/sealevel/text.html]

Tyler. S.W.. "Review of Soil Moisture Flux Studies at the Nevada Test Site. Nye County. Nevada." Publication no. 45058. Reno. NV. Desert Research Institute. 1987.

Tyler. S.W.. J.B. Chapman. S.H. Conrad. and D. Hammermeister. "Paleoclimatic Response of a Deep Vadose Zone in Southern Nevada. USA. as Inferred from Soil Water Tracers." *Applications of Tracers in Arid Zone Hydrology. Proceedings of the Vienna Symposium. Volume* 232. Vienna. Austria. International Association of Hydrological Sciences. 1995. pp. 351–361.

Tyler. S.W.. and R.L. Jacobson. "Soil Moisture Flux Studies on the Nevada Test Site: A Review of Results an: Techniques." *Hydraulics/Hydrol: gy of Arid Lands. Proceedings of the Internationa: Symposium*. American Society of Civil Engineers. 1990. pp. 718–724.

Tyler. S.W.. and G.R. Walker. "Root Zone Effects on Tracer Migration in Arid Zones." *Soil Science Society of America Journal*. 58(1). 1994. pp. 25–31

Waddell R K J H Robison and R K Blankennagel "Hydrology of Yucca Mountain and Vicinity Nevada-California—Investigative Results Through Mid-1983" Water-Resources Investigations Report 84-4267 Denver, CO. U S Geological Survey 1984

Wallace, A., and E M Romney. "Radioecology and Ecophysiology of Desert Plants at the Nevada Test Site." TID-25954, Riverside, CA, University of California, 1972

Watson, P., P Sinclair, and R Waggoner. "Quantitative Evaluation of a Method for Estimating Recharge to the Desert Basins of Nevada," *Journal of Hydrology*, 31, 1976, pp. 335–348

Winograd, I.J., and G.C. Doty, "Paleohydrology of the Southern Great Basin with Special Reference to Water Table Fluctuations Beneath the Nevada Test Site During the Late (?) Pleistocene," USGS Open-File Report 80-569, Reston, VA, U.S Geological Survey, 1980.

Wolfsberg, A.V., B.A. Robinson, and J.T. Fabryka-Martin, "Migration of Solutes in Unsaturated Fractured Rock at Yucca Mountain: Measurements, Mechanisms, and Models," *Scientific Basis for Nuclear Waste Management XIX*, W M. Murphy and D A Knecht, eds., Pittsburgh, PA, Materials Research Society, Symposium Proceedings, 412, 1996, pp 707–714

Yang, I C., G W Rattray, and P Yu, "Interpretations of Chemical and Isotopic Data from Boreholes in the Unsaturated Zone at Yucca Mountain, Nevada," Water Resources Investigations Report 96-4058, Denver, CO, U S Geological Survey, 1996.

APPENDIX A

DRAFT FIGURE ILLUSTRATING ELEMENTS OF THE NRC STAFF'S TOTAL SYSTEM PERFORMANCE ASSESSMENT

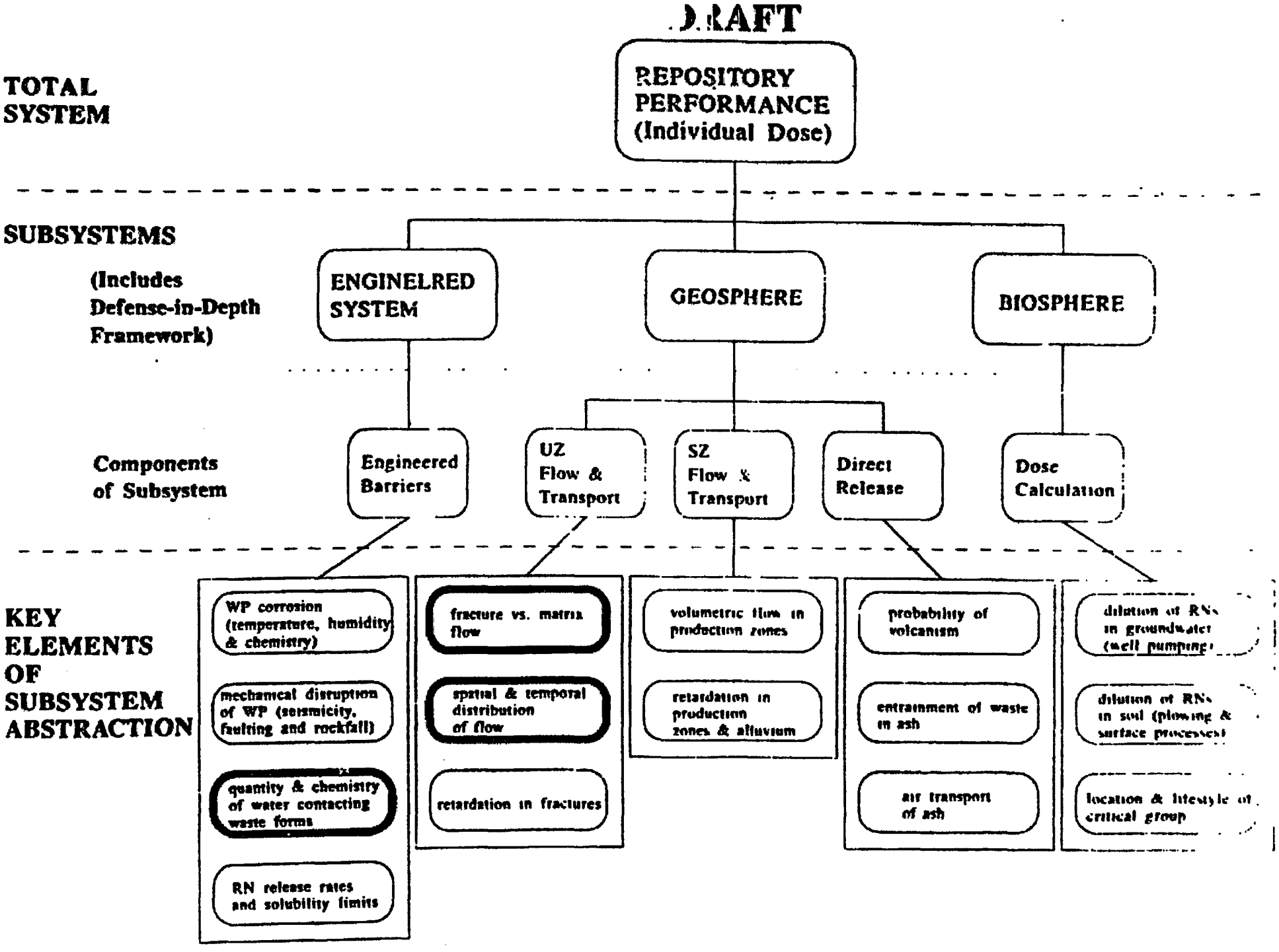

Figure A-1. Flowdown diagram for total system performance assessment. The subissue of "Present-Day

APPENDIX B

CONCEPTUAL MODEL OF INFILTRATION AT YUCCA MOUNTAIN

CONTROLLING INFLUENCES ON NET INFILTRATION

Net infiltration is one component of a general water-balance equation that is usefully written for a control volume that extends from the ground surface to a depth below the rooting zone Descriptions of the water-balance equation and example applications are provided by any soil-science textbook [e.g. Jury, et al. (1991) and Hillel (1980)]; Flint, et al. (1996) provides a description that is specific to Yucca Mountain (YM). The water balance for the control volume over a specified period of time can be written

$$P + A - I_{net} + O_{net} + L_{net} + R_{net} - E_{net} - T = \Delta S_a + \Delta S_b + \Delta S_p$$

where

- P - net precipitation (including rain, snow, dew, and frost)
- A - applied moisture (human induced)
- I_{net} - net infiltration (liquid and vapor flow across the bottom of the control volume)
- O_{net} - net overland flow (runon and runoff)
- L_{net} - net lateral subsurface flow (liquid and vapor)
- R_{net} - net lateral subsurface root flow
- E_{net} - net vapor transport out of the top of the system (excluding transpiration)
- T - transpiration
- ΔS_a - change in above-ground storage
- ΔS_b - change in below-ground storage
- ΔS_p - change in plant-biomass storage

A schematic diagram of the components of the water balance equation is shown in figure B-1.

Depending on the time period of interest and the location of the control volume, some of the components may be negligible (i.e., changes in storage; human-induced moisture). Over long time periods (decades to centuries), net infiltration is typically only a small component of the water balance [e.g., a few percent or less (Maxey and Eakin, 1949; Montazer and Wilson, 1984; Watson, et al., 1976; Winograd and Thordarson, 1975)], particularly in arid and semiarid environments such as occur at YM. Factors to consider when evaluating components of the water-balance equation are discussed in the following subsections.

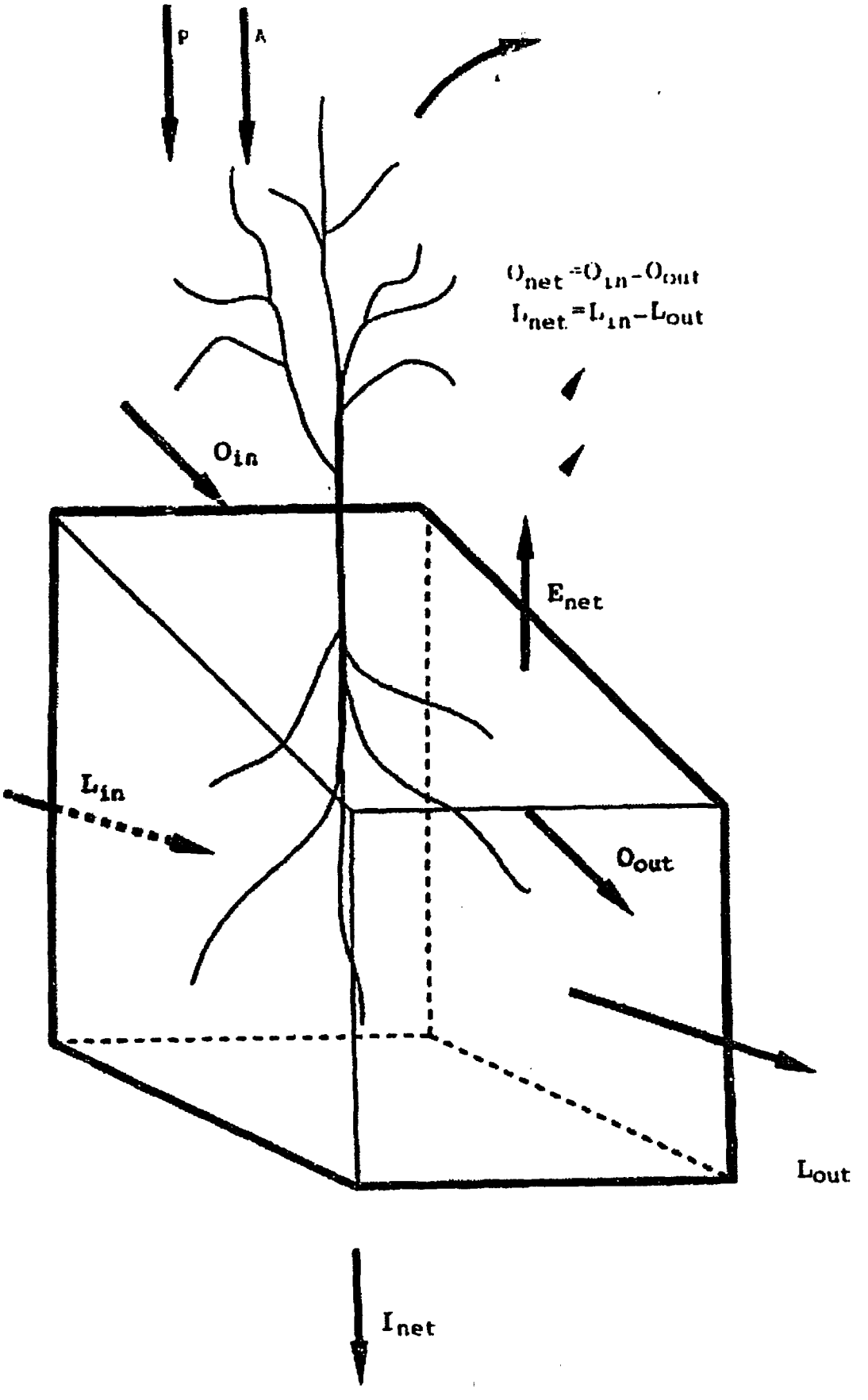

Figure B-1. Schematic diagram of the components of the water balance equation.

PRECIPITATION

Precipitation is one of the most significant factors in determining net shallow infiltration as precipitation is the source of infiltrating water Flint, et al (1996) provide a good qualitative description of precipitation processes active at YM Historical precipitation records are available for a number of locations in the YM area, including Beatty, Lathrop Wells, Mercury, and locations within the Nevada Test Site Mean annual precipitation generally increases with elevation and is affected by the rain shadow of the Sierra Nevada and other mountain ranges. Mean annual precipitation data in the YM region is summarized by Hevesi, et al. (1992) and references therein. At YM, mean annual precipitation under current climatic conditions is generally reported to be in the range of 150 to 170 mm/yr.

Precipitation at YM is seasonal, with winter precipitation consisting predominantly of frontal storms that cover large areas, while summer precipitation consists predominantly of convective storms that may be quite local. Winter storms are controlled by storm tracks that are set up by the position of the jet stream, and may be strongly influenced by global circulation patterns that are in turn influenced by the El Niño Southern Oscillation. As shown by Hessing, et al. (1996), annual precipitation at United States Geological Survey (USGS) weather station 4JA, near YM, is highly cyclic over the 35-yr period of record from water year 1961 through 1995, supporting assertions that oscillations such as the El Niño events drive precipitation. The record also suggests that wet years are getting wetter

Flint, et al (1994) notes that summer storms can produce runoff in one wash while the next wash receives no rainfall; summer storms are generally less than 10 km in radius and have total precipitations of tens of mm to as much as 100 mm (Flint, et al., 1996). Regression equations presented by French (1986) suggest that precipitation is about 2.5 times more strongly affected by elevation in the summers than in the winters, which may be explained by the phenomenon of virga (evaporation of rain while falling)

Under current climatic conditions, snow occurs at the higher elevations and can remain on the ground for several weeks (Flint, et al., 1994). Under cooler conditions, snow might accumulate to greater depths and for longer periods of time, perhaps serving as an efficient source of infiltrating water (Gee and Hillel, 1988).

In arid and semiarid areas, it is commonly accepted that recharge may not occur every year Instead, an occasional exceptionally large precipitation event or series of events allows moisture to move below the evapotranspiration trap (Barnes, et al., 1994; French, et al., 1996; Gee and Hillel, 1988; Gee, et al., 1994; Lane and Osterkamp, 1991; Phillips, 1994), particularly when the precipitation occurs when evapotranspiration demands are low. Precipitation is known to be highly variable in the YM area; for example, at Beatty annual precipitation ranged from 1.8 to 26.3 cm in the period of 1949 to 1979, and at Lathrop Wells recorded precipitation ranged from 2.4 to 13.4 cm in the same period (Nichols, 1987). As a corollary, it may be most important to properly characterize the return period and magnitude of these anomalous types of events, rather than magnitudes and frequencies of small and isolated medium-size events.

The historical record does not extend more than 50 yr in the vicinity of YM, so it is difficult or impossible to defensibly characterize events with long return periods. Most of the historical record consists of daily precipitation totals, while most events occur on time scales of minutes

to hours For winter storms, with low evapotranspiration demands and longer-duration events daily records are more representative than for the typically much shorter and more intense summer storms

EVAPOTRANSPIRATION

Evaporation is the process of vapor transfer from the soil surface to the atmosphere, while transpiration is the process of vapor transfer from plants to the atmosphere. Evaporation and transpiration are commonly lumped into a single term for convenience. It is physically possible for vapor to transfer from the atmosphere to the soil surface (e g , dew, frost), however, it is difficult to conceive of a situation at YM where any net infiltration will occur due to this reversed vapor transfer.

Evaporation occurs under two conditions: (i) climate limited, where sufficient moisture exists at the ground surface to evaporate as fast as the atmosphere will accept it; and (ii) soil limited, where the ability of the soil to deliver moisture to the ground surface is the rate-limiting factor Evaporation typically occurs in the top few centimeters of the ground

Potential evapotranspiration is the amount of water that could be evaporated under climate-limited conditions, reported as 876 mm/yr by Flint, et al. (1996) and estimated by Shevenell (1996) to be approximately 1,200 to 1,500 mm/yr Nichols (1987) reports that pan evaporation at the low-level waste site near Beatty probably exceeds 2,500 mm/yr and measured pan evaporation at Boulder City, NV, is 2,800 mm/yr. If all precipitation was subject to evaporation at the potential rate, clearly no net infiltration could occur at YM

Climatic controls on evaporation include temperature, net solar radiation, net longwave radiation, atmospheric vapor density, and windspeed. Evaporation flux is from higher to lower vapor density. Relative humidity is the ratio of the actual vapor density to the maximum possible vapor density for the same gas temperature Typically the relative humidity of the soil is almost 100 percent unless the soil is quite dry, while the relative humidity of the atmosphere is significantly less than 100 percent. The larger the gradient, the faster that evaporation can take place. The relative humidity of the atmosphere is largest during winter months and smallest during the summer months. Therefore, evaporative demand is least in the winter and greatest in the summer.

The rate at which evaporation takes place is also controlled by the vapor conductance. The vapor diffusion conductance increases as atmospheric turbulence in the surface boundary layer increases, which in turn increases as the windspeed increases. Also, the less stable the atmosphere is, the larger the conductance. Atmospheric instability is fostered by a hot ground surface relative to the atmosphere, so that the vapor conductance is larger in regions where relatively more net radiation is available to heat the ground. Accordingly, south-facing slopes with their increased solar load have an increased evaporative demand over north-facing slopes and would be expected to have a smaller net infiltration. The difference in evaporation from north-facing and south-facing slopes may only be a few percent; however, the difference between 98 percent and 99 percent removal of precipitation through evaporation translates into a factor of 2 change in net infiltration.

Coarse materials at the ground surface can limit evaporation by providing shelter from winds. For example, studies presented by Kemper et al (1994) comparing evaporative losses from bare soil and soil covered by sand or gravel mulches indicate that while bare soil had about 81 percent of applied moisture evaporated, only 15 to 19 percent evaporated when the same type of soil was covered with 5 cm of gravel. Scree slopes at YM may be local areas where significant net infiltration could occur unless adjacent vegetation is able to take advantage of the moisture. Desert vegetation does not grow within scree piles because desert vegetation is typically adapted to growing with sunlight almost immediately available upon germination and does not have the energy reserves to reach sunlight from deep within a scree pile[1]

Barometric pumping, thermosyphons, and windpumping are other ways vapor can be exchanged with the atmosphere. Barometric pumping refers to short-term gas-flow cycles induced by barometric-pressure variation in the atmosphere, and can occur in both soil and fractured-rock outcrops. A thermosyphon refers to a circulation pattern in the soil due to temperature-induced pressure differences between atmospheric and rock gases, where dry atmospheric air enters at one end of the syphon and moist rock air exits at the other end, and requires a significant difference in elevation. Windpumping occurs due to the airfoil effect of wind being forced to move around a barrier. Both thermosyphons and windpumping are expected to occur primarily on Yucca Crest and ridges east of Yucca Crest. Measurements and simulations assessing the magnitude of gas flow through these mechanisms are discussed by Patterson, et al (1996). The calculated net exchange of moisture through these effects is on the order of 0.02 mm/yr (E. Weeks, presentation at the U.S. Department of Energy's (DOE's) Unsaturated Zone Expert Elicitation Workshop, February 4, 1997). All of these mechanisms exchange gas between the atmosphere and the soil, thus may be effectively removing vapor from below the root zone.

Transpiration is a significant process for removing soil moisture. Desert shrubs can be extremely efficient at removing water stored in a soil column, as demonstrated by lysimeter studies at Beatty, Nevada, and at the Hanford site (Gee, et al., 1994). The effectiveness of desert vegetation at removing water from shallow soils over fractured bedrock has not been established to date, due to the difficulty in performing measurements.

The vegetation at YM is transitional between Mojave and Great Basin associations (Flint, et al., 1996), with Mojave species (bursage and range rhatany) dominating on the warmer south-facing slopes and Great Basin species (yellow rabbitbrush, green ephedra, big sagebrush, and burrobrush) dominating on the cooler north-facing slopes. As soils change from deep, loose, and sandy to rockier but still relatively flat to steep and shallow, the vegetation associations change from the *larrea-ambrosia* association (creosote bush and bursage) to the *larrea-lycium-grayia* association (creosote bush, desert thorn, and spiny hopsage) to the *lycium-grayia* association. The Great Basin *coleogyne* association (blackbrush) dominates in cooler and flatter areas, particularly where lateral flow provides additional moisture. The pinyon-juniper association is not found in the immediate repository area but can be found at higher elevations, on Shoshone Mountain about 18 km northeast the proposed repository, and might be expected to move south in cooler climatic conditions. An isolated population of junipers currently exists on the Prow just north of the repository site. The general description of vegetation distributions is adapted from that presented by Flint, et al. (1996) based on a cursory confirmatory field survey.

---

[1] D. Groeneveld, oral communication, 1997

Characterization of transpiration patterns due to desert vegetation is currently somewhat poorly constrained Little site-specific measurement of transpiration has been attempted with most efforts concentrating on describing plant dynamics rather than water-uptake dynamics Available information on rooting depths is typically obtained under conditions where the roots are not constrained by bedrock, while the presence of bedrock and bedrock fissures is strongly constraining on ridgetops and sideslopes There is a strong seasonality component to desert vegetation with the growing season synchronized within the autumn-winter-spring period Annuals can respond within weeks to significant soil moisture An invading alien species, cheatgrass, tends to be most active in the winter

Mathematical relationships describing transpiration are most fully developed for areas with deep soil and are most poorly characterized in areas with shallow, rocky soil, particularly with bedrock constraints on roots For comparison, estimates of bare-soil net infiltration tend to be relatively small in deep soils and relatively high in shallow soils (Stothoff, 1997).

Relationships between precipitation, plant biomass, edaphic constraints, phenologic constraints, seasonality, soil moisture distributions, and transpiration are more qualitative in nature than quantitative, although some phenologic events have predictable outcomes For example, a significant rainfall (greater than 25 mm) in late September through early December is a good predictor of seasonal activity through the spring, while lack of such a rainfall causes perennial plants to remain dormant from March through May and annual plants to be absent (Beatley 1974) Drought periods can dramatically change the percent cover of the species as well (Flint, et al., 1996) with the implication that the first rainy period subsequent to a drought has reduced vegetation available for transpiration

MOISTURE REDISTRIBUTION

Moisture redistribution can be conveniently partitioned into vertical and lateral redistribution. Vertical redistribution is the component of flow that contributes to net shallow infiltration. Lateral redistribution can be defined as any nonvertical flow [above the representative elementary volume (REV) scale]. Lateral redistribution can occur as overland flow, where water is moving across the ground surface, or it can occur in the soil matrix. Lateral redistribution can be a concentrating mechanism, increasing effective precipitation in local areas (e.g., wash channels, local depressions, fractures), or it can be a dissipating mechanism, decreasing effective precipitation (e.g., ridgetops). Barring capillary effects, the more permeable that a medium is, the less lateral redistribution occurs.

When considering wetting-front penetration during a rainfall event, important factors include K_{sat} (governing how fast water can infiltrate relative to rainfall rate); porosity (governing how deep a wetting pulse can move); and depth to a restricting layer (governing the total volume of water that can infiltrate before runoff occurs). The last two factors are often multiplied to yield storage capacity. Low-permeability rocks within a soil matrix effectively reduce the porosity and thus the storage capacity At the time scales of infiltration events (minutes to days), the matrix of a fractured low-permeability bedrock has minimal effect on flow and the fractured medium can be considered to have very low porosity and thus low storage capacity.

For small to medium storms soils with a high storage capacity tend to return the infiltrated water to the atmosphere through evapotranspiration while soils with a low storage capacity above a fractured bedrock may have some water enter the fractures and escape downward as net infiltration On the other hand, if the fractures in the low storage-capacity area have restricted K and flow concentration occurs in the high storage-capacity area (i e , wash channels), large events may cause water to penetrate below the evapotranspiration zone in the areas with large storage capacity and yield more net infiltration than in the low storage-capacity areas for the same event

The primary cause of overland flow is when the ground cannot accept water at the rate of precipitation, so the excess water either locally concentrates or flows downhill After an equilibration period where capillary effects are dominant, a porous medium accepts water due to gravity, with a maximum rate of K_{sat}. An intense storm might have intensities of over 100 mm/hr for 5 minutes, but only infrequently will average precipitation over an hour be more than 25 mm [based on depth-duration frequency curves presented by French (1983)]

Welded tuff typically has very low K_{sat} on the order of 10^{-8} to 10^{-1} mm/hr (Flint, 1996) so that overland flow is expected wherever unfractured welded tuffs crop out Nonwelded tuff typically has higher K_{sat} on the order of 10^{-1} to 10 mm/hr (Flint, 1996) so that overland flow is also expected for at least some precipitation events wherever nonwelded tuffs crop out

Flint, et al (1996) asserts that 2 5, 25, and 250 μm fractures have K_{sat} values of about 20, 650, and $3\ 1 \times 10^{5}$ mm/hr, respectively while fracture-fill materials are reported to have K_{sat} values that average about 1 8 mm/hr Open fractures of an appreciable size should limit overland flow if the fractures intercept a rivulet, while a filled fracture would not appreciably limit overland flow The upper washes east of Yucca Crest and the west flank of YM are likely candidates for exposed fractures

Soils at YM have similar compositions for all environments (Schmidt, 1989). YM soils tend to have higher K_{sat} than tuffs or fracture-fill materials, with estimated values based on texture analysis of about 20 mm/hr (Schmidt, 1989) or on the order of 20 to 140 mm/hr (Flint, et al, 1996) with measured values of as much as 500 mm/hr (Guertal, et al., 1994), and with wash channels having as much as 2,500 mm/hr (trip report by S Stothoff and J. Winterle, 1997), so runoff would only occur for intense storms or for cases where the soils become saturated due to contact with bedrock or other impeding layers such as carbonate deposits (caliche). Note that considerable volumes of water can be imbibed into wash channel soils when the wash is flowing.

Another source of overland flow is when lateral subsurface flow moves from topographic highs to topographic lows and emerges as a permanent or intermittent spring, then moves off downhill At YM, no permanent springs exist and intermittent springs would be most likely to occur at the base of sideslopes

Lateral subsurface flow tends to occur whenever there is

- a focused source of water (e g , washes),
- heterogeneity and layering,
- and a soil-rock interface, particularly when the interface is tilted

Even in apparently homogeneous media there can be lateral movement of water (McCord and Stephens 1987) due to microtextural effects however other factors should be far more significant for lateral subsurface flow at YM

A significant focused source of water at YM occurs when water is flowing in wash channels due to overland flow Where soils are shallow or nonexistent fractured bedrock is exposed to flowing water and any open fractures would be expected to flow at full capacity Where soils exist, water would be expected to imbibe radially at early times, due to capillary forces, and relatively quickly (due to the relatively coarse materials in wash channels) convert to predominantly vertical flow If sufficient water imbibes that a wetting pulse contacts the soil-bedrock interface, lateral flow along the interface would be expected to take place According to Flint, et al. (1996) channels cover about 2 percent of the surface area, so that lateral flow due to a channel source should be a relatively local phenomenon

Another focused source of water occurs when water runs off of exposed bedrock into a local depression (e g., a pocket of soil or a fracture). The local wetting front is then deeper than would otherwise have been the case and water is likelier to drain below the evapotranspiration zone Significant focusing through this mechanism should be most likely along Yucca Crest and on the west flank of YM

Due to the relatively large K_{sat} values for soils at YM and the relatively shallow soils everywhere but in washes, soil heterogeneity and soil layering are not expected to strongly impact moisture redistribution except, perhaps, in deep alluvium Calcium carbonate (caliche) layers, however have the potential to strongly impact redistribution Well-developed caliche is observed at YM in earth flow and colluvial deposits on steep slopes in low positions (Schmidt, 1989). In soils caliche layers tend to form in the root zone from calcium in eolian dust (Schlesinger, 1985) and were more likely to have formed during a wetter Pleistocene with cooler winters than under current climatic conditions (Marion, et al., 1985) Depth of caliche-layer formation is strongly affected by the depth of wetting pulses from extreme precipitation events (Marion, et al., 1985) Reported values for caliche K_{sat} are generally on the order of 40 to 120 mm/hr (Baumhardt and Lascano, 1993), so that no runoff can be expected for most precipitation events; however, strong capillary barriers to flow may form (Hennessy, et al., 1983), which would tend to hold water in the evapotranspiration zone and lower net infiltration

At YM, carbonate contents are generally less than 5 percent of the fine fraction (<2 mm) of soils deposited since the late Holocene and are associated with thin coats on clast undersides, while late Pleistocene soils are more cemented with a maximum carbonate content of less than 10 percent of the fine fraction and with cementation occurring at depths greater than 30 cm (Lundstrom, et al., 1995). Little information is available on the spatial distribution of caliche at YM, but it would be reasonable to assume that caliche would not be present in soils anywhere but in alluvium that is greater than 30 cm in depth. On the other hand, the soil-bedrock interface can form a barrier to flow that fosters evaporation and thus carbonate deposition, so that it would not be unexpected to have caliche deposits on top of the bedrock covered by shallow soils (e.g., sideslopes and ridgetops) at YM

An excellent candidate for substantial lateral subsurface flow within the soil exists wherever there is a sloping soil-bedrock interface at a sufficiently shallow depth that a wetting pulse could

contact the interface Particularly good candidates exist on the sideslopes in washes east of Yucca Crest where the soil is sufficiently permeable to allow most or all of the precipitation to imbibe during precipitation events and the soil-bedrock interface is steeply tilted Vegetation tends to be relatively sparse at the top of the slopes and locally heavier where the slope breaks Neutron probes provide evidence of lateral flow when moistures increase at depth without increasing closer to the surface although it cannot be determined whether the lateral flow is due to a fast vertical pathway just outside the range of the probe or due to lateral flow at depth At Abandoned Wash, in the spring of 1993, neutron-probe evidence suggestive of lateral flow along the sideslopes was documented in the form of increased moisture at about 7 m of depth in N58 (located in a terrace adjacent to a sideslope), appearing well below a wetting front from the surface.

ENVIRONMENTS TO CONSIDER AT YM

The conceptual model laid out by Flint and Flint (1995) and Flint, et al. (1994, 1996) proposes four hydrologic environments [ridgetop, sideslope (north-facing and south-facing), terrace, and channel] covering 14, 62, 22, and 2 percent of the site-scale model The conceptual model laid out by Long and Childs (1993) is similar, with three hydrologic environments [shallow (soil depth <0 35 m), slopes (soil depth 0 35 to 2 m), and basins (deep soils)] covering 18, 70, and 12 percent of the repository footprint.

The NRC staff agrees that these broad divisions are reasonable, particularly east of Yucca Crest although the categories may be somewhat too generic The ridgetop category may have two different infiltration behaviors depending on whether crystal-rich (Tpcr) or crystal-poor (Tpcp) bedrock is exposed, due to significantly different bedrock-fracturing patterns As generally described, the sideslope category is representative of the washes east of Yucca Crest but may inadequately account for the west flank of Yucca Crest.

1 Ridgetop

The ridgetop environment is generally flat to gently sloping, characterized by shallow (roughly 30 to 40 cm, with deeper pockets in scattered locations) to no surficial deposits. The soils have a significant fine eolian component Flint, et al. (1996) classify the soils as lithic haplocambids with a K_{sat} of 24 mm/hr (based on texture analysis), porosity of 0.33, and rock fragments of 15 2 percent. From personal observation, both the number of rock fragments and their size increase with depth, and permeameter measurements suggest that a representative K_{sat} may be as much as 150 to 175 mm/hr (Stothoff and Winterle, 1997) In general, K_{sat} for the ridgetop soils is large enough to accept most or all rainfall and overland-flow runoff should be minimal until the soil storage capacity is reached. Assuming that representative and maximum soil depths are 20 and 60 cm, representative and maximum soil capacities are about 5.5 to 17 cm^3/cm^2.

Two general classes of bedrock are present along ridgetops and the hydrologic behavior of the two classes may be significantly different

a. Crystal-Rich Tiva Canyon Bedrock (Tpcr)

The first bedrock class is crystal-rich Tiva Canyon Tpcr [cuc using the notation of Scott and Bonk, 1984)] overlying Yucca Crest and extending somewhat to the east along some ridges This bedrock is somewhat permeable with K_{sat} on the order of 0 1 mm/hr (Flint, 1996) and weathers into monolithic boulders. The vegetation is typically crack loving and can form linear features aligned with fissures in the bedrock even in soils as deep as 40 cm (Stothoff and Winterle, 1997). Based on cursory field checking, bedrock fissures can be 5 to more than 10 cm in aperture; are typically filled with soil to at least some depth, although fissures may be cemented at depth; there is no evidence of significant carbonate layering above the bedrock; and there are relatively few rock fragments in the soil.

The hydrologic regime of the first bedrock class is expected to be primarily vertical, with lateral flow locally focussing runoff from outcrops into soil and from soil into fissures. For soil-filled fissures, there is no capillary or permeability barrier to prevent water from escaping to depth quickly. If the fissure has carbonate fillings at depth, permeability and capillary barriers may retard wetting pulses. In general, it is expected that water may quickly escape to depth. Although vegetation rooting is strongly preferential to the fissures, it is not yet clear what proportion of a precipitation event can be intercepted through vegetation.

Bomb-pulse ^{36}Cl was located to depths of at least 17 m in seven of the eight ridgetop neutron-probe boreholes discussed by Fabryka-Martin, et al. (1996) with no trace in the other borehole. All eight ridgetop boreholes were completed in Tpcr. Moisture-content records in the boreholes (Flint and Flint, 1995) appear consistent with the bomb-pulse ^{36}Cl data. One borehole had bomb-pulse ^{36}Cl to a depth of 62 m, although this may be due to lateral flow One-dimensional simulations by Flint, et al (1996) and Stothoff, et al. (1996) suggest that infiltration should be quite significant in this environment.

b. Crystal-Poor Tiva Canyon Bedrock (Tpcp)

The second bedrock class is crystal-poor Tiva Canyon, or Tpcp. This bedrock class is exposed at lower elevations where the overlying Tpcr has eroded away. Few data are available to quantify infiltration in this environment. The Tpcp bedrock is somewhat less permeable with K_{sat} on the order of 0.04 mm/hr (Flint, 1996) and is densely fractured. Overlying soils are also classified as lithic haplocambids by Flint, et al. (1996) but may be somewhat shallower than for the Tpcr unit. Fractures typically have much smaller apertures and are generally filled with carbonate materials with K_{sat} on the order of 1.8 mm/hr (Flint, et al., 1996). Carbonate materials should have a strong capillary attraction for water relative to the soils so that considerably increased sorption rates would be anticipated at early times in a precipitation event.

For large precipitation events, the hydrologic regime of the second bedrock class is expected to have a larger lateral-flow component than for the Tpcr unit, due to somewhat smaller soil storage capacity, greater slopes, and restricted capacity for infiltration into the bedrock. The hydrologic regime however, may allow a greater amount of net infiltration for small events, due to small soil storage capacity and capillary attraction of fracture-fill materials. Vegetation is relatively sparse in this environment. It does not appear that vegetation rooting is able to significantly penetrate the carbonate-filled fractures.

2 Sideslopes

The sideslope category covers the largest portion of the area over the potential repository footprint Over the footprint to the east of Yucca Crest, the sideslope category represents the sides of washes incised into Tpcp subunits To the west of Yucca Crest, the sideslope category represents the east flank of Solitario Canyon and exposures of all units from Tpcr through Tptpll (TCw, PTn, and TSw through the lower lithophysal unit)

Scree formation is a common characteristic of all sideslopes Based on about two dozen observations in washes east of Yucca Crest[2], scree is generally not present on slopes less than about 30 percent slope, linearly increases with slope above 30 percent, and completely covers areas with about 60 percent slope, with a coefficient of determination of 0.67 (i.e., a substantial correlation exists between slope and the presence of scree). This relationship may overpredict scree cover on fault-controlled sideslopes such as the west flank of YM.

a. Sideslopes East of Yucca Crest

The sideslopes of washes east of Yucca Crest fit the common conceptualization of the sideslope category Ground slopes are as much as 35 degrees Soil depth is 0 to roughly 1 to 2 m, typically less than 0.5 m, with fragments of rock increasing in size and plentitude as bedrock is approached Over the repository footprint, bedrock is exclusively Tpcp with characteristics described in section 1 b. (Crystal-Poor Tiva Canyon Bedrock)

The general east-west trend of the washes results in north-facing and south-facing slopes with significantly increased solar loading for the south-facing slopes. Mojave vegetation typically dominates on south-facing slopes, and plant activity is likely to be strongly seasonal. Great Basin vegetation dominates north-facing slopes and plant activity may be less seasonal. The soil-bedrock interface is irregular in locations while the soil surface is much smoother, so vegetation may locally take advantage of pockets of deeper soil for moisture requirements.

Lateral subsurface flow is more likely on sideslopes than on ridgetops based on the steep slopes, low soil storage capacity, and bedrock permeability (in common with the Tpcp ridgetops) The sparsity of vegetation at the top of slopes and relative abundance of vegetation at the foot of slopes is indirect evidence for lateral flow. Overland flow undoubtedly occurs on sideslopes in upper washes based on lack of soil cover and smooth rock surfaces in such areas. Overland flow is probably minimal elsewhere on the sideslopes, due to the lack of evidence for gully formation and the rather high soil permeabilities.

Three neutron-probe boreholes in lower sideslopes were sampled for bomb-pulse ^{36}Cl as discussed by Fabryka-Martin, et al. (1996). Two boreholes in WT-2 Wash (N53 and N55, each with soil covers of about 0.7 m) had bomb-pulse ^{36}Cl to depths of 58 and 79 m. Both had bomb-pulse ^{36}Cl throughout the TCw and into the PTn with the deeper borehole also showing bomb-pulse ^{36}Cl in the TSw unit. On the other hand, no bomb-pulse ^{36}Cl was found in N61 (with soil cover of 3.1 m) in Abandoned Wash. In borehole N54, in the channel of WT-2 Wash between N53 and N55, all bomb-pulse ^{36}Cl was found in alluvium at depths less than 4.6 m and

[2] D. Groeneveld, written communication, 1997

the infiltration rate for N54 calculated using chloride mass balance is 0 06 to 0 29 mm yr (Fabryka-Martin et al 1996) Sideslopes with shallow soil cover can be far more effective at providing net infiltration than channels in deep alluvium As bomb-pulse ^{36}Cl is found deeper in N53 and N55 than in typical ridgetop environments lateral flow may supply additional water downslope to both N53 and N55

In Pagany Wash, there are contradictory interpretations of infiltration at UZ-4 (terrace with 12 m of alluvium) and UZ-5 (sideslope with little or no soil cover) Percolation fluxes calculated using pore-water chloride mass balance in the PTn are 1 1 and 1 5 to 2 5 mm/yr for UZ-4 and UZ-5 (Fabryka-Martin, et al, 1996). Using tritium and ^{14}C data yields 35 1 and 20 mm/yr for UZ-4, and ^{14}C data yields 4 mm/yr for UZ-5 (Kwicklis, et al, 1993) Thermal-flux calculations using 1995 data suggest that infiltration fluxes are 18 and 5 mm/yr at UZ-4 and UZ-5 (Rousseau, et al, 1996), although the authors expect the methodology to yield fluxes too high for UZ-4 and too low for UZ-5. As discussed by Tyler and Walker (1994), the use of bomb-pulse tracers can overestimate recharge by an order of magnitude or greater when the impact of transpiration on the flow velocities is neglected. Tyler and Walker (1994) consider chloride balance to be far more reliable The thermal-flux calculations may have been influenced by nonrepresentative wet years to some extent It may also be that channel infiltration dominates sideslope infiltration, at least occasionally, in Pagany Wash Moisture-content data from a set of neutron probes in Pagany Wash (N2 through N9 and N63) are indicative of lateral flow from the channel, lateral flow from the sideslopes in the TCw bedrock cannot be precluded, either Nevertheless, it appears that flow may be predominantly vertical

Approaches considering flow to be essentially vertical have been used to model infiltration on YM sideslopes (Flint, et al, 1996 Stothoff, et al, 1996) Despite the apparent contradiction of perhaps significant lateral flow, the approach may not be unreasonable for the washes east of Yucca Crest as long as the modeling approach assumes that any water not infiltrating runs off to be accounted for separately Salvucci and Entekhabi (1995) present a modeling study examining hillslope controls on equilibrium shallow-water-table profiles that demonstrated that hills with long slopes relative to the soil thickness have an extended domain with equilibrium profiles essentially parallel to the bedrock surface. If this characteristic is reproduced for the highly intermittent conditions at YM, lateral inflow would be almost balanced by lateral outflow for most of the hillslope and the one-dimensional (1D) approach would be appropriate except at ridgetops (drier than predicted) and at the base of the slope (wetter than predicted).

Approaches considering flow to be 2D (two-dimensional) or 3D (three-dimensional) have not been considered for YM sideslopes If the 1D approach is used for sideslopes, it is critical to consider lateral flow to and from channels separately.

b. Sideslopes West of Yucca Crest

Although the bulk of the potential repository footprint lies below and to the east of Yucca Crest, the west flank of YM is of interest as it may be possible for infiltration to enter the TSw below the PTn and move laterally into the repository horizon without being buffered by the PTn.

The sideslope environment along the west flank of YM is more heterogenous than in the washes east of Yucca Crest, due to the wider range of bedrock exposures and gullying due to the steeper slopes. Slopes are greater than 30 degrees Vegetation is dominated by crack-loving

species Solar loading is far more spatially uniform than on the east of Yucca Crest, due to the western exposure

Above the PTn exposure, scree is dominant, channels expose bedrock, and where scree is not present, soils only exist in pockets and cracks In the PTn exposure, slopes flatten with shallow soils developing in places, although bedrock is exposed in channels and local patches Below the PTn exposure, slopes are generally less than 15 degrees and soils begin to develop although gullies expose bedrock even near the bottom of Solitano Canyon

As with the washes east of Yucca Crest, the predominant modeling approach has been vertical and 1D. The steep slopes and presence of gullies suggest that overland flow is significant. It is anticipated that overland flow is relatively short so that although the fractured bedrock exposed in the channels might accept water rapidly, total volume entering the bedrock may be limited. Due to shallow to nonexistent soils, the 1D approach may once again be appropriate, as long as overland flow is explicitly accounted. Overland flow to provide infiltration into channels will likely be the predominant source of net infiltration on the west face of YM.

3. Wash Bottoms

All wash bottoms have a channel that exposes bedrock in upper reaches and lies within alluvial fill in lower reaches. In addition, lower reaches have alluvial terraces that the channel may be incised within. Total depth of alluvial fill may be as much as 10 m over the repository footprint and Solitano Canyon and hundreds of meters in Jackass Flats. In the relatively narrow washes between Yucca Crest and the Exploratory Studies Facility (ESF), wash terraces are shallow to nonexistent

a. Wash Terraces

Lower washes have a terrace of alluvial fill, at least 1 m in depth to as much as 10 m, in which a channel may be incised. Terraces were formed in climates with runoff events larger than observed historically (Lundstrom, et al., 1995). Terraces have shallow slopes and are characterized by deep-rooted vegetation such as creosotebush. As with the ridgetop and sideslope soils, terrace soils have a significant eolian component near the ground surface (Lundstrom, et al., 1995).

Net infiltration is expected to be small to nonexistent in wash terraces unless there is significant lateral flow from sideslopes. The storage capacity of the terraces is large relative to precipitation events so that vegetation should be efficient in transpiring soil moisture before it can escape to depth. Wash terraces are analogous to the deep alluvium cases commonly studied in the literature. Recharge is typically found to be small in deep alluvium unless concentrating mechanisms exist (e.g., active channels, depressions).

Heterogeneity is probably significant in terrace soils based on complex ^{36}Cl signatures (Fabryka-Martin, et al., 1993), making calibration of 1D simulations difficult. Flow fields in terraces are likely to be inherently 2D or 3D due to lateral redistribution from sideslopes and channels.

b Wash Channels

All washes in the YM area are ephemeral Bedrock is exposed in upper washes while in lower washes the channel may be incised into alluvial fill Soils in lower-wash channels are coarser and more permeable than in adjacent terraces Vegetation is sparse in active channels, due to scouring from occasional runoff events, although roots typically should extend under the channel from adjacent terraces.

Net infiltration may be large in the channels, due to concentration of flow from large areas and high permeability of channel bottoms. As discussed in section 2.a. (Sideslopes East of Yucca Crest), evidence based on heat-flux arguments is available suggesting that net infiltration from the Pagany Wash channel may be on the order of 20 mm/yr (Rousseau, et al., 1996), although it is not clear over what area this infiltration rate applies. In 1983, about 15 months after the previous reading, temperature perturbations were also observed in UE-25 a#7 following a major storm. Borehole UE-25 a#7 lies on or near the Drillhole Wash fault zone. The perturbations developed to a depth of 150 m, which Sass, et al. (1988) assessed as possibly attributable to borehole-annulus fluxes. If annulus fluxes were significant, the temperature anomalies are meaningless. Since the temperature anomaly persisted for at least 1 year and was not atypical of previous conditions, the anomaly may represent an infiltration event moving through the fault. If so, the moisture penetrated 47 m of alluvium, 4 m of TCw, 42 m of PTn, and 58 m of TSw in as little as 1 week to as much as 15 months

To date channel flow over the potential repository footprint has not been rigorously considered in modeling efforts. Recharge from channels is considered to be 3 percent of precipitation by Flint, et al. (1996) based on regressions from neutron-probe measurements.

CALCULATED DISTRIBUTION OF INFILTRATION AT YM

A map of estimated spatial distribution of net infiltration was presented by Bagtzoglou, et al. (1996) based on abstractions of 1D simulations considering the impact of soil properties, soil depths, bedrock-fracture properties, elevation, and solar loading on net infiltration The simulations are based on the assumptions that (i) where unfilled fractures exist, they dominate the hydrologic response of the bedrock; and (ii) a few unfilled fractures exist everywhere. Using the same assumptions as Bagtzoglou, et al. (1996), a map of estimated net infiltration in the area of the proposed repository footprint is presented in figure B-2.

Figure B-2 is in qualitative agreement with the conceptual model of distributed net infiltration being dominated by areas with shallow soil depths (i.e., higher infiltration along ridgetops and sideslopes). The distribution of infiltration in figure B-2 does not explicitly account for lateral flow or localized infiltration under scree and only qualitatively addresses infiltration in areas where PTn crops out. Further, the impact of vegetation is not considered, which is anticipated to significantly decrease net infiltration in areas with deep soils. Infiltration resulting from channel flow is indirectly accounted for by occasional shallow soil depths within active wash channels and distributed recharge in areas with deep soils that also have drainage channels.

Net infiltration values predicted by the 1D simulations were found to be insensitive to the hydraulic properties of unfilled fractures as long as some fractures existed (i.e., nonzero fracture porosity), but the net infiltration was found to be very sensitive to soil depth (Stothoff, 1997)

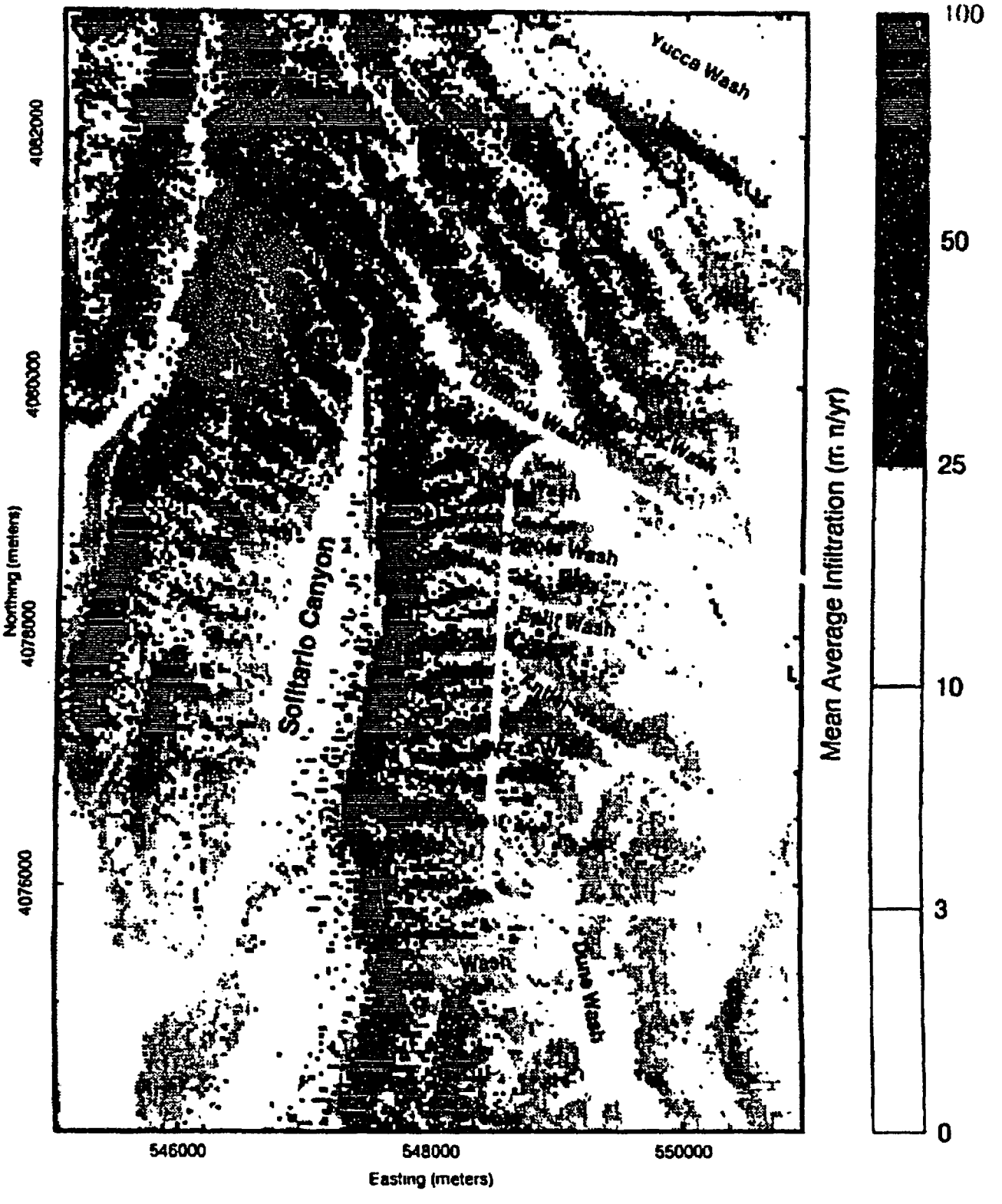

Figure B-2. Estimated net infiltration in the vicinity of the proposed repository footprint.

Subsequent unpublished simulations assumed that the bedrock was impermeable aside from filled fractures having saturated hydraulic conductivities similar to those reported by Flint et al (1996) It was suggested that in cases where all fractures are filled with carbonates net infiltration is comparatively less sensitive to soil depth In contrast to cases with unfilled fractures, net infiltration in carbonate-filled fractures is quite sensitive to the hydraulic properties of the fillings, particularly bubbling pressure and saturated hydraulic conductivity As with unfilled fractures, the (nonzero) porosity assigned to the fractures does not appear to have a significant influence on net infiltration implying that as long as a few fractures exist, it is not important to characterize the number of fractures or their apertures

REFERENCES

Bagtzoglou, A C . E C Pearcy, S A Stothoff, G W Wittmeyer, and N M Coleman, "Unsaturated and Saturated Flow under Isothermal Conditions," B Sagar ed . NRC High-Level Radioactive Waste Program FY96 Annual Progress Report, Volume NUREG/CR-6513, No 1, Washington, DC, U S Nuclear Regulatory Commission, 1996, pp 10-1 through 10-28

Barnes, C.J., G Jacobson, and G D Smith, "The Distributed Recharge Mechanism in the Australian And Zone," *Soil Science Society of America Journal*, 58(1), 1994, pp. 31–40

Baumhardt, R.L., and R.J. Lascano, "Physical and hydraulic properties of a calcic horizon," *Soil Science*, 155(6), 1993, pp. 368–375

Beatley, J.C., "Phenological Events and Their Environmental Triggers in Mojave Desert Ecosystems," *Ecology*, 55, 1974, pp. 856–863.

Fabryka-Martin, J., M Caffee, G Nimz, J. Southon, S. Wightman, W Murphy, M Wickham, and P. Sharma, "Distribution of Chlorine-36 in the Unsaturated Zone at Yucca Mountain: An Indicator of Fast Transport Paths," *Proceedings of the Topical Meeting on Site Characterization and Model Validation: Focus '93*, La Grange Park, IL, American Nuclear Society, 1993, pp. 58–68

Fabryka-Martin, J.T . H J. Turin, A V Wolfsberg, D Brenner, P R Dixon, and J A. Musgrave, "Summary Report of Chlorine-36 Studies," LA-CST-TIP-96-003, Los Alamos, NM, Los Alamos National Laboratory, 1996

Flint, L.E., "Matrix Properties of Hydrogeologic Units at Yucca Mountain, Nevada," Open-File Report 96-xx [draft dated September 25, 1996], Denver, CO, U S. Geological Survey, 1996

Flint, L.E., and A.L. Flint, "Shallow Infiltration Processes at Yucca Mountain, Nevada—Neutron Logging Data 1984-93," Water-Resources Investigations Report 95-4035, Denver, CO, U.S. Geological Survey, 1995.

Flint, L.E., A.L. Flint, and J.A. Hevesi, "Shallow Infiltration Processes in Arid Watersheds at Yucca Mountain, Nevada," *Proceedings of the Fifth Annual International Conference on High-Level Radioactive Waste Management*, La Grange Park, IL, American Nuclear Society, 1994, pp. 2,315–2,322.

Flint, A.L., J.A. Hevesi, and L.E. Flint, "Conceptual and Numerical Model of Infiltration for the Yucca Mountain Area, Nevada," Water-Resources Investigations Report, Denver, CO, U.S Geological Survey, 1996.

French, R.H., "Precipitation in Southern Nevada," *Journal of Hydraulic Engineering*, 109(7), 1983, pp. 1,023–1,036.

French, R.H., "Daily, Seasonal, and Annual Precipitation at the Nevada Test Site, Nevada," Publication No. 45042, Reno, NV, Desert Research Institute, 1986.

French R H R L Jacobson and B F Lyles "Threshold Precipitation Events and Potential Ground-Water Recharge." *Journal of Hydraulic Engineering*. 122(10) 1996 pp 573–578

Gee. G W and D Hillel "Groundwater Recharge in Arid Regions Review and Critique of Estimation Methods," *Hydrological Processes* 2. 1988 pp 255–266

Gee. G W. P J Wierenga. B J Andraski. M H Young. M J Fayer and M L. Rockhold "Variations in Water Balance and Recharge Potential at Three Western Desert Sites." *Soil Science Society of America Journal*, 58(1) 1994 pp 63–72

Guertal, W.R., A.L Flint. L.L Hofmann, and D B Hudson. "Characterization of a Desert Soil Sequence at Yucca Mountain. NV," *Proceedings of the Fifth Annual International Conference on High-Level Radioactive Waste Management*. La Grange Park, IL. American Nuclear Society 1994. pp 2,755–2,763.

Hennessy. J T.. R P Gibbens J M Tromble, and M Cardenas. "Water Properties of Caliche " *Journal of Range Management*, 36(6). 1983. pp 723–726

Hessing, M.B . G E Lyon. G T Sharp. W K Ostler R A Green. and J P Angerer "The Vegetation of Yucca Mountain Description and Ecology." B00000000-01717-5705-00030 Rev 00. Las Vegas. NV TRW Environmental Safety Systems Inc . 1996

Hevesi, J.A . J D Istok. and A L Flint, "Precipitation Estimation in Mountainous Terrain Using Multivariate Geostatistics. Part I. Structural Analysis." *Journal of Applied Meteorology* 31(7) 1992. pp. 661–676

Hillel, D , "Introduction to Soil Physics." New York. NY. Academic Press. 1980

Jury. W.A , W.R. Gardner. and W H Gardner "Soil Physics," New York, NY. John Wiley & Sons 1991.

Kemper, W D., A.D. Nicks, and A T Corey, "Accumulation of Water in Soils under Gravel and Sand Mulches," *Soil Science Society of America Journal*, 58(1). 1994. pp. 56–63.

Kwicklis, E.M., A.L. Flint, and R W. Healy, "Estimation of Unsaturated Zone Liquid Water Flux at Boreholes UZ#4, UZ #5. UZ #7, and UZ #13. Yucca Mountain, Nevada, from Saturation and Water Potential Profiles," *Proceedings of the Topical Meeting on Site Characterization and Model Validation: Focus '93*, La Grange Park, IL, American Nuclear Society, 1993, pp. 53–57.

Lane, L.J., and W.R. Osterkamp, "Estimating Upland Recharge in the Yucca Mountain Area," *Irrigation and Drainage Proceedings 1991*, American Society of Civil Engineers, 1991, pp. 170–176.

Long, A., and S.W. Childs, "Rainfall and Net Infiltration Probabilities for Future Climate Conditions at Yucca Mountain," *Proceedings of the Fourth Annual International Conference on High-Level Radioactive Waste Management*, La Grange Park, IL, American Nuclear Society, 1993, pp. 112–121.

Lundstrom S.C., S.M. McDaniel, W. Guertal, M.H. Nash, J.R. Wesling, J. Cidziel, S. Cox, and J. Coe. "Characteristics and Development of Alluvial Soils of the Yucca Mountain Area, Southern Nevada." USGS Open-File Report 95GCH510M. Denver, CO: U.S. Geological Survey, 1995.

Marion, G.M., W.H. Schlesinger, and P.J. Fonteyn. "CALDEP: A Regional Model for Soil $CaCO_3$ (Caliche) Deposition in Southwestern Deserts." *Soil Science*, 139(5), 1985, pp. 468–481.

Maxey, G.B., and T.E. Eakin. "Ground Water in White River Valley, White Pine, Nye, and Lincoln Counties, Nevada." Bulletin 8. Carson City, NV: Department of Conservation and Natural Resources, State of Nevada, 1949.

McCord, J.T., and D.B. Stephens. "Comment on Effect of Groundwater Recharge on Configuration of the Water Table Beneath Sand Dunes." *Journal of Hydrology*, 95, 1987, pp. 365–367.

Montazer, P., and W.E. Wilson. "Conceptual Hydrologic Model of Flow in the Unsaturated Zone, Yucca Mountain, Nevada." USGS Open-File Report 84-4345, Lakewood, CO: U.S. Geological Survey, 1984.

Nichols, W.D. "Geohydrology of the Unsaturated Zone at the Burial Site for Low-Level Radioactive Waste Near Beatty, Nye County, Nevada." Water-Supply Paper 2312. Denver, CO: U.S. Geological Survey, 1987.

Patterson, G.L., E.P. Weeks, J.P. Rousseau, and T.A. Oliver. "Interpretation of Pneumatic and Chemical Data From the Unsaturated Zone Near Yucca Mountain, Nevada." Denver, CO: U.S. Geological Survey, 1996.

Phillips, F.M. "Environmental Tracers for Water Movement in Desert Soils of the American Southwest." *Soil Science Society of America Journal*, 58(1), 1994, pp. 15–24.

Rousseau, J.P., E.M. Kwicklis, and D.C. Gillies, eds. "Hydrogeology of the Unsaturated Zone, North Ramp Area of the Exploratory Studies Facility, Yucca Mountain, Nevada." Water-Resources Investigations Report. Denver, CO: U.S. Geological Survey, 1996.

Salvucci, G.D., and D. Entekhabi. "Hillslope and Climatic Controls on Hydrologic Fluxes." *Water Resources Research*, 31(7), 1995, pp. 1,725–1,739.

Sass, J.H., A.H. Lachenbruch, W.W. Dudley, Jr., S.S. Priest, and R.J. Munroe. "Temperature, Thermal Conductivity, and Heat Flow Near Yucca Mountain, Nevada: Some Tectonic and Hydrologic Implications." USGS Open-File Report 87-649. Denver, CO: U.S. Geological Survey, 1988.

Schlesinger, W.H. "The Formation of Caliche in Soils of the Mojave Desert." *Geochimica et Cosmochimica Acta*, 49, 1985, pp. 57–66.

Schmidt, M.R. "Classification of Upland Soils by Geomorphic and Physical Properties Affecting Infiltration at Yucca Mountain, Nevada." Master's thesis, Colorado State University, 1989.

Scott. R B and J Bonk "Preliminary Geologic Map (1 12 000 scale) of Yucca Mountain Nye County. Nevada. with Geologic Cross Sections." USGS Open-File Report 84-494 Denver CO U.S Geological Survey. 1984

Shevenell. L., "Statewide Potential Evapotranspiration Maps for Nevada." Nevada Bureau of Mines and Geology. Report 48. University of Nevada. 1996

Stothoff. S A . "Sensitivity of Long-Term Bare Soil Infiltration Simulations to Hydraulic Properties in an Arid Environment," *Water Resources Research*. 33(4). 1997. pp. 547–558.

Stothoff. S.A., H.M. Castellaw, and A.C. Bagtzoglou. "Simulating the Spatial Distribution of Infiltration at Yucca Mountain, Nevada," San Antonio. TX. Center for Nuclear Waste Regulatory Analyses. sent under cover letter from E. Pearcy (CNWRA) to N. Coleman (NRC). dated July 3. 1996.

Stothoff. S.A. and J.R. Winterle. "Trip Report - Trip to Yucca Mountain for Hydrology Field Work." Documenting trip to Yucca Mountain (March 26-28. 1997) by staff and contractors of the Center for Nuclear Waste Regulatory Analyses. San Antonio. TX. dated April 9. 1997. 6 pp

Tyler. S.W., and G R Walker. "Root Zone Effects on Tracer Migration in Arid Zones." *Soil Science Society of America Journal*. 58(1). 1994. pp 25–31

Watson. P . P. Sinclair. and R. Waggoner. "Quantitative Evaluation of a Method for Estimating Recharge to the Desert Basins of Nevada." *Journal of Hydrology*. 31. 1976. pp 335–348

Winograd. I J., and W. Thordarson. "Hydrologeologic and Hydrochemical Framework. South-Central Great Basin. Nevada-California. with Special Reference to the Nevada Test Site." Professional Paper 712-C. Washington. DC. U.S. Geological Survey. 1975

APPENDIX C

DOE'S UNSATURATED ZONE FLOW MODEL EXPERT ELICITATION PROJECT

From the Fall of 1996 through the Spring of 1997, the U.S. Department of Energy (DOE) performed an expert elicitation assessing issues related to modeling the Yucca Mountain unsaturated zone at the site scale (DOE, 1997). In section 1.1 of DOE's report, the objectives of the elicitation are spelled out (DOE, 1997, p. 1-1).

> This report presents results of the Unsaturated Zone Flow Model Expert Elicitation (UZFMEE) project at Yucca Mountain, Nevada. This project was sponsored by the U.S. Department of Energy (DOE) and managed by Geomatrix Consultants, Inc. (Geomatrix), for TRW Environmental Safety Systems, Inc. The objective of this project was to identify and assess the uncertainties associated with certain key components of the unsaturated zone flow system at Yucca Mountain. This assessment reviewed the data inputs, modeling approaches, and results of the unsaturated zone flow model (termed the "UZ site-scale model") being developed by Lawrence Berkeley National Laboratory (LBNL) and the United States Geological Survey (USGS). In addition to data input and modeling issues, the assessment focused on percolation flux (volumetric flow rate per unit cross-sectional area) at the potential repository horizon. An understanding of unsaturated zone processes is critical to evaluating the performance of the potential high-level nuclear waste repository at Yucca Mountain.
>
> A major goal of the project was to capture the uncertainties involved in assessing the unsaturated flow processes, including uncertainty in both the *models* used to represent physical controls on unsaturated zone flow and the *parameter values* used in the models. To ensure that the analysis included a wide range of perspectives, multiple individual judgments were elicited from members of an expert panel. The panel members, who were experts from within and outside the Yucca Mountain project, represented a range of experience and expertise. A deliberate process was followed in facilitating interactions among the experts, in training them to express their uncertainties, and in eliciting their interpretations. The resulting assessments and probability distributions, therefore, provide a reasonable aggregate representation of the knowledge and uncertainties about key issues regarding the unsaturated zone at the Yucca Mountain site.

Table 3-1 of the expert elicitation (DOE, 1997) summarizes key issues discussed with the experts and the responses of the experts to the issues. Portions of that table relevant to

shallow infiltration are reproduced here as Table C-1 Table 3-2 of the expert elicitation (DOE, 1997) presents a summary of the estimates of percolation flux provided by the experts this table is reproduced as Table C-2. Six of the seven experts thought that the statistical distributions for net shallow infiltration and deep percolation fluxes were identical. the remaining expert (G. Campbell) thought that slightly higher values would occur for net shallow infiltration than for deep percolation flux. Median percolation flux estimated by the experts is 7.2 mm/yr; mean percolation flux estimated by the experts is 10 3 mm/yr

The NRC staff cautions that the tables reproduced here from DOE (1997) are provided as a summary for the convenience of the reader. The information should not be interpreted without full consideration of the text within DOE's (1997) expert elicitation report, and especially the elicitation interview summaries for each of the seven expert panelists.

The NRC staff is not bound by the conclusions of an elicitation *a priori* solely based on adherence to guidance provided by the staff. As noted in NUREG-1563 (NRC, 1996, p. 8), "...the use of a formal elicitation process, even when conducted in a manner consistent with guidance provided in this BTP [NRC, 1996], [does not] guarantee that specific technical conclusions will be accepted and adopted by the staff, a Licensing Board, the Commission itself, or any other party to a potential HLW licensing proceeding."

References

DOE (U.S. Department of Energy), "Unsaturated Zone Flow Model Expert Elicitation Project." WBS 1.2 5 7, prepared for DOE by Geomatrix Consultants, Inc., San Francisco, CA, and TRW, Las Vegas, NV under Contract No. DE-AC01-91RW00134, 1997

NRC (U.S. Nuclear Regulatory Commission), "Branch Technical Position on the Use of Expert Elicitation in the High-Level Radioactive Waste Program," NUREG-1563, November 1996.

	Gaylon Campbell	Glendon Gee	James Mercer	Shlomo Neuman	Karsten Pruess	Daniel Stephens	Edwin Weeks
Net Infiltration Temporal Issues	+ Major storm events with intervals of ~ 10 yrs + Essentially no infiltration between these events	+ Major storm events with intervals of about 1 yr + Essentially no infiltration between these events	+ Episodic storm events with average intervals of about 5 yrs give rise to most (~ 80% of infiltration)	+ Major storm events lead to infiltration recurrence interval tied to precipitation record	+ Infiltration occurs from few isolated storm events, 1-2 per yr + Infiltration near zero or negative between these events	+ Infiltration occurs during short bursts of severe storm events that have recurrence intervals of 20 yrs + Between these events infiltration occurs but in low amounts	+ Storm event or sequence every few yrs leads to infiltration event; intervening time essentially no net infiltration + More severe events with longer recurrence intervals
Net Infiltration Spatial Issues	+ Agree with basic Flint map and relative importance of various factors + Horse-tailing faults important	+ Flint map generally OK but expect more infiltration at upper reaches of washes + Funneling of water into faults and fractures (~ 5% of surface area) is important process	+ At lower net infiltration values, Flint map is OK + At higher values would expect higher values in washes and lower values on ridge tops + Lateral flow within alluvium into fractures is important	+ Expected to be heterogeneous, but Flint map is consistent intuitive; highs expected in washes, lows on ridge tops + Lateral flow at bedrock alluvium contact into fractures (faults) high permeability paths	+ May be nonlinear relationship between amount of infiltration and spatial distribution	+ Flint infiltration map is generally OK, but would expect moderate infiltration amounts on ridgetops and high rates in washes + Underflow at alluvium bedrock surface is important process	+ Net infiltration map would be smoother than Flint - with lower highs on the ridges and higher rates in the washes + Flow at alluvium bedrock contact into open fractures is important
Net Infiltration Temporal and Spatial Average (Note mean values are calculated)	Mean 7.4 mm/yr Median 7 mm/yr 5th 1 mm/yr 95th 15 mm/yr Averaged over 50-1,000 yr	Mean 12.7 mm/yr Median 12.7 mm/yr 5th 7 mm/yr 95th 18 mm/yr Average over ~ 100 yr	Mean 8.4 mm/yr Median 7.5 mm/yr 5th 2 mm/yr 95th 20 mm/yr Average over ~ 100 yr	Assessed percolation flux and thus net infiltration on the basis of deeper subsurface data	Mean 11.3 mm/yr Median 7 mm/yr 5th 0.5 mm/yr 95th 40 mm/yr Averaged over several major storm events	Mean [illegible] mm/yr Median [illegible] mm/yr 5th [illegible] mm/yr 95th 10 mm/yr Averaged over 100 yr	Assessed percolation flux and thus net infiltration on the basis of deeper subsurface data
Temporal Behavior of UZ flow System	+ Episodic infiltration events, dampening of pulsed flow at PTn, essentially steady-state below PTn (except fast-flow component, which is transient)	+ Episodic infiltration events lead to pulse of water that can reach depth quickly, as evidenced by ^{36}Cl	+ Transient pulse related to infiltration is significantly dampened as it moves through system, fast-flow component remains transient	+ Transient pulse related to episodic infiltration events dampened in PTn + Fast flow components transient and slightly dampened	+ Episodic pulses can flow through system + Pulses dampened as they pass through PTn and other layers with different hydraulic properties + System may not be steady state	+ Fast-flow components years to tens of yrs, fracture components travel times are ~ thousands of yrs, matrix component ~ hundreds of thousands of yrs	+ Transient pulse related to infiltration events moves through system with little matrix interaction + At high percolation fluxes [illegible]

Table C-1. Summary of key issues (reproduced in part from Table 3-1, pp. 3-27 to 3-30, DOE, 1997)
(page 1 of 3)

	Gaylon Campbell	Glendon Gee	James Mercer	Shlomo Neuman	Karsten Pruess	Daniel Stephens	Edwin Weeks
Method(s) Used to Estimate Percolation Flux at Repository Horizon	Relative weights: Net infiltration/surface water balance (0.3) ^{36}Cl (0.3) Flux through PTn (0.2) Concentration heat flux (0.05) Radiocarbon decay (0.05) Mineral coating (0.05) Perched water (0.05)	+ Net infiltration, checked with water potentials and isotopic evidence	+ Net infiltration, checked with chloride mass balance, temperature gradients, and perched water	+ Saturations and water potentials within PTn supplemented by isotopic evidence and ESF moisture balance	+ Net infiltration	+ Net infiltration	+ Temperature gradients + Radiocarbon gas + Perched Water
Percolation Flux Estimate, Temporal and Spatial Average (Note: mean values are calculated)	Mean 5.3 mm/yr Median 4 mm/yr 5th 1 mm/yr 95th: 14 mm/yr Based on net infiltration, ^{36}Cl, and flux through PTn	+ Same spatial and temporal average as net infiltration	+ Same spatial and temporal average as net infiltration	Mean 21.1 mm/y Median 17 mm/y 5th 0 mm/y 95th 50 mm/y	+ Same spatial and temporal average as net infiltration	+ Same spatial and temporal average as net infiltration + Lateral input from Solitario Canyon to TSw is probably minor	Mean 7.4 mm/yr Median 6 mm/yr 5th 1 mm/yr 95th 22 mm/yr
Percolation Flux: Spatial Issues	+ Generally same as net infiltration map, but smoother + As predicted by LBNL model results	+ Generally same as net infiltration map	+ More uniform distribution than infiltration because of diffusion into TSw fracture network (which contains ubiquitous fractures)	+ Should generally correlate with infiltration map but local lateral flow, medium heterogeneities and fast flow channels will modify	+ Not known, may be similar to net infiltration map, or heterogeneities may develop new variability	+ Generally same as infiltration map (highs and lows generally the same locations) + Superimposed are local highs at faults and fractures	+ Map expected to be subdued replica of net infiltration map
Modeling Issues	+ 1-d finite difference model for net infiltration is OK	1-d infiltration modeling doesn't adequately address runoff + Need mass balance model for infiltration + Neutron probe data do not capture episodic nature of storm events	+ Dual-K above PTn, ECM probably OK below, as long as fast-flow component included	+ 1-d modeling is not capable of incorporating lateral flow at bedrock alluvium contact + Uncertainty and error analyses of local flux estimates and measured temperature profiles should be conducted	+ A WEEPS-type model embedded in a more complex model may be way to portray fast-flow component + Continuum description of flow assumes volume-averaging and may miss much of localized flow volume + Role of faults is not understood, may not be needed in PTn + Spatial stability of flow paths through time is uncertain	+ No confidence in Richards model for infiltration. Manty Lakes not satisfactory for points within a watershed + Perched water balance and overall water balance including water table fluctuations should be modeled + TOUGH2 modeling should predict key observations such as the wet spot at ESF station 75+00	+ Transport paths through PTn and deeper in saturated zone with both matrix interactions + Episodic pulses, not steady state + Predictability of which fractures in TSw will carry flow should be modeled as random

Table C-1 (cont.). (page 2 of 3)

	Gaylon Campbell	Glendon Gee	James Mercer	Shlomo Neuman	Karsten Pruess	Daniel Stephens	Edwin Weeks
Additional Data Collection/Future Work to Reduce Uncertainties	+ Water potential, water content, hydraulic properties measurements in situ in ESF + Unsaturated conductivity measurements should be high priority + Surface water balance info: plant uptake, rock cover on slopes, snow, washes, rock-alluvium contact	+ Mass balance using drip line source above ESF and pan + Inject water above sealed-off room of ESF to test for seepage + Perform non-linear fit to temperature data to see if profiles show curvature	+ Run UZ model to examine the effect of higher infiltrations + Evaluate effect of more infiltration in washes	+ Develop a detailed database of saturations, pressure, hydraulic conductivities at ambient saturations, and PTn thicknesses to obtain vertical and lateral resolution of percolation flux in PTn	+ Monitoring and data collection related to net infiltration should continue	+ Thoroughly study and instrument small drainage basin above repository, including rain gauges, mapping of fractures, nests of piezometers, [illegible] of bedrock-alluvium[illegible], buried pan lysimeters, and TDR probes + More unsaturated hydraulic conductivity measurements + More accurate measurements of water potentials in PTn using tensiometers and heat dissipation probes + Infiltration study of Solitario Canyon and development of hydrographs of perched water	+ Obtain temperature logs with measurements at close intervals

Table C-1 (cont.). (page 3 of 3)

Percolation Flux (mm/yr)						
Expert	Mean	5th	15th	50th	85th	95th
G. Campbell	5.3	1.1	2.0	3.8	9.4	13.6
G. Gee	13.2	3.0	5.5	**12**	21.7	27.5
J. Mercer	8.4	**2**	4.4	7.5	10.8	**20**
S. Neuman	21.1	**6**	9.0	17.3	34.2	**50**
K. Pruess	11.3	0.5	1.8	7.0	25.0	40.0
D. Stephens	3.9	0.7	1.3	3.1	6.3	**10**
E. Weeks	7.4	1.0	2.3	6.1	11.7	21.7
Aggregate	10.3	1.0	2.3	7.2	19.3	30.0
Numbers in bold were assessed directly by the experts. The other numbers were interpolated from their assessed distributions						

Table C-2. Summary of estimates of percolation flux (from Table 3-2 of DOE, 1997)

APPENDIX D

OPEN KTI ITEMS UNRESOLVED AT THE STAFF LEVEL

TSPA95	Area of Concern (USFIC) - Infiltration and deep percolation calculations presented in Chapter 7 of TSPA-95 lack defensibility
TSPA95	Area of Concern (USFIC) - Dilution factor calculations presented in Chapter 7 of TSPA-95 lack defensibility.
TSPA95	Statement of Concern (USFIC) - The lower limit chosen for the "satiated matrix saturation" remains unrealistically high and not adequately conservative.
SCA	Comment 15 - Solitario Canyon horizontal borehole activity inadequate to address impact of faults on fluid flow.
SCA	Comment 19 - Activities for the saturated zone flow system are inadequate to characterize boundaries, flow directions, magnitudes, and paths
SCA	Comment 20 - Current and proposed well locations inadequate for defining the potentiometric surface in the controlled area
SCA	Comment 21 - No consideration of I-129 and Tc-99 in characterization of saturated zone hydrochemistry.
SCA	Comment 22 - Inadequate saturated zone hydrology sample collection methods.
SCA	Question 55 - No analysis of potential test interference from water storage facilities.
SP 831212	Comment 1 - The NRC staff considers that specific attention should be given to the study of surface runoff flows from the west face of YM and in Solitario Canyon.
SP 831214	Comment 1 - The study needs to identify what minimum information and documentation about pre-existing wells will be acceptable to support the use of those wells in calibrating regional models.
SP 831214	Comment 2 - The study needs to be updated with respect to available literature on the alternate conceptual models for the regional ground water system. The study plan does not adequately describe the approach for modifying existing conceptual models based on new hydrogeologic data.

SP 831214	Comment 3 - Data may be insufficient to adequately construct and calibrate subregional or regional groundwater models
SP 831214	Question 1 - What approaches will be used to evaluate evapotranspiration and recharge on a regional basis?
SP 831228	Question 1 - How will laboratory-scale models and data be used to estimate model parameters in the corresponding site-scale models?
SP 831228	Question 2 - Why have particular modeling strategies been assigned to address particular technical issues?
SP 831228	Question 3 - Is the method used by Cacas, et al. (1990) for the determination of fracture network hydraulic aperture distributions applicable for unsaturated flow?
SP 831228	Question 4 - How can one build confidence in conceptual models if every time a conceptual model is refuted by experimental data, the experiment is redesigned as inappropriate or not sensitive enough to capture the essence of the model?
SP 831228	Question 5 - What modeling strategies will be used to address technical issues for fluid flow studies?
SP 831229	Comment 1 - Solitario Canyon fault as a water infiltration pathway
SP 831229	Question 1 - Evaluation of wetting front instabilities for modeling the Yucca Mountain hydrologic regime
SP 831229	Question 2 - Obtaining hydrologic parameters for fractures.
SP 831229	Question 3 - Measurement of local water gradients in fractures to infer net moisture flux rates.
SP 831229	Question 4 - Calibration of hydrologic sub-models using experimental perturbations.
SP 831229	Question 5 - Evaluation of modeling the non-Darcian flow regime in specific fault zones.
SP 831233	Comment 1 - Hydrochemical data should be used to support conceptual and numerical groundwater models for the saturated zone.
SP 831233	Question 1 - Which hydrologic codes may be used to model complex heterogeneities in the saturated zone?
SP 831233	Question 2 - What methods will be used to incorporate "soft" information in analyses of hydrologic parameters?

SP 831233	Question 3 - How will site saturated-zone hydrologic modeling be integrated with other site characterization activities?
SP 831233	Question 5 - How will upper and lower boundary conditions be selected for a three-dimensional groundwater model at the scale of the controlled area?
SP 831233	Question 6 - If additional multiple-well sites are not constructed, how will DOE demonstrate that fracture-network models represent the saturated groundwater system in portions of the controlled area beyond the vicinity of the C-well complex?
SP 831521	Comment 2 - Planned thermal scanner flight data may not provide sufficient areal coverage to characterize regional properties.
SP 831521	Question 6 - Will tracer isotopic compositions be determined for analog deposits and compared to those in Trench 14?
SP 831522	Comment 1 There appears to be a gap in the documentation of groundwater modeling work under this study
SP 831522	Question 1 - How will the work in regional surface water and saturated zone modeling be integrated with the site unsaturated zone modeling?
SP 831522	Question 2 - How will infiltration be simulated under the surface water modeling activity?